INVESTIGATION OF CONTROL OF HUMAN BALANCE-RECOVERY REACTIONS

A THESIS SUBMITTED TO
THE GRADUATE SCHOOL OF NATURAL AND APPLIED SCIENCES
OF
MIDDLE EAST TECHNICAL UNIVERSITY

BY

NURDAN BILGIN

IN PARTIAL FULFILLMENT OF THE REQUIREMENTS
FOR
THE DEGREE OF DOCTOR OF PHILOSOPHY
IN
MECHANICAL ENGINEERING

SEPTEMBER 2015

Approval of the thesis:

INVESTIGATION OF CONTROL OF HUMAN BALANCE-RECOVERY REACTIONS

submitted by **NURDAN BILGIN** in partial fulfillment of the requirements for the degree of **Doctor of Philosophy in Mechanical Engineering Department, Middle East Technical University** by,

Prof. Dr. Gülbin Dural Ünver
Dean, Graduate School of **Natural and Applied Sciences** ________________

Prof. Dr. R. Tuna Balkan
Head of Department, **Mechanical Engineering** ________________

Prof. Dr. M. Kemal Özgören
Supervisor, **Mechanical Engineering Department, METU** ________________

Examining Committee Members:

Assist. Prof. Dr. Ergin Tönük
Mechanical Engineering Department, METU ________________

Prof. Dr. M. Kemal Özgören
Mechanical Engineering Department, METU ________________

Prof. Dr. Kemal Leblebicioğlu
Electrical and Electronics Engineering Department, METU ________________

Prof. Dr. Metin Uymaz Salamcı
Mechanical Engineering Department, Gazi University ________________

Assoc. Prof. Dr. Yiğit Yazıcıoğlu
Mechanical Engineering Department, METU ________________

Date: ________________

I hereby declare that all information in this document has been obtained and presented in accordance with academic rules and ethical conduct. I also declare that, as required by these rules and conduct, I have fully cited and referenced all material and results that are not original to this work.

Name, Last Name: NURDAN BILGIN

Signature :

ABSTRACT

INVESTIGATION OF CONTROL OF HUMAN BALANCE-RECOVERY REACTIONS

Bilgin, Nurdan
Ph.D., Department of Mechanical Engineering
Supervisor : Prof. Dr. M. Kemal Özgören

September 2015, 201 pages

In this study, a natural control law has been conjectured, which is assumed to be applied by the central nervous system of a human being in order to maintain the erect posture after being exposed to a suddenly occurring impulsive disturbance. The control law is conjectured as PD (proportional-derivative) control, because it has to be compatible with the physiological facts. The conjectured control law has been validated by comparing a set of experimental results with the corresponding set of simulation results generated by applying the conjectured control law to a biomechanical model of a typical human being. For the sake of simplicity, the model is confined to the sagittal plane with three degrees of freedom having the ankle, knee, and hip joints as the only actuated joints. The other joints are assumed to be kept fixed. The experiments are carried out in a way compatible with the model by using a tilt platform and by requesting the human subjects to keep their hands in their pockets while standing on the platform. During the experiments, the impulsive disturbance is given by tilting the platform suddenly and then the balance recovery motions of the human subject are recorded. The experiments and simulations are repeated several times on different human subjects. In all the test runs, it has been possible to match the simulation and experimental results only if the simulations are made by changing the gains of the conjectured PD control law as particular functions of time.

The experimentally inferred fact of changing PD control gains leads to a major hypothesis that the central nervous system applies the conjectured PD control law by changing its gains according to a certain adaptation law. Naturally, it is difficult to estimate this adaptation law because it is probably very much dependent on the past physiological and psychological experiences of the human beings. Nevertheless, it may be possible to estimate at least a set of major arguments along with a functional relationship between them and the adapted gains. In this study, it has been possible to arrive at such an estimation by means of the renown "canonical correlation method". When this method is applied to correlate the experimental and simulation results, it has been found out that the adaptation law seems to be a linear relationship that gives the PD control gains in terms of the error state and input variables as long as they remain small in magnitude.

Furthermore, upon examining the experimental results gathered from the repeated runs for different human subjects, another evident correlation is detected, which is between the initial posture of the human subject on the platform and the subsequent pattern of the balance-recovery response that occurs after a sudden tilt of the platform. In order to express this correlation mathematically, the initial postures and the balance-recovery responses are classified by using classification algorithms. Afterwards, the expression obtained for this correlation has been tested and verified to a large extent with Monte Carlo simulations by using the decision tree created in accordance with the classification.

Keywords: Biomechanics, Postural Control, Physiological Feedback Control, Proportional Derivative Control, Musculosceletal Model, Time-Varying Feedback Gains, Least Square Method, Unexpected External Disturbance

ÖZ

İNSAN DENGE KURTARMA REAKSİYONLARININ KONTROLÜNÜN ARAŞTIRILMASI

Bilgin, Nurdan
Doktora, Makina Mühendisliği Bölümü
Tez Yöneticisi : Prof. Dr. M. Kemal Özgören

Eylül 2015 , 201 sayfa

Bu çalışmada, ani bir eğim değişimine maruz kalan insanın dengesini koruyabilmek için merkezi sinir sistemince uygulanan doğal kontrol kuralı tahmin edilmeye çalışılmaktadır. Bu tahmin çerçevesinde doğal kontrol kuralı, fizyolojik bulgularla uyumlu olması gözetilerek oransal-türevsel kontrol olarak modellenmiştir. Bu doğal denge kurtarma tepkileri için önerilen kontrol kuralı modelinin doğrulaması, deneysel veriler ile benzetim verilerinin karşılaştırması yoluyla yapılmıştır. Sözü edilen benzetimler, insanın karakteristik biyomekanik modeline, önerilen kontrol kuralının uygulanması ile, elde edilmiştir. Kontrol modelinde kullanılan basitlik ilkesinden ayrılmaksızın, biyomekanik model, eyleticiler ayak bileği, diz ve kalça eklemlerinde olmak üzere, üç serbestlik dereceli ve sagital düzlemle sınırlıdır. Diğer eklemlerin sabit tutulduğu kabul edilmiştir. Deneyler sırasında, ani dış sarsı, özel yapım sarsma platformu ile verilmekte ve deneklerin gösterdiği denge kurtarma tepkileri kaydedilmektedir. Deneyler ve devamında benzetimler farklı denekler üzerinde bir çok kez tekrarlanmıştır. Bütün test çalışmalarında, deneysel veriler ile benzetim verilerinin uyumunun sadece önerilen oransal-türevsel kontrolün kazançlarının zaman içinde değiştirilmesi ile mümkün olduğu görülmüştür.

Oransal türevsel kazançların değiştiği gerçeğinin deneysel olarak anlaşılması önemli bir hipoteze yol açmıştır. Şöyle ki, merkezi sinir sistemi gelen duyusal geri bildirim ve çevresel değişimlere bağlı olarak denge kurtarma tepkilerini yöneten kontrol kuralının kazançlarını uyarlamaktadır. Doğal olarak, bu uyarlama kuralını, insanın geçmiş fizyolojik ve psikolojik deneyimlerine çok bağlı olması nedeniyle, kesinlikli olarak tahmin etmek oldukça zordur. Bu zorluğa rağmen, duyusal geri bildirim ve çevresel değişimler ile uyarlanan kazançlar arasında fonksiyonel ilişkiler betimlenmesi yoluyla en azından uyarlama kuralının varlığı ve niteliğine ilişkin önemli argumanlar elde edilebilir ve merkezi sinir sisteminin kullanmış olabileceği uyarlama kuralı tahmin edilebilir. Bu çalışmada, çok bilinen ve kullanışlı "kanonik korelasyon yöntemi" aracılığıyla böyle bir tahmine varmak mümkün olmuştur. Bu yöntem, deneysel verilerle benzerliği karşılaştırılmak üzere benzetim sonuçlarına uygulandığında, değişkenlerin büyüklüklerinin belirli bir sınırlılıkta kalması koşuluyla, uyarlama kuralı ile oransal türevsel kontrolun kazançlarının hata ve girdi değişkenleri terimleriyle, doğrusal bir ilişki olarak ifade edilebileceği görülmüştür.

Ayrıca, farklı deneklerden toplanan, deneysel verilerin değerlendirilmesi sırasında, deneklerin başlangıç duruşları ile ani eğim değişiminin ardından ortaya çıkan denge kurtarma reaksiyonu arasında belirgin bir ilişki tespit edilmiştir. Ortaya çıkan bu olgunun ardından, matematiksel olarak bu ilişkiyi ifade etmek üzere, ilk duruş ve denge kurtarma reaksiyonları, sınıflandırma algoritması kullanarak sınıflandırılmıştır. Ardından, bu sınıflandırma sonucu elde edilen karar ağacı kullanılarak yapılan Monte Carlo benzetimleri ile ilk duruş ile denge kurtarma reaksiyonları arasındaki ilişki örüntüsü deneysel veriler ile elde edilen örüntülere büyük bir benzerlikle yeniden elde edilmiş ve benzerlik ilişkisi istatistiksel olarak ortaya konulmuştur.

Anahtar Kelimeler: Biyomekanik, İnsan Denge Kontrolü, Fizyolojik Geribeslemeli Kontrol, Oransal Türevsel Kontrol, Biyomekanik Model, Zamana Bağlı Geribesleme Kazançları, En Küçük Kareler Yöntemi, Beklenmeyen Dış Etki

I would like to dedicate my thesis to my loving father and mother.

ACKNOWLEDGMENTS

I would like to express my deep gratitude to Prof. Dr. M. Kemal Özgören, my supervisor, for his guidance, contribution to me for overcoming obstacles and useful critiques of this thesis. Last, but the most, I would thank him from my all heart for allowing me to gain self-confidence.

I would like to deliver my appreciations to Assoc. Prof. Dr. Senih Gürses and Mr. Emre Akçay for their help in conducting my experiments.

I am particularly grateful for the enthusiastic encouragement and support given by Prof. Dr. Metin Uymaz Salamcı.

My thesis committee members Prof. Dr. Kemal Leblebicioğlu, Assoc. Prof. Dr. Yiğit Yazıcıoğlu and Asst. Prof. Dr. Ergin Tönük are greatly acknowledged for their valuable key suggestions.

Finally, I would like to thank to my parents for their everlasting support, patience and love. They have always and forever my heartfelt thanks.

TABLE OF CONTENTS

ABSTRACT v

ÖZ vii

ACKNOWLEDGMENTS x

TABLE OF CONTENTS xi

LIST OF TABLES xvii

LIST OF FIGURES xix

LIST OF ABBREVIATIONS xxiii

CHAPTERS

1 INTRODUCTION 1

1.1 Motivation 2

1.2 Hypotheses 3

1.3 Brief Summary of the Thesis Background 5

1.4 Thesis Contributions 8

1.5 Thesis Outline 9

2 PHYSIOLOGICAL BACKGROUND 11

2.1 Key Terms Related with Balance-Recovery 12

2.1.1 Balance 12

2.1.2 Automatic Postural Responses 13

2.1.3 Postural Strategies 15

2.1.4 Postural Synergies 19

2.1.5 Relation between postural strategies and postural synergies 22

2.2 The Main Physiological Elements Participating in Human Postural Control 23

2.2.1 The Central Nervous System 23

2.2.2 The Peripheral Nervous System 24

2.2.3 The Musculoskeletal System 25

2.2.4 Sensory System: Somatosensory, Vestibular and Visual Contributions to Postural Control 25

2.2.5 Sensory Integration and Sensory Re-weighting . . 26

3 THE RELEVANT BALANCE CONTROL THEORIES 29

3.1 To Understand the Neural Control of Movement 30

3.1.1 Feedback Control of Movement 31

3.1.2 The Most Appropriate Simple Model for Human Postural Control 31

3.2 Current Studies 35

3.2.1 Examples of Experimental Studies 36

3.2.2 Examples of Current Models 38

3.3 Open Questions and Challenges 45

4 EXPERIMENTAL SETUP AND BIOMECHANICAL MODEL . . . 47

4.1 Experimental Setup 48

4.1.1 Support-Surface Tilt Platform 48

4.1.2 Sensors 51

4.2 Experimental Protocol 54

4.2.1 Key Ideas about Experiment Protocol 55

4.2.2 Attained Experimental Protocol 59

4.3 Biomechanical Model 60

4.3.1 Key Ideas about Model 61

4.3.2 Limitations, Simplifications and Assumptions . . . 62

4.3.3 Mathematical Representation of Basic Biomechanical Model for Human Standing on a Tilt Platform 62

5 PROPOSED CONTROL LAW TO MODEL AUTOMATIC POSTURAL RESPONSES 65

5.1 Literature Review 67

5.1.1 Why is the PD Control Strategy? Why is not Optimal Control? 67

5.1.2 Time-varying Feedback Gains 69

5.1.3 Difference between the Actual and Desired Body Configuration 71

5.2 Physiological Basis of Proposed Control Law 73

5.3 The Results of Examination of Experimental Data 75

5.3.1 Behavioral Patterns; Individual Specificity for the Balance-Recovery Responses. 75

5.3.2 Diversity Between Initial and Final Body Configuration 78

5.3.3 Uncorrelation Between Initial and Final Body Configuration 78

5.3.4 Arbitrariness at the Selection of the Initial and Final Body Configuration 79

5.4 Simplified Schematic Representation of CNS as a Controller 79

5.5 Definition of the Control Law Mathematically 81

5.5.1 Feedback gains are Used in Principle Axis 83

5.5.2 All Sensors and Actuators are Assumed Perfect . . 83

5.5.3 Delays are not Included the Model 84

6 COMPARISON OF SIMULATION RESULTS WITH EXPERIMENTAL DATA 85

6.1 Identification of the Feedback Gains 86

6.1.1 Least Square Method for Parameter Estimation . . 87

6.2 Determination of the Body Reference Angles 91

6.3 Verification of Investigated Control Law 93

6.3.1 With Identified Feedback Gains: Simulation with all Initial Conditions Measured during Experiments 94

6.3.2 With Identified Feedback Gains: Monte Carlo Simulations with Random Initial Conditions 98

7 THE ADAPTATION LAW FOR ADAPTIVE MODIFICATION OF AUTOMATIC POSTURAL RESPONSES 105

7.1 Literature Review 106

7.2 Neural Mechanisms Responsible for Adaptive Modification . 108

7.3 Variables which Possibly Contribute to the Adaptation Law . 109

7.4 The Canonical Correlation Analysis in Identification of the Adaptation Law 111

7.4.1 The Canonical Correlation Analysis Method 111

7.4.2 Identification of the Adaptation Law with CCA . . 115

7.5 Verification of the Adaptation Law: Simulation for All Experimental Trials 120

8 CORRELATION BETWEEN INITIAL POSTURE AND BALANCE-RECOVERY RESPONSE 125

8.1 Literature Review 126

8.2 A Correlation Rule Established by Using Classification Algorithms 129

8.2.1 Illustration of "Agile" and "Slouchy" Postures and Responses 129

8.2.2 Classification Algorithm 132

8.2.3 Decision Three 134

8.3 Statistical Evidence with Monte Carlo Simulations for Correlation between Initial Posture and Balance-Recovery Response 138

9 SUMMARY AND CONCLUSIONS 145

9.1 Summary of Thesis 146

9.2 Discussion 148

9.3 Future Prospects 153

9.4 Conclusions 153

REFERENCES 155

APPENDICES

A DERIVATION OF EQUATIONS FOR MUSCULOSKELETAL STRUCTURE 165

B THE METHOD FOR ESTIMATION OF THE MODEL INERTIAL PARAMETERS 171

C ANTHROPOMETRIC MEASURES 175

C.1 Segment Dimensions 176

C.2 Center of Masses of the Segments 177

D INITIAL AND FINAL LIMB ANGLES 179

E DETAILED ANALYSIS: COMPARISON OF SIMULATIONS AND EXPERIMENTAL DATA 183

F CANONICAL CORRELATION ANALYSIS METHOD 185

G TABULATED RESULTS OF STATISTICAL ANALYSIS FOR CCA 191

H IDENTIFICATION OF THE "AGILE" AND "SLOUCHY" INITIAL STANCE 193

CURRICULUM VITAE 199

LIST OF TABLES

TABLES

Table 2.1 The meaning of the muscle abbreviations in Fig. 2.3 18

Table 4.1 Description of Specific Locations (Adapted From [120]) 51

Table 4.2 Conducted Pre-Experiments 55

Table 5.1 Uncorrelation between initial and final body configuration 79

Table 6.1 Comparison of Subject 1 and Subject 2 according to analysis results of simulations. 97

Table 6.2 Evaluation of Monte Carlo Simulations for Subject 1 in terms of the number of repetitions 101

Table 6.3 Evaluation of Monte Carlo Simulations for Subject 1 in terms of the number of repetitions (Backward Trials) 102

Table 6.4 Evaluation of Monte Carlo Simulations for Subject 2 in terms of the number of repetitions 103

Table 6.5 Evaluation of Monte Carlo Simulations for Subject 2 in terms of the number of repetitions (Backward Trials) 104

Table 7.1 List of variables for six independent case 116

Table 7.2 Average values of ρ for all directions and all subjects 117

Table 7.3 Correlation coefficients of sixth forward trials of subject 1 118

Table 7.4 Comparison between Subjects depending on deviation from experimental data. 122

Table 8.1 Trial Numbers Classified as an "Agile" and "Slouchy". 130

Table 8.2 Training Set for Subject 2 Forward Trials 135

Table 8.3 Extracted Rules 138

Table 8.4 Algorithm for Testing the Extracted Rules by Using MCS 140

Table D.1 Initial and final limb angles for forward trials of subject 1 179

Table D.2 Initial and final limb angles for backward trials of subject 1 180

Table D.3 Initial and final limb angles for forward trials of subject 2 181

Table D.4 Initial and final limb angles for backward trials of subject 2 182

Table E.1 The analysis results of simulations of subject 1 183

Table E.2 The analysis results of simulations of subject 2 184

Table G.1 Tabulated results of statistical analysis for subject 1 191

Table G.2 Tabulated results of statistical analysis for subject 2 192

Table H.1 Subject#1, Statistics for Forward Trials 194

Table H.2 Subject#1, Statistics for Backward Trials 194

Table H.3 Subject#2, Statistics for Forward Trials 195

Table H.4 Subject#2, Statistics for Backward Trials 195

LIST OF FIGURES

FIGURES

Figure 2.1 Representation of the center of body mass, base of support and limit of stability. 13

Figure 2.2 Classification of the Postural Strategies (Quoted from [67]). 16

Figure 2.3 A conceptual framework for the emergence of strategies that are plans for action (Adapted From [39]). 17

Figure 2.4 The new muscle synergy concept (Quoted from [101]). 20

Figure 2.5 Postural Synergies in Automatic Postural Responses (Quoted from [101]). 21

Figure 2.6 Relation between postural strategies and postural synergies due to increasing external perturbation. (Quoted from [38]). 22

Figure 2.7 Descending signals from the brain stem and motor cortex initiate locomotion. (Quoted from [52].) 24

Figure 3.1 A schematic representation of the postural control system from a control theory perspective. (Quoted from [49]). 32

Figure 3.2 Peterka's Model (Adapted From [86]) 39

Figure 3.3 van der Kooij's Model (1999) (Adapted From [106]) 40

Figure 3.4 van der Kooij's Model (2001) (Adapted From [107]) 41

Figure 3.5 Kuo's Model (Adapted From [57]) 42

Figure 3.6 Yao Li and William S. Levine's Model (Adapted From [61]) 43

Figure 3.7 Park's Model (Adapted From [84]) 44

Figure 4.1 General View of Support-Surface Tilt Platform [75] 48

Figure 4.2 Motion Profile 50

Figure 4.3 Presented Motion Profile in [97] 50

Figure 4.4 Wearable motion tracker sensors (adapted from [120]) 52

Figure 4.5 Measurement Device and Parameters 52

Figure 4.6 Proposed model for a subject standing on a tilt platform. 60

Figure 5.1 Comparison between PD and optimal control in terms of time delay (Quoted from [49]). 68

Figure 5.2 A simple model of proposed neural pathways involved in the cortical control of short, medium and long latency automatic postural responses to external perturbations. (Quoted from [47]) 74

Figure 5.3 Behavioral pattern of Subject 1 76

Figure 5.4 Behavioral pattern of Subject 2 77

Figure 5.5 Simplified schematic representation of CNS as a controller. 81

Figure 5.6 Simplification of the balance-recovery reaction as a block diagram. 81

Figure 6.1 Scheduled Characteristics of the Control Parameters for Selected Trial (Using LS method). 92

Figure 6.2 The results of the estimated control parameters in terms of fitting the experimental data. 94

Figure 6.3 Automatic Postural Responses of Subject 1 on the Forward and Backward Trials. 95

Figure 6.4 Automatic Postural Responses of Subject 1 on the Forward and Backward Trials. 96

Figure 6.5 Monte Carlo Simulations for Subject 1 (Forward Trials). 100

Figure 6.6 Monte Carlo Simulations for Subject 1 (Backward Trials). 102

Figure 6.7 Monte Carlo Simulations for Subject 2 103

Figure 6.8 Monte Carlo Simulations for Subject 2 (Backward Trials). 104

Figure 7.1 The General Structure of Canonical Correlation Analysis [56]. . . . 114

Figure 7.2 Comparison of gains estimated by using CCA with gains estimated by using LS. 119

Figure 7.3 Illustration of control inputs estimated by using experimental data, LS method and CCA method. . . . 119

Figure 7.4 Simulations of Automatic Postural Responses of Subject 1 by using CCA. . . . 121

Figure 7.5 Simulations of Automatic Postural Responses of Subject 2 by using CCA. . . . 121

Figure 7.6 For Sixth Forward Trials: Comparisons of Simulations obtained by using LS and CCA. . . . 122

Figure 8.1 This figure is a reproduction of Fig.3 in [3]. Stick figure shows link movements in response to different rotational perturbations in the pitch and roll planes. . . . 127

Figure 8.2 "Agile" and "Slouchy" Postures and Responses of Subject 1 for Forward Trials. . . . 130

Figure 8.3 "Agile" and "Slouchy" Postures and Responses of Subject 1 for Backward Trials. . . . 131

Figure 8.4 "Agile" and "Slouchy" Postures and Responses of Subject 2 for Forward Trials. . . . 131

Figure 8.5 "Agile" and "Slouchy" Postures and Responses of Subject 2 for Backward Trials. . . . 132

Figure 8.6 Decision Tree Showing "Agile" and "Slouchy" Postures together with the Related Terminology. . . . 136

Figure 8.7 Averages of Agile and Slouchy Trials for Subject 1 . . . 139

Figure 8.8 Averages of Agile and Slouchy Trials for Subject 2 . . . 139

Figure 8.9 Monte Carlo Simulations for Testing the Extracted Rules for Subject 1, Forward Trials . . . 141

Figure 8.10 Monte Carlo Simulations for Testing the Extracted Rules for Subject 1, Backward Trials . . . 141

Figure 8.11 Monte Carlo Simulations for Testing the Extracted Rules for Subject 2, Forward Trials . . . 142

Figure 8.12 Monte Carlo Simulations for Testing the Extracted Rules for Subject 2, Backward Trials . . . 143

Figure A.1 Proposed model for a subject standing on a tilt platform. 165

Figure A.2 The geometric features of the tilt platform. 166

Figure B.1 Body Segment Parameters (Adapted from [121]) 171

Figure B.2 Regression Coefficients (Adapted from [121]) 173

Figure B.3 Regression Coefficients (Adapted from [121]) 174

Figure C.1 Body segment lengths expressed as a fraction of body height H (Adapted from [116]) 176

Figure C.2 Body segment lengths expressed as a fraction of body height H (Adapted from [116]) 177

Figure H.1 Weka Output for decision three, Forward Trials of Subject 1 196

Figure H.2 Weka Output for decision three, Backward Trials of Subject 1 . . . 196

Figure H.3 Weka Output for decision three, Forward Trials of Subject 2 197

Figure H.4 Weka Output for decision three, Backward Trials of Subject 2 . . . 197

Figure H.5 Visualized Decision Tree by Weka, Forward Trials of Subject 2 . . 198

LIST OF ABBREVIATIONS

CNS	Central Nervous System
PD	Proportional-Derivative
θ_{ref}	The Set of Reference Angles
DoF	Degree of Freedom
CoM	Center of Mass
BoS	Body of Support
LoS	Limit of Stability
PID	Proportional-Integral-Derivative
EoM	Equation of Motion
M_{sh}	Mass of Shank
M_{th}	Mass of Thigh
M_{tr}	Mass of Trunk
I_{sh}	Mass Moment of Inertia of Shank
I_{th}	Mass Moment of Inertia of Thigh
I_{tr}	Mass Moment of Inertia of Trunk
d_{sh}	Length of Shank
d_{th}	Length of Thigh
d_{tr}	Length of Trunk
q_{sh}	Length of the CoM of Shank from Ankle Joint
q_{th}	Length of the CoM of Thigh from Knee Joint
q_{tr}	Length of the CoM of Trunk from Hip Joint
T_A	Ankle Joint Torque
T_K	Knee Joint Torque
T_H	Hip Joint Torque
θ_{sh}	Angles of the Shank Deviated from the Vertical Axis
θ_{th}	Angles of the Thigh Deviated from the Vertical Axis
θ_{tr}	Angles of the Trunk Deviated from the Vertical Axis
θ_p	Specified Disturbance Angular Position Deviated from Horizontal Axis

LS	Least Square
MCS	Monte Carlo Simulation
CCA	Canonical Correlation Analysis

CHAPTER 1

INTRODUCTION

There are, very complex and not understood clearly yet, control laws for driving the movement of the human in daily life. Very likely, these laws are very different for three categories of human daily activity. The classification of human activity can be expressed as follows:

- The maintenance of the specified static posture, for example, lying down, sitting or standing.
- Voluntary movement, for example, bringing a glass of water to one's mouth.
- The reaction to an external disturbance, for instance, a trip, a slip or a push.

In this thesis, the control law, which is responsible for the reaction to an external disturbance, is tried to be understood. The following sections provide a general overview of the topics studied in this thesis. This chapter involves the following sections which are titled as motivation, hypotheses, brief summary of the thesis, thesis contributions and thesis outline.

1.1 Motivation

In this study, it is attempted to understand how the balance-recovery reactions are realized. The results of the this study may provide benefits in terms of some humanistic and social aspects. Understanding of the postural control clearly is vitally important for early and effective diagnosis of balance disorders. For instance, falls, which are the natural result of various balance disorders, can be prevented. In this case, the life quality of older people (the largest falling group) can increase; the health care costs can decrease in the country, therefore social welfare can increase. In more specific perspective, revealed results from studies about balance-recovery reactions can be used in neuroprosthetics and artificial balancers.

There are numerous unresolved important questions to achieve the above-mentioned general purpose. In daily life, humans are capable of maintaining postural stability over a wide range of complex scenarios. How can the central nervous system select different postural control strategies depending on these scenarios? How are postural strategies and postural synergies depending on these strategies formed by central nervous system (CNS)? How do environmental content and initial body configuration affect the selection of the postural strategies and synergies?

1.2 Hypotheses

This study is based on testing three basic hypotheses:

1. It is widely known that information about the body orientation and motion is used to detect the postural instabilities. In the same way postural stability responses are generated by CNS using the same bodily and environmentally sensory feedback. The generation of the postural responses by CNS are realized by activating of the selected multiple muscles. At the same time, during the balance-recovery process, selection and coordination of the multiple muscles are modulated by CNS. In this manner, desired body configuration is reconstructed based on new environmental conditions. Widely accepted theory given above can be expressed with the known control terms. The results of the experiments have supported this theory.

   The first hypothesis of this thesis claims that the proportional-derivative (PD) control can mimic balance-recovery reactions that are generated by CNS. Proposed PD control law involves time-varying adapted parameters. It appears that CNS has adapted the appropriate upright posture and the proportional and derivative feedback gains according to an adaptation law.

2. The central nervous system uses the muscle co-activation patterns to keep and recover balance standing upright. These mentioned patterns of muscle activations are referred to as postural synergies and due to a common theory, they are used and modulated by CNS to postural adjustments. According to this theory, the modulation of the postural synergies depend on the bodily and environmentally acquired sensory information transmitted to CNS.

   Therefore, it can be hypothesized that the gains of the motor command to the muscles for generating torque can be expressed as a function of the most basic sensory feedbacks and the most observable environmental changes.

   This hypothesis can be clarified with the following explanation. It is known that balance-recovery reactions arise when human beings are stimulated with sudden external perturbations. Although these arisen responses are quite rapid and sudden, it is widely acknowledged theory that they have to adapt to changing conditions to be functional. It is impossible to identify an unchangeable, definite rule for this adaptation. However, it is possible to identify a function which involves the relative contributions of the changing variables.

It is suggested that the adaptation law depends on the difference between the actual and reference angular position, on the angular velocity of the body limbs and on the direction and amount of the perturbation substantially.

3. There is an evident correlation between the initial body configuration and the subsequent pattern of balance-recovery reaction to a sudden tilt disturbance. This relation between initial posture and balance-recovery response pattern can be systematized as a rule by using classification algorithms.

1.3 Brief Summary of the Thesis Background

In daily life, frequently, the balance-recovery action is required to protect the body against external disturbance acting suddenly. For instance, the reaction of the standing upright passenger in the suddenly accelerated vehicle, slipping old people on wet, icy or compliant surfaces; or pushing the kids by their playmates during the game can be exemplified. While standing upright is already a very complicated control problem, understanding of how balance recovery action is achieved under the effect of a sudden external disturbance is very important and open problem. The primary scope of this thesis is to find out the control law which is used by humans to keep their balance under the effect of external disturbances

The effort to understand how the balance-recovery reactions are realized has been questioned for the last 30 years. How does the CNS manage the body to stay in the limit of stability and how does it decide to change the current strategy? When the studies trying to understand these questions are reviewed, two main approaches were seen. The first approach is the perturbation of support surface and the second basic approach is that subjects are pushed from their waist or back. As a result of this review, it is understood that the perturbation is absolutely required for the investigation of the balance-recovery reactions.

Considering that the infinite number of possibilities for application center and size of disturbance, it is impossible to examine experimentally. The most efficient way to cope with this problem is thought that the solution is model-based working on the problem. A large number of model-based simulations can give an insight about the solution. Experimental and model-based studies have nested with and supported each other.

Determination of the experimental procedure diligently to meet all requirements should be considered as the most important key point for this study. At very short time collecting various type and meaningful data is necessary. Because the transition phase is extremely small (approximately 500 ms). Therefore, the whole body kinematic data and force plate data are collected.

The main question of this thesis is what and how is done in order to recover sudden emerging disturbances. When this question is tried to be answered by using the simplest and the most straightforward model, inverted pendulum models suggest themselves immediately because of their simplicity. When worked with large disturbance, researchers prefer the models at least with 2, 3 and even 4 degrees of freedom.

Some studies about the control model of the balance-recovery process propose optimal control. In these studies, optimal state estimation is used as an internal model for decision-making about body orientation and processing sensory information. The most likely, the CNS (Central Nervous System) can behave optimally by using redundant sets of both actuators and sensors. However, there are not enough valid arguments about the possible optimization criteria. Besides, it does not seem plausible that the CNS can handle complicated algorithms with heavy computational loads, e.g., solving matrix Riccati equations, required in general by optimal control laws. Therefore, in this thesis, the control law is chosen as the PD (proportional-derivative) control. This control law is thought to be the most probable basic structure. Additionally, it is as simple as possible, and it is compatible with the physiological facts and it is sufficient to simulate the behavior of the system. This model fits the physiological facts because the muscle spindle is the sensory organ in the muscle, and it senses the muscle length and the changing rate (derivative) of the muscle length. This physiological fact naturally leads to the conjecture of the PD control. On the other hand, there is not any clue about the existence of an organ that works as an error integrator. Therefore, due to the physiological unrealizability of the integral control action, the PID control is not conjectured in this thesis.

Human balance control is a rather difficult topic to study, because of the parametric variability of the postural control strategy. The parameters of the postural control strategy can change depending on many factors such as redundancies, nonlinear features of the sensing system, uncertainties, etc.

Redundancies in the human body is a problem on its own. Additionally, postural control involves nonlinear feature at various different levels. Some recent studies [60, 61] take into account the nonlinear character of the system and importance of sensory and motor delays. However, these attempts have not produced reasonable results. The nonlinear features create huge complexity in the model. Nonetheless, they create a very small contribution to understand of the basis of human balance control. Additionally, it is impossible to take all nonlinear features into consideration.

Furthermore, uncertainties in the sensory system are at least as important as the nonlinear character of the sensory system. Source of uncertainty can be both random processes and nonrandom processes [82]. For instance, the sensory organs such as somatosensory, proprioceptive, vestibular, and visual are the source of random errors. On the other hand, ambiguities, such as lifting an unknown weight, serve as a typical example of nonrandom error. The source of the ambiguity can be thought as CNS has the lack of ability to predict the weight accurately. Therefore, it causes to be generated more or fewer forces at the muscles. However, some recent studies about uncertainty claim that the central nervous system has knowledge of its own sensory and motor uncertainty [82]. As well as, they also state that CNS learns to cope with these uncertainties over time. Therefore, for the sake of simplicity, all sensors and actuators can be assumed as perfect in the model.

Some other recent studies [51, 54, 84] have introduced the variable gain coefficient and full state feedback in parallel with physiological findings. In these studies, variability of gain coefficients has been investigated at the different conditions that are the support surface perturbations and pushing from the back of the body. However, they have only shown that variability of gain coefficients are only correlated with the magnitude of the perturbation. It is also known that CNS can act differently at changing environmental condition via sensory reweighting. Therefore, adaptation is the other key point of these studies. In this case, the transition phase of the body responses after the sudden external disturbance has to be analyzed for revealing the existence of the adaptation. It is thought that it is extremely important for modeling and understanding of the balance-recovery.

In summary, for the understanding of human balance-recovery control, it must be thought about human-environment interaction, skeletal anatomy, physiological mechanism that generates muscle forces, sensory inputs and central processor with an unknown control law. This multiple part problem can be handled with very different engineering approaches as mentioned above. This complexity is a result of the nature of the problem. There are many questions with no answer about how automatic postural responses are realized. However, each new finding triggers new developments in the medical and robotic studies.

1.4 Thesis Contributions

The physiological controller model that is revealed for description of the automatic postural responses is an important contribution all on its own. The validity of this control law has been demonstrated with the matching of the results of the simulations and the experiments closely enough. However, the most important contribution of this thesis is that a functional relationship about how time-varying gains are managed by CNS can be revealed.

To uncover of the evident correlation between the initial body configuration and the subsequent pattern of balance-recovery reaction can be regarded as the second most important contribution.

In addition to these two major contributions, it should be mentioned two more important findings that are obtained from the examination of the experimental data. First is an existence of the individual behavioral patterns that appear during balance-recovery reactions. According to observations, these patterns are related to perturbation types, magnitudes, and musculoskeletal geometry. Second important observation is that initial and final body configuration after the perturbations are always different for all trials and each subject. However, this configuration difference cannot be identified as a relationship between the position of the body segments in the initial and final posture.

1.5 Thesis Outline

This dissertation is organized into nine chapters. Following this introduction is the physiological background about human automatic postural responses. In this chapter, key terms related with balance-recovery such as postural strategies, postural synergies, sensory integration and sensory reweighing are explained. Additionally, the main physiological elements participating in human postural control are briefly reviewed, including the central nervous system, the peripheral nervous system, and the musculoskeletal system. Chapter 3 reviews the relevant balance control theories, experimental studies, and the existing modeling work. At the beginning of this chapter, information about the physiological background of neural control of movement is introduced. In Chapter 4, experimental setup and protocol are described. Furthermore, a simple biomechanics model using a 3 DoF inverted pendulum is derived. These four chapters are introductory parts of the thesis.

Chapter 5 presents a control law to model automatic postural responses against sudden external disturbance. In that chapter, at the same time, the proposed control model is underlined depending on the diversity and similarity of previous studies and its physiological basis.

In Chapter 6, the proposed control model to balance-recovery reactions is verified by using simulations. At the beginning of this chapter, least squares method, which is used for parameter estimation, is described. After the explanation of the method, validation of the estimated time-varying feedback control gains and upright reference position (θ_{ref}) is tested with their achievement to fit the experimental data. Simultaneously, simulations and experimental results are compared. Besides, simulations are repeated to test whether it is possible to obtain the individual behavioral pattern characteristics by using random initial body configurations.

Chapter 7 explores the adaptation law for adaptive modification of automatic postural responses. Firstly, at the beginning of the chapter, experimental evidence for several potential neural mechanisms responsible for adaptive modification of automatic postural responses are reviewed. As a result of this review, variables that possibly contribute to the adaptation law are determined. Afterward, adaptation law is identified by using the canonical correlation analysis. Finally, proposed adaptation law is verified by using simulations.

Chapter 8 demonstrates the correlation between the initial body configuration and the subsequent pattern of balance-recovery reaction to a sudden tilt disturbance. In continuation of the chapter, the relation between initial posture and balance-recovery response pattern is systematized as a rule by using classification algorithms. This chapter is completed with the Monte Carlo simulations as a statistical evidence.

Finally, in Chapter 9, this dissertation is summarized and concluded. At the same time, the main findings and results are discussed widely. This chapter is closed by considering further prospects of this research field.

CHAPTER 2

PHYSIOLOGICAL BACKGROUND

The scope of this thesis is to propose a realistic model for the very sensitive and flexible postural control system to cope with unpredictable external disturbance. Postural control is a continuous effort for providing postural equilibrium and postural orientation[38]. Postural equilibrium includes two main obligatory tasks to maintain balance. These tasks are coordination of sensory integration and coordination of motor strategies. Whereas, postural orientation includes the correct relative positions of body with respect to gravity, the support surface, visual environment and other sensory reference frames[38]. At this point, it is a requirement to give some definitions related with the postural control. Therefore, in this chapter, definitions of some important terms mentioned above are given and their relevance of the balance-recovery responses are discussed. This chapter is organized into two sections. They are titled as key terms related with balance-recovery and the main physiological elements participating in human postural control.

2.1 Key Terms Related with Balance-Recovery

In this section, four key terms are explained. These terms are respectively balance, automatic postural responses, postural strategies and postural synergies. Additionally, another topic is titled as relation between postural strategies and postural synergies. All key terms involve various secondary terms and their definitions. For sake of understanding easily, all definitions are discussed as simple as possible. At the same time, related figures with definitions are given to strengthen the meaning.

2.1.1 Balance

The extended definition of ***balance*** combines conscious and automatic motor controls, conscious and unconscious brain processes, with sensory information from the visual, inner ear vestibular and proprioceptive systems[80]. However, the more technical and simple definition of the balance is the ability to maintain the position of the center of body mass (CoM) over its base of support (BoS), or within stability limits[38]. The related terms such as center of body mass, base of support and limit of stability (LoS) can be described as follows.

The center of mass (CoM) is a hypothetical point in or near the body where total body mass is concentrated. Center of mass of the body is calculated using the locations and masses of individual body segments. Naturally, it depends on body build, posture, gender, and age. It is assumed that the center of mass location is just anterior to the lower lumbar/upper sacral vertebrae for an average individual standing erect with arms at the side [38].

Base of the support (BoS) is an area where body contacts the environment and allows supporting ground reactions forces to be generated [85].

Limits of stability (LoS) is the greatest distance in any direction that a person can lean away from a mid line vertical position without falling, stepping, or reaching for support [22]. Limit of stability may be represented with a hypothetical cone as shown in Fig.2.1. According to [37], equilibrium is not a particular position but a space determined by the size of the support base (the feet in stance) and the limitations on joint range, muscle strength and sensory information available to detect the limits. In [37], it is also stated that the CNS has an internal representation of this cone of stability that it uses to determine how to move to maintain equilibrium.

Following these definitions, it has to be discussed dynamic equilibrium under the effect of the external disturbance. In that context, the movement of the CoM is taken into account. This fact has been expressed in [83] with following explanations. Classical definition of the balance, which is the ability to maintain the position of CoM over its BoS, does not guarantee maintenance of balance. For example, the body can be dynamically unstable when it moves with sufficient horizontal velocity. On the contrary, body can be dynamically stable even though the location of the CoM is outside the static stability limits of the BoS.

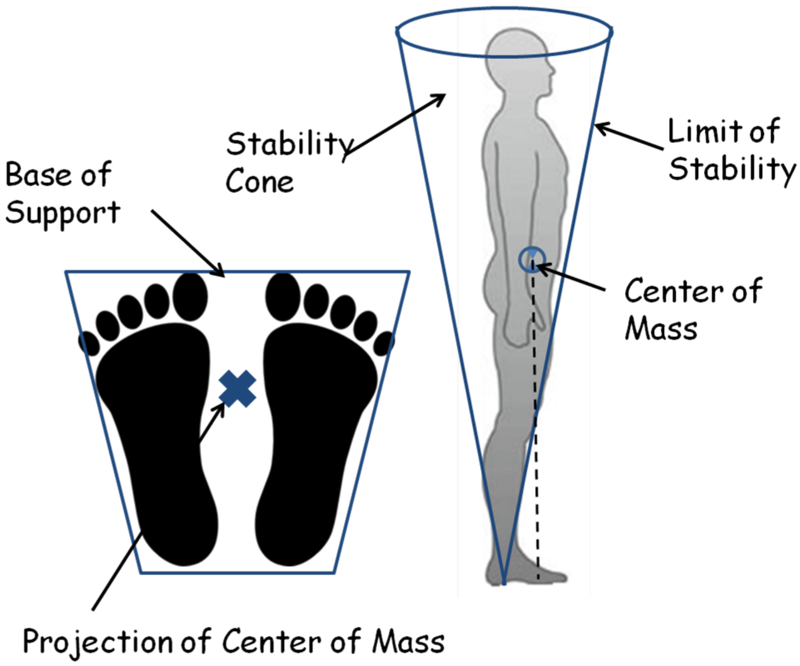

Figure 2.1: Representation of the center of body mass, base of support and limit of stability.

2.1.2 Automatic Postural Responses

Balance-recovery reactions of the body against unexpected disturbances are referred to as automatic postural responses. The definition of the automatic postural responses is given in [1] as follows.

This part is directly quoted from [1]

The automatic postural response is a muscular response to a postural perturbation that is thought to be mediated by brainstem centers. The response can be modulated in amplitude by many factors, including habituation, anticipation, prior experience, etc. However, it is "automatic" because it cannot be completely suppressed and is therefore neither completely fixed nor completely voluntary.

Balance recovery reactions depend on stereotyped postural responses, which are referred to as postural strategies. In humans, these responses arise approximately ~100 ms later from applied external disturbance. Due to this latency, automatic postural responses are slower than the stretch reflexes but faster than voluntary postural reactions [38].

This part is directly quoted from [2]

The stretch reflex is a reflex that causes a muscle to contract and shorten after it is stretched. The elongation of a muscle, usually by an external perturbation is encoded by the firing of muscle spindle receptors within the muscle.

Although the definition of the muscle spindle may be derived from the stretch reflex definition, for the sake of clarity, it can be given again as follows.

This part is directly quoted from [113]

Muscle spindles are sensory receptors within the belly of a muscle that primarily detect changes in the length of this muscle.

The stretch reflex is very important in posture. It is very useful for maintaining proper posturing. The stretch reflex gives very quick response and it can cope with a slight lean to either side causes a stretch in the body segments. However, it cannot generate enough force to maintain body posture against sudden external perturbation [38]. Therefore, in nature, automatic postural responses involve responses in muscles that are shortened, as well as stretched [100].

It is widely acknowledged that automatic postural responses can be modulated in amplitude by many factors, including habituation, anticipation, prior experience, etc. For instance, it has been found that its modulation is affected some emotional factors such as fear, anxiety and depression [14, 15]. Anticipation have also been studied in [19]. There is reciprocity between central set and sensorimotor systems.

Automatic postural responses mainly can be expressed in terms of postural strategies and postural synergies. Their definitions are given below, respectively. They also can be expressed with the following analogies. Postural strategy can be thought as "plan of action" and postural synergies can be expressed as "implementation plan".

2.1.3 Postural Strategies

Postural strategies are specific patterns of muscle activation, joint torque, joint rotation and/or limb movement. It is needed to evoke the balance with an external perturbation for existence of postural strategies. They can be initiated by multiple sensory inputs. Their existence protects the body against fall. They also provide to recover the balance. Triggered by multiple sensory inputs, they involve polysynaptic spinal and supraspinal neural pathways and are highly adaptable to meet functional demands [67].

Strategy selection and modulation depend on four main features as seen the following items quoted directly from [67]:

i. The features of the perturbation (timing, direction, magnitude, predictability),

ii. The individual factors (affect, arousal, attention, expectations, prior experience),

iii. Ongoing activity (cognitive or motor) and

iv. Environmental constraints (on reaction force generation and limb movement).

Postural Strategies for Responding to Unexpected External Disturbance

When it is thought about the daily life activities, it is not difficult to reach a result that very complicated muscle activation is needed to maintain the upright balance. It is widely accepted that postural strategies are used to cope with these difficulties, especially against unexpected external disturbance. For this purpose, CNS has to continuously control the interrelation between the CoM and the BoS [83]. This control can be realized with two main ways: first is deceleration of the CoM and second is changing of the BoS. Correspondingly, postural strategies are classified as follows. They can be seen in Fig.2.2

i. Fixed-support (feet-in-place) strategies, in which the BoS is not altered.

ii. Change-in-support reactions, in which the BoS is altered via rapid stepping or by reaching movements of the limbs toward nearby support points [66].

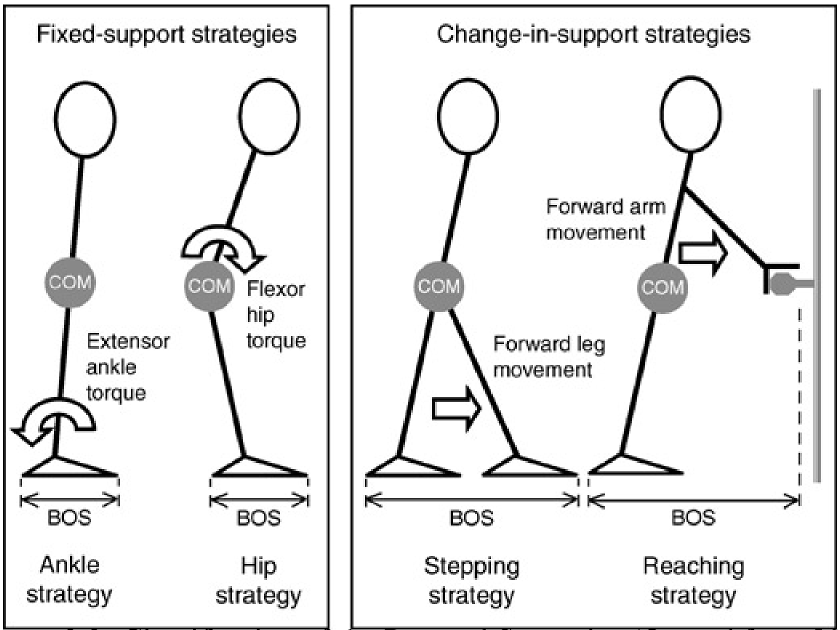

Figure 2.2: Classification of the Postural Strategies (Quoted from [67]).

For the emergence of postural strategy, sensory information about the body orientation and motion is required, especially when balance is disturbed unexpectedly by a sudden perturbation. This external disturbance can be defined as a force applied to the body or motion of the support surface. The mentioned sensory information is used to detect instability and to generate appropriate stabilizing responses.

Postural strategies relate to multiple sensory inputs such as somatosensory, vestibular and visual. Additionally, postural strategies are highly adaptable than stereotyped short-latency reflexive responses. For instance, when the perturbation involves the movement of the support surface, responses may involve ankle muscle spindles, on the contrary, when the perturbation involves a force applied to the upper body the role of the vestibular system and/or somatosensory inputs from other joints cannot be ruled out [4].

Strategies are emphasized here because it is claimed that strategies are emergent neural control processes providing an overall "plan for action" based on the behavioral goals, environmental context, and particular task or activity [39]. Selection of strategy is changeable related to magnitude and speed of disturbance.

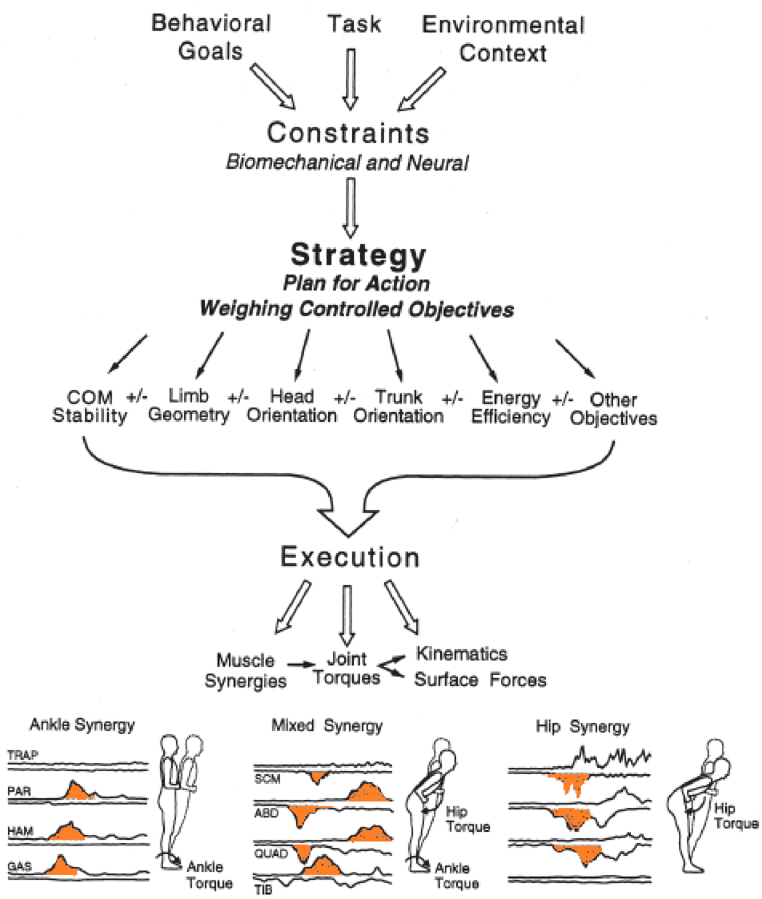

Figure 2.3: A conceptual framework for the emergence of strategies that are plans for action (Adapted From [39]).

Biomechanically, the upright human body is redundantly actuated. At this point, there is a fact that it can be probable to construct many combinations of muscle torques at the various joints. These different combinations could be used to re-establish postural equilibrium against a given postural perturbation. According to common acceptance, CNS uses this redundancy for the benefit to simplify the control problem. During the life cycle, each individual has constructed a finite number of specific response patterns or weighted combinations of these patterns. Their classification is discussed above previously such as fixed-support and change-in-support strategies. At the scope of this thesis, only fixed-support strategies, which are divided into subcategories as

Table 2.1: The meaning of the muscle abbreviations in Fig. 2.3

Abbreviation	Meaning
TRAP	trapezius muscle
SCM	sternocleidomastoid muscle
PAR	lumbar paraspinal muscles
ABD	rectus abdominis muscle
HAM	hamstring muscles
QUAD	rectus fernoris muscle
GAS	gastrocnemius muscles
TIB	tibialis anterior muscle

ankle, hip and mixed strategies, are handled.

i. Ankle strategy. The CoM is moved by rotating the body as an approximately rigid mass about the ankle joints, which is also referred to as *ankle strategy*. This strategy rotates the body by exerting torque onto the ankle joints while stabilizing the proximal knee and hip joints. However, because the feet are much shorter than the body height, the ability to generate torque about the ankles is limited. Hence, the ankle strategy is effective only when CoM movements are relatively slow and the CoM is positioned well within the LoS perimeter [80, 42].

ii. Hip strategy. The CoM moves by rapidly rotating the hip joints, which is referred to as *hip strategy*. This strategy relies on the inertia of the trunk rapidly accelerating in one direction to generate a horizontal shear force against the support surface and move the CoM in the opposite direction. Because there are no biomechanical limitations on the horizontal shear force, hip strategy is effective when the CoM is positioned near the LoS perimeter. However, conditions that limit horizontal force, such as standing on ice, render the hip strategy ineffective [80, 42].

iii. Mixed strategy Mixed strategies contain all components of both ankle and hip strategies such as early activations in both dorsal ankle and ventral trunk muscles.

Modulation of Strategies

Postural strategies are highly modifiable. The most basic physiological base of *automatic postural response* is the early ankle activation. This early activation is not highly modifiable. Nonetheless, the automatic postural response is not a stereotyped response. The magnitude of the activation is scaled according to the direction and the magnitude of the perturbation. Additionally, it is influenced by the predictability of the perturbation, and the individual factors [67].

2.1.4 Postural Synergies

The central nervous system uses the postural synergies to keep and recovery balance standing upright. Basically, postural synergy is defined as a preferred muscle co-activation pattern. Each postural synergy represents a pattern of muscle activation across many muscles. Postural behaviors arise by using different combinations of postural synergies. The main advantage of the postural synergies is to eliminate the requirement of selecting and coordinating multiple muscles across the body independently. Postural synergies are the way for simplification of the neural control task. The relation between postural strategy and postural synergy can be defined as follows.

A postural strategy defines the general objectives included in the keeping of balance. According to context, postural strategies can change. The context depends on the postural configuration and the particular postural task performed. Postural synergies define the muscle activation patterns that are used by the nervous system to implement various postural strategies[101].

It can be shown in Fig.2.4, according to new muscle synergy concept, more than one muscle synergy can be activate during a postural response and each muscle can also be activated by more than one synergy. Many muscle activation patterns can be generated by adjusting the magnitude of the neural command signals to just a few muscle synergies [100, 101].

The neural mechanism and origin of muscle synergies for postural control remain unknown. It is claimed that muscle synergies are encoded within the neural control hierarchy and formed in the brainstem. Moreover, it is thought that it may also be task dependent.

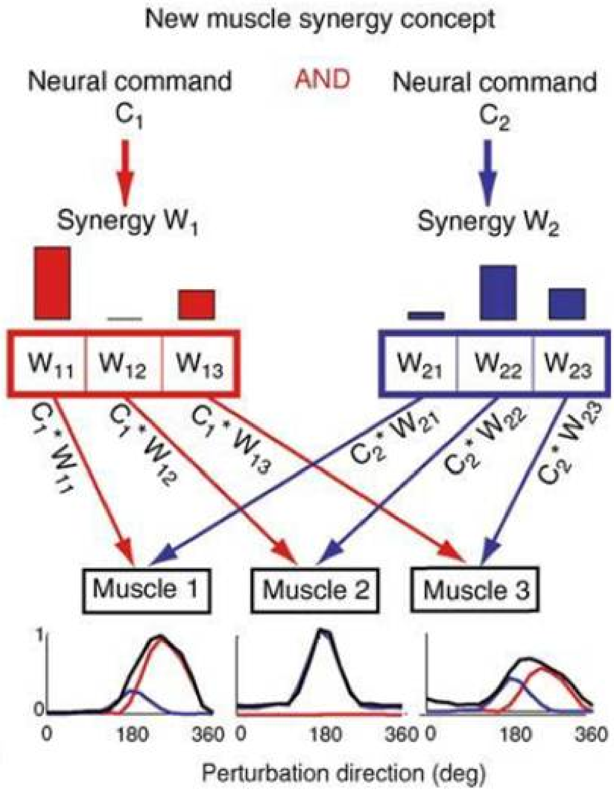

Figure 2.4: The new muscle synergy concept (Quoted from [101]).

Postural Synergies in Postural Control

According to the observations of different muscle activation patterns, moveable support surface platform can be shifted either forwards or backwards. As a result of this process, two different postural synergies can be seen as in Fig.2.5a. Similarly, during postural responses to perturbations in different directions, many varying patterns of muscle activation are generated because of the activation of the multiple muscles across the body as in Fig.2.5b. The muscle activation occurs after the platform motion begins, but before the center of mass moves appreciably, with a latency of around –100 ms. This latency is about twice the stretch reflex latency for distal muscles and evokes a much larger response than the stretch reflex [101]

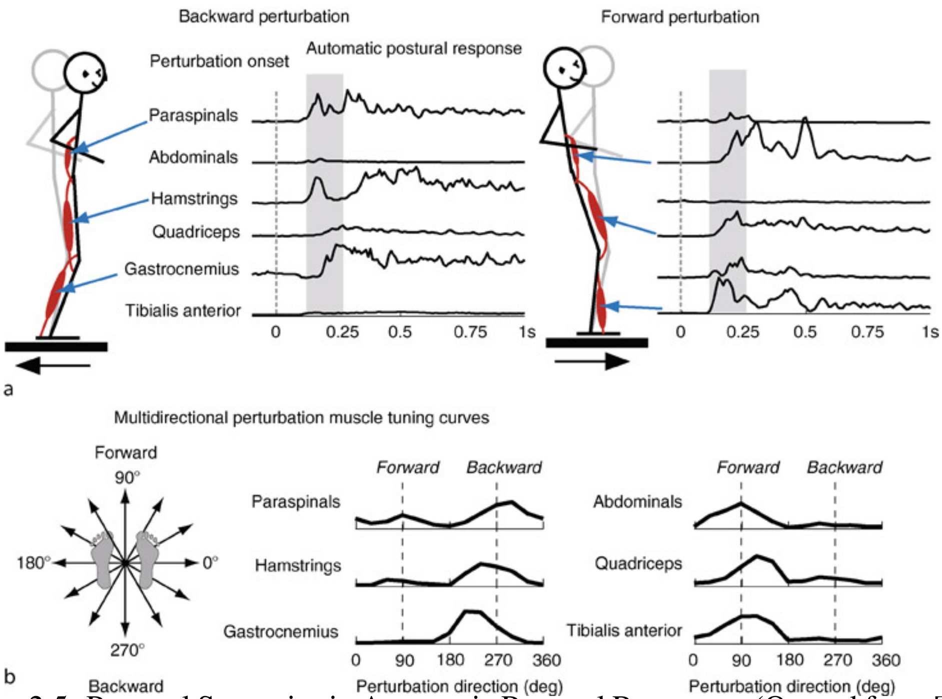

Figure 2.5: Postural Synergies in Automatic Postural Responses (Quoted from [101]).

Neural Mechanism of Muscle Synergies in the CNS

Today it is now understood that postural synergies cannot be explained just by reflexes acting in response to muscle stretch. It has been shown that the same muscle synergies can be initiated by stretching the muscles with different perturbations. It is widely believed that muscle synergies are related to global variables such as the direction of CoM displacement caused by the perturbation [101].

How postural synergies are encoded in the nervous system is not known. However, brainstem is known that it has the important role at the maintenance of postural orientation and equilibrium. The studies on the neural circuitry of the spinal cord imply that neural mechanisms producing postural synergies reside in brainstem. Moreover, studies on patients who suffer from postural impairments due to lesions in higher brain centers show different fact. These patients have the ability to generate postural synergies that are similar to control subjects, but they have difficulty changing the muscle synergy that is activated when perturbation conditions change. The theory of postural synergies is widely accepted that there is the role of various nervous system structures in postural control [101].

2.1.5 Relation between postural strategies and postural synergies

Postural synergies define the muscle activation patterns that are used by the nervous system to implement various postural strategies. Depending on the increasing of perturbation, postural strategies and postural synergies are adjusted. It can be seen in Fig.2.6, several muscles activated in the ankle, hip and mixed ankle-hip postural muscle synergies in response to forward sway perturbations.

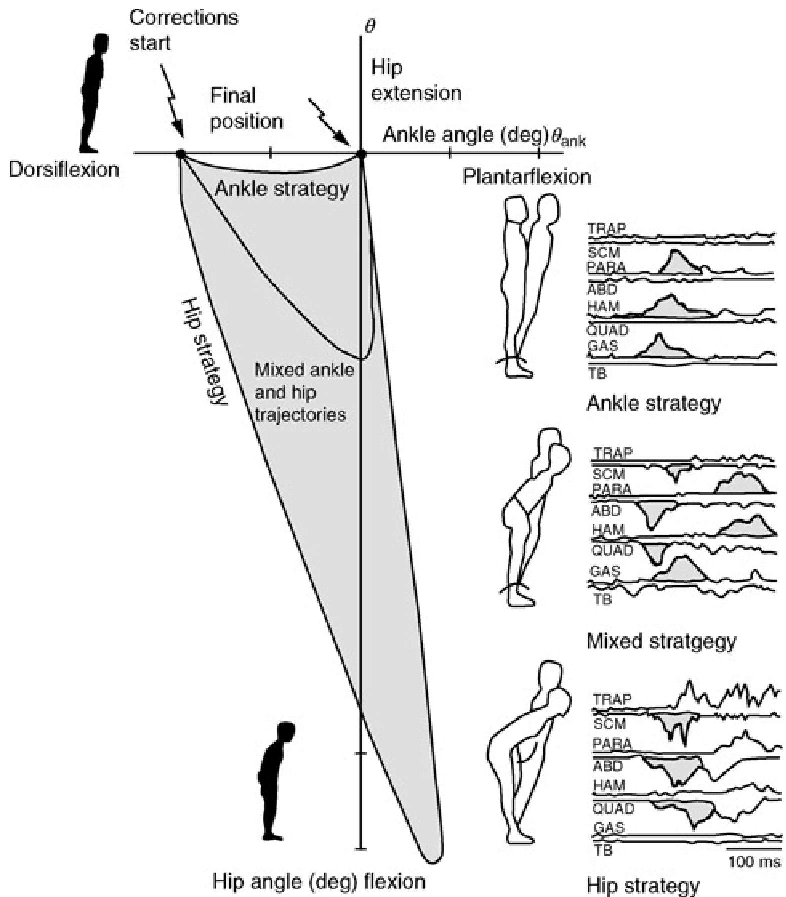

Figure 2.6: Relation between postural strategies and postural synergies due to increasing external perturbation. (Quoted from [38]).

2.2 The Main Physiological Elements Participating in Human Postural Control

In this section, it is reviewed cortical structures with related to automatic postural responses triggered by external postural perturbations. Responses to postural perturbations suggest greater potential for modification by the cortex. Obtaining evidence from recent studies, it is widely acknowledged that the cortex is connected with changing postural responses with adaptation in cognitive state. Studies suggest that the cerebellar-cortical loop is responsible for adapting postural responses based on prior experience and the basal ganglia-cortical loop is responsible for pre-selecting and optimizing postural responses based on current context. Thus, the cerebral cortex likely influences longer latency postural responses both directly via corticospinal loops and shorter latency postural responses indirectly via communication with the brainstem centers that harbor the synergies for postural responses, thereby providing both speed and flexibility for preselecting and modifying environmentally appropriate responses to a loss of balance [38].

2.2.1 The Central Nervous System

The CNS including the spinal cord, brain stem, cerebellum, basal ganglia and cerebrum are used for achieving the balance-recovery action.

The spinal cord receives sensory information from the skin, joints, and muscles of the trunk and limbs and contains the motor neurons responsible for both voluntary and reflex movements. The cord also receives sensory information from internal organs [52].

The brain stem contains ascending and descending pathways that carry sensory and motor information to other divisions of the central nervous system [52].

The cerebellum receives somatosensory input from the spinal cord, motor information from the cerebral cortex, and input about balance from the vestibular organs of the inner ear. It is important for maintaining posture and for coordinating head and eye movements. Cerebellum is also involved in fine tuning the movements of muscle and in learning motor skills [52].

The basal ganglia have four nuclei which have an important role in the control of motion, but they do not directly depend to spinal cord. They receive their primary input from the cerebral cortex and send their output to the brain stem [52].

The cerebrum is the largest part of the brain. The surface of the cerebrum is referred to the cerebral cortex which has many areas that are concerned primarily with processing sensory information or delivering motor commands [52].

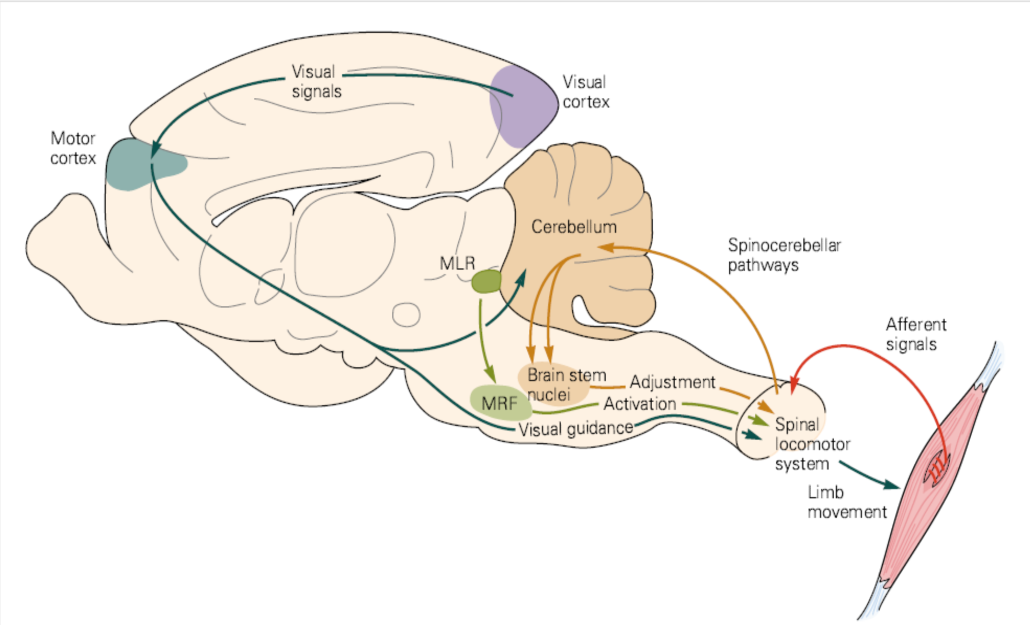

Figure 2.7: Descending signals from the brain stem and motor cortex initiate locomotion. (Quoted from [52].)

2.2.2 The Peripheral Nervous System

The peripheral nervous system is divided into somatic and autonomic divisions.It is with somatic division that this study is related. It includes the sensory neurons that innervate the skin, muscles, and joints. Receptors provide sensory information to the central nervous system about muscle and limb position and about touch and pressure at the body surface [52].

2.2.3 The Musculoskeletal System

This section provides a brief overview of the bones, joints and ligaments, muscles and other associated components of the motor system. The musculoskeletal system is driven by the nervous system via motor neurons. Movement of the body depends on more than just the contractile properties of agonist and antagonist muscles. Bones of the human body make contact with three types of joints: fibrous joints, cartilaginous joints, and synovial joints. Only some synovial joints, such as the ankle, knee and hip will be modeled in this study. Ligaments attach the bones at a synovial joint. Joints may have one to three degrees of rotational freedom with a limited range of rotational motion about each axis. Movement of bones about joints is caused by the contraction of skeletal muscles. Skeletal muscles are very complicated structures, but their complexity is used as an advantage in coping with unanticipated perturbations by the nervous system. In a flat surface, it is needed little or no ankle muscle activity for standing upright. However, in any perturbed surface such as the deck of a boat, large forces must be applied rapidly for stabilizing the balance. The stiffness of the ankle joint is increased by the co-contraction of the ankle muscles in this situation [52].

2.2.4 Sensory System: Somatosensory, Vestibular and Visual Contributions to Postural Control

In this section, it is given that some information about somatosensory, vestibular and visual systems.

Somatosensory inputs for posture include pressure information from skin in contact with surfaces, limb segment orientation from muscle proprioceptors and joint receptors, as well as muscle length, velocity and force information. Somatosensory inputs are important for triggering the earliest automatic postural responses against external perturbations. Somatosensory inputs are also important for providing information about the direction of perturbation and the texture and stability of the support surface so that appropriate postural strategies can be selected [38].

The somatosensory system has very wide responsibilities such as mentioned above. However, this study is more relevant with one of the responsibilities that give information about the position and movement of body (proprioception). It has some receptors in the joints and muscles. Joint receptors provide information about angular displacement and velocity.

Vestibular inputs for posture are important for orientation of the trunk and head to gravity, especially when the surface is unstable. The vestibular system can measure head rotational and linear acceleration. It can sense a different direction of head rotation. Vestibulospinal inputs are particularly important for controlling orientation of the head and trunk in space but are not necessary to trigger automatic postural responses to external perturbations [38].

Visual information is an important sensory input in the postural control system. Especially, when the vestibular system is lost, vision has greater influence on postural control. Stable gaze is necessary for accurate visual orientation information which is used to reduce the destabilizing effect of the balance perturbation [80].

When stable stance is disturbed suddenly, early vestibular, somatosensory, and visual signals are processed by CNS and used to select, trigger, and control the appropriate postural response [91].

2.2.5 Sensory Integration and Sensory Re-weighting

Sensory systems in postural control have been known to be changeable depended to the inner and outer environment. Postural control depends on the central neural interpretation of convergent sensory information from somatosensory, vestibular, visual systems. Sensory information has to be integrated in order to realize complicated and changeable sensory environments. This interpretation process of sensory information is referred as *sensory integration* and this changeable nature of sensory systems is generally called as *sensory re-weighting*.

Consequently, the nervous system controls posture via estimates of position and motion of the body and the environment by combining sensory inputs from several canals. Additionally, kinematic and kinetic body information must be integrated for control of posture. In postural control studies, feedback control has been classified in two different terms as negative and positive feedback. CNS uses the negative feedback control to minimize postural motion. In this control, sensory systems give information about kinematic position and motion of the body. Contrary, positive feedback control is used to maximize joint torque when tilting. In this process, sensory systems give information about kinetic force [38].

CHAPTER 3

THE RELEVANT BALANCE CONTROL THEORIES

This chapter consists of four sections. First, the perspectives for the understanding of the neural control of movement are discussed. Then, based on this discussion, literature about experimental studies and current feedback control models are reviewed. Some of these recent studies are summarized here to allow a comparison with the proposed control law. After these two review sections, open questions and challenges are analyzed by using together interpretation of experiments and reviewing background knowledge.

3.1 To Understand the Neural Control of Movement

All animals must move to interact with the environment or other organisms. For instance, cheetahs must catch their prey rapidly, or human must show an expressive dance gesture, in general, all must stabilize their postural adjustments. In summary, the motor repertoire of an organism defines the nature of its environmental interactions. Various structures in the human body are in charge of finding the most direct solution with these environmental interactions. These structures are the periphery of the motor system, the musculoskeletal system, and spinal cord. The actions of central brain regions such as cortex, cerebellum, or basal ganglia all ultimately have to pass through these peripheral structures. Understanding the properties of these peripheral systems is, therefore, critical to our understanding of the neural control of movement[104].

Environmental components of the motor system can be handled with two common perspectives. In one common perspective, these systems are problems that the CNS must overcome. For suppression, reversal or bypassing of these complications central motor systems develops strategies. In perspective mentioned above, these strategies are needed to the complex properties of muscles, limb mechanics, motor neurons, and spinal circuits. Complexity could, therefore, cause greater complexity: evolutionary changes in the periphery could require the co-evolution of more complex mechanisms to maintain performance [104].

In the second perspective, peripheral systems might simplify for motor control. The complexities of spinal systems or nonlinear properties of the musculoskeletal system might reflect adaptations that allow simplified control by descending systems. In [104], the following examples are given as evidence of the second perspective. For example, passive mechanics can be used to assist movements [17]. Muscle properties can contribute to stability [81]. Basic reflexes allow for rapid control [62]. And defining adaptive muscle coordination patterns can potentially simplify movement [105]. In this perspective, energetic costs associated with inefficient, complex control might lead to evolutionary adaptations that simplify control and neural processing [104].

3.1.1 Feedback Control of Movement

In neurophysiology, feedback is used to describe the signals entering the central nervous system from sensory afferents. The CNS uses these signals to control of bodily functions. Signals from a variety of receptors are involved in the achievement of the control of bodily movement. These signals take their source from mechanoreceptors in muscles, joints, and skin. Additionally, higher-order receptor organs such as the eyes, ears, and vestibular apparatus contribute to the formation of these signals. All levels of the CNS from the spinal cord to the cerebellum and cerebral cortex receive feedback from mechanoreceptors, and all these levels are involved to some extent in controlling even the simplest limb movements [88].

3.1.2 The Most Appropriate Simple Model for Human Postural Control

In natural, human upright stance, which has even no external disturbance, is unstable. Therefore, possibly, the neural control process has existed evolutionary. According to discussion adapted section from [104], to start with the simplest possible model is the most appropriate for the adventure of the understanding of neural control process under the effect of external disturbance. The mentioned section is titled *"To Understand the Neural Control of Movement"*. Naturally, control process needs corrective joint torques that maintain the body upright. It should be noted that there are various studies and many controversies among them about how the nervous system generates these corrective torques. In this thesis, simplification approach is adopted.

This section is explained based on [49]. It is traced because of its clarity at the ability of illustration the issues by starting with the simplest possible model. This fundamental postural control model for upright posture has three elements such as a plant, sensory systems, and a neural controller. It can be seen in Fig.3.1. The plant involves body and movement of the body depends on muscle and tendon and the mechanics of the body. It can be seen that it is a simple model, and it does not include the external disturbance. Motor commands drive the muscle and tendon. It is constructed a hypothetical loop for expression between body and its motion.

Sensory systems measure the body's position and movement and send related sensory signals to the neural controller. Then, the neural controller integrates these incoming sensory signals. As a result, it produces new motor commands. Control theory addresses the question of how to design a controller based on the properties of the plant and sensory systems. This controller is capable of producing the desired behavior of the plant, in this case, maintenance of stable upright stance [49].

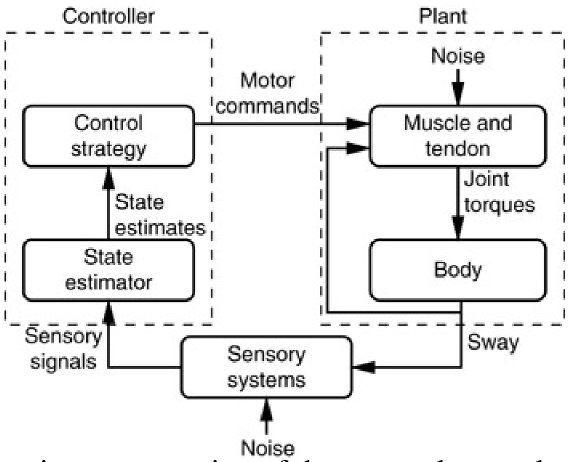

Figure 3.1: A schematic representation of the postural control system from a control theory perspective. (Quoted from [49]).

Traced paper for this section [49], has described the postural control with the control theory perspective by using the simple plant and sensory models and a suitable neural controller.

A Simple Plant Model

In [49], the body without the effect of any external disturbance, is modeled as a single inverted pendulum. [49] has declared that the motivation for the single-joint approximation is not only to simplify the control problem but is also based on empirical results demonstrating that modulation of muscle activity during quiet stance. The derived plant model in [49] with some simplification and assumption is given in the box below. Simplification is that [49] has used linear model with a small angle assumption. Additionally, actuator, which rotates the ankle joint in the sagittal plane, is assumed perfect.

This part is directly quoted from [49]

$$J\ddot{\theta} = mgh\theta(t) + u(t) + \sigma\xi(t)$$

where t is time, $\theta(t)$ is the angular deviation of the body from vertical, $\ddot{\theta}$ is the body's angular acceleration, u(t) (the motor command) is the net forward ankle-muscle torque specified by the neural controller and $\xi(t)$ is a white noise.

The noise in the model is meant to account for the fact that the actual torque produced by ankle muscle will not be exactly equal to the torque specified by the motor command.

The model parameters are:

J, the body's moment of inertia around the ankle joint;

m, the mass of the body;

h, the height of the body's center of mass above the ankle joint (J, m and h do not include the mass of the feet);

g, the acceleration due to gravity; and

σ, the noise level.

[49] have expressed that their highly simplified plant model, which is given in the above box, includes basic characteristics of the control problem the nervous system must solve. They have said that, according to their model, if the control signal u is zero (or constant), the body will quickly deviate from vertical due disturbances. If the *Noises* shown in the Fig.3.1 is not equal zero, then sensory *Noise* can be represent the internal disturbances such as physiological tremor. Similarly *Noise*, which is affected the muscle and tendon, shows the effect of external disturbance such as support surface tilt. As a summary, the body modeled as the plant is unstable. Therefore, it needs an effective feedback control process to detect deviation from vertical and generate motor commands for a corrective torque to keep the body upright.

A Simple Sensory Measurement Model

According to [49], there are two common approaches to modeling sensory feedback. The first approach assumes the sensors include noise because of their nature. This approach is accepted by the studies focused on the sensory integration. Contrarily, sensors are assumed perfect by the second approach. It is approved by the studies focused on the understanding of general principles of the postural control. At the recent times, it is widely discussed that the central nervous system have knowledge of its own sensory and motor noises. As well as, CNS learns to cope with these noises over time.

> This part is directly quoted from [49]
> For simplicity, the second approach is illustrated. If the plant is assumed to be a single-joint inverted pendulum, as in
>
> $$J\ddot{\theta} = mgh\theta(t) + u(t) + \sigma\xi(t)$$
>
> It is completely described by two variables, the angular position and velocity of the body. Therefore, we assume that the neural controller has access to these two sensory signals:
>
> $$z_1(t) = \theta(t), z_2(t) = \dot{\theta}(t)$$
>
> Although the sensory model is not usually explicitly presented when it is this simple, here it paves the way for the discussion of more complicated sensory models below.

A Simple Neural Controller

The control law is considered as a possible basic structure, so it is chosen as proportional-derivative control (PD). It will be discussed later, but, it is widely accepted that this control law is as simple as possible, and it is the most convenient law in accordance with the physiological facts.

> This part is directly quoted from [49]
> It is well known from control theory that stabilization of an inverted pendulum requires that the control signal (corrective ankle torque) depends on both body position and velocity:
>
> $$u(t) = -K_P\theta(t) - K_D\dot{\theta}(t)$$
>
> This is an example of proportional-derivative (PD) control, where K_P and K_D are the proportional and derivative gains, which are assumed to be positive.

A Simple Posture Model

This part is directly quoted from [49]

Combining the plant model,

$$J\ddot{\theta} = mgh\theta(t) + u(t) + \sigma\xi(t)$$

the sensory measurement model

$$z_1(t) = \theta(t), z_2(t) = \dot{\theta}(t)$$

and the controller model

$$u(t) = -K_P\theta(t) - K_D\dot{\theta}(t)$$

results in the postural control model

$$J\ddot{\theta} = (mgh - K_P)\theta(t) - K_D\dot{\theta}(t) + \sigma\xi(t)$$

According to derived postural control model that shown in the above box, the proportional gain K_P must be greater than mgh. Additionally, due to $\sigma\xi(t)$, an offset, which depends on the magnitude of the noise, occurs at the steady state. It means that body's orientation fluctuates around vertical.

3.2 Current Studies

Recently, many researchers have been studying on neural control of balance with various motivations. Both their methods and their curiosity can be different from their colleagues. Two mainstreams can be noticed in this research area such as experimental studies and model-based studies. Experimental studies focus on the balance disorders in terms of early diagnosis, assessment of the patients and selective lesion studies. Additionally, cognitive processing studies, such as ongoing activities (cognitive or motor), arousal (fear), attention and expectation, occupy an important field. Understanding of physiological systems such as sensory systems and their different contributions to postural control is topic for each mainstream.

On the contrary, model-based studies focus on the understanding of the control law, which is responsible for maintaining balance. Moreover, higher-brain contribution to postural control, muscle, and tendon properties are also topics of model-based studies.

3.2.1 Examples of Experimental Studies

Mostly, in the experimental studies, two types of support surface perturbation are used, one of them is rotation in the pitch direction, and the other is the forward and backward translation. Surface rotation is more useful than the forward and backward translation because it gives more information about the role of lower leg proprioception on balance control. Different surface perturbation causes different muscle responses. In experimental studies generally, two subject groups are preferred, normal individuals and patients. The main reason for this choice is the possibility to compare.

Balance Disorders

Firstly, in many of the studies about balance disorders, subjects are normal individuals and patients, and they are assessed on the synergy and strategy of balance corrections [5]. Secondly, experimental studies about balance disorder based on postural control have been classified into three categories in [108]. These categories are making the (differential) diagnosis, estimating fall risks and assessing the effect of treatment. Natural processes as aging, disorders related with central and peripheral nervous system have been studied at these categories.

Cognitive Processing Studies

Postural control is affected to change the cognitive load such as given additional tasks, which are referred to as "dual task" or multitask paradigm. They present an opportunity to assess the subject's ability to manage the increasing cognitive load. Additionally, subjects are evaluated in terms of their strategy selections for dealing with complex task [9, 108].

Furthermore, attention is important contributors to instability in both healthy and balance-impaired older adults [65, 119]. Dual-task paradigms are also used for examining the relation between attention and the control of posture. Postural control is also affected by fear and anxiety. Some recent studies, which are related to quantitative and qualitative assessment of perceived and physiological effects of fear and anxiety at the postural control, are reviewed in [27]

Understanding of Physiological Systems

[39] has declared that postural responses are shaped by CNS mechanisms related to expectations, attention, experience, environmental context, and intention, as well as by preprogrammed muscle activation patterns called synergies. Additionally, they have stated that the concept of muscle synergies has changed over the last 20 years. According to [39], while muscle synergy was described as stereotyped patterns of bursts of muscle activity in the past, the concept of muscle synergies has evolved toward a concept of "flexible" synergies. Now it is defined as centrally organized patterns of muscle activity that are responsive to initial conditions, perturbation characteristics, learning, and intention. Furthermore, the most important argument of [47] is that cerebral cortex is contributing to postural responses. The behavioral evidence can be seen below list, they are quoted directly from [47].

- changes in cognitive load and attention when performing concurrent tasks
- changes in a subject's intentions to respond with a specific strategy
- learning and modification of postural responses with prior experience and with changes in initial conditions

3.2.2 Examples of Current Models

When model based studies are reviewed, it can be seen wide spectrum from the most simple to the most sophisticated models. This variety is related to the researcher's aims. Beginning of the research has to be made many decisions about modeling of the body and its musculotendon dynamics, complexity of the sensory systems, type of neural control strategies and more specifically nonlinearities and uncertainties, etc. In this section, the previous studies are reviewed for understanding of the strengths and weaknesses of published models.

Peterka's Model

According to [6, 51, 60], Peterka can be named the well-known and the most criticized scientist at the postural control field. Peterka's studies focus on the understanding of the sensory integration of visual, proprioceptive, and graviceptive systems. Peterka has modeled the postural sway and proposed a single link inverted model. Peterka suggested PID controller as neural control model. At this point, Peterka's model can be criticized due to three aspects.

- Single inverted pendulum cannot represent the body dynamics.
- Suggested controller (PID) as a neural controller is not is based on the real physiological structure.
- Simulations with proposed models do not fit experimental data exactly.

An example of the Peterka's studies can be seen in Fig.3.2, where W_{prop} represents sensory orientation information from proprioceptors sensing body orientation relative to the support surface. This information is processed by a neural controller (NC) with a time delay (TD) to generate corrective torque T_c. This corrective torque drives the body.

Modified version can be seen in (b) there are added two new features to the model. One of them is passive muscle dynamics P that generate passive corrective torque T_p that sums with active torque T_a. The second modification is force feedback loop that are conveying force related sensory information F to the back (From [86]).

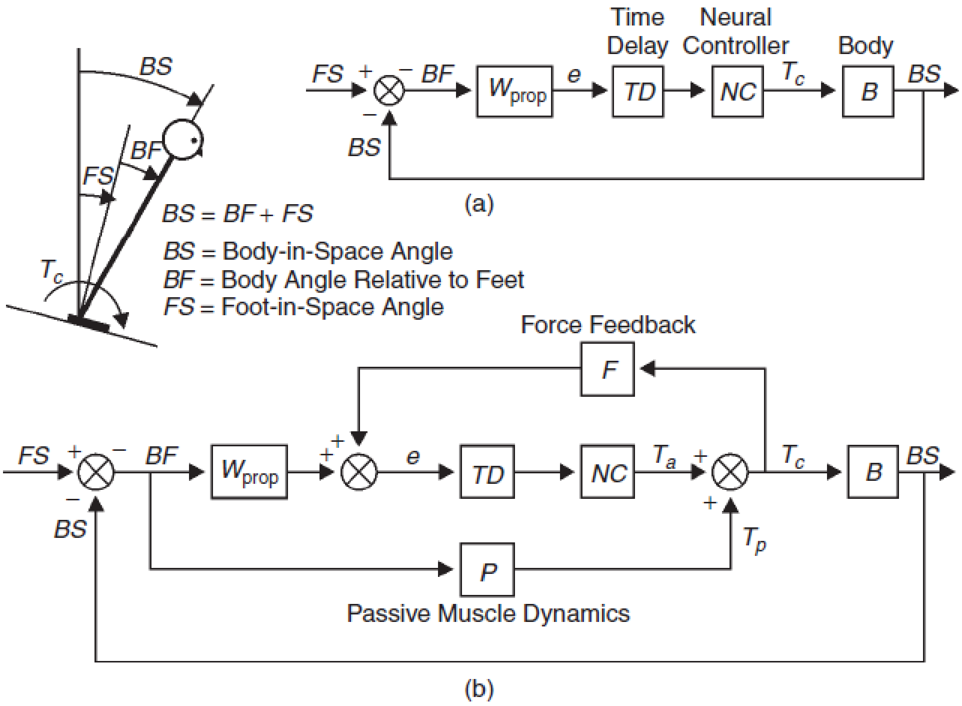

Figure 3.2: Peterka's Model (Adapted From [86])

In spite of some critiques, Peterka is an important figure in the sensory integration studies, and his ideas have to take account for the future studies. Peterka summarizes his ideas in [87] as follows:

- Redundancy of the sensory sources and a weighted combination of sensory information may be beneficial for central nervous system.
- The sensory integration process is limited with the physics of the body and its interaction with the environment.
- The effects of external disturbances while maintaining stability can be minimized by using the sensory re-weighting and its combination of kinematic and kinetic sensory information.
- Sensory reconstruction and re-weighting including thresholds have been modeled relatively simple models. They can give an explanation for a wide variety of experimental data.

- Similarly, engineering tools such as optimal estimation methods have been used to the understanding of postural control. Many experimentally observed features of sensory integration can be rationalized with these tools.

- Determination of the actual neural mechanisms of sensory integration systems is open field yet.

van der Kooij's Model

Given in Fig.3.3, van der Kooij's model from 1999 emphasizes the weight of sensory information to human standing. Optimal estimation theory is applied for quantification of the weights. The model includes the delay in the sensory system. The controller includes a predictive element to compensate for time delay.

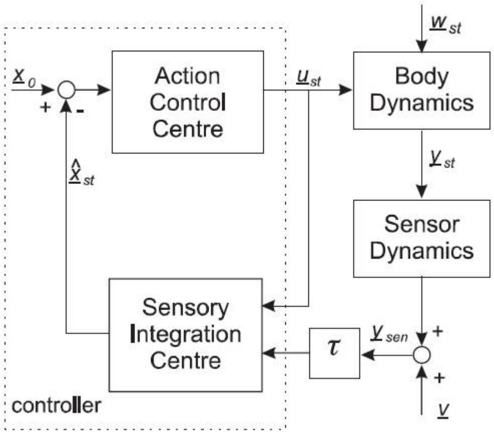

Figure 3.3: van der Kooij's Model (1999) (Adapted From [106])

Given in Fig.3.4, van der Kooij's model from 2001 presents an adaptive estimator model of human spatial orientation. Proposed adaptive model weights sensory error signals as a function of environmental conditions. Sensory error signals are defined as the difference between expected and actual sensory signals.

The special feature of Kooij's models is that they include the dynamics of the environment in the overall human postural control model. These models show that proposed adaptive controller can produce many of the responses with a simple linear time-invariant system.

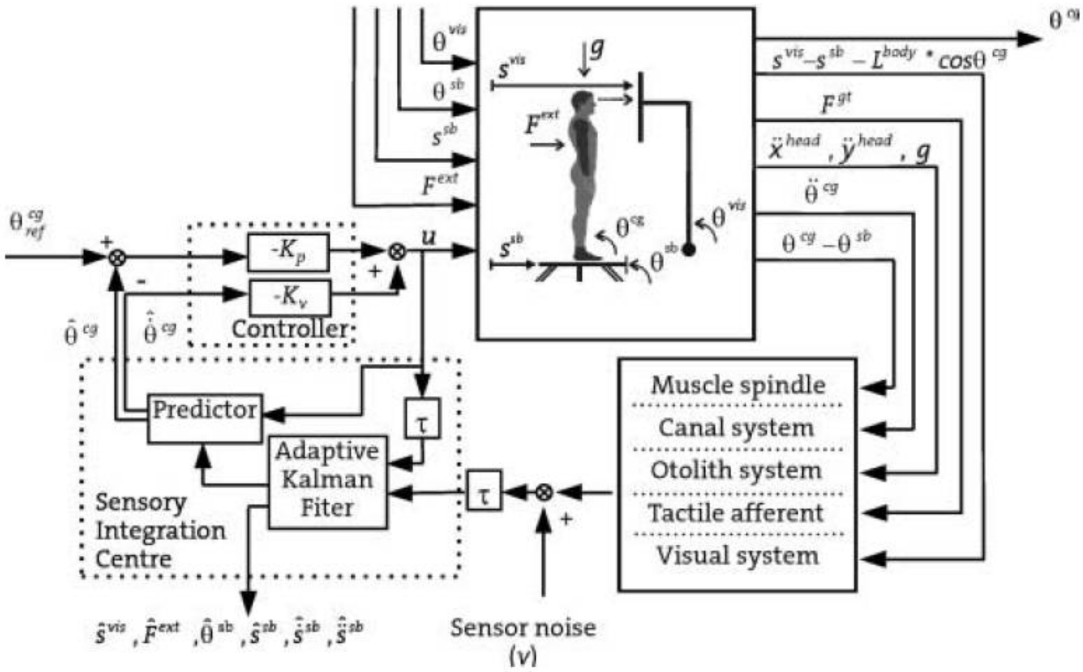

Figure 3.4: van der Kooij's Model (2001) (Adapted From [107])

Kuo's Model

In Fig.3.5, at the upper left schema, it is shown general feedback model. CNS produces motor commands u that drives the body dynamics. Human movements are described by state x. Sensory dynamics translate the state into sensory outputs y. Sensory output y is processed in sensory processing unit then it feeds the CNS as an input. Feedback control K is modeled as state feedback.

In the upper right schema, it is given sensor model. Sensor dynamics consists of ankle proprioception, hip proprioception, semicircular canals, otoliths, visual translation and visual rotation; each of these sensors has dynamics that temporally filter the state x [57].

In the lower left schema, it is shown direct feedback model. It is said in the [57] that motor command u is produced from sensory outputs y which are multiplied by directly weights matrix.

In the lower right schema, it is shown that the state estimator model. State estimation is a different method of sensory processing from direct feedback model. It uses an internal model of body and sensor dynamics. Efference copy and estimator output are used as an input to the internal model, and it produces the state estimate $\hat{x}$ that enters the feedback control gain matrix. The internal model also predicts the sensory output $\hat{y}$, and the error of this prediction $(y - \hat{y})$ is used to estimator input. Then estimator output (estimator correction) goes to internal model. It is used to correct $\hat{x}$. In [57], it is given an explanation about state estimation that can temporally process information from multiple sensors. Each with distinct dynamics, so that disparate and noisy data can be integrated to yield an optimal estimate [57].

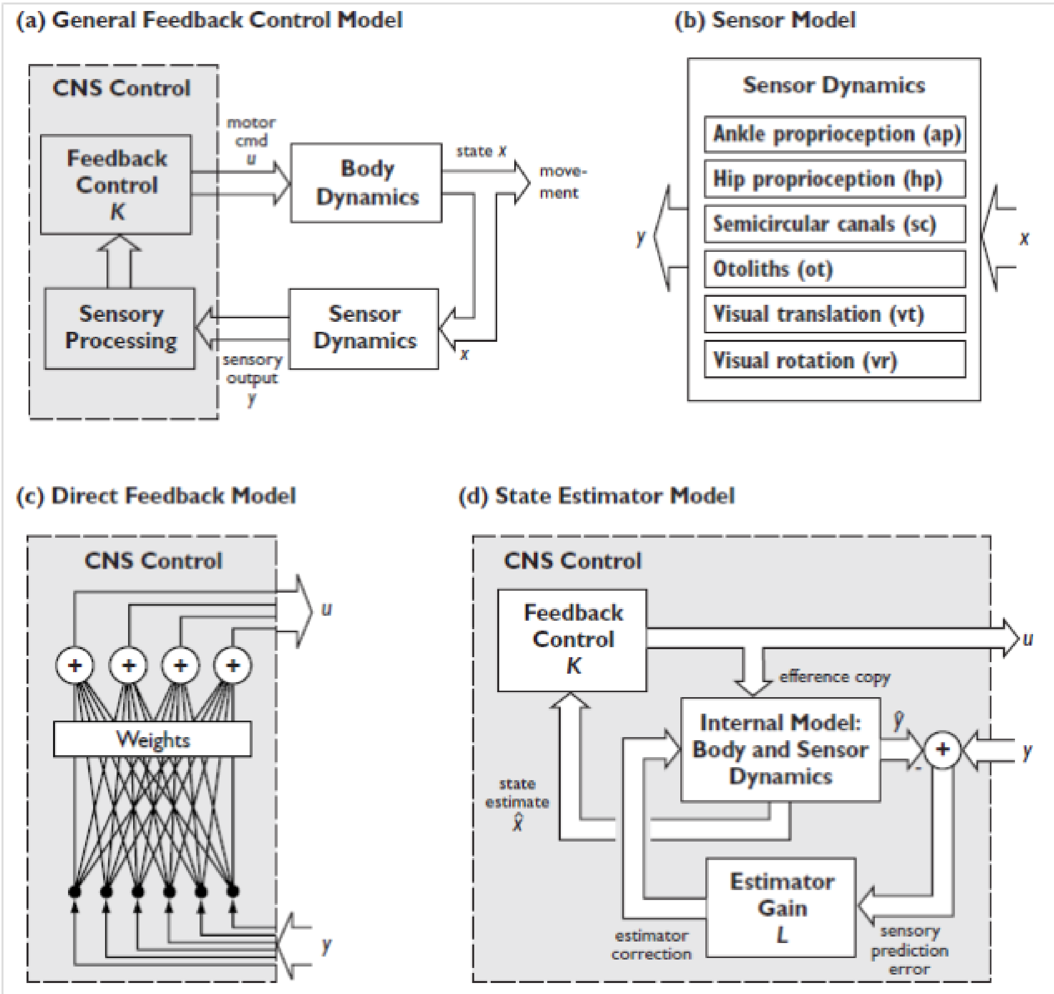

Figure 3.5: Kuo's Model (Adapted From [57])

Yao Li and William S. Levine's Model

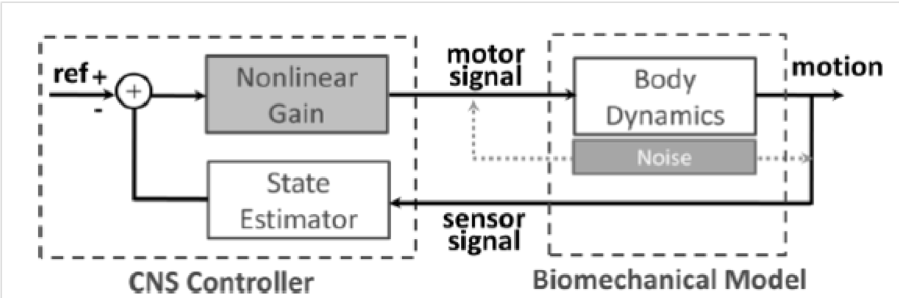

Figure 3.6: Yao Li and William S. Levine's Model (Adapted From [61])

In this study, Kuo's model has been criticized in many aspects as below.

- Muscle dynamics was not included.
- Joint torques were directly proportional to the motor output of the controller.
- Neural delays were mentioned but not quantified.

In their model, a double inverted pendulum has been used to approximate the human responses that are controlled by joint torques at the ankle and hip. It has been claimed that the neural delays from sensation, perception, transduction and execution were incorporated into the neuromusculoskeletal dynamics. The performance measure has been chosen nonlinear quartic in the center of pressure and quadratic in the controls. This nonlinear quartic regulator problem has been solved approximately by the model predictive control technique.

Both Kuo and Li can be criticized for their optimal control methods. The most likely, the CNS can behave optimally via using redundant sets of both actuators and sensors. However, there are not enough valid arguments about optimization criteria.

Additionally, there are some opinions in favor to abandon optimal control. [63] has stated that computational methods for ensuring a globally optimal solution require an inverse model of the plant to be controlled. It is also declared that the model of a biological neuromusculoskeletal system involves some nonlinearities; it is almost impossible to invert its model without making simplifications.

Park's Model

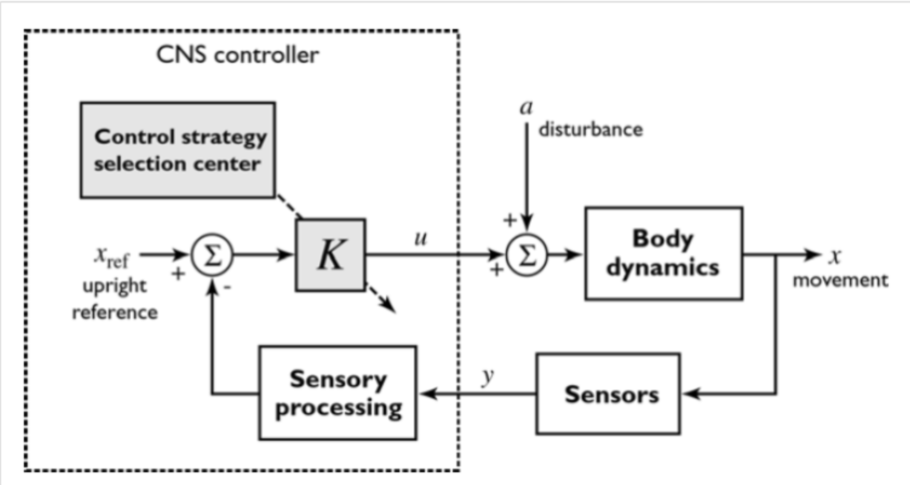

Figure 3.7: Park's Model (Adapted From [84])

In Fig.3.7, feedback gains are producing joint torque commands u as a function of body movement x. Where a is disturbances inputs to the body dynamics. The movement of a body is measured by the body sensors. Sensory information is processed by the central nervous system to estimate the positions and velocities of the body segments. Then this information is fed back for using to generate the compensatory joint torque commands u. [84] is related with selection of K conveniently. This process is realized by the CNS in agreement with biomechanical constraints and body dynamics. In their model, sensors and sensory processing have not been studied intentionally.

Park's model has underlined the linear scaling of the time-invariant feedback gain values concerning the magnitude of the perturbation. Park has minimized error measured and simulated angular position and velocity of the links by using least-squares optimization. As a result, Park showed that the feedback gain values "gradually" scale with the magnitude of the perturbation. There are some weaknesses as well as its important contributions. Common weaknesses of [84] can be summarized as follows.

- The body dynamics may be represented with a double inverted pendulum, but it is a fact that increasing the degree of freedom increases accuracy. In our experiments for all trials, knee motion is observed.

- The other important limitation of this study is the use of LTI (linear time invariant) gain set.
- The other limitation is that they don't care about deviation from the equilibrium position. (i.e. final positions of subjects differed from their initial positions)

3.3 Open Questions and Challenges

According to literature review, the most fundamental open question is how to model adaptive control processes. For instance, adjustment of sensory information and re-weighting by changing the environmental conditions or internal changes such as attention or expectation are open questions. Because of indispensability of taking into account of all level adaptations, higher level systems in the brain, which are responsible for postural control, have to be considered a part of modeling.

For the construction of appropriate postural control model, there are some lower level questions and challenges beyond adaptation. They can be listed as follows.

- Complexity vs. simplicity,
- Modeling of the body and its musculotendon dynamics,
- Complexity of the sensory systems and inner dynamics of sensory modalities,
- Prediction of the control strategies used by the nervous system,
- All level nonlinearities and uncertainties such as considering noise in sensors and actuators.

All these questions and challenges will be discussed in the next related chapters of the thesis.

CHAPTER 4

EXPERIMENTAL SETUP AND BIOMECHANICAL MODEL

In this chapter, experimental setup and protocol, and biomechanical model are presented. Construction a model, which is perfectly adequate for the representation of human balance-recovery reactions, is very difficult and complex action. Consequently, these difficulties and complexities lead to cascaded study plan as naturally. The concatenated study plan consisted of following steps.

- Literature review,
- Conducting a set of experiment,
- Interpretation of the experimental data,
- Constructing a biomechanical model,
- Conducting a new set of experiment,
- Interpretation of the new experimental data.

Therefore, in this chapter, beside the experimental setup and protocol, the interpretation of the experimental data is brought up for discussion along with the assumptions made.

4.1 Experimental Setup

All experiments are conducted by using the facilities of METU-MODSIMMER Posture Laboratory. Experimental setup consists of a 2-dof custom-made high-precision hydraulic support surface tilt platform, a wearable inertial sensor set, an LVDT and a force plate. In the experiments, subjects are exposed to perturbations that are generated by mentioned custom-made support surface tilt platform. The full body kinematics data during the experiment are recorded by the wearable inertial sensors. Position of the platform is measured by the LVDT. The ground reaction forces of subjects are recorded by force plate to make sure their standing on the platform with two feet.

4.1.1 Support-Surface Tilt Platform

2-dof high-precision hydraulic tilt platform is embedded in the shown cabin at the left side in Fig.4.1. Force plate is located in the middle of the platform, which can be seen at the right side of the same figure. The cabin provides an opportunity for the perception experiments, besides postural control experiments. The illumination inside the cabin is adjustable by changing light intensity and frequency. Additionally, it is possible to realize the absolute dark room experiments [75].

Figure 4.1: General View of Support-Surface Tilt Platform [75]

Application Reasons and Type of the Perturbation

For detection of the postural control, it is required to perturb the body's equilibrium orientation with a sudden external disturbance. Sensory system perceives the disturbance, and balance-recovery reactions arise. This external disturbance can be defined as a force applied to the body or motion of the support surface. Nearly all body muscles generate torque for the correction of the posture against the perturbation of the support surfaces [100]. It means that it can be obtained more information about body.

There are two types of support surface perturbations; one is rotational generally in pitch or roll directions. The other is translational in backward-forward directions. At the beginning of the study, literature was reviewed for answering the question about what type of support surface perturbation was more convenient for revealing the internal control. [5, 55, 92, 97, 109].

Support surface tilt and translation reveal very similar reactions. However, [21] states that bilateral vestibular loss has not affected postural reactions to translation because relative displacement is not changed between limbs and trunk. Translational perturbations are more convenient for the studies about the loss of thick afferent fibers from limbs and loss of cutaneous afferents [21]. On the other hand, the tilt of support surface has been stated in [21]. The rotation of support surface has a crucial role in understanding the basic mechanisms generating corrective postural reactions by the lower levels of CNS, with the brain stem and cerebellum.

Technical Details about Support-Surface Tilt Platform

The maximum amplitude the support-surface tilt platform is $\pm 9°$. It completes this maximum amplitude in 600 ms. And its average velocity during motion is $15°/s$. Typical angular position and velocity profiles are shown in Fig.4.2.

Determination of the motion profile is significantly important for the reliability of experiments. Available support-surface tilt platform in the laboratory is not as fast as the platform presented in [97]. The mentioned platform technical specifications are $\pm 7.5°$ in amplitude, 150 ms in time and $60°/s$ in average velocity, which can be seen in Fig.4.3.

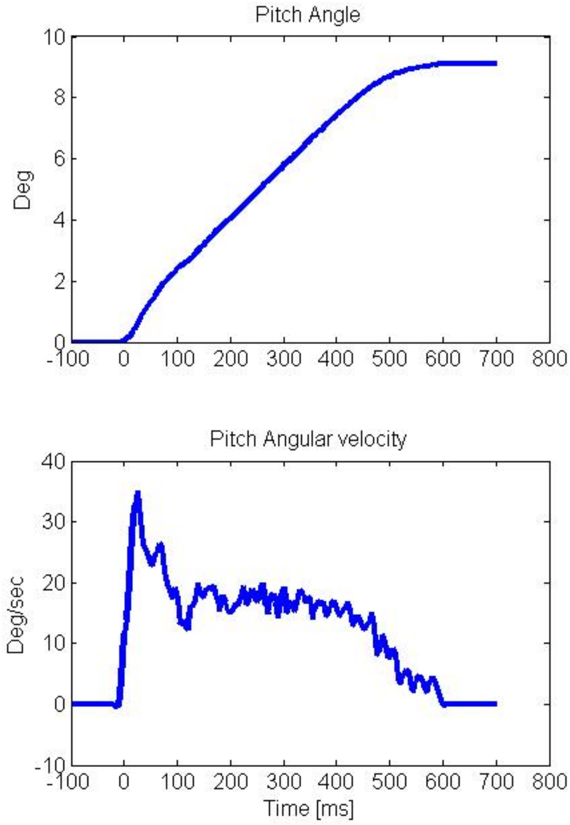

Figure 4.2: Motion Profile

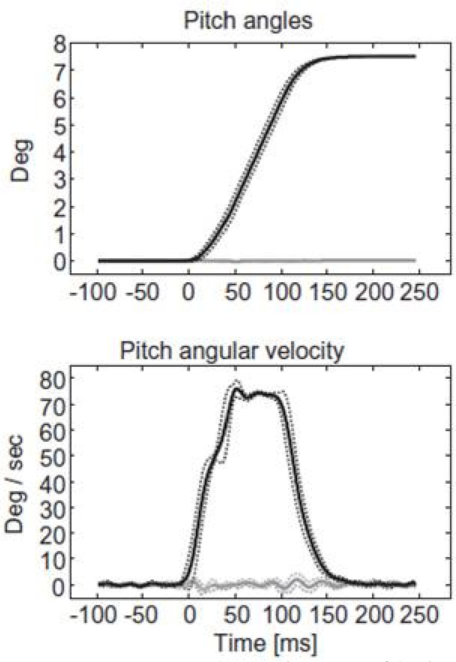

Figure 4.3: Presented Motion Profile in [97]

Naturally, there is an influence of the motion profile on the subject's postural responses. However, in daily life, the human can remain exposed to various external disturbances. Due to nature of this external perturbations, only nature of the control can change. Therefore, as long as the same protocol is applied to all subjects, the motion profile does not have a negative effect on the experiment.

4.1.2 Sensors

Present posture laboratory has a set of wearable miniature inertial measurement units. Each measurement unit consists of 3D linear accelerometers, 3D rate gyroscopes, and 3D magnetometers. Wearable means that each measurement units are placed at specific locations (See Table 4.1) on the body and are fixed with straps, to measure the motion of each body segment. It can be seen in 4.4.

Table 4.1: Description of Specific Locations (Adapted From [120])

Location	Abbreviation	Optimal Position
Foot	FOOT	Middle of bridge of foot
Lower leg	L-LEG	Flat on the shin bone (medial surface of the tibia)
Upper leg	U-LEG	Lateral side above knee
Pelvis	PELV	Flat on sacrum
Sternum	STER	Flat, in the middle of the chest
Shoulder	SHOU	Scapula (shoulder blades)
Upper arm	U-ARM	Lateral side above elbow
Fore arm	F-ARM	Lateral and flat side of the wrist
Hand	HAND	Backside of hand
Head	HEAD	Any comfortable position

Mentioned measurement unit, which are comprised of accelerometers, magnetometers, and gyroscopes, is a small orange box shown in Fig.4.5. A set of measurement units is used to record measurements of a set of parameters from the body limb during the performed perturbation. These parameters recorded from the device are listed at the background in the Fig.4.5. It is preferred to use "Matlab" for analyzing these parameters.

Figure 4.4: Wearable motion tracker sensors (adapted from [120])

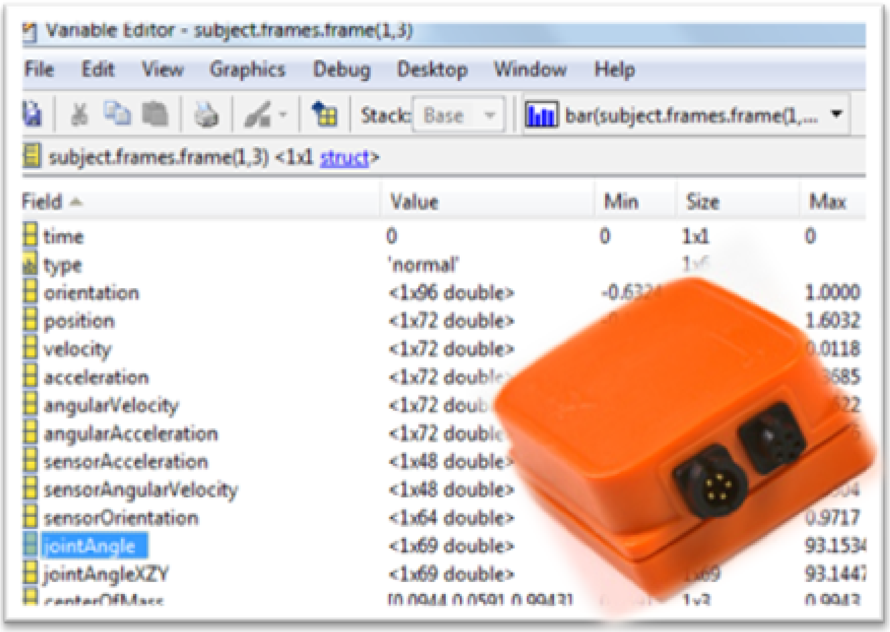

Figure 4.5: Measurement Device and Parameters

Just "jointAngle" and "position" from parameters represented in Fig.4.5 have been used in the analysis. It is defined that there are 22 joints and 23 body segments for a full body.

Global reference frame (with respect to an earth-fixed reference coordinate system) is defined as for wearable motion tracker sensors.

- X positive when pointing to the local magnetic North.
- Y according to right-handed coordinates (West).
- Z positive when pointing up.

Local coordinate frame is defined for each body individually that are segments in anatomical pose, and center of rotation is origin of the frame on the proximal body.

- X forward.
- Y up, from joint to joint.
- Z pointing right.

The difference between the global and local frames does not affect the results. Therefore, the orientation convention of the global frame has been replaced with that of the local frame for the sake of simplicity.

Sign Convention and Notation

Wearable sensors, which are explained in the previous section, are a commercial product. Therefore, creators of this product have preferred using standards, which are declared by International Society of Biomechanics (ISB). It has declared in 1993 that their first aim for standardization matches the clinical terminology; the other is to create the easier interpretation of data by clinicians.

The mentioned notation has accepted in this thesis with an exception. Xsens (manufacturer of sensors) has defined two different frames such as the global and local frame. Two distinct frame could create some unnecessary ambiguity while interpreting the data, for this reason, the global frame have been transformed to the local frame.

4.2 Experimental Protocol

To find out the control algorithm that is used by humans to keep their balance under the effect of suddenly occurring external disturbances is very hard and open problem. As well as its difficulty, the handling of the problem has to be parallel with the design of experiments.

The experimental protocol was defined by using the results of several experiments (see Table.4.2). The evaluation of these experiments led to a decision about the final experimental protocol. This nested activity should be explained for the understanding of the attained protocol. Additionally, the other importance of the set of experiments allows one to make accurate assumptions for biomechanical model and conjectured control law (For assumptions see section 4.2.1).

For all level, at the design procedure, it is taken defined criteria listed below into account:

- Definition of the factors which effect the experiment, clearly,
- Requirement of control condition,
- Background variables of the subjects,
- Sample size i.e. how many subjects must be taken part in the experiment,
- Trial size i.e. how many times must be repeated,
- Disturbance and noise.

Detailed explanation of all pre-experiments does not have to be specified. However, their results are the remarkable effect on selections and assumptions of both experimental protocol and biomechanical model. The analysis of the obtained data reveals some key ideas. They can be categorized depending on their effects such as ideas about experiment protocol, ideas about the nature of control and ideas about the biomechanical model. In this section, ideas about experiment protocol and attained experimental protocol are introduced. The other key ideas will be expressed in the next sections.

Table 4.2: Conducted Pre-Experiments

Definition	Date	Purpose	Explanation
PE.#1.S.#1	12.07.2013	Tested Range of the Angles [1:9 in deg.]	Many angles tested randomly.
PE.#1.S.#2	12.07.2013		S. could not stand on the platform.
PE.#2.S.#1	02.09.2013	Tested Specified Angles [5,7 and 9 in deg.]	Three specified angles are performed with random order and random direction.
PE.#3.S.#1	13.11.2013	Only one Angle [9 in deg.], gender and personal differences	Woman; Her posture has changed.
PE.#3.S.#2	13.11.2013		Short and thin man
PE.#3.S.#3	13.11.2013		Tall and athletic man
PE.#4.S.#1	07.01.2014	Sign Convention and Notations	Totally 17 trial
PE.#5.S.#1	04.04.2014	Tested final position of the body differ from initial position.	Many angles tested dynamically and statically
PE.#5.S.#1	04.04.2014	Tested final position of the body differ from initial position.	Many angle tested dynamically and statically
PE.#6.S.#1	16.05.2014	Tested Usability of the Electromyography.	Which muscles are available for data acquisition?
PE.#7.S.#1	05.07.2014	Tested Predictable perturbation effect.	2 set Forward 2 Set Backward, the same magnitude and equal time interval
PE.#8.S.#1	08.07.2014	Tested Predictable perturbation effect.+ Electromyography	1 set Forward 1 Set Backward, the same magnitude and equal time interval

4.2.1 Key Ideas about Experiment Protocol

The pre-experiments have revealed various observations and ideas, which are very effective on the specified the experimental protocol. Following items should be noticed for planning the new experiments.

- ***Automatic postural responses are individual.*** It is observed that each subject has a distinctive behavioral response pattern. However, there are also some general characteristics for all subjects. Firstly common attributes and secondly individual features of responses are given below:

  1. Observed general characteristics of postural responses.
     - After the perturbation, toe and ankle joints start to move, their movement is in the same direction with the tilt platform. Approximately 50-100 ms later, the other joints start the movement.
     - It is not observed all subjects, but some of them have adjusted their posture to cope with the external suddenly occurring perturbation. It is thought that it can be a clue about adaptation.
     - Moreover, some subjects have learned using appropriate joints to cope with the perturbation.
     - Although it is not clear exactly, there are some clues about unexpected responses. So, bad performance can follow two successive good performances. This situation may be explained by decreasing the attention.
     - Forward perturbations are coped with more easily.
     - There is a clue that subject's physique correlates with their selections.
     - It is obviously observed that there is a significant difference between the first and other trials during the experiment.
  2. Detected individual features of behavioral patterns.
     - Gender differences and subject's physique are correlated the behavioral pattern.
     - For forward perturbations, two of subjects, have behaved as a two part beam that consists of fixed rigid lower part and flexible upper part. Their upper body is flexed as a flexible beam, or it can be explained as a whip-like movement counter the perturbation direction.
     - For backward perturbations, in the same way, the same two subjects have behaved as an only one part beam. Whereas one of them behaves as a rigid inverted pendulum jointed on the ground, the

other behaves as a flexible beam fixed on the ground. First one has used her ankle joint very efficiently. During the first backward perturbation, the second one has lost his balance and took a step to back. He rarely used his ankle joint. His movement started 100 ms later from perturbation. The whole body is flexed as a flexible beam to counter direction of perturbation.

- Towards the end of the trials, some subjects have changed their behavior. One has changed her posture. The other one has learned to use his ankle joint.
- In general, some subjects could prefer to use their arms to recover the balance.
- One subject, who is the tall and athletic man, has coped with the perturbation easily. His responses can be described as: at first 50 ms, ankle and toe joints are changing the same direction with the perturbation. Then, knee and hip joints start motion. Knee joint's maximum value is seen at 200 ms after the perturbation. At this point, upper body is flexed toward the back by hip, ankle, and toe. After finishing the perturbation, all body components try to come to their starting points.
- However, the responses given backward perturbation differ from given forward perturbation as follows: at first 50 ms, ankle, and toe joints are changing the same direction with the perturbation. Then, knee and hip joints start motion. Upper body is flexed toward forward at the hip. In contrast to forward prototype, upper body show more flexible behavior at the backward perturbations.

In this thesis, it is not sought a relation between subjects. Naturally, there is a need to study with many and appropriate subjects for interpersonal studies. However, a human subject is sufficient in this study, only with the main condition. The subject response must be consistent with the general characteristic of postural behavior under the effect of external disturbance. In experiment protocol, it can be better to study ***with two subjects to provide the control criteria*** of the basic principles of the design of experiments.

- In pre-experiments, it is observed that predictable and unpredictable perturbations cause different responses. At this case, perturbation trains were determined in a sequence unpredictably. Waiting time between the perturbations is also determined by unpredictable size. As a result of this case, very complex and incomprehensible data set was obtained. Therefore, the sake of simplicity purposes, ***predictable case is preferred***. Perturbations are given the same direction and the same magnitude with the equal time interval in predictable case.

- Subjects should be selected ***considering some features*** such as having the same gender, educational and cultural background and providing similarity between their physiques.

- In pre-experiments, when experiments were conducted with a group of subjects, they could affect to each others. It was a bias factor. Therefore, ***experiment for each subject should be realized differently and individually.***

- Experimental procedures can be exhausting, strenuous and boring over time for subjects. Therefore, it should be conducted with possible the least number of trials. However, ***the quantity of trials must be meaningful, statistically***.

- In preliminary experiments, it has been observed that talking, noise and the other disturbance at the environment could influence on subjects. Therefore, ***laboratory must be isolated*** against noise and other external disturbances.

- Subject could have different initial posture at the beginning of the trials. This distinctive initial posture and body configuration could cause the complexity. Therefore, subjects should be informed to protect as possible as their initial posture and initial body configuration. For simplification of modeling, ***they can be forced to a specific body configuration, such as upright posture with hands in pockets.*** This enforcement does not adversely affect the experiments because it is a natural posture.

4.2.2 Attained Experimental Protocol

Experiment protocol is the most important issue for an experimental study. Therefore, given the above explanation, it is decided as follows.

Predictable case: perturbations are given with custom-made support surface tilt platform that can produce maximum tilt angle of $\pm 9^{\circ}$. Perturbations are given the same direction and the same magnitude with equal time interval.

Two sets of the experiments are conducted for each subject. The first set experiment starts with quiet stance upright posture that takes 30 s. And then perturbation is given toward forward (toes down) which takes 600 ms and subject stands in this position 15 s. Then platform was turned back to the horizontal position and again the subject stands 15 s. This loop is repeated 20 times. The second set is different from the first set with respect to tilted direction. The second stage of the experiment is the backward direction (toes up).

Subjects: two healthy young male subjects participated in this experiment. (Their age: 27 and 32 yr, height: 185 and 179 cm, body mass: 86 and 67 kg) and They have the same educational and cultural background. Both were instructed to stand upright with their hands in their pockets and to recover an upright posture under the effect of perturbation without stepping, if possible.

Data acquisition: the full body kinematics data, the ground reaction forces and the position of the platform were recorded during the experiments. Kinematic data were measured at a sampling rate of 100 Hz by the wearable inertial sensors (The Xsens MTx sensors) which consist of 3D gyroscopes, accelerometers and magnetometer that are reported to provide drift-free motion data.

The manufacturers report a static accuracy of 0.5 degrees for roll and pitch, 1 degree for yaw, and a 2 degrees RMS dynamic accuracy. The ground reaction forces were recorded on a force plate (Bertec FP-4060) at a sampling rate of 100 Hz, and the position of the platform was measured by an LVDT (Sick-MPA sensor) placed under the platform at a sampling rate of 200 Hz.

4.3 Biomechanical Model

The actual DoF of human rigid body dynamics in the sagittal plane is greater than 3. However, in this thesis, its DoF is reduced to 3 by using a 3-DoF inverted pendulum model with some assumptions and limitations (see section 4.3.2). The Fig.4.6 shows an erect human posture standing on a movable platform and trying to keep an erect posture on this moving platform.

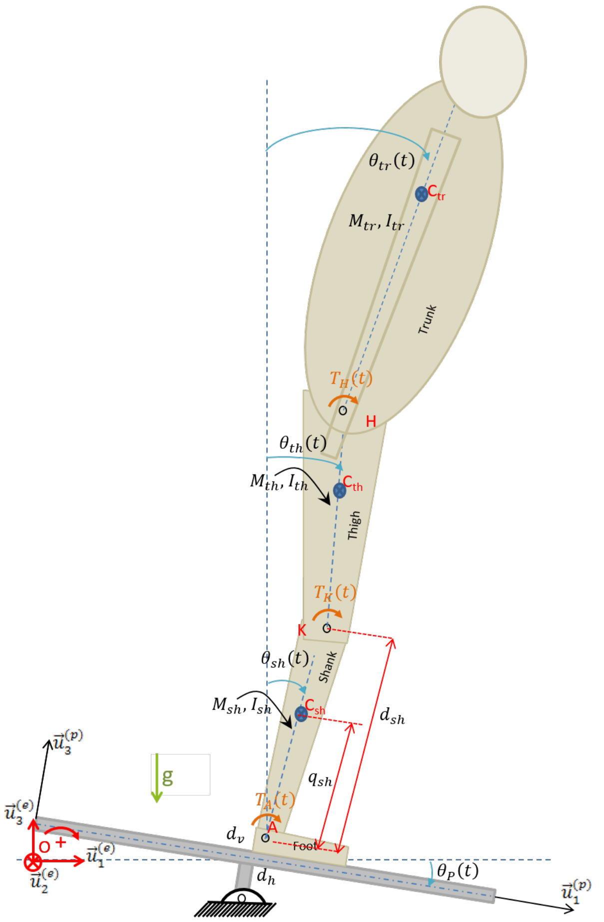

Figure 4.6: Proposed model for a subject standing on a tilt platform.

This section consists of three sub-sections. In the sub-section named as key ideas about the model, interpretation of the experimental data and observations during this process are evaluated in terms of making decisions about modeling. The second sub-section declares the limitations, simplifications and assumptions on the modeling process. The last subsection is devoted to mathematical representation of the model.

4.3.1 Key Ideas about Model

During interpretation of the preliminary data, it was obtained a little foresight to judge what is important for the modeling process accurately. It is known that human body is very complex, and it has a lot of redundancies. At this point, some assumptions for limitation and simplification of complexity have to be done. They are listed below.

- Ankle joint, foot and related muscles may have a crucial role in automatic postural responses. Because the first and rapid reaction to the perturbation comes from this joint during the experiment.

- It is observed that knee joint has been used for absorption of the first impact coming from the platform. It is also noticed that motion depending on knee joint arises immediately after ankle joint's movement.

- Bending of the trunk may also be thought as an important factor in balance recovery-reactions. However, it is very difficult to create a model of the vertebral structure because of its multiple segmental compositions.

- Can be constructed a model for describing the motion of the human body based on limb segment angles with respect to gravity vertical axis? Is it realistic? It is known that feedback related with body position comes from mechanoreceptors in muscles, joints, and skin. As well as, higher-order receptor organs such as the eyes, ears, and vestibular apparatus contribute to the formation of feedback signals. Naturally, all distinct sensory system has a different reference frame. They can be assumed to be integrated perfectly by CNS. Thus, it can be assumed that it gives instantaneous feedback information about the position and velocity of the moving body with respect to gravity vertical.

- There is a significant clue that subject's physique correlated with their selections. Therefore, parameters such as the mass and inertia of the segments of the human body and length and position of the center of mass should be defined individually for each subject.

4.3.2 Limitations, Simplifications and Assumptions

The proposed model is confined to the sagittal plane with three degrees of freedom having the ankle, knee, and hip joints as the only actuated joints. This general assumption is a widely used approach in terms of simplification. In the sagittal plane, [7] has evaluated a generalized model of human postural dynamics are represented as a planar open-chain linkage system supported by a triangular foot. It has been stated that the proposed model is valid for analysis of postural control mechanisms.

The model of the human subject can be constructed basically like a three-body inverted pendulum by assuming such that

- The hands are kept in the pocket.
- The feet remain fixed on the platform.
- The feet are assumed massless.
- The legs remain parallel to each other.
- Trunk is assumed rigid and the relative motion of the head with respect to the torso is negligible.

Thus, the modeled three bodies happen to be the shank pair, the thigh pair, and the torso-head combination. The relevant neuromuscular actuation system is modeled as if it consists of three torque actuators placed on the axes of the ankle joint pair, knee joint pair, and the hip joint pair.

4.3.3 Mathematical Representation of Basic Biomechanical Model for Human Standing on a Tilt Platform

In this model, mass and mass moment of inertia are represented as by $M_{sh}, I_{sh}, M_{th}, I_{th}$ and M_{tr}, I_{tr}. Where "sh", "th" and "tr" represent shank, thigh, and trunk respectively. Similarly, d_{sh}, d_{th} and d_{tr} shows length of limbs and q_{sh}, q_{th} and q_{tr} shows length of the CoM from joint. The subjects use the torques $(T_A(t), T_K(t)$

and $T_H(t)$) to maintain their balance. In other words, it was assumed that there were rotary actuators at the ankle, knee, hip and shoulder joints. Naturally, the torques that were generated by rotary actuators were assumed to be equal to torques that were generated by related muscle group. The motions of the body members (shank, thigh, and trunk) are described by the angles $\theta_{sh}(t), \theta_{th}(t)$ and $\theta_{tr}(t)$. They are the measures of deviation from the vertical axis $\vec{u}_3^{(e)}$ so the differential equations were derived based on these angles (the detailed derivation is given in Appendix A). $\theta_p(t)$ represents specified disturbance, d_h and d_v are constant values that depend on dynamic of the tilt platform. Lastly, C_{sh}, C_{th} and C_{tr} are mass centers of the segments. Averaged anthropometric measures are model-based in this study. For instance, the mass and inertia of the segments of the human body are calculated by using the model in [121] (see Appendix B in detailed). The length of the segments and the length and position of the center of mass of segments are found the values for the parameters in the model in [116]. In summary proposed model can be represented as,

$$M(\theta)\ddot{\theta} + V(\theta, \dot{\theta})\dot{\theta} + D(\theta, \theta_p, \dot{\theta}_p, \ddot{\theta}_p) + G(\theta) = Q \tag{4.1}$$

Where $\theta = [\theta_{sh} \quad \theta_{th} \quad \theta_{tr}]^T$ and M is square mass matrix; V is a square matrix which represents the effects of the centrifugal and Coriolis forces; D is a vector dependent on external perturbation, G is a vector of gravity dependent terms and Q generalized torques which can be shown as,

$$Q = \begin{bmatrix} T_A - T_K \\ T_K - T_H \\ T_H \end{bmatrix} \tag{4.2}$$

CHAPTER 5

PROPOSED CONTROL LAW TO MODEL AUTOMATIC POSTURAL RESPONSES

In this chapter, a control law is conjectured in order to model the automatic postural responses of human beings to sudden external disturbances. The chapter starts with a brief and specific literature review. Afterward, the main physiological elements participating in human postural control are briefly reviewed, including the central nervous system, the peripheral nervous system, and the musculoskeletal system. In section 5.3, it is discussed the main basis of the conjectured control law as depending on the examination of experimental data. It is expected to be easier to understand the selections and assumptions about control law with the following four subsections. Then, the schematic representation of proposed postural control law is constructed. Finally, conjectured control law is defined mathematically.

This chapter can be summarized with three main steps as follows. The first step is to explain the observed behavioral pattern under the given external disturbance. For this purpose, experimental data is examined again for attaining the key ideas about the nature of control. Behavioral patterns mean that balance-recovery responses have individual specificity. This observation is supported by [38]. It has been claimed that automatic postural responses depend on adjustable postural strategies and synergies [38]. This adjustment is realized by central nervous system for an upcoming event based on initial conditions, prior experience and expectations [38]. The second step is to understand the other important observation that there is diversity between initial and final body conditions. However, there is no correlation between body configurations. The selection of the body configuration seems to be arbitrary.

Finally, the third step is to conjecture the control law that handles the reaction to an external disturbance.

In the lights of these observations, control law can be considered as PD control. It is based on the idea that feedback gains that are producing joint torque commands as a function of body movement have been claimed in [54, 84]. However, it is the hypothesis of this thesis that the feedback gains are time-varying and these gains are managed by CNS. According to the second observation, it has been proposed time-dependent upright reference angles (θ_{ref}). It has been claimed that the difference between the desired upright body segment position and sensed position is the main dynamics of producing the torque on muscles. And these differences are tried to be eliminated by feedback at the feedback control models [28, 59, 73].

5.1 Literature Review

In this literature review section, three important questions are answered basically. The essential issues can be listed as follows:

1. Why is the PD control strategy selected to model the human neural control? Why is not optimal control?
2. Why must the feedback gains of the PD control be time-varying? What is the analogy between time-varying gains and adjustable muscle synergies?
3. How can we prove that the difference between the actual and desired body configuration are main dynamics to generate torque. Has similar experimental evidence ever been found by others?

5.1.1 Why is the PD Control Strategy? Why is not Optimal Control?

PD control strategy can be considered as the most elementary control law, which is probably used even by the most primitive creatures. Besides its simplicity, it is the most convenient to simulate the behavior of the system, because measured bodily control signal depends on both body position and velocity [49]. The most referenced criticism to PD control strategies for using as postural control model is instability problem for large delay magnitudes. However, there are many studies against the great renowned criticism [49, 70, 71]. Fig.5.1 shows that the PD control model is near optimal for time delays of about 100 ms or less. In this thesis scope, the maximum delay for automatic postural responses is under these limits [38]. Additionally, time-varying control gains can be a solution to the instability problem depending on longer time delays.

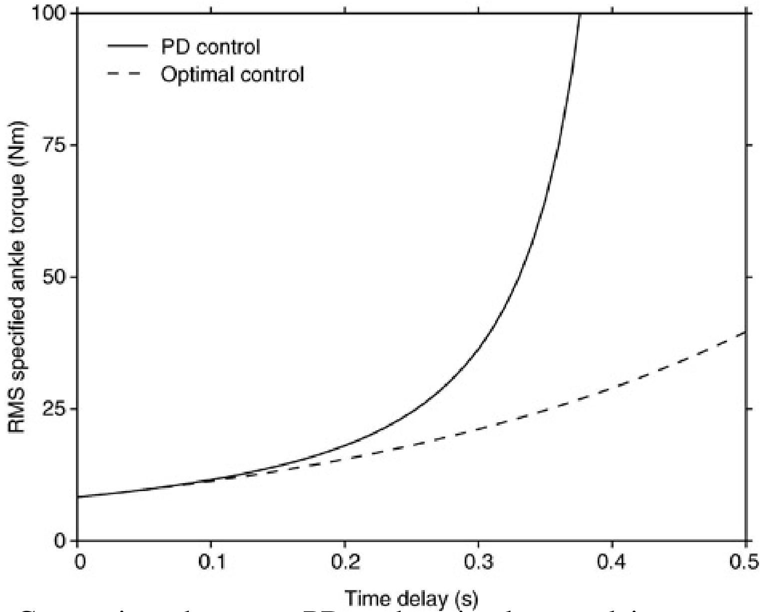

Figure 5.1: Comparison between PD and optimal control in terms of time delay (Quoted from [49]).

On the other side, optimal control is criticized for many ways. For instance, the optimal control can be applicable with satisfying some principles given below but these are not true for biological organisms, likely. [63] has listed these principles as follows.

(i) A single, known cost function to be optimized,

(ii) An invertible model of the plant, and

(iii) Simple noise interfering with optimal performance.

In addition to these structural criticisms, In [63], it is claimed that the motion of a biological organism cannot be globally optimal. The reasons are shown as "physical limits of the body" and "trial-and-error learning mechanism". These reasons lead to a good enough solution rather than the globally optimal solution. A biological organism prefers a robust solution rather than the optimal solution. Therefore, the evolution of the organisms is probably based on the robustness criterion instead of the optimality criterion.

There is another major criticism for an optimal control law due its *algorithmic complexity* and *heavy computational load*, which cannot be expected to be achievable by a biological organism.

Beyond this discussion, this thesis does not claim that the PD control is the real neural control. However, due to its simplicity, it is a useful tool for understanding some complex aspects related to the modulation of postural control. At this point, it can be expressed that, at all levels of the CNS, the noises and time delays are assumed to be ignorable in the conjectured control strategy, for the sake of simplicity. The main justification of this assumption is the improving effect of the sensory fusion process, which involves the somatosensory, proprioceptive, vestibular, and visual senses.

5.1.2 Time-varying Feedback Gains

The central nervous system (CNS) plays a major role in the balance-recovery control process [38, 42, 84]. Depending on given information, the gains of the PD control must be adjustable, if it is needed.

Naturally, an explanation is required about the adaptable gains which are the main idea of this section. For this purpose, it is consulted to two important sources. One is [84] that time-varying gains are mentioned first as an idea there. The study as mentioned above has strengths and weaknesses. Therefore, its weaknesses are handled for improvement in this thesis. The other is [103] that it is the theoretical basis of the time-varying gains idea.

In [84], feedback gains are producing joint torque commands $u = K(x - x_{ref})$ as a function of body movement x. Where $x = [\theta_{ank}, \theta_{hip}, \dot{\theta}_{ank}, \dot{\theta}_{hip}]^T$ is state information and "ank" and "hip" represent ankle and hip joints, respectively. θ_{ank} and θ_{hip} have been measured relative to upright vertical position. K is the (2x4) feedback control gain matrix, and x_{ref} is the state corresponding to the upright reference position.

The movement of body has been measured by the body sensors. Sensory information has been processed by the central nervous system to estimate the positions and velocities of the body segments. Then this information have been fed to back for using to generate the compensatory joint torque commands u. [84] is related with selection of K conveniently. This process is realized by the CNS in accordance with biomechanical constraints and body dynamics. In their model, sensors and sensory processing have not been studied intentionally.

Park's model has underlined the linear scaling of the time-invariant feedback gain values concerning the magnitude of the perturbation. Park has minimized error measured and simulated angular position and velocity of the links by using a least-squares optimization. As a result, Park showed that the feedback gain values "gradually" scale with the magnitude of the perturbation. There are some weaknesses as well as its important contributions.

Common weaknesses of [84] can be summarized as follows.

- The body dynamics may be represented with double inverted pendulum but it is the fact that increasing the degree of freedom increases accuracy. In our experiments for all trials, knee motion is observed.
- The other important limitation of this study is the use of LTI (linear time invariant) gain set.
- The other limitation is that they don't care about deviation from the equilibrium position. (i.e., they ignore the fact that the final positions of the subjects differ from their initial positions)

According to [84], feedback gain values scale with the magnitude of the perturbation. According to the evaluation of the experimental data, it is thought that feedback gain values may not be only related to perturbation but also may be correlated with changing the position and velocity of the body. Similarly, but more specifically, [99, 103] states that intertrial variability in muscle activation patterns show that the desired task-level biomechanical functions are produced by modulating the activity of the various muscle synergies.

According to[103], the contributions of each muscle synergy may be modulated by descending influences on postural strategy regulated through sensory feedback to perform motor behaviors. In summary, corresponding to this statement, *feedback control gains are* determined as *time-varying* for the conjectured control law.

5.1.3 Difference between the Actual and Desired Body Configuration

In [84], x_{ref} is defined as constant and it represents the state corresponding to the upright reference position. At the scope of this thesis, the second distinction from [84] is related to the definition of the upright reference position. It is again based on experimental observation that subjects have found their balance for each trial, but their body segment positions differed from their initial positions. This observation causes a necessity to explain with the difference between desired position (θ_{ref}) and measured or sensed position. At this point, it has been hypothesized that upright reference body angles may also be modified by CNS. However, according to observations (see 5.3 section), desired upright references are changing quite slowly from initial value to the final equilibrium value. Therefore, it is thought that, the selection of the desired body configuration can be defined as a time-dependent gradually changing curve. It may also depend on the sensory feedback information. However, in this study, it is only defined time-dependent for simplification. At first 50 ms, (θ_{ref}) is equal to initial value of the experimental data. In that time, the subjects are supposed to be standing without moving. Because a drift is observed at the tilt direction. It is assumed (θ_{ref}) changes between the initial and final position linearly during the external disturbance that takes 600 ms. After the effect of disturbance, subjects adjust their body position which is assumed to be equal to final experimental positions.

This difference between desired position (θ_{ref}) and measured or sensed position has been claimed that it is the main dynamics of the producing the torque on muscles. At the feedback control models, sensed error between desired and actual forces are tried to be eliminated by feedback [79, 73, 28]. In [25], it has been stated that the muscles and reflexes generate position- and velocity-dependent responses that resist deviations from the initial posture if they are elicited by external perturbations. It has also been stated that this fact can be explained with equilibrium point theory. The basis of this theory can be explained with an example. Let us think a robot arm which is replaced each of motors with a pair of opposing rubber bands. In this case, if the robot arm is released free, its position is the equilibrium point of the system. Now, if the length-tension properties of the rubber bands are changed, the equilibrium point of the system will change. Muscles share the same property with rubber bands.

Muscles generate the forces depending on the length changes. The greater the length is the greater the force. Motor neurons are activated by commands from the brain or/and the spinal cord. The activations received by motor neurons can change the force-length relation for each muscle. This muscle length changes cause to change in the equilibrium position of the system [79].

5.2 Physiological Basis of Proposed Control Law

In this section, physiological circuits and responsibilities of higher brain structures are explained briefly. Much knowledge and sense go to the higher brain directly, for example, sensory information, knowledge of the environment, etc. Some of the senses do not go to higher brain directly, but higher brain always observes the all structures. Today, the role of the higher brain structures is accepted widely. For instance, in [69], it has been declared to reach a consensus on the precise role played by the cerebellum in movement control. Similarly, [98] emphasizes the plasticity of the sensorimotor system, particularly the spinal and supraspinal structures. It exemplifies neurophysiological adaptations caused by balance training and their effect on motor behavior. [48] presents almost the same way with the first two examples that cerebral cortex is partly responsible for modifying forthcoming postural responses to external perturbations. In [48], it is concluded that cortical activity before an externally triggered perturbation is related with modifications of the resulting postural response.

Explanation of the physiological circuits and responsibilities of higher brain structures is a very hard issue. For the sake of the integrity, this issue is summarized from [47].

Fig.5.2, which has been presented in [47] originally, shows a simple model of the neural loops taken part in automatic postural response. According to [47], balance-recovery reactions evoked by external disturbance consist of short-, medium- and long-latency responses. Short-latency response represents a mono- or oligo- synaptic spinal circuit depends on the initial conditions surrounding the perturbation. Its existence can be a proof of the spinal cord's contribution to the postural response. Moreover, this contribution is too small short-latency response has minimal effect on stabilization of the balance. Therefore, spinal-mediated short-latency response is excluded from automatic postural response because of its non-functional effect. Stabilization of the balance under the effect of external disturbance provides with muscle synergies including the medium-latency and long-latency responses. As mentioned earlier, it is referred to as the automatic postural response.

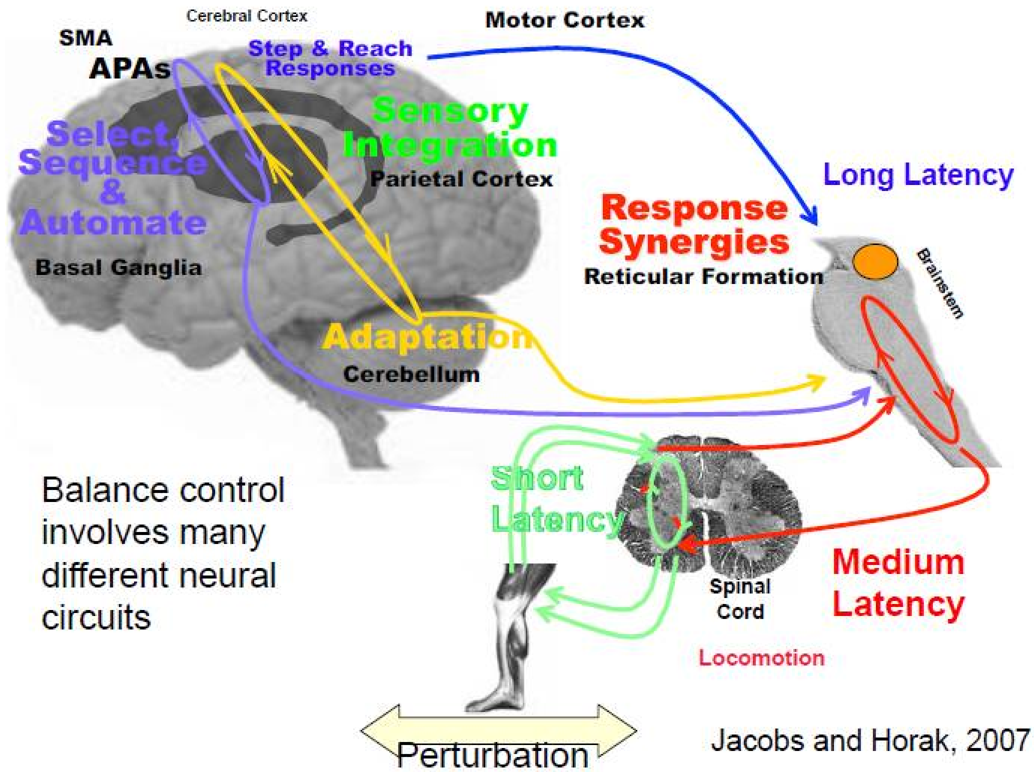

Figure 5.2: A simple model of proposed neural pathways involved in the cortical control of short, medium and long latency automatic postural responses to external perturbations. (Quoted from [47])

In aforementioned study, it is suggested that the initial response to the external perturbations likely arises from the brainstem instead of the cortex. After the earliest part of the postural response, cortical circuits is recruited that it is likely responsible for shaping the postural response. Cortical loop is composed of the cerebellum, the parietal cortex and dorso-lateral premotor cortex. The cerebellum receives somatosensory input from the spinal cord, motor information from the cerebral cortex, and input about balance from the vestibular organs of the inner ear. It is important for maintaining posture and for coordinating head and eye movements. The cerebellum is also involved in fine tuning the movements of muscle and in learning motor skills. Balance recovery reactions need to be fast, the earliest phases are most automatic with peripheral sensory input triggering synergies pre-set in the brainstem, whereas the later phases of the same responses are less automatic and can be modified to accomplish goals involving cortical loops (for more information turn back to section 2.2.1).

5.3 The Results of Examination of Experimental Data

The analysis of the experiments has provided an important foresight to judge accurately balance-recovery responses of subjects. It is observed that all participants have shown approximately the same reactions that can be specified individually. This fact referred to as behavioral patterns. The other noticeable feature is the deviations from the initial and final positions. This observation is the basis of the time-varying upright body configuration ($\theta_{ref}(t)$). However, there is no correlation between the initial and final reference angles. The selection of the initial and final condition is likely arbitrarily. All items are discussed below more extensively.

5.3.1 Behavioral Patterns; Individual Specificity for the Balance-Recovery Responses.

Observation, which is called as behavioral pattern, is convenient with literature in terms of changing of the patterns with perturbation directions and magnitudes [42] and relation with the physique of the subjects [58].

Naturally, experimental data includes only kinematic data; it is not muscle activation pattern. However, there is a cause-effect relation between kinematic data and muscle activation data. These patterns can be represented modulation of the postural synergies, which depend on the bodily and environmentally acquired sensory information transmitted to CNS. Fundamental basis of behavioral patterns have been formulated by [94]. They have been paraphrased as follows.

- Patterns of behavior are determined by inner states. It causes persistence of the patterns over time and under changing conditions.
- It is the definition of the state variables that are the smallest set of the system variables such that knowledge is necessary and sufficient to determine the behavior of the system. Sensory and motor information within a neural network generates the state variables. Evaluation and integration of the state variables can be modeled as a dynamical system, which is affected many factors. Physical dynamics of the body, material properties of the body,

material properties of the environment, sensory inputs with internal sensory feedback are some of these factors.

- The nervous system is extensively interconnected with variable sensory inputs and the complex and temporally variable natural environment.

- Complexity of the behavior may be generated from stable and unstable linear or nonlinear dynamical structures.

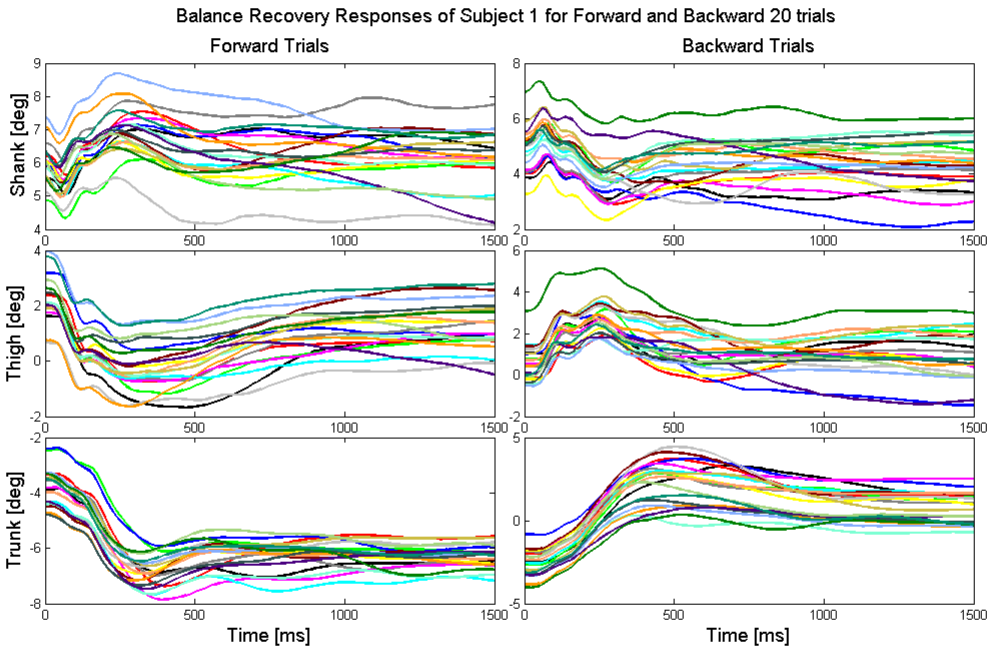

Figure 5.3: Behavioral pattern of Subject 1

In Fig.5.3 and Fig.5.4, the behavioral pattern of subjects for an experimental set that contains 20 trials for forward and backward directions can be seen. Each color represents a trial. The angles of the shank, thigh and trunk that deviate from vertical are shown in the graphs. In Fig.5.3 and Fig.5.4, the very first noticeable feature is that they are quite different from each other. This fact can be referred to as the individual specificity of the balance-recovery responses. Although they are very different interpersonally, all trials forward and backward directions distinctly are similar to each other.

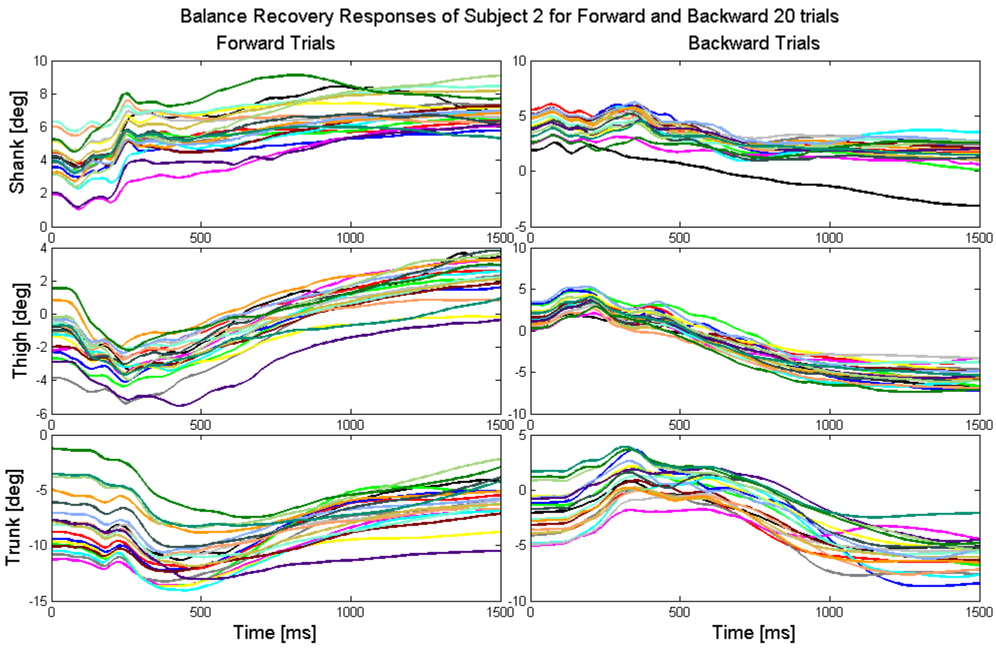

Figure 5.4: Behavioral pattern of Subject 2

The transient phase for all trials last about 500 ms. Additionally, they resemble each other significantly. It can be thought that the responses can depend on the state variables such as initial posture, perturbation magnitude and changing of the body configurations. However, there is a noticeable difference in terms of direction between forward trials, which are seen at the left and backward trials, which are seen at the right. For time-varying gains hypothesis, it is the biggest reason that any trial do not success to produce the same results.

When Fig.5.3 and Fig.5.4 are inspected, two more important features can be noticed. The first noticeable feature is the deviations from the initial and final positions. The second noticeable feature is the difference between the first (black) and other trials. Although it is out of the scope of this study, it must be mentioned from diversity between the first trial and others. This observed effect is an issue widely studied. For instance, [97] has explained that first trial responses appear to consist of movement strategy imposed on an adapted response strategy. They have also stated that it is a failure of the CNS to weight properly lower leg proprioceptive and vestibular inputs.

5.3.2 Diversity Between Initial and Final Body Configuration

Detailed view of Fig.5.3 and Fig.5.4, it can be seen that there is no correlation between the initial and final body configurations. Thus, the deviation between the initial and final positions has been thought that the reference angles (or body configurations) may be changed by CNS. This hypothesis will be one of the main components of the suggested control law. The mean of diversity between the initial and final value is that the desired posture changes during the balance-recovery reaction time. The perception of upright being may change depending on feeling comfortable in the balance after each trial. For example, subjects do not mind the position of the shank up to 2- 3 degrees. They only want to feel comfortable in the upright position and in the balance.

Therefore, desired angular positions (θ_{ref}) have to define depending on time. For this purpose in this study, θ_{ref} has been defined as the following procedure: at first 50 ms, θ_{ref} is equal to the initial value of the experimental data. In that time, the subjects are supposed to be standing without moving. Because of observed drift in the tilt direction, it is assumed that θ_{ref} changes between the initial and final position linearly during the external disturbance that takes 600 ms. After the effect of disturbance, subjects adjust their body position that is assumed to be equal to final experimental positions.

5.3.3 Uncorrelation Between Initial and Final Body Configuration

If there were a correlation between the position of the body segments in the initial and final configuration, it would not be needed to define a hypothetical desired upright body configuration in the previous section. Instead, it could be defined a function between the initial and final configurations. Table.5.1 shows the uncorrelation between the associated displacements of the body segments.

Table 5.1: Uncorrelation between initial and final body configuration

	Subject 1		Subject 2	
	Forward Tr.	Backward Tr.	Forward Tr.	Backward Tr.
Shank	0.3269	0.6399	0.2732	0.5204
Thigh	0.6080	0.5135	0.3673	-0.2357
Trunk	0.3619	0.7898	0.6002	0.4938

Correlations are calculated using the initial and final limb angles with respect to gravity vertical that can be seen in the Appendix-D.

5.3.4 Arbitrariness at the Selection of the Initial and Final Body Configuration

The body configurations may be crucial for balance-recovery reactions. However, there is not any correlation between the initial and final configurations. It is almost impossible to say anything about the selection of the initial and final body configurations by CNS. However, the experimental data shows that a different selection of the body configuration leads to a different response to the perturbation. The reasons of selecting different body configurations and their effects on the balance-recovery reactions have not been revealed yet. There are many favorable [109] and unfavorable [78] studies on the initial body configuration and its effects on the balance-recovery reactions. Until this issue is enlightened, for the time being, it will be assumed in this study that the initial and final configurations are determined by CNS arbitrarily.

5.4 Simplified Schematic Representation of CNS as a Controller

In this thesis, it is hypothesized that higher brain structures are responsible for balance-recovery reactions. Just before, not given the mathematical expression of the conjectured control law, the contribution of the higher brain structures to balance-recovery reaction is the topic of this section. Therefore, physiological structures and their responsibilities are explained briefly and shown schematically in Fig.5.5

The CNS including the spinal cord, brain stem and higher brain structures (cerebellum, basal ganglia and cerebral cortex) are used for achieving the balance-recovery action. The relation between the higher brain structures are very complex, and information flows between them via thalamus. Therefore, due to the simplicity principle, it is not shown in Fig.5.5. The spinal cord receives sensory information from the skin, joints, and muscles of the trunk and limbs; besides, it contains the motor neurons responsible for both voluntary and reflex movements. Brain stem contains ascending and descending pathways that carry sensory and motor information to other divisions of the central nervous system [52]. The cerebellum receives somatosensory input from the spinal cord, motor information from the cerebral cortex, and input about balance from the vestibular organs of the inner ear [52]. They are important for maintaining posture and for coordinating head and eye movements. The basal ganglia have four nuclei which have an important role in the control of motion [52], but there is no direct transmission between the basal ganglia and the spinal cord. The nuclei of basal ganglia receive their primary input from the cerebral cortex and send their output to the brain stem [52]. Surface of the cerebrum is called as the cerebral cortex which has many areas concerned primarily with processing sensory information or delivering motor commands [52].

Generally, muscles and tendons are classified in the peripheral nervous system, but in Fig.5.5, they are added to the central nervous system for simplification of the control algorithm. Thus, control input u can be defined as generalized torque (Q).

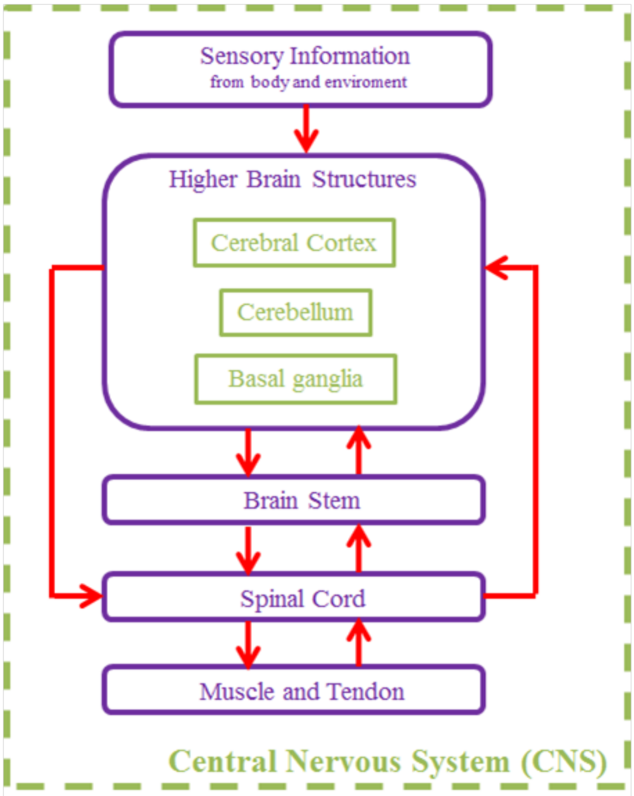

Figure 5.5: Simplified schematic representation of CNS as a controller.

5.5 Definition of the Control Law Mathematically

The above-mentioned physiological structures have been placed inside the green lines on the block diagram in Fig.5.6. The output of the CNS, motor command u is the control input for the musculoskeletal system in Fig.5.6.

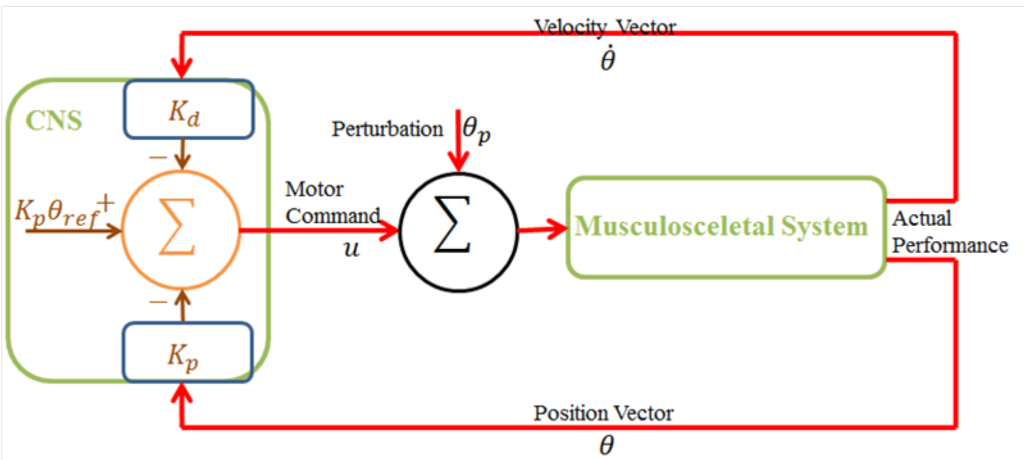

Figure 5.6: Simplification of the balance-recovery reaction as a block diagram.

θ and $\dot{\theta}$ describe augmented position and velocity vectors of the member with respect to the inertial frame under the assumption of perfect sensors (This conjecture will be discussed in the following sub-section). Selected strategy and muscle synergies may be modulated by CNS. Therefore, feedback control input u can be represented for simplification as

$$u = K_p(t)\left[\theta_{ref}(t) - \theta\right] - K_d(t)\dot{\theta} \tag{5.1}$$

where the proportional and the derivatives gains are defined as

$$K_p(t) = \begin{bmatrix} k_{1p} & 0 & 0 \\ 0 & k_{2p} & 0 \\ 0 & 0 & k_{3p} \end{bmatrix} \tag{5.2}$$

and

$$K_d(t) = \begin{bmatrix} k_{1d} & 0 & 0 \\ 0 & k_{2d} & 0 \\ 0 & 0 & k_{3d} \end{bmatrix} \tag{5.3}$$

$K_p(t)$ ***and*** $K_d(t)$ ***are the time-varying feedback control gain matrices.*** Actually, non-diagonal terms which appear to be zero in the matrix $K_p(t)$ and $K_d(t)$ are not zero. It is known that muscles which pass through two joints have affected each of joints in a certain percentage, but their contribution to the stability of the body was found very little [48]. Therefore, they are neglected. The presence of non-diagonal terms increases the computational load, consequently, the recommended method to determine parameters that cannot be used without the mentioned neglect. It will be shown by simulations that the neglect of the non-diagonal terms does not have a dominant effect. It is known that feedback control gains are selected by the CNS via taking sensory information that have originated from the body and environment, previous experiences and expectations and adaptation processes into account. The selection of gain matrices effectively determines the postural response strategy. ***Similarly,*** $\theta_{ref}(t)$ ***is the upright reference position which depends on time.*** It is observed that the upright reference position changes with respect to the desires and the expectations of the human. Lastly, $\theta = \begin{bmatrix} \theta_{sh} & \theta_{th} & \theta_{tr} \end{bmatrix}$ and $\dot{\theta} = \begin{bmatrix} \dot{\theta}_{sh} & \dot{\theta}_{th} & \dot{\theta}_{tr} \end{bmatrix}$

It is known that this study is focused on to define a control law for human balance recovery reactions under the relatively big sudden external disturbance. In this study, the time scale of human responses is enormously larger than time constants of the inner dynamics of sensors and actuators. Therefore, their dynamics can be neglected, so they are assumed perfect.

Conjectured control law is constructed on the three main assumptions. They can be listed as feedback gains are used in principle axis, all sensors and actuators are assumed perfect and time delays are not included the model.

5.5.1 Feedback gains are Used in Principle Axis

In the current study, feedback gains are used in principle to indicate the sending signals to the muscles. These signals are multisynaptic and feedback to both agonists as well muscles that cross other joints [11]. It means that a group of muscles can act to two joints, but the contribution of all others than the major gains to the control of the body was found very little [84]. Therefore, gains can be assumed to be independent of each other. Thus, three rotational actuators in the mechanical model are driven by the same control law but they are assumed to be driven independently from each other.

5.5.2 All Sensors and Actuators are Assumed Perfect

The same way, a further simplification can be made that all sensors and actuators can be assumed perfect. However, naturally, uncertainty arises at all levels of this process [24]. On the top of that, the central nervous system has knowledge of its own sensory and motor uncertainty, as well as it learns to cope with these uncertainties over time [82]. Additionally, the error sensitivity of the actuator is assumed as perfect. Since, in [77], which have presented a computational model of limb impedance control, it is stated that uncertainty in the optimal motor plan that results from uncertainty in model parameters is compensated by co-contraction. Additionally, the highly accurate movement of the human has been reported [13, 23].

5.5.3 Delays are not Included the Model

Naturally, there are the time delays in CNS feedback control. However, in this study, all level time delays are neglected. These distinct time delays are sourced from mechanical stiffness, spinal reflexes, and longer feedback loops. All of them have different time constants. It is almost impossible to model all delays realistically. Additionally, it is not necessary for identification of the possible control law in terms of generality and simplicity.

Simulations, which are presented in the next chapter, show that all assumptions and neglects are not affect general conclusions of this study.

CHAPTER 6

COMPARISON OF SIMULATION RESULTS WITH EXPERIMENTAL DATA

In this chapter, the conjectured control law has been tested through detailed simulations on a 3 DoF biomechanical model. Then, these simulations have been compared with experimental data. This chapter is composed of three sections; the first two components include the preparation statements for simulations, which have been used for verification of the suggested control law. These sections are called as identification of the feedback gains and determination of the body reference angles. The last section includes simulations and it is called as verification of investigated control law.

6.1 Identification of the Feedback Gains

According to the current literature review, [84] is one of the remarkable model-based control studies about balance-recovery reactions. They have been attempted to find a set of feedback gains by using sequential quadratic programming algorithm. In the aforementioned study, their aim was to explain the relation between the human response and the magnitude and speed of the perturbation were tried to find a set of feedback gains. They have given used numerical analysis method as follows.

An optimization technique has been used to describe the postural response strategy in terms of the feedback parameters. The objective was to minimize the sum-squared, normalized deviations of the model states x_{sim} from the experimental data x_{exp} and the model torques u_{sim} from the data u_{exp}:

This part is adapted from [84]

$$J(K) = \sum \delta x^T Q \delta x + \delta u^T \delta u$$

where $\delta x = (x_{exp} - x_{sim})/|x_{exp}|$, $\delta u = (u_{exp} - u_{sim})/|u_{exp}|$ and the summation occurs over samples of recorded data. The Q matrix was used to weight the relative contributions of errors in state and control and was chosen to be $Q = 0.01 I^{4x4}$ where I is the identity matrix. This places equal weighting on all states relative to each other, with the overall scaling factor of 0.01 chosen to place some weighting on matching experimentally-derived joint torques. One constraint was placed on the optimization, requiring a stable closed-loop system, i.e., eigenvalues of the system matrix having non-positive real parts. Therefore, the constrained optimization problem is written mathematically as follows:

$$\min_K J(K) \text{ subject to } Re\{eig(A - BK)\} \leq 0$$

They said that we had to repeat optimization several times using random initial guesses for K (feedback gains matrix), to check for local minima in the optimization.

To summarize again, Park's model has underlined the linear scaling of the time-invariant feedback gain values concerning the magnitude of the perturbation.

Park has minimized error measured and simulated angular position and velocity of the links by using a least-squares optimization. However, the results of conducted experiments in this thesis scope show that the responses of the subjects could differ without changing the magnitude and speed of the perturbation. The most important inference drawn from these experiments, CNS may not only select the suitable strategies but also may modulate the strategies by changing postural feedback gains and desired upright reference. Therefore, (See Chapter 5 for details) feedback gains are defined as time-varying. These time-varying adaptive gains can be identified by using following least-square method.

6.1.1 Least Square Method for Parameter Estimation

The method has been suggested in [50] and it has been called as automatically adjustable variable-length sliding-window blockwise-applied least squares (LS) method. This method has been applied for identification of time-varying adaptive gains as follows. The equation, which is shown below,

$$M(\theta)\ddot{\theta} + V(\theta,\dot{\theta})\dot{\theta} + D(\theta,\theta_p,\dot{\theta}_p,\ddot{\theta}_p) + G(\theta) = Q \tag{6.1}$$

can be evaluated with subject's kinematics data, the kinematic data of support surface perturbation platform and the other model parameters such as the mass and inertia of the segments of the human body and length and position of the center of mass. Control torques can be found for each data point. With the assumption given above, joint torques are equal to control torques.

$$Q = u = K_p(t)\left[\theta_{ref}(t) - \theta\right] - K_d(t)\dot{\theta} \tag{6.2}$$

In this case, all components of Eq.6.2 except the control gain set can be known. Eq.6.2 can be written widely as follows:

$$u = \begin{bmatrix} u_A \\ u_K \\ u_H \end{bmatrix} = \begin{bmatrix} K_{1p}(t)\left[\theta_{shref}(t) - \theta_{sh}\right] - K_{1d}(t)\dot{\theta}_{sh} \\ K_{2p}(t)\left[\theta_{thref}(t) - \theta_{th}\right] - K_{2d}(t)\dot{\theta}_{th} \\ K_{3p}(t)\left[\theta_{trref}(t) - \theta_{tr}\right] - K_{3d}(t)\dot{\theta}_{tr} \end{bmatrix} \tag{6.3}$$

In 6.3, "sh", "th" and "tr" represent shank, thigh and trunk respectively. Similarly, "A", "K" and "H" show ankle, knee and hip. For each component of the column vector u can be written as follows.

$$u_A = \left[\begin{array}{cc} \theta_{shref}(t) - \theta_{sh} & -\dot{\theta}_{sh} \end{array} \right] \left[\begin{array}{c} K_{1p}(t) \\ K_{1d}(t) \end{array} \right] \tag{6.4}$$

Eq.6.3 can be generalized and written as follows. In control torque expression (u_j), the subscript j can be equal to ($j = A, K, H$).

$$u_j = \varphi_j K_j \tag{6.5}$$

Eq.6.5 is called the regression model [44]. φ_i is the regression variable (with known value). φ is the regression vector (with known value). Regression variables consist of angular positions, the desired values of angular positions (θ_{ref}) and the angular velocities. K_j is an unknown gain coefficients column vector which includes proportional and derivative gains of the joint j. Assume that there are m corresponding values of u and φ. Then it can be written the following m equations according to the model:

$$\underbrace{\begin{bmatrix} u_1 \\ \vdots \\ u_m \end{bmatrix}}_{U} = \underbrace{\begin{bmatrix} \varphi_{11} & \cdots & \varphi_{1n} \\ \vdots & \ddots & \vdots \\ \varphi_{m1} & \cdots & \varphi_{mn} \end{bmatrix}}_{\phi} \underbrace{\begin{bmatrix} K_1 \\ \vdots \\ K_m \end{bmatrix}}_{K} \tag{6.6}$$

Eq.6.6 is a set of equations from which we will calculate or estimate a value of the unknown K using the LS-method. Prediction-error vector, $E = U - \phi K$, can be defined as the difference between the left side and the right side of Eq.6.6. At this point, the problem is to estimate a value of the unknown parameter-vector K so that the following quadratic criterion function, $V(K)$, is minimized:

$$V(K) = E^T E \tag{6.7}$$

Since $V(K)$ in Eq.6.7 is a quadratic function of the unknown parameters K, the minimum value of $V(K)$ can be calculated by setting the derivative of V with respect to K equal to zero: The result is

$$K = (\phi^T \phi)^{-1} \phi^T U \tag{6.8}$$

which is the LS-solution of Eq.6.6. All right side terms in Eq.6.6 are known. The sample data can be divided into many parts. Hence, $K(k)$ can be written alternatively as follows [50].

$$K(k) = (\phi_k^T \phi_k)^{-1} \phi_k^T U_k \tag{6.9}$$

When LS is applied to non-stationary environments, e.g. system identification and parameter estimation in the presence of unknown parameter changes, its performance is dependent on the true setting of the window length. For time-invariant systems, the longer the window length, the higher the estimation accuracy. However, the fast tracking of the changed parameters must be achieved for the system with abrupt parameter changes. Therefore, the window length should be adjusted accordingly so that the out-of-date information from the past measurements can be discarded effectively to assign a relatively heavier weight on the latest measurement [50]. Therefore, in this study, for improving the tracking capability of the algorithm was used variable-length sliding windows.

To select the length of the sliding window, proposed algorithms in [50] can be used, such as a change detection mechanism and a window length adjustment strategy.

Change detection mechanism:

Many algorithms have been developed to detect parameter changes [50, 8]. Taking account easily implementation, change detector was selected as given in [50]. This detector is based on the prediction error of the system within the sliding-window. Mentioned prediction error can be expressed as follows:

$$\varepsilon(k) = U_{k-L+1}^{k} - \phi_{k-L+1}^{k} K_L(k) \tag{6.10}$$

In Eq.6.10, L is defined as window length. Thus, $\varepsilon(k)$ is the prediction error that occurs in each step along the window that length is L. Averaged detection index given below is obtained as the sum of the squared prediction-error values are divided by the length of the window [50].

$$d(k) = \frac{1}{L} \sum_{i=k-L+1}^{k} \varepsilon^T(i)\varepsilon(i) \tag{6.11}$$

Parameter change detection mechanism can be expressed by the following equation; where ρ is a predefined threshold value.

$$\begin{aligned} d(k) > \rho \Rightarrow H_1 \\ d(k) \leq \rho \Rightarrow H_0 \end{aligned} \tag{6.12}$$

According to Eq.6.12, if detection index does not exceed the pre-set threshold value ρ, then the decision is H_0 that means "No change in the system parameters". On the contrary, if detection index exceeds the pre-set threshold value ρ, then it is H_1 that means "Parameter changes have occurred in the system".

Window length adjustment strategy:

In the problem which is described in this thesis scope, transition phase (first 600 ms) is very important. Therefore, window length adjustment strategy has been changed a little. Original strategy can be seen in [50]. The changed strategy aimed to show the best correlation in transition phase. According to defined new window length adjustment strategy, first 600 ms window length is pre-defined as 100 ms. After 600 ms later, this pre-definition set to 500 ms. Additionally, if the decision of the change detection mechanism is H_1, then the pre-defined window length is divided by two and this process continues until to take the answer H_0. When answer is H_0, $K(k)$ is calculated and window is slid to forward as $k = k + L$.

6.2 Determination of the Body Reference Angles

Why do we need to define a time-varying reference position (θ_{ref})? In the previous chapter, it is mentioned some important experimental observations. One of them is that subjects have found their balance for each trial, but their final body positions differ from their initial positions. This observed phenomenon has been also found out in many experimental studies. According to the literature review, the central nervous system produces some effective strategies for trying to reduce the effects of the *unpredictable* perturbation [77]. The result of these strategies is kinematic variability that in human motion originates from some inevitable sources such as neuromuscular noise and environmental disturbances [76]. It is widely accepted that CNS forms an internal forward dynamics model to compensate for delays, the uncertainty of sensory feedback, and environmental changes [53, 118]. These internal and external uncertainties have stochastic characteristics [24]. However, it is stated that humans have the ability to learn not only the dynamics but also the stochastic characteristics of tasks, in order to optimally learn the control of a complex task [95]. The notion of internal model uncertainties becomes important for neuromuscular control during adaptation [77]. Therefore, each trial with the updated dynamics along the current trajectory is different from each other.

This literature review is an explanation of a variety of the initial and final configurations between trials. At this point, an embedded parameter in the model is required to represent this fact. The mentioned parameter is referred to as desired position (θ_{ref}). It has been claimed that the difference between the desired upright body segment position and sensed position is the main dynamics of producing the torque on muscles [28, 59, 73]. Additionally, the internal model is updateable with newly available training data from the limbs [77]. At this point, it has been hypothesized in this thesis that upright reference body angles may also be modified by CNS.

It is a fact that there are differences between the initial and final body configurations. However, there are contradictory studies on the relationship between the position of the body segments in the initial and final frames and the associated displacement of the body segments. Although [78] has stated that there is no relation between the initial and final body configurations, [109] has claimed that the body configuration at the instant of first stepping foot contact accurately predicted successful balance recovery after a backward postural perturbation. This thesis is in favor of the claim of the existence of the relation between initial body configuration and balance recovery responses (see chapter 8). However, it has been not found out a functional relation between the initial and final body configurations. Therefore, time-varying reference position (θ_{ref}) is suggested as follows. At first 50 ms, θ_{ref} is equal to the initial value of the experimental data. In that time, the subjects are supposed to be standing without moving. Because of observed drift in the tilt direction, it is assumed that θ_{ref} changes between the initial and final position linearly during the external disturbance that takes 600 ms. After the effect of disturbance, subjects adjust their body positions that are assumed to be equal to final experimental positions.

Simulation results can be used, in order to verify that proposed PD control with estimated variable gains and suggested upright reference (θ_{ref}) are capable of approximating reality. It is said that conjectured control law for human balance-recovery reactions are produced by CNS with time-dependent feedback control gains, i.e., $K_p(t)$ and $K_d(t)$, along with a time-dependent upright reference position, i.e., $\theta_{ref}(t)$. However, $\theta_{ref}(t)$ depends on the initial state as well.

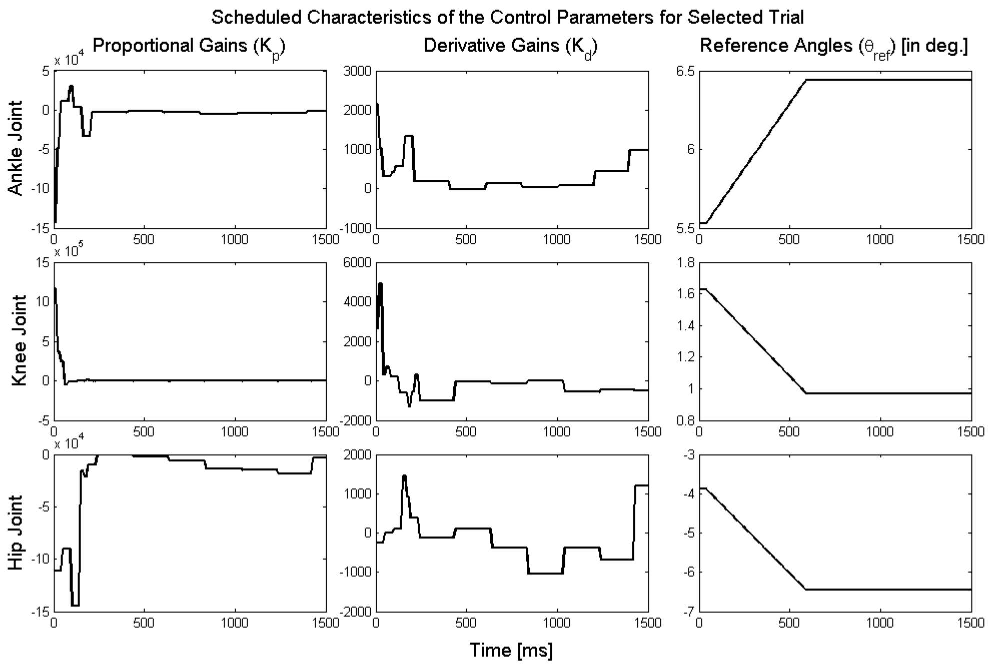

Figure 6.1: Scheduled Characteristics of the Control Parameters for Selected Trial (Using LS method).

The time-dependent feedback control gains and upright reference position of the first forward trial of Subject 1 can be seen in Fig.6.1. In the first two columns, scheduled characteristics of the proportional and derivative gains are shown. Desired angular positions can be seen in the leftmost column. However, it has to be said that estimated control parameters are not unique. There can be many solutions. Multiple sets of parameters are possible as basically and mathematically. However, it is also true as physiologically. Conjectured control law implemented by the CNS depends on the appropriate selection of feedback control gains and the upright reference position. It can be based on the redundancy of the muscular apparatus. Therefore, the solution can be not unique and infinitely many muscle patterns can generate the same force output.

In the following section, first the justification of the selection of LS method is explained. Then, the validation of these found sets of parameters with LS methods for all trials can be tested with the achievement of the estimated parameters to fit the experimental data at the following sub-section. It is verified two different forms. First, simulation algorithm runs for all initial conditions measured during experiments. Second, random initial conditions, which are generated in compliance with experimental data, are used for simulations.

6.3 Verification of Investigated Control Law

It can be stated that there can be infinitely many solutions depending on the selection of $K_p(t)$, $K_d(t)$ and $\theta_{ref}(t)$. Estimated time-varying gains and upright reference angles set (they are shown in Fig.6.1) is only one of these infinitely many solutions. In Fig.6.2, simulation of the balance-recovery reactions with the estimated control parameters can be seen. In Fig.6.2, balance-recovery reactions of the shank, thigh and trunk are shown in terms of angular positions. These angles are absolute angles i.e. they are the deviation from vertical with respect to ground. Graphs are drawn on experimental data to allow comparison between them. It can be seen in the Fig.6.2 that simulations deviate from experimental data. The main reason for this deviation is the limitations of the LS method that is used to estimate the gains. These limitations can be exemplified as the determination of the predefined threshold value accurately for all intervals, or determination of the window lengths. Elimination of these limitations requires spending too much time and effort. Additionally, the characteristic of the proposed LS method turns to manual from automatic.

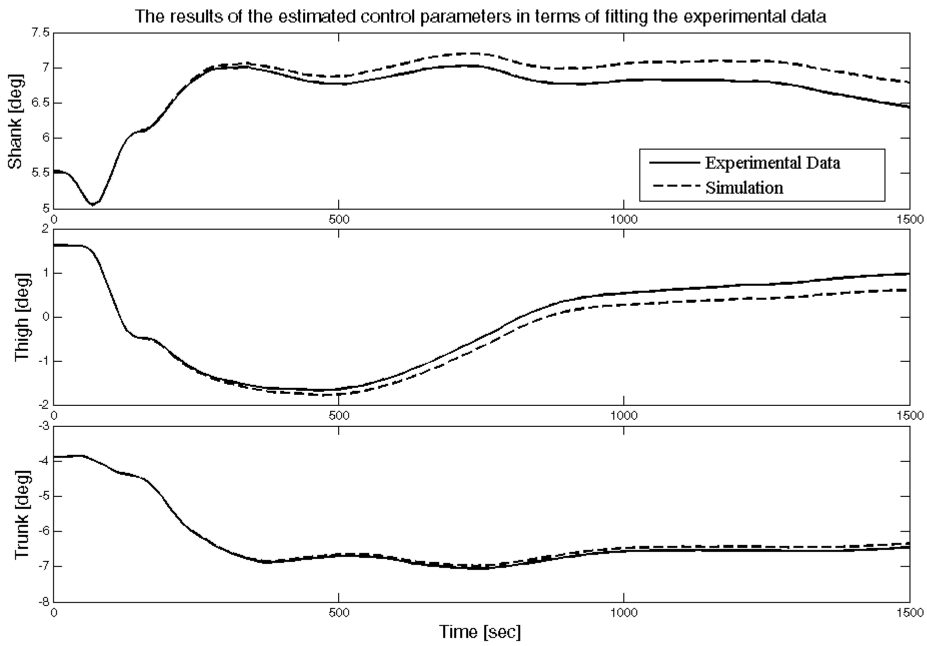

Figure 6.2: The results of the estimated control parameters in terms of fitting the experimental data.

6.3.1 With Identified Feedback Gains: Simulation with all Initial Conditions Measured during Experiments

In this study, a control law is conjectured in order to describe and simulate the automatic postural responses of human beings to sudden external disturbances. Conjectured control law has two original attributes different from previous studies [54, 84, 92]. These attributes are time-varying control gains and the concept of time varying upright reference angles. For the validation of the propounded control law including mentioned attributes, it has been evaluated through detailed simulations on a 3 DoF biomechanical model. In these simulations, time-varying control gains are identified with the automatically adjustable variable-length sliding-window blockwise-applied least squares (LS) method. Furthermore, the model is simulated for two different cases, which are used experimental initial conditions and random initial conditions.

Estimated time-varying feedback control gains and upright reference position (θ_{ref}) have been tested for their achievement in terms of fitting the experimental data. Fig.6.3 and Fig.6.4 illustrate the test results for all trials at forward and backward directions for two different subjects.

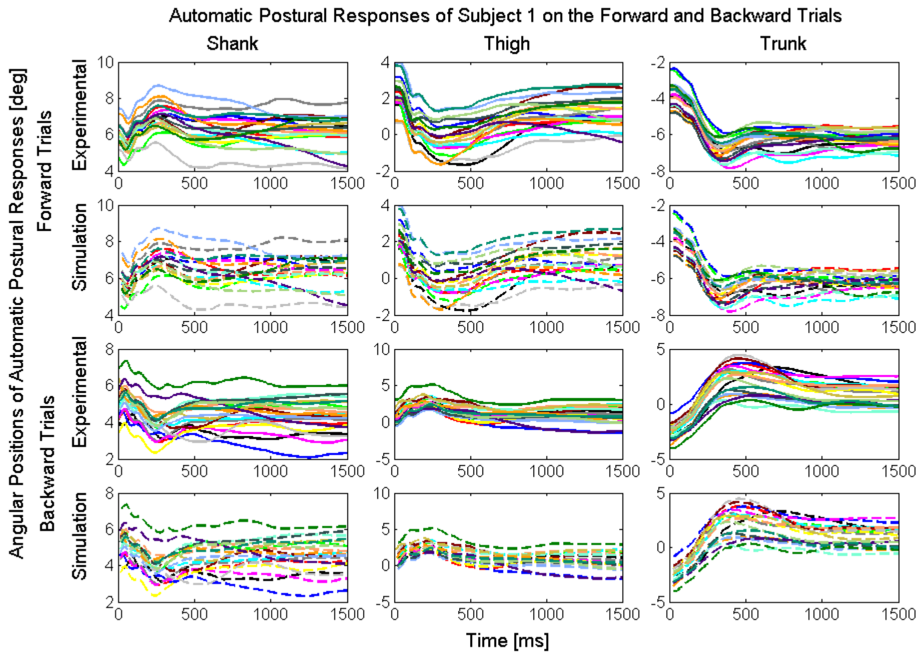

Figure 6.3: Automatic Postural Responses of Subject 1 on the Forward and Backward Trials.

Upper two rows show forward trials. Backward trials are also shown in the lower two rows. Experimental results of automatic postural responses of the shank, thigh, and trunk, are drawn with solid lines and each color represent a different trial. Dotted lines are used for representation of simulated data. The same way, each color represent a different trial. Illustrated angular positions are absolute angles i.e. they are the deviation from vertical with respect to ground. In those illustrations, it can be seen that simulated angular positions and experimental angular positions show the same behavioral patterns. It is very difficult to understand the differences between them. Therefore, the detailed analysis is required. These differences were analyzed in two ways such as the final value differences and root mean square deviation that measures the deviation between simulated data and experimental data. The detailed analysis is tabulated, and it can be seen in Appendix-E.

In Table.E.1, all trials for Subject 1, forward and backward, are assessed, final value differences and root mean square deviations are given. The maximum final value differences of forward trials are smaller than backward trials. Its maximum numerical value is $0.4695°$. Averaged final value differences are given as follows. For forward trials, they are $0.254°$ in the shank, $0.2325°$ in the thigh and $0.052°$ in the trunk. For backward trials, similarly but greater than forward trials, averaged final value differences for shank, thigh and trunk are $0.2796°$, $0.3548°$ and $0.1812°$, respectively.

Moreover, any significant variation between forward and backward trials in terms of root mean square deviations is not found. If they are expressed quantitatively for forward trials then averaged deviation from experimental data in the shank, thigh and trunk are equal to $0.0105°$, $0.0102°$ and $0.0025°$. Similarly, the same values for backward trials are $0.0093°$, $0.0117°$ and $0.0059°$.

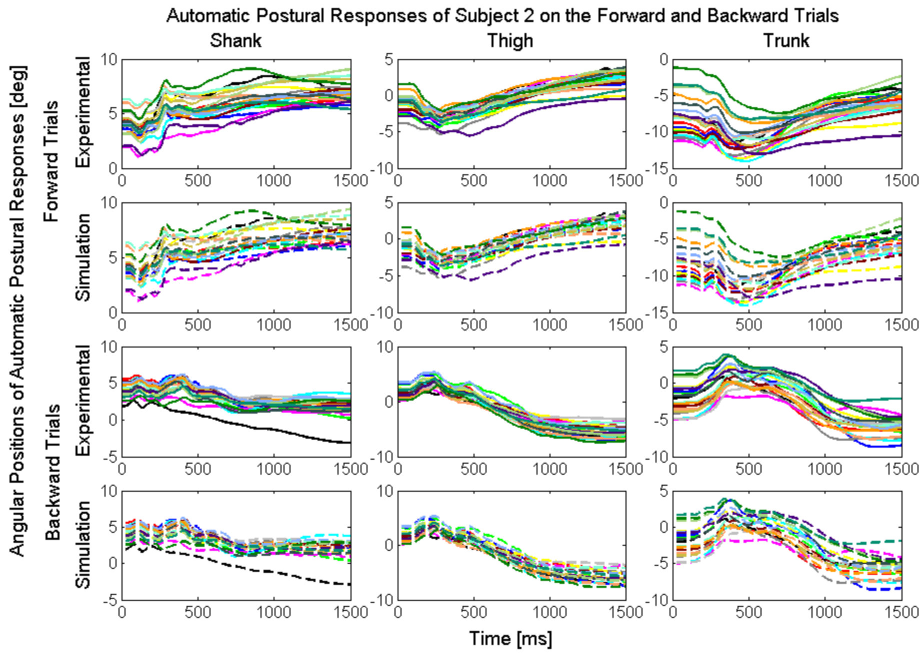

Figure 6.4: Automatic Postural Responses of Subject 1 on the Forward and Backward Trials.

Table.E.2 shows analysis of the simulations, depending on fitting the experimental data. All trials for Subject 2 are assessed with the same procedure, which is used for Subject 1. It is observed again that the maximum final value differences of forward trials are smaller than backward trials. Its maximum numerical value is $0.3823°$. Averaged final value differences are given as follows. For forward trials, they are $0.2426°$ in the shank, $0.2241°$ in the thigh and $0.0498°$ in the trunk. For backward trials, similarly but greater than forward trials, averaged final value differences for shank, thigh and trunk are $0.2453°$, $0.3217°$ and $0.1636°$, respectively.

Moreover, there is not found significant variation between forward and backward trials in terms of root mean square deviations. If they are expressed quantitatively for forward trials then averaged deviation from experimental data in the shank, thigh and trunk are equal to $0.0138°$, $0.0143°$ and $0.0047°$. Moreover, the same values for backward trials are $0.0117°$, $0.0218°$ and $0.0174°$.

Success expectation in the LS method, which is used for estimation parameters, is realized. According to Table.8.1, there are not significant differences between the subjects averaged values. Although behavioral patterns of the subjects are very different from each other, they have been simulated with estimated parameters, successfully. Final value differences and root mean squares deviations can be decreased with more convenient methods, no doubt about that. However, it is not needed to be sought more successful parameter estimation methods in terms of fitting experimental data. Because conjectured control law has produced with estimated parameters almost the same responses with the experimental data.

Table 6.1: Comparison of Subject 1 and Subject 2 according to analysis results of simulations.

	Forward Trials						Backward Trials					
	Averages of Final Values			Averages of RMS			Averages of Final Values			Averages of RMS		
Subject 1	0.254	0.2325	0.052	0.0105	0.0102	0.0025	0.2796	0.3548	0.1812	0.0093	0.0117	0.0059
Subject 2	0.2426	0.2241	0.0498	0.0097	0.0096	0.0022	0.2453	0.3217	0.1636	0.0067	0.0086	0.0044

As a summary in this section, the experimentally observed motions of the human subjects have been simulated by using the three-body model and the conjectured control law. Very satisfactory imitations are obtained by updating the control gains and the set points appropriately. However, in that point, it can be considered how behavioral patterns observed in Fig.6.3 and Fig.6.4 are modified by CNS. This question will be started to discuss at next section.

6.3.2 With Identified Feedback Gains: Monte Carlo Simulations with Random Initial Conditions

Over the last 20 years, it is widely accepted that automatic postural coordination is flexible and adapted to particular tasks and contexts based on the sensory information specific to each condition [39]. Although there are many arguments for and against the notion of muscle synergies [105], today, it is more approved that adaptation is provided by CNS by using flexible muscle synergies [39]. In this section, it will be discussed an important argument given in [39] that muscle synergies activated in response to an external perturbation depend on initial body position. The same argument has also been claimed in [39] that muscle synergy are responsive to initial conditions, perturbation characteristics, learning, and intention. Similarly, [33] has also suggested that a flexible continuum of muscle synergies that are modifiable in a task-dependent manner be used for equilibrium control in stance. Moreover, in [64], it is studied postural responses to the same perturbations have changed with initial stance posture. As a result, the general view is that different initial stance positions cause changing in postural strategies. However, [41] has stated that this changing cannot be predicted based on simple stretch or load reflexes, but match predictions from computational, biomechanical models of human stance coordination.

Above mentioned studies provides insight into the relation between initial body configuration and behavioral pattern. The hypothesis that postural responses to the same perturbations change with initial stance posture can be tested by using random initial body configurations. It has to be expected that individual behavioral pattern characteristics can be obtained. If selected random body configuration is entirely consistent with stance posture, which is used by the individual. For this purpose, a statistical method called as Monte Carlo simulation (MCS) have been applied.

Thus, two main idea can be tested as follows.

- The alleged definition range for the estimated parameters can be verified.
- Postural responses can be predicted by using computational ways. For example, behavioral patterns, which is shown in Fig.6.3 and Fig.6.4, can be produced again. For reproduction of behavioral patterns, the suggested control law can be run by using random initial body configuration and biomechanical model.

It is known that the general procedure of Monte Carlo simulation method is to solve mathematical problems by the simulation of random variables. Main steps in MCS are as below [12]:

1. Define the relation between the inputs and the response
2. Generate a vector of random variables for inputs
3. Evaluate the response
4. Repeat 2^{nd} and 3^{rd} steps until enough number of trials are performed.

The Monte Carlo method relies on realizations (draws) from a probability density function. Ideally, to correctly apply the Monte Carlo method and obtain valid results, the sampling method employed should be completely random. In a random sample, each draw must be independent of every other draw, that is, there must be no correlation between samples. Previous observations of the random variable have no bearing on future draws. The number of realizations has to be sufficiently large to represent accurately the distribution of the input variables [90, 74].

MCS is implemented with the following steps. Firstly, random initial and final conditions are generated within identified limits individually. Selected initial and the final configurations are categorized in terms of its similarity to experimental data. In other words, Making a decision about the resembling of the experimental data is required. Following this judgment, θ_{ref} is determined depending on random initial and final body configurations. At the same time, control parameters have to determine the estimated parameters for experimental data, because any rule for parameter determination is not found yet. Afterward, control law, which is suggested for balance recovery responses, has been tested through simulations on a $3DoF$ biomechanical model with the random initial condition and estimated parameters for related experimental data. Lastly, it is shown that behavioral patterns, which are seen in experimental responses, can be simulated with Monte Carlo simulations. The numbers of repetitions are determined three different sample size such as 20, 50 and 100. Then, they are compared with experimental data. This comparison depends on correlation between each set of simulations and experimental data in terms of representation of the behavioral patterns. Fig.6.5 shows Monte Carlo simulations of Subject 1 for forward trials.

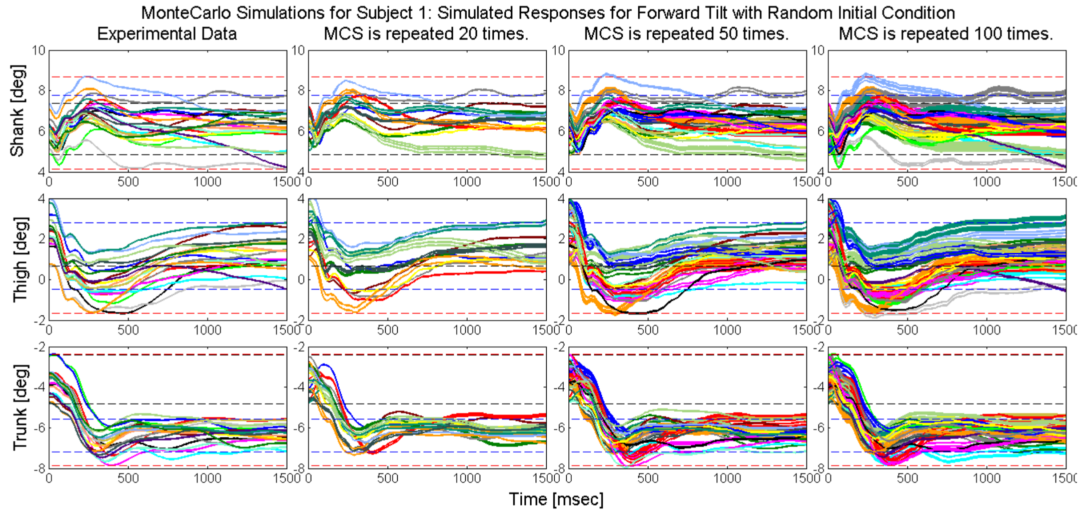

Figure 6.5: Monte Carlo Simulations for Subject 1 (Forward Trials).

Fig.6.5 consists of 3 rows and 4 columns. The rows involve angular positions of body segments with respect to gravity vertical, where body segments are the shank, thigh, and trunk. In the first column, experimental data is shown. In the second column, MCS, where the number of repetition is 20, is illustrated. For third and fourth columns, the numbers of repetitions are 50 and 100. In Fig.6.5, dashed horizontal lines, and their colors represent limits of body segment angles. Red dashed lines show maximum and minimum limits for all trials during the balance-recovery reactions. Black dashed lines demonstrate the range of the initial angles of body segments and blue dashed lines represent the range of the final angles of body segments.

Naturally, it is aimed to check the accuracy of representation of behavioral pattern with three different repetition numbers. If the probability density function can be constructed correctly, then it can be possible to obtain valid results. The validation of the simulation results can be verified with the correlation between experimental data and each independent MCS. Therefore, in Table.6.2 , it is given the averaged values each set of simulations and experimental data concerning the initial and final body configurations. The correlations of the set of MCS (including 20, 50 and 100 repetition) with experimental data are obtained as 0.9984, 0.9994 and 0.9996, respectively. It can be noticed that the correlations are considerably high, besides, slightly upward inclination of correlations depending on the number of repetition have to be seen.

Table 6.2: Evaluation of Monte Carlo Simulations for Subject 1 in terms of the number of repetitions

Averaged Data	Initial Shank Angle	Initial Thigh Angle	Initial Trunk Angle	Initial Knee Angle	Initial Hip Angle	Final Shank Angle	Final Thigh Angle	Final Trunk Angle	Final Knee Angle	Final Hip Angle
Experimental	0.1046	0.0387	-0.0669	-0.0659	-0.1056	0.106	0.0206	-0.1102	-0.0854	-0.1308
MCS: 20 times	0.1092	0.0425	-0.0638	-0.0667	-0.1063	0.0985	0.0216	-0.1148	-0.0769	-0.1364
MCS: 50 times	0.1072	0.0403	-0.061	-0.0669	-0.1012	0.1015	0.0168	-0.1108	-0.0846	-0.1276
MCS: 100 times	0.108	0.0384	-0.0635	-0.0696	-0.1019	0.1029	0.0194	-0.1109	-0.0835	-0.1303

After this point, it is given remaining simulations such as backward trials for Subject 1 and each two trials for Subject 2. It is expected that similar phenomenon will be observed. The same evaluation procedure will be followed i.e. figures containing simulations, averaged value tables and correlations will be presented, respectively. After demonstrations, this section will be finished a brief discussion.

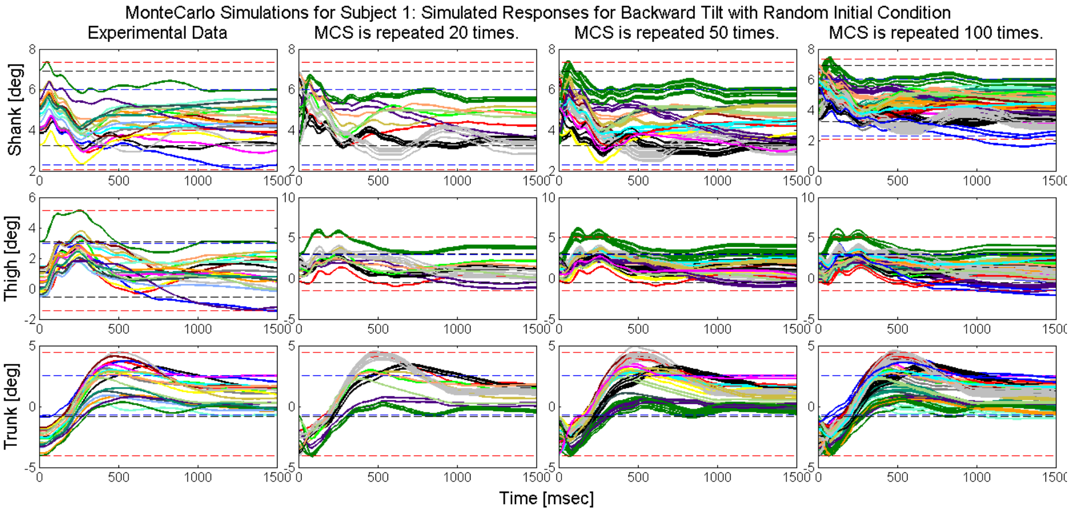

Figure 6.6: Monte Carlo Simulations for Subject 1 (Backward Trials).

Fig.6.6 shows Monte Carlo Simulations of Subject 1 for Backward Trials. The correlations are a bit smaller than found for forward trials. They are found as 0.9865, 0.9889 and 0.9948 for 20, 50 and 100 repetition, respectively, besides, the correlation coefficients are big enough to validate the results. The same upward inclination of correlation coefficient related with repetition number reveals again. The same phenomenon is also observable in Table.6.3, where the similarities between averaged body configurations can be seen.

Table 6.3: Evaluation of Monte Carlo Simulations for Subject 1 in terms of the number of repetitions (Backward Trials)

Averaged Data	Initial Shank Angle	Initial Thigh Angle	Initial Trunk Angle	Initial Knee Angle	Initial Hip Angle	Final Shank Angle	Final Thigh Angle	Final Trunk Angle	Final Knee Angle	Final Hip Angle
Experimental	0.0843	0.0099	-0.0445	-0.0745	-0.0544	0.0752	0.0157	0.0142	-0.0595	-0.0015
MCS: 20 times	0.0912	0.0243	-0.0475	-0.067	-0.0718	0.0683	0.0137	0.0214	-0.0546	0.0077
MCS: 50 times	0.0893	0.0262	-0.0422	-0.0631	-0.0684	0.0713	0.0132	0.0164	-0.058	0.0032
MCS: 100 times	0.089	0.022	-0.0406	-0.0669	-0.0626	0.0764	0.0135	0.0133	-0.0629	-0.0002

Although Subject 1 and Subject 2 are very different in terms of their behavioral patterns, their responses can be mimicked very well by using MCS. For comprasion, the Figures (Fig.6.5, Fig.6.6, Fig.6.7 and Fig.6.8) can be assessed together.

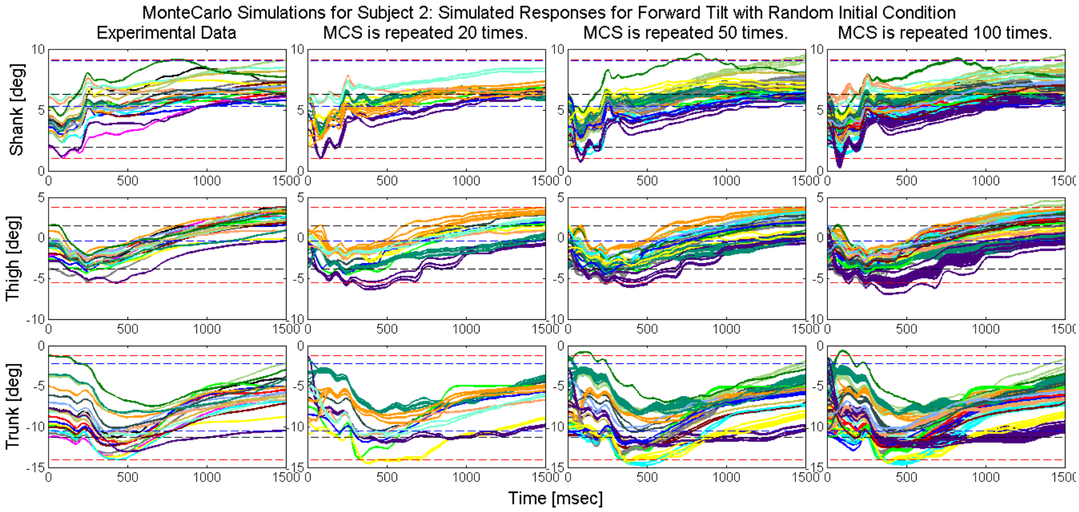

Figure 6.7: Monte Carlo Simulations for Subject 2

Fig.6.7 shows Monte Carlo Simulations of Subject 2 for Forward Trials. The correlations, which are found for Subject 2 are a bit smaller than found for forward trials of Subject 1. They are found as 0.9859, 0.9887 and 0.9906 for 20, 50 and 100 repetition, respectively. The relation between the correlation coefficients and repetition size are also appeared. It is observed again a slight increase in correlation coefficients. Table.6.4 shows the similarities between averaged body configurations.

Table 6.4: Evaluation of Monte Carlo Simulations for Subject 2 in terms of the number of repetitions

Averaged Data	Initial Shank Angle	Initial Thigh Angle	Initial Trunk Angle	Initial Knee Angle	Initial Hip Angle	Final Shank Angle	Final Thigh Angle	Final Trunk Angle	Final Knee Angle	Final Hip Angle
Experimental	0.0718	-0.0195	-0.1349	-0.0913	-0.1153	0.1204	0.0383	-0.1005	-0.082	-0.1388
MCS: 20 times	0.0791	-0.0173	-0.1037	-0.0964	-0.0864	0.1282	0.0311	-0.1095	-0.0971	-0.1406
MCS: 50 times	0.0715	-0.0287	-0.1182	-0.1002	-0.0895	0.1294	0.028	-0.1036	-0.1015	-0.1316
MCS: 100 times	0.0762	-0.0209	-0.1129	-0.0971	-0.092	0.1247	0.0277	-0.1069	-0.097	-0.1346

The last graph of this section can be seen in Fig.6.8, which includes Monte Carlo Simulations of Subject 2 for backward trials. Table.6.5 is placed just below it. The correlation coefficients are found as 0.9821, 0.9772 and 0.9854. For this case, the correlation found for 50 repetitions is smaller than the others. This phenomenon can be thought that it is needed more repetition for this case.

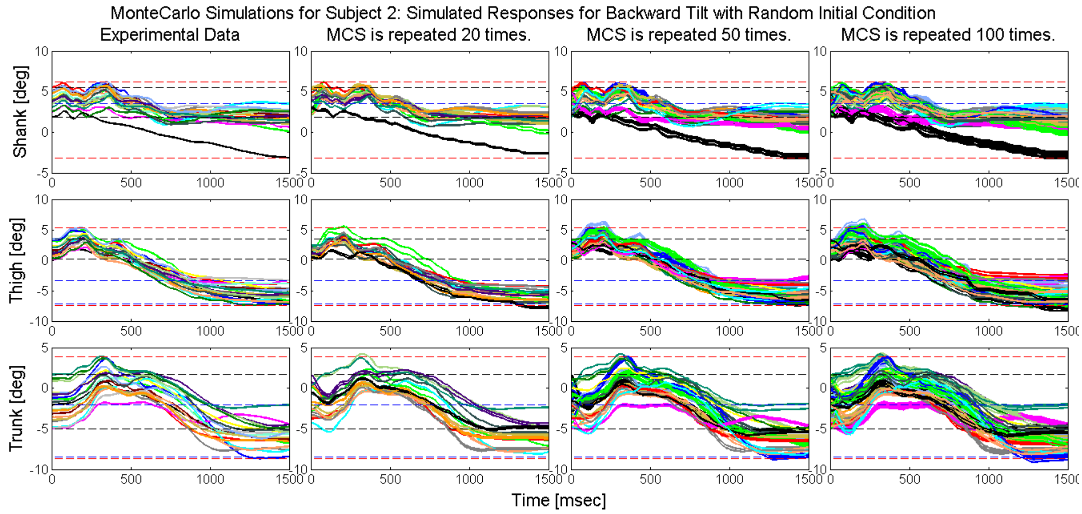

Figure 6.8: Monte Carlo Simulations for Subject 2 (Backward Trials).

Table 6.5: Evaluation of Monte Carlo Simulations for Subject 2 in terms of the number of repetitions (Backward Trials)

Averaged Data	Initial Shank Angle	Initial Thigh Angle	Initial Trunk Angle	Initial Knee Angle	Initial Hip Angle	Final Shank Angle	Final Thigh Angle	Final Trunk Angle	Final Knee Angle	Final Hip Angle
Experimental	0.0729	0.0265	-0.0379	-0.0464	-0.0645	0.0292	-0.0949	-0.102	-0.1241	-0.0071
MCS: 20 times	0.0663	0.0187	-0.0259	-0.0475	-0.0447	0.0061	-0.092	-0.0846	-0.0981	0.0074
MCS: 50 times	0.0606	0.0309	-0.0315	-0.0297	-0.0624	-0.0001	-0.0894	-0.0928	-0.0893	-0.0034
MCS: 100 times	0.0646	0.0334	-0.0368	-0.0312	-0.0702	0.009	-0.0903	-0.09	-0.0992	0.0003

As a summary of this chapter, it can be stated that the proposed control model to balance-recovery reactions was verified by using simulations. At that point, it can be said that estimated parameters at the beginning of this chapter with least squares method could be tested. The validation of the estimated time-varying feedback control gains and upright reference position (θ_{ref}) was verified with the achievement of the estimated parameters to fit the experimental data. Simultaneously, simulations and experimental results were compared. Besides, simulations are repeated to test whether it was possible to obtain the individual behavioral pattern characteristics by using random initial body configurations.

CHAPTER 7

THE ADAPTATION LAW FOR ADAPTIVE MODIFICATION OF AUTOMATIC POSTURAL RESPONSES

In this chapter, it is tried to explore the adaptation law for adaptive modification of automatic postural responses. Naturally, it is difficult to estimate this adaptation law because it is probably dependent on the past physiological and psychological experiences of the human beings. Nevertheless, it may be possible to estimate at least a functional relationship between major arguments that possibly contribute to the adaptation law and the adapted gains.

Firstly, recent studies, which are related to adaptation of postural response, are reviewed. The adaptation can be realized by changing gains or synergies that is a general idea in [40].

Secondly, neural mechanisms, which are responsible for adaptive modification of automatic postural responses, are discussed on the basis of evidence came from experimental studies.

Thirdly, variables that possibly contribute to the adaptation law are described. These variables can be categorized as bodily and environmentally sensory information. It is widely accepted that automatic postural responses are adaptable. According to particular tasks and contexts, they can be adapt by using sensory information [36, 39].

Fourthly, adaptation law is identified by using the canonical correlation analysis. Because, the experimentally inferred fact of changing PD control gains leads to a major hypothesis that the central nervous system applies the conjectured PD control law by changing its gains according to a certain adaptation law.

In this study, it has been possible to arrive at such an estimation by means of the renown "canonical correlation method". Finally, proposed adaptation law is verified by using simulations.

7.1 Literature Review

It is generally accepted that the CNS can modify the gain of even simple reflexes based on expectation, instruction and experience [41]. However, the neural mechanism of adaptation has not been revealed yet clearly. Naturally, there are many experimental studies. In [40], they have been reviewed in terms of behavioral evidence and possible mechanisms for the short-term adaptation of postural coordination in response to external perturbations. More recently, the other study is [110], and it wonders about how adaptation occurs in task-level balance control during responses to perturbations. [36] is another major study for this section. [36] has stated that the nervous system must adapt not only due to change in base of support and initial position, but also to change in the mass, strength, and stiffness of segments. These changes can occur gradually during the lifespan or can emerge suddenly depending on the environmental conditions. On the basis of these four studies, the literature review has been expanded.

20 years ago, possibly for the first time, it was stated that functional flexibility of postural coordination has been provided by afferent inflow based on current conditions and the particular parameters of the stimuli [40]. Where afferent inflow means to bring or to direct inwards to a part or an organ of the body, especially towards the brain or spinal cord [18]. Additionally, the stimulus can be categorized as external and internal. This study is interesting with external disturbance as support surface perturbation. Internal stimulus can be exemplified as arousal, attention, expectations and prior experience. The more recent study is supported the same idea with experimental evidence. According to [72], experimental results have revealed task-specific facilitation of sensory inputs to the cortex and inhibition of the spinal reflex pathway. Mentioned experiments in [72] have been conducted to examine modulation of proprioceptive inputs during balance tasks of varying difficulty.

A very recent study presents evidence for motor adaptation primarily in reactive sensorimotor response to perturbations during standing balance [110]. Where sensory-motor is a term that it has been defined in [114] as the integration of the sensory system and motor system. The explanation given in [114] is continuing as follows.

> Sensorimotor integration is not a static process. For a given stimulus, there is no one single motor command. Neural responses at almost every stage of a sensorimotor pathway are modified at short and long timescales by biophysical and synaptic processes, recurrent and feedback connections, and learning, as well as many other internal and external variables

After this explanation, it can be proceeded to review of [110]. Its hypothesis is that adaptation occurs in task-level balance control during responses to perturbations due to central changes in the control of both anticipatory and reactive components of balance. They have also stated that adaptation has been found in the evoked long-latency muscular response, and also in the sensorimotor transformation mediating that response.

Adaptation can affect both the gain and the temporal synergy of the responses and strategy selection. It is also influenced by the sensory information that is available [40, 39].

[40] shows a way for future studies. [40] has proposed that it is needed to determine what variables are optimized by postural adaptation and whether the optimized variables can vary depending on the specific task and context. Additionally, according to [40], the cerebellum appears to be a critical contributor to adaptive gain modification of postural responses based on the sensorimotor set. In the next section, neural mechanisms responsible for adaptive modification will be discussed. In addition to experimental studies, in fewer studies [110, 26], they have been attempted to identify the adaptation. A quantitative measure of adaptation can be used for the evaluation of balance disorders and diseases. In evaluating treatment efficacy, it can be an important tool in monitoring the progress of patients [26]. The new tools have been developed for system identification and determination of correlation. For instance, in [26], two new methods have been proposed for

describing the adaptation of postural control. These methods were named 'added exponential function' denoted AEF and 'analysis with reduction' denoted AWR. Moreover, [110] has used one-sample Kolmogorov-Smirnov test and Bonferroni correction to evaluate the degree of adaptation.

In this study, it is aimed to find functional relations, which can express the contributions of the variables involved in the adaptation process. For this purpose, the canonical correlation analysis method is selected. To verify the obtained results, the model is simulated by using these functions that are found by the canonical correlation analysis method.

7.2 Neural Mechanisms Responsible for Adaptive Modification

On the contrary of the majority of the mechanistic theories, a section of [69] has claimed that the cerebellum does not manage the coordination of movement directly and primarily. The mentioned section is called as the cerebellum and the control of movement-related sensory data acquisition. [69] proposed that the cerebellum coordinates the acquisition of sensory data on which motor systems and all other brain systems depend.

Adaptation involves the trial-by-trial adjustment of the magnitude of muscle activation (gain) or the gradual modification of the pattern and timing of muscles (synergy) activated by the perturbation [40]. The set-dependent adaptation of postural response gain or synergies most likely involves higher centers such as the cerebellum, brainstem, and cortex [40].

A recent review paper [46] has summarized the studies about the role of the cerebellum in the reorganization of posture. To review all studies again is not necessary. However, one of them is directly related to this study. Therefore, [35] is reviewed again for the understanding of its details. According to [35], the anterior cerebellum has been shown to play a critical role in modifying the magnitude of automatic postural responses to a platform displacement to anticipated displacement conditions based on prior experience [46]. It is said in [35, 46] that there is a lot of controversy between reviewed studies. However, a great majority of them have accepted that the cerebellum is involved in the control of learned automatic postural reactions, particularly in their temporal and magnitude structure.

7.3 Variables which Possibly Contribute to the Adaptation Law

The postural adaptation is a very difficult issue to study depending on its nature. The main reason for this challenge is its complexity. Adaptation is the result of a series of processes such as the acquisition of sensory data, interpretation of sensory information, adjustment of sensory information and re-weighting by changing the environmental conditions. Additionally, adaptation is affected excessively by many factors such as anticipation, arousal, attention, expectations and prior experience. However, these emotional effects could not be taken into account in the adaptation law model, which is proposed within the scope of this thesis. Instead, for sake of simplicity, the proposed adaptation law model only consists bodily sensory information (measured position and velocity) and external disturbance (generated by support surface tilt platform) transmitted to CNS (higher brain structure).

Actually, given literature review and introduced neural mechanisms of adaptation is only beneficial to show the consistency between proposed model and currently accepted the physiological theory. In other words, proposed model does not involve details, for example, it does not include a cerebellum model. Yet, the simulation studies have shown that it has been possible to match the simulation and experimental results only if the simulations are made by changing the gains as functions of time. On the other hand, as discussed above, the apparent time variation of the gains is due to a certain adaptation law implemented somehow by the CNS. So, in this section, without considering the physiological details, an adaptation law is conjectured and then it is verified based on the experimental results.

It is known that automatic postural responses arise when human beings are stimulated with sudden external perturbations when they are in balance in an upright posture. Moreover, it is discussed above that automatic postural responses have to be adapted to the changing conditions until the balance is recovered. Moreover, it is also said that adaptation is affected by many internal and external factors. Therefore, it is impossible to identify an unchangeable, definite rule for this adaptation. However, it is possible to identify a function that involves the relative contributions of the changing variables. In this section, these variables will be discussed depending on their possible contribution of the proposed adaptation law model. Before talking about the selection of these variables, it can be said that the adaptation law seems to depend substantially on the difference between the actual and reference angular position, on the angular velocity of the body limbs, and on the direction and amount of the perturbation.

As mentioned above, the adaptation of the gains depends on sensory information and external disturbance. At this point, it must be said that sensory information is limited with the proposed $3DoF$ biomechanical model. Similarly, the external disturbance is also represented with the motion of the support surface tilt platform. Therefore, variables of the functions, which will identify the gains, are thought on the basis of equation of motion of the biomechanical model given below.

$$M(\theta)\ddot{\theta} + V(\theta,\dot{\theta})\dot{\theta} + D(\theta,\theta_p,\dot{\theta}_p,\ddot{\theta}_p) + G(\theta) = -K_p(t)\left[\theta - \theta_{ref}(t)\right] - K_d(t)\dot{\theta} \quad (7.1)$$

Regarding Eq.7.1, it can be said that the variables that are expected to be the arguments of the conjectured adaptation law are the ones listed below. They are related to the postural error and the disturbance input.

- $[\theta - \theta_{ref}(t)]$ the difference between the actual and reference angular position.
- $\dot{\theta}$ the angular velocity of the body limbs.
- θ_p the angular position of the support surface tilt platform.
- $\dot{\theta}_p$ the angular velocity of the support surface tilt platform.

Actually, angular acceleration of the body segments ($\ddot{\theta}$) and the support surface tilted platform ($\ddot{\theta}_p$) are the variables of the biomechanical model. However, they are not included intentionally because of their effects on the functions. Their contribution was seen as a slight wiggle at the responses of the obtained functions. They have also increased the calculation load, besides, their negative effects on responses.

7.4 The Canonical Correlation Analysis in Identification of the Adaptation Law

In the previous section, it was mentioned functions that could represent the gains. Additionally these functions were expressed that they could be identified with the relative contributions of the changing variables determined. In this section, it is presented a method referred to as canonical correlation analysis. This method can be used to identify such a function. This section is composed of two parts.

In the first part, the canonical correlation analysis method will be introduced in terms of its selection reasons. Then, the theoretical and historical background of the method will be given. And then, a brief literature review about the usage of the method will be presented.

7.4.1 The Canonical Correlation Analysis Method

Canonical correlation analysis (CCA) is a statistical technique that determines if there is a relationship between two sets of variables. This method is appropriate for determining the functional relation between two sets of variables. For example, in [68], 16 colonies of the butterfly Euphydryas editha in California and Oregon have been studied. For each colony values are available for four environmental variables and six gene frequencies. The question of [68] is what relationships, if any, exist between the gene frequencies and the environmental variables. Finally, in [68], it is declared that canonical correlation analysis is convenient to investigate this type relations. Canonical correlation analysis can address a wide range of objectives.

These objects have been expressed in [29, 102] as follows:

- Whether the two sets of variables are statistically independent of one another can be determined.
- The magnitude of the relationships that may exist between the two sets can be expressed
- The linear combinations of each set must be maximally correlated. Therefore, the weights for each set of dependent and independent variables can be set for this purpose.
- Additional linear functions that maximize the remaining correlation are independent of the preceding set(s) of linear combinations.
- That the nature of whatever relationships exist between the sets of dependent and independent variables can be explained.
- The relative contribution of each variable to the canonical functions can be extracted.

Historical Background

Canonical correlation analysis is developed by Hotelling in 1936 [43]. According to realized search results on the scientific database (ScienceDirect), it was used in various application areas from 1980 to present. These application areas can be classified into two main groups such as science and technology and social science. Generally, social science studies are related to psychology, especially personality and individual differences. On the other side, the main topics of science and technology studies are biology, neuroscience, and signal processing. The majority of the studies in neuroscience have been published about neuroimage. As a result of this searching, it was discovered practically that, canonical correlation analysis is very useful in describing the nature of the relationship between two latent variables. At the same time, it is beneficial to determine easily how many dimensions are needed to account for the relationship.

For sake of clarity, it might be best to take more concrete examples of each main application areas. [96, 20, 45] may be good examples for this purpose. [96] brings a new insight into the interpretation of canonical correlation analysis. A new approach, which can deal with automatically irregularly or sparsely observed functional data, has been proposed in [96]. It is also verified by using two real datasets: the first one is AIDS dataset, and the second is the primary biliary cirrhosis (PBC) dataset. Their aim has been declared as finding out a relation between viral load and immunity level by canonical correlation analysis. It must be emphasized that proposed new approach for canonical correlation analysis can produce result despite irregularly or sparsely data. Another example can be given about neuroimage studies. Many researchers in recent years are related with the understanding of brain function, organization, and structure. Brain functions and complementary spatio-temporal information about brain function are tried to be understood by using functional magnetic resonance imaging (fMRI) data and electroencephalography (EEG) data [20]. Canonical correlation analysis method is widely used at the studies about neuroimagine. [20] proposes a data fusion method for simultaneously acquired fMRI and EEG data. In [20], they have stated that it could be obtained a decomposition of the two modalities (fMRI and EEG), by using multi-set canonical correlation analysis (M-CCA). The topic of the last example is pattern recognition, more specifically face recognition. Canonical correlation analysis (CCA) is used in [45], in order to determine a coherent subspace in which the statistical correlation between intrinsic structures of low-resolution and high-resolution images is maximized.

Theoretical Background

The canonical correlation analysis is a standard tool of multivariate statistical analysis for discovery and quantification of associations between two sets of variables. In this part, the canonical correlation analysis is explained shorty because the method is presented almost all textbooks related with multivariate data analysis, for example, [29, 32, 68]. However, for sake of integrity of the thesis, theoretical background and mathematical description of the method are presented in Appendix F.

The method can be summarized as follows.

Suppose, it is given two independent datasets such as

$$\mathbf{X} = \begin{pmatrix} x_{11} & x_{12} & \dots & x_{1p} \\ x_{22} & x_{22} & \dots & x_{2p} \\ \vdots & \vdots & \ddots & \vdots \\ x_{n1} & x_{n2} & \dots & x_{np} \end{pmatrix} \text{ and } \mathbf{Y} = \begin{pmatrix} y_{11} & y_{12} & \dots & y_{1q} \\ y_{22} & y_{22} & \dots & y_{2q} \\ \vdots & \vdots & \ddots & \vdots \\ y_{n1} & y_{n2} & \dots & y_{nq} \end{pmatrix}$$

In canonical correlation analysis, the objective is to project X and Y datasets onto basis vectors a and b, respectively, such that the correlation between the projections of the variables onto these basis vectors is mutually maximized. In other words, the aim is to maximize the correlation between the linear combinations $a^T X$ and $b^T Y$. Where, a and b are called the canonical correlation vectors. Using these canonical correlation vectors, it can be defined the canonical correlation variables as follows:

$$\begin{aligned} U &= a^T X \\ V &= b^T Y \end{aligned} \tag{7.2}$$

the canonical correlation vectors (a and b) are the solution to the maximization problem of given below:

$$\rho(a, b) = \mathrm{corr}(a^T X, b^T Y) \tag{7.3}$$

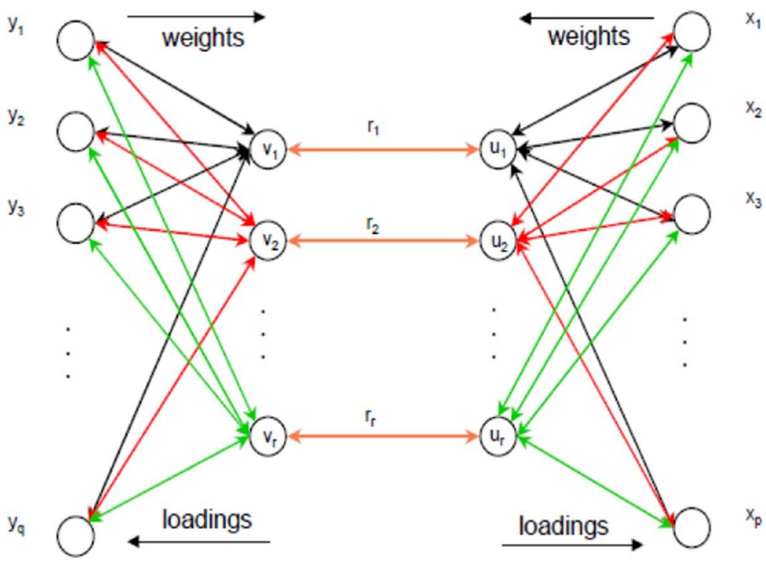

Figure 7.1: The General Structure of Canonical Correlation Analysis [56].

As a summary of this section, the canonical-correlation analysis is defined in [111] briefly as follows. Canonical-correlation analysis seeks vectors a and b such that the random variables $a^T X$ and $b^T Y$ maximize the correlation $\rho = \mathrm{corr}(a^T X, b^T Y)$. The random variables $U = a^T X$ and $V = b^T Y$ are the first pair of canonical variables. Then one seeks vectors maximizing the same correlation subject to the constraint that they are to be uncorrelated with the first pair of canonical variables; this gives the second pair of canonical variables. This procedure may be continued up to $\min\{m, n\}$ times.

7.4.2 Identification of the Adaptation Law with CCA

As stated in the previous section, the aim of this section is to identify a reasonable adaptation law depending on bodily and environmentally sensory information. The canonical correlation analysis is a very useful tool for this purpose because it investigates the relation between the two variables.

The canonical correlation analysis is performed on the datasets X and Y that correspond to the values gain and the difference between the actual and reference angular positions, angular velocity of the body limbs, angular position of support-surface tilt platform, angular velocities of support-surface tilt platform, respectively. However, there are six different datasets must be defined for six different control gains which were expressed in chapter 6. They are written below again for remembering.

$$u = \begin{bmatrix} u_A \\ u_K \\ u_H \end{bmatrix} = \begin{bmatrix} K_{1p}(t)\left[\theta_{shref}(t) - \theta_{sh}\right] - K_{1d}(t)\dot{\theta}_{sh} \\ K_{2p}(t)\left[\theta_{thref}(t) - \theta_{th}\right] - K_{2d}(t)\dot{\theta}_{th} \\ K_{3p}(t)\left[\theta_{trref}(t) - \theta_{tr}\right] - K_{3d}(t)\dot{\theta}_{tr} \end{bmatrix} \tag{7.4}$$

In Eq.7.4, six different gains are represented with K_{1p}, K_{1d}, K_{2p}, K_{2d}, K_{3p} and K_{3d}. Where "1", "2" and "3" represent ankle joint, knee joint and hip joint respectively. On the other hand, it has to be remembered that these 6 different gains were found by using a type of least squares method in Chapter 6. In this section, 6 different functional relations are estimated by using CCA as a function of variables, which are the difference between the actual and reference angular positions, angular velocities of the body limbs, angular position of support-surface tilt platform, angular velocity of support-surface tilt platform. These functions are substituted into Eq.7.4, in this case, u has turned into a functional expression, which is composed of three independent functions. For six independent case, the variables, which are involved in the datasets X and Y, are shown in Table.7.1

Table 7.1: List of variables for six independent case

Case	X	Y
1	K_{1p}	$[\theta_{sh} - \theta_{shref}], \dot{\theta}_{sh}, \theta_p, \dot{\theta}_p$
2	K_{1d}	$[\theta_{sh} - \theta_{shref}], \dot{\theta}_{sh}, \theta_p, \dot{\theta}_p$
3	K_{2p}	$[\theta_{th} - \theta_{thref}], \dot{\theta}_{th}, \theta_p, \dot{\theta}_p$
4	K_{2d}	$[\theta_{th} - \theta_{thref}], \dot{\theta}_{th}, \theta_p, \dot{\theta}_p$
5	K_{3p}	$[\theta_{tr} - \theta_{trref}], \dot{\theta}_{tr}, \theta_p, \dot{\theta}_p$
6	K_{3d}	$[\theta_{tr} - \theta_{trref}], \dot{\theta}_{tr}, \theta_p, \dot{\theta}_p$

It is discussed in the previous section that canonical-correlation analysis attempts to find maximum correlation between the canonical variables such as $U = a^T X$ and $V = b^T Y$. For this purpose, it seeks coefficients a and b. This can be expressed mathematically as follows.

$$\begin{gathered} \text{If } \rho = \mathrm{corr}(U,V) = 1 \text{ Then } U = V \\ \text{If } 0.5 < \rho < 1 \text{ Then } U \cong V \end{gathered} \tag{7.5}$$

Average values of ρ are given in the Table.7.2 for each subject and for each direction. It can be detected in Table.7.2 that maximum correlation is found as 0.9459 and minimum correlation is found as 0.4936. It must be expressed that correlations, which were found for backward trials of Subject 2, are not big enough. At this point, it has to be remembered that adaptation is affected excessively by many factors such as anticipation, arousal, attention, expectations and prior experience. Additionally, identified functions for gains are only correlated with the gains, which were estimated by using LS method.

Table 7.2: Average values of ρ for all directions and all subjects

	Subject 1		Subject 1	
Corr. Coef.	Forward Trials	Backward Trials	Forward Trials	Backward Trials
$\rho(K_{1p})$	0.6677	0.7120	0.6712	0.6069
$\rho(K_{1d})$	0.7932	0.6567	0.8990	0.5669
$\rho(K_{2p})$	0.8791	0.5807	0.7348	0.5563
$\rho(K_{2d})$	0.9459	0.6420	0.8629	0.4936
$\rho(K_{3p})$	0.8000	0.8007	0.6649	0.5854
$\rho(K_{3d})$	0.9243	0.7910	0.7686	0.5632

Some correlations, whose averages can be checked from Table.7.2, are smaller than 0.5, but the averages of the gain couples, such as $\rho(K_{2p})$ and $\rho(K_{2d})$ are bigger than 0.5. Moreover, this phenomenon is seen only in backward trials of Subject 2. As a result, it can be written the following relations from Eq.7.5.

$$U \cong V \Leftrightarrow a^T X \cong b^T Y \tag{7.6}$$

For all cases for this study, X contains only one variable set so a^T is a scalar, therefore, $a^T = a$ and the relation can be written as follows:

$$\widetilde{X} = \begin{bmatrix} b_1/a & b_2/a & b_3/a & b_4/a \end{bmatrix} \begin{bmatrix} y_{11} \\ y_{12} \\ y_{13} \\ y_{14} \end{bmatrix} \tag{7.7}$$

Eq.7.7 can be rewritten in the following form.

$$\widetilde{X} = C_1 y_{11} + C_2 y_{12} + C_3 y_{13} + C_4 y_{14} \tag{7.8}$$

Example 7.4.1. *Sixth forward trials of Subject 1 is chosen as an example. The six different gains (K_{1p}, K_{1d}, K_{2p}, K_{2d}, K_{3p} and K_{3d}),which are found by using CCA, can be shown as following expressions. Related correlation coefficients are given in Table.7.3 Estimated expressions by using CCA are substituted into Eq.7.4. Thus, an adaptation law, which can be expressed with body and platform kinematics, can be obtained this trial.*

Table 7.3: Correlation coefficients of sixth forward trials of subject 1

Corr. Coef.	Num. Value
$\rho(K_{1p})$	0.7714
$\rho(K_{1d})$	0.6656
$\rho(K_{2p})$	0.8640
$\rho(K_{2d})$	0.8859
$\rho(K_{3p})$	0.8772
$\rho(K_{3d})$	0.8859

$$\begin{aligned}
\widetilde{K}_{1p} &= 10^5 \left[-5\left[\theta_{sh}-\theta_{shref}\right]+0.5853\dot{\theta}_{sh}+2.4483\theta_p+0.7194\dot{\theta}_p\right] \\
\widetilde{K}_{1d} &= 10^5 \left[0.2358\left[\theta_{sh}-\theta_{shref}\right]-0.0286\dot{\theta}_{sh}-0.2663\theta_p+0.0268\dot{\theta}_p\right] \\
\widetilde{K}_{2p} &= 10^5 \left[-2.7599\left[\theta_{th}-\theta_{thref}\right]+0.2659\dot{\theta}_{th}-1.1056\theta_p-0.1784\dot{\theta}_p\right] \\
\widetilde{K}_{2d} &= 10^4 \left[5.3214\left[\theta_{th}-\theta_{thref}\right]+0.2264\dot{\theta}_{th}-0.3835\theta_p+0.4110\dot{\theta}_p\right] \\
\widetilde{K}_{3p} &= 10^5 \left[-2.7977\left[\theta_{tr}-\theta_{trref}\right]-0.3498\dot{\theta}_{tr}+0.0333\theta_p-0.6242\dot{\theta}_p\right] \\
\widetilde{K}_{3d} &= 10^4 \left[6.4564\left[\theta_{tr}-\theta_{trref}\right]+0.4219\dot{\theta}_{tr}+0.2871\theta_p+0.7375\dot{\theta}_p\right]
\end{aligned} \tag{7.9}$$

The expressions for gains, which are shown in Eq.7.9, are linear functions. As a first impression, their linear characteristics can lead to illusions about that gains can diverge. However, variables can appear in the limited ranges. For instance, the motion of the support surface tilt platform last about 600 ms. and motion of the joints have biological limitations. A bit later, they will be shown as illustratively.

Estimated gains, which are shown in Eq.7.9, are substituted into 7.4. Therefore, adaptable control input can be obtained as follows.

$$\widetilde{u} = \begin{bmatrix} \widetilde{u}_A \\ \widetilde{u}_K \\ \widetilde{u}_H \end{bmatrix} = \begin{bmatrix} \widetilde{K}_{1p}(t)\left[\theta_{shref}(t)-\theta_{sh}\right]-\widetilde{K}_{1d}(t)\dot{\theta}_{sh} \\ \widetilde{K}_{2p}(t)\left[\theta_{thref}(t)-\theta_{th}\right]-\widetilde{K}_{2d}(t)\dot{\theta}_{th} \\ \widetilde{K}_{3p}(t)\left[\theta_{trref}(t)-\theta_{tr}\right]-\widetilde{K}_{3d}(t)\dot{\theta}_{tr} \end{bmatrix} \tag{7.10}$$

It can be noticed that this new control law only depends on the difference between the actual and reference angular positions, angular velocities of the body limbs, angular position of support-surface tilt platform, angular velocity of support-surface tilt platform. The functional expressions given in Eq.7.9 and Eq.7.10 are illustrated in Fig.7.2 and Fig.7.3

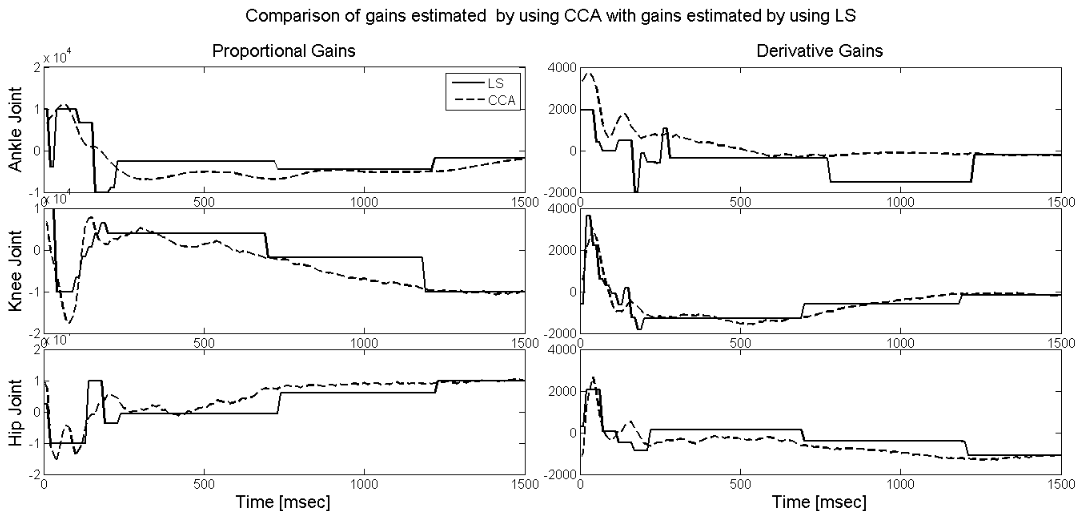

Figure 7.2: Comparison of gains estimated by using CCA with gains estimated by using LS.

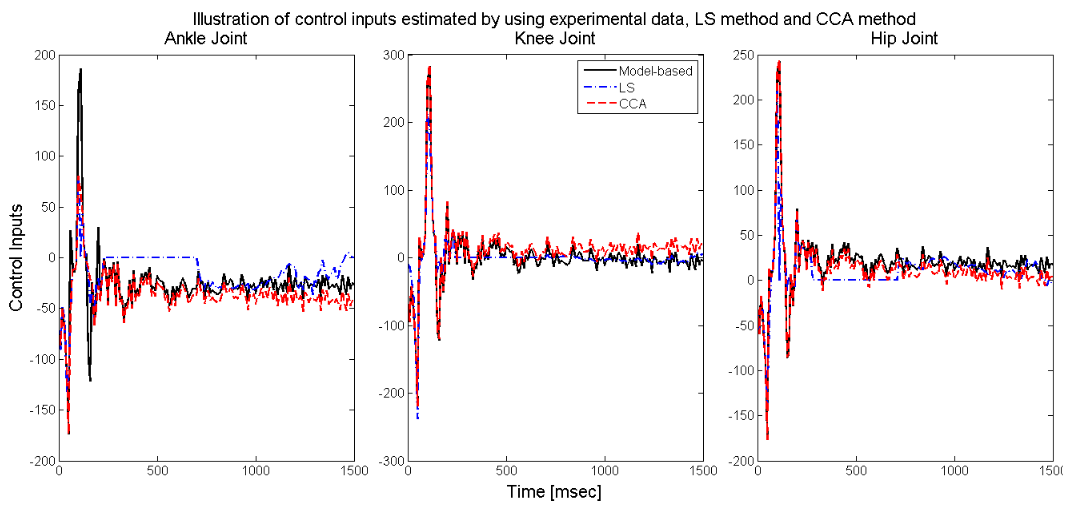

Figure 7.3: Illustration of control inputs estimated by using experimental data, LS method and CCA method.

In Fig.7.2, by using CCA, the revealed functional expressions for gains are compared to gains based on LS method, which was described in chapter 6. The functions of gains that are referred to in Eq.7.9 are evaluated with experimental data for each time increments. Thus, the numerical values of gains depending on time are obtained. Fig.7.3 shows control inputs, which are calculated with three distinct method. Black lines, which are referred to as model-based, are obtained from directly equation of motion.

$$M(\theta)\ddot{\theta} + V(\theta, \dot{\theta})\dot{\theta} + D(\theta, \theta_p, \dot{\theta}_p, \ddot{\theta}_p) + G(\theta) = Q = u \tag{7.11}$$

Left side of the Eq.7.11 can be evaluated with subject's kinematics data, the kinematic data of support surface perturbation platform and the other model parameters such as the mass and inertia of the segments of the human body and length and position of the center of mass. Control torques can be found for each data point.

Fig.7.2 and Fig.7.3 are illustrative examples of Eq.7.9 and Eq.7.10. Therefore, it is not needed to assess these figures in detail. Verification of the method will be given at next section.

7.5 Verification of the Adaptation Law: Simulation for All Experimental Trials

In the previous section, the adaptation law was estimated. The functional expressions of adaptation law depend on the difference between the actual and reference angular positions, on the angular velocities of the body limbs and on the direction and amount of the perturbation substantially.

In this section, adaptation law will be applied to correlate the experimental and simulation results. In this way, the proposed adaptation law will be verified by using simulations on a 3 DoF biomechanical model. The proposed model is simulated by using experimental initial conditions. Furthermore, obtained simulations are compared to the experimental data by using simple statistical analysis tools. They are the instruments related to the final value differences and root mean square deviations. All results can be seen in Appendix.G.

Fig.7.4 and Fig.7.5 illustrate the simulations with CCA for all trials at forward and backward directions for two different subjects. Upper two rows show forward trials. Backward trials are also shown in the lower two rows. Experimental results of automatic postural responses of the shank, thigh, and trunk, are drawn with solid lines and each color represent a different trial. Dotted lines are used for representation of simulated data. The same way, each color represent a different trial.

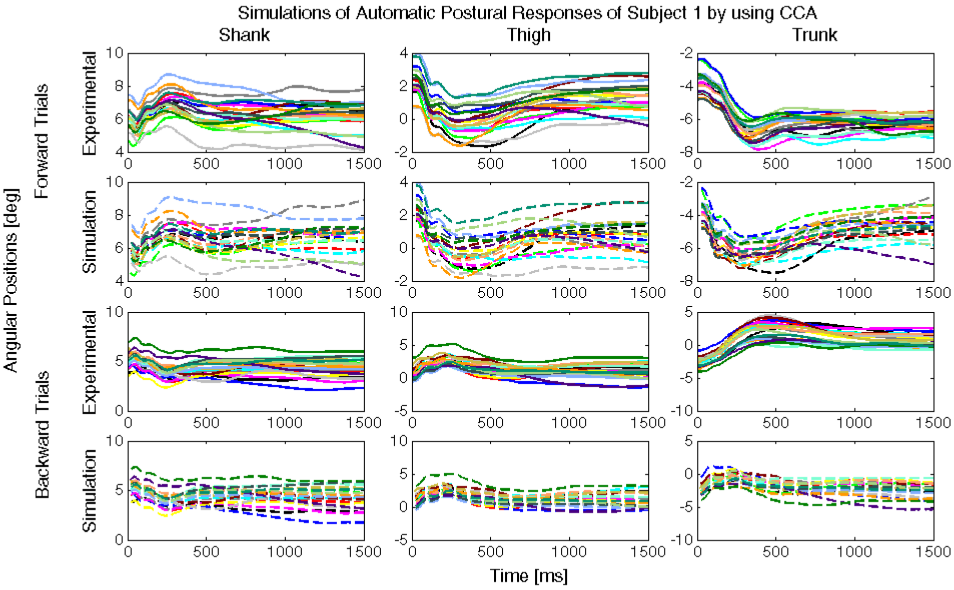

Figure 7.4: Simulations of Automatic Postural Responses of Subject 1 by using CCA.

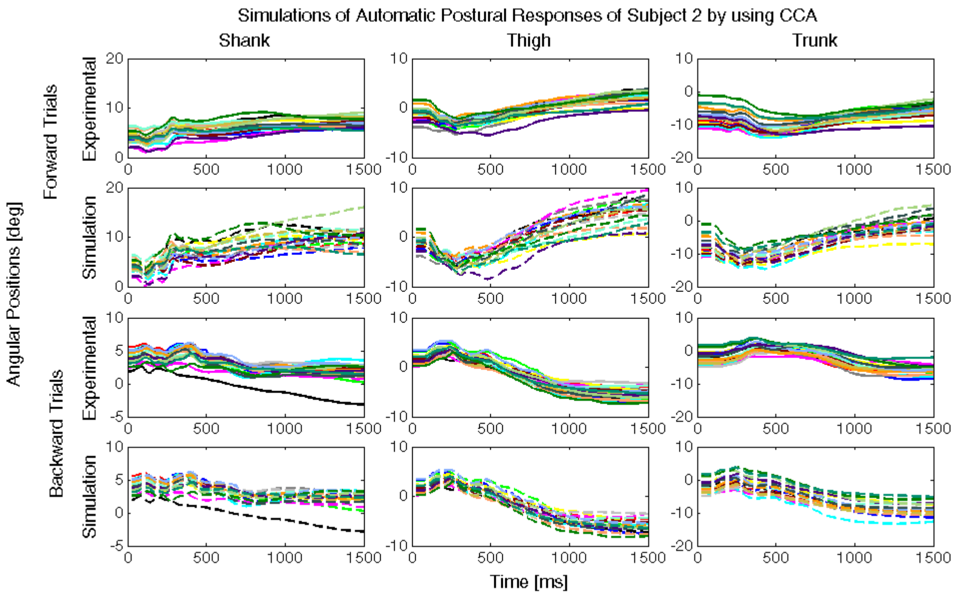

Figure 7.5: Simulations of Automatic Postural Responses of Subject 2 by using CCA.

Illustrated angular positions are absolute angles i.e. they are the deviation from vertical with respect to ground. In those illustrations, it can be seen that simulated angular positions and experimental angular positions show the same behavioral patterns. However, it can be seen in Fig.7.4 and Fig.7.5 that simulated and experimental data do not fit, especially in trunk part. Therefore, it is needed to understand the differences more clearly between them. For the averaged value, Table. 7.4, which is given below, can be checked.

Table 7.4: Comparison between Subjects depending on deviation from experimental data.

	Forward Trials						Backward Trials					
	Averages of Final Values			Averages of RMS			Averages of Final Values			Averages of RMS		
Subject 1	0.7799	0.9844	1.8994	0.0293	0.0389	0.0719	0.5233	0.9109	2.9917	0.0142	0.0228	0.2173
Subject 2	0.7462	1.0182	1.6452	0.032	0.044	0.1148	1.2182	1.572	2.6869	0.0546	0.0716	0.2167

Addition to Table. 7.4, all detailed statistical analysis are given in Appendix G. Nevertheless, it can be better to give an illustrative example of a trial only. Thus, the differences between experimental data, simulation with LS method and simulation with CCA method can be animated very well.

Example 7.5.1. *(Continued from example 7.4.1.) In this example, again, sixth forward trials of Subject 1 is chosen as an example. Obtained adaptation law is simulated, and the results are compared to experimental data and simulation, which is ran with gains estimated with LS method.*

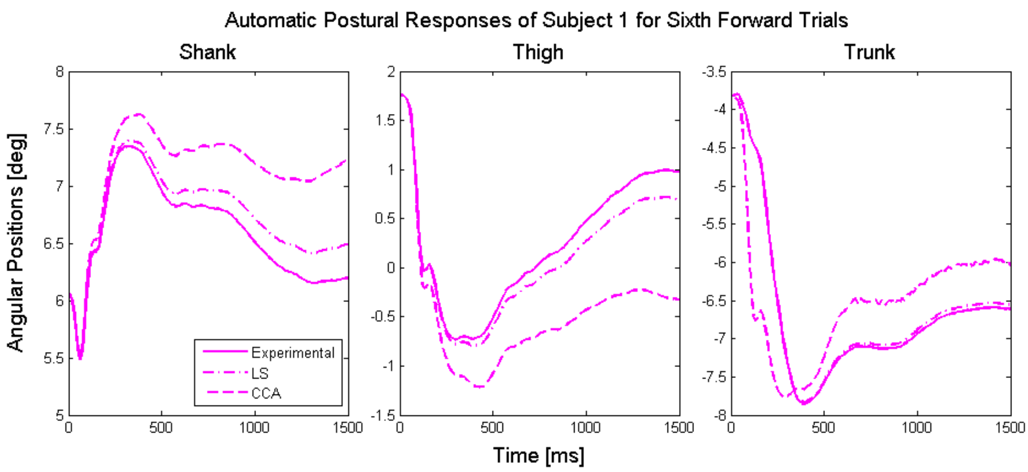

Figure 7.6: For Sixth Forward Trials: Comparisons of Simulations obtained by using LS and CCA.

Success expectation in the adaptation law is realized. It is formed by using bodily sensory information (measured position and velocity) and external disturbance (generated by support surface tilt platform). Additionally it is estimated by using CCA. No doubt about that there are highly visible differences between experimental data and simulations. Naturally, a correction method such as genetic algorithm basis methods can be sought to obtain more successful simulations in terms of fitting experimental data. Additionally, new corrective terms can be added to adaptation law, which may represent the emotional factors such as anticipation, arousal, attention, expectations and prior experience. On the other hand, more powerful LS methods can be available in order to more accurately estimate the control gains.

However, although there can be possible an improvement on simulations in terms of fitting to experimental data, it is not essential. At the beginning of this chapter, it was declared that estimation of the adaptation law was very difficult depending on many factors related to the past physiological and psychological experiences of the human beings. Nevertheless, it is achieved to estimate functional relationships, which symbolize adjustment of sensory information and re-weighting by changing the environmental conditions. As a result, obtained simulations not only parallel to experimental data but also they support to the idea given in [36, 39]. This idea is that automatic postural coordination is flexible and adapted to particular tasks and contexts based on the sensory information specific to each condition.

CHAPTER 8

CORRELATION BETWEEN INITIAL POSTURE AND BALANCE-RECOVERY RESPONSE

In this chapter, the effect of the initial body configuration on balance-recovery reactions is studied. Upon examining the experimental results gathered from the repeated trials for different human subjects, an evident correlation is detected. This correlation is between the initial posture of the human subject on the platform and the subsequent pattern of the balance-recovery response that occurs after a sudden tilt of the platform. This chapter involves three section. In the first section, it is given related literature. Following the literature review, the initial postures and the balance-recovery responses are classified to express the correlation between them by using classification algorithms in the second section. Afterwards, in the last section, the expression obtained for this relationship has been tested with Monte Carlo simulations by using the decision tree created in accordance with the classification.

8.1 Literature Review

In the previous parts of this thesis, it has been mentioned that the body configurations might be crucial for balance-recovery reactions. There are many studies on initial body configuration and its effects on balance-recovery reactions [64, 41, 39, 3, 10, 34, 16, 115, 78, 109].

[64] is one of the earliest studies on this topic. In [64], it has been studied the effect of initial stance (bipedal and quadrupedal stance) configuration on automatic postural responses in humans. Naturally, the change in strategy has been found, in other words, quadrupedal stance were remarkably different from the bipedal stance in terms of usage of the muscles. It is not surprised that postural responses of the human subjects and cats during quadrupedal stance are similar to each other. The results of this study led to new studies.

In [41], the relation between prior leaning and human postural responses have been studied. The most important finding of this study is that if the initial postures of the subjects are closer to their limits of stability, then they use hip motions to keep their body in stability limits. Furthermore, [41] has suggested that the CNS can be triggered a new muscle activation pattern based on the initial posture. The main result of [41] is that different initial stance positions cause changing in postural strategies. However, this changing cannot be predicted based on simple stretch or load reflexes, but match predictions from computational, biomechanical models of human stance coordination. The same argument has been improved in [39] that selection of the muscle synergy depends on not only initial conditions but also perturbation characteristics, learning, and intention.

[3] is an important review, which has been composed of five distinct parts. Each part has explained an experimental study and its results. At the end of the review, all experimental studies have been discussed in terms of effects of the trunk and hip motion on human balance corrections. Especially, one of these experimental studies is parallel with this thesis according to its experimental method. This part is called as "contributions of proprioceptive and vestibular inputs to postural control in the roll and pitch planes" in [3]. In the mentioned study, the relationship between the initial

stance and the balance-recovery reaction is a recognized phenomenon. However, it is also declared as a limitation for the experimental studies because the initial stance may differ considerably among the subjects. The purpose of this mentioned experiment has been declared in [3] that it was to determine the directional sensitivity in balance corrections and, it was to discover the relative contributions from the hip, knee, and ankle proprioceptive inputs in triggering automatic postural responses to unexpected perturbations. As seen in the Fig.8.1, body configuration has been changed to cope with the support surface perturbation. It is dependent upon the direction of the perturbation. Although it changes from trial to trial, it shows a typical posture. Besides, this posture is also different for different subjects.

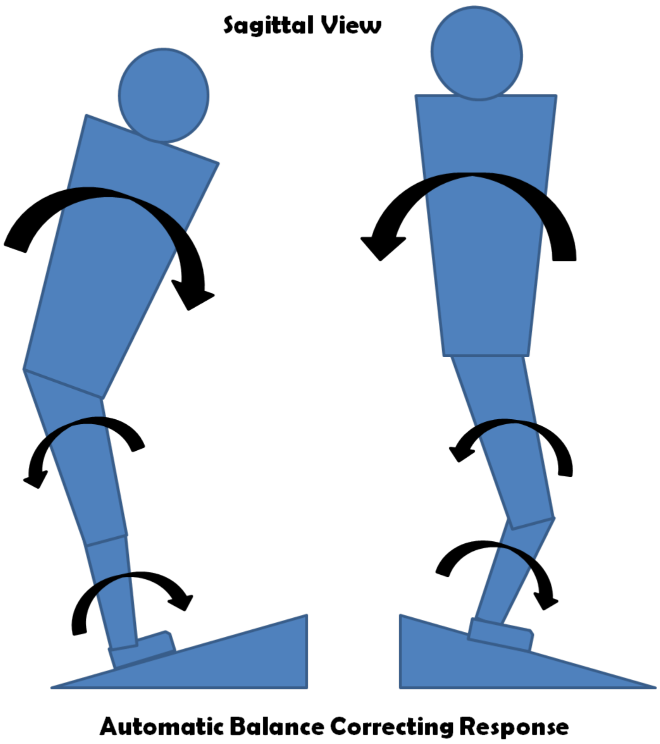

Figure 8.1: This figure is a reproduction of Fig.3 in [3]. Stick figure shows link movements in response to different rotational perturbations in the pitch and roll planes.

The other key study is [10], which is curious about whether the automatic postural responses of patients who suffer from Parkinson can be mimicked. These patients have a stooped posture. In experiments, healthy subjects mimicked this posture, and their responses were measured. [10] has stated that responses of the patients could be reproduced in healthy subjects mimicking a stooped parkinsonian posture.

The initial stance width, which is the distance between feet, is also another initial condition for this type experiments. In [34], it has been studied the altering stance width effects on postural response to multi-directional support surface translations. As a result, [34] has stated that postural strategies have changed depending on initial stance width. The other influence on postural reactions is anxiety. [16] has studied the effect of postural anxiety on postural reactions to unexpected surface rotations in multiple directions. The results of this study revealed that postural responses have changed with increased anxiety. In their experiment, the postural anxiety provided by changing the altitude of the support surface platform. Fatigue also has to be taken account into as an effect on postural responses. This effect has been studied in [115]. Their findings have illustrated that neuromuscular fatigue can influence postural strategy in response to a balance perturbation.

[78] is opposed to the concept that compensatory postural adjustment is associated with the alignment of body segments. Their claim is based on the idea that initial and final postures are similar but not exactly same for all trials. As a conclusion, [78] has stated behavior of the body segments during compensatory postural adjustment can not be predicted by evaluating only static posture. On the other hand, [109] has demonstrated that the body configuration at the instant of first stepping-foot contact is a very strong predictor of successful balance recovery (vs. falling) after a backward postural perturbation.

8.2 A Correlation Rule Established by Using Classification Algorithms

There is a little controversy over the idea that postural responses are related to initial posture. In this chapter, it will be examined whether the initial posture and the balance-recovery reactions against a sudden external disturbance are correlated. The experimental results of the subjects show that the initial posture of the subject happens to be different at each trial. It is also observed that the initial posture and the balance-recovery reaction patterns are noticeably correlated. In this respect, the initial postures are classified here into two fuzzy membership categories designated as "agile" and "slouchy" postures. The results give the impression that a subject with an agile initial posture can recover balance effectively with few oscillations, whereas a subject with a slouchy initial posture can recover balance ineffectively with too many oscillations. For example, an excessive initial inclination of the trunk seems to be one of the main causes of an ineffective balance recovery. The results also imply that initially bent knees have an improving effect on the balance recovery like that of a shock absorber, especially during the backward tilts.

It is thought that these two fuzzy membership categories can be classified by using decision trees algorithms. Afterward, a rule, which can describe the responses as "agile" and "slouchy" depending on random initial and random final configurations, can be written from decision trees. It is discussed in this section.

8.2.1 Illustration of "Agile" and "Slouchy" Postures and Responses

During the evaluation of the experimental data, it is observed that some responses are more oscillatory than the others. It can be thought that this observation can depend on the initial body configuration. At this point, the data is inspected more detail by means of given figures and tables. The assessments of the tables without any spreadsheet software are very difficult. Therefore just for information, they are given in the Appendix H. However, figures can be seen as follows. When Fig.8.2, Fig.8.3, Fig.8.4, Fig.8.5 and tables given in Appendix H are analyzed, responses are categorized into two distinct groups, which are referred to as "Agile" and "Slouchy". The following table shows the classification of the trials.

Table 8.1: Trial Numbers Classified as an "Agile" and "Slouchy".

	Forward Trials	
	Agile	Slouchy
Subject 1	5, 6, 7, 8, 10, 11, 12, 13, 16	1, 2, 3, 4, 9, 14, 15, 17, 18, 19, 20
Subject 2	2, 3, 4, 5, 8, 9, 10, 11, 12, 13, 15	1, 6, 7, 14, 16, 17, 18, 19, 20
	Backward Trials	
	Agile	Slouchy
Subject 1	2, 5, 7, 8, 14, 15, 16, 18, 20	1, 3, 4, 6, 9, 10, 11, 12, 13, 17, 19
Subject 2	2, 5, 8, 9, 10, 11, 12, 13, 14	1, 3, 4, 6, 7, 15, 16, 17, 18, 19, 20

The grouping of responses by their oscillatory behavior will be used as training set. Therefore, the visual inspection is very important step for the achievement of the classification algorithm. There are two main advantages of using classification algorithm. First, it gives a systematic assessment of the visual inspection. Second, a set of IF-THEN rules can be extracted to help identify the responses depending on the initial and final body configurations.

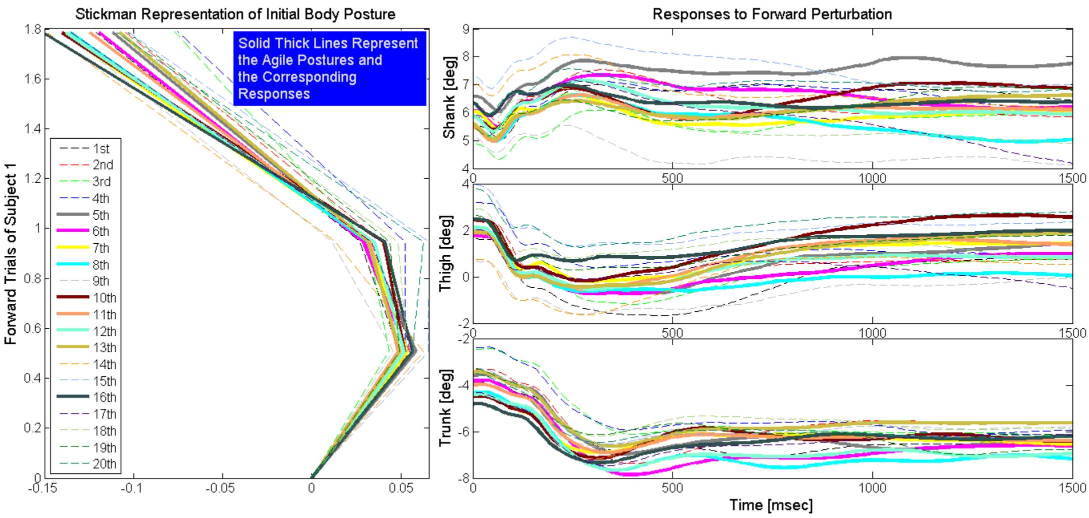

Figure 8.2: "Agile" and "Slouchy" Postures and Responses of Subject 1 for Forward Trials.

Fig.8.2 are composed of two columns, the first column shows the initial body configurations in stick man representation form. The right part is divided into three; each part shows the responses of the body parts, which are included the biomechanical model such as shank, thigh and trunk. Solid thick lines represent the "Agile" initial posture and corresponding responses. Thin dashed lines are used for showing the "Slouchy" initial posture and corresponding responses.

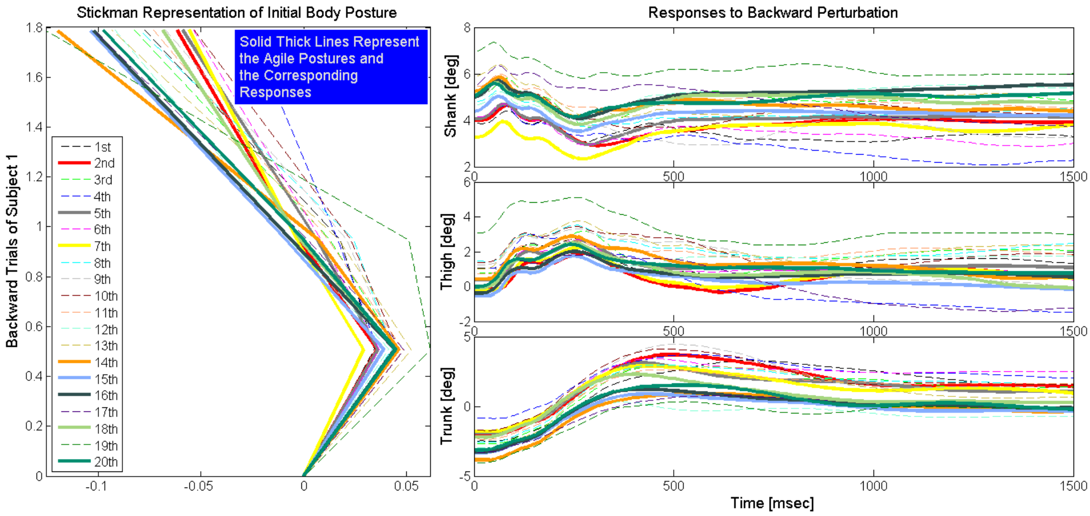

Figure 8.3: "Agile" and "Slouchy" Postures and Responses of Subject 1 for Backward Trials.

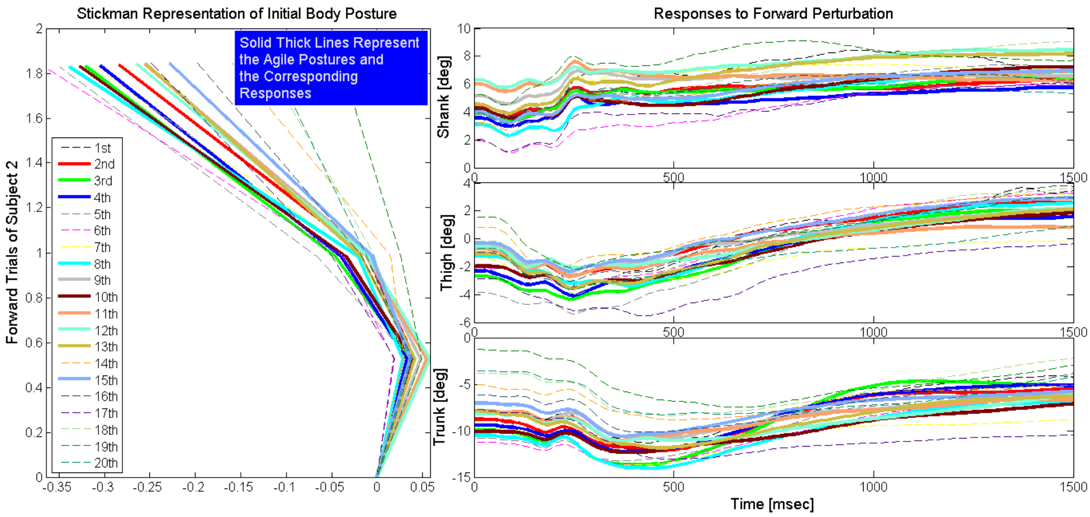

Figure 8.4: "Agile" and "Slouchy" Postures and Responses of Subject 2 for Forward Trials.

The figures belonging to each subject can be compared in terms of their oscillatory behaviors and initial body configurations with each other. At this point, it can be said that Subject 1 behaves less oscillatory. With this view, the axis limits of the figures can be checked. The categorization as "Agile" and "Slouchy" can be understood from the figures. The posture of the subject in an agile posture looks similar to a bow of archery in figures. Visually, non-classified postures of the subjects are called as a slouchy posture. The figures give the impression that a subject with an agile initial posture can recover balance effectively with few oscillations, whereas a subject with a slouchy initial posture can recover balance effectively with too many oscillations. For example, an excessive initial inclination of the trunk seems to be one of the main causes of an ineffective balance recovery. The figures also show that initially bent knees have an improving effect on the balance recovery like that of a shock absorber.

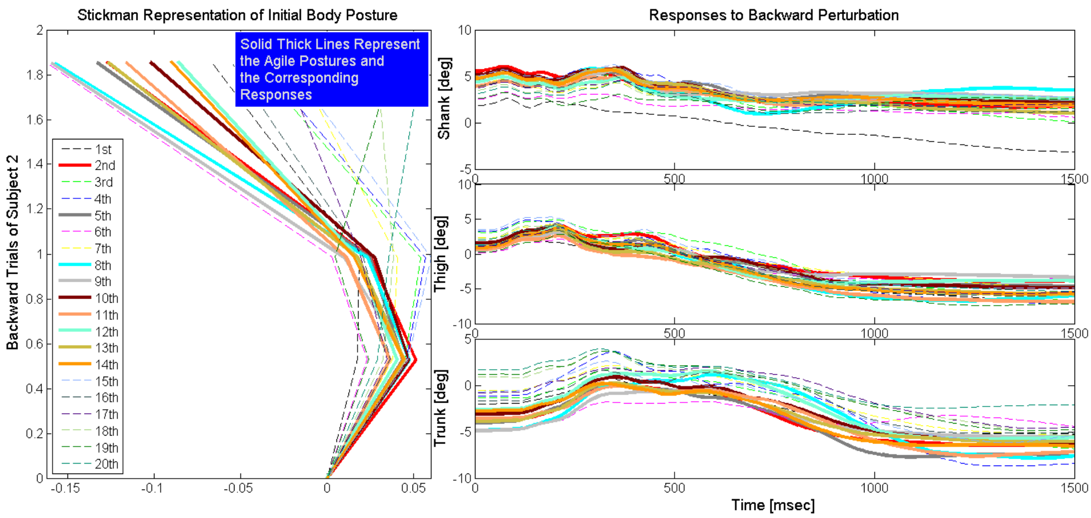

Figure 8.5: "Agile" and "Slouchy" Postures and Responses of Subject 2 for Backward Trials.

8.2.2 Classification Algorithm

For rule extraction, decision tree method is a widely used data mining approach. Actually, data mining is a collection of data processing methods which can be listed as association, clustering, classification, and prediction [112]. Naturally, data mining involves various techniques; just one of them is decision tree algorithms, which is often used for the classification of data. It is the task of generalizing known structure to apply to new data [31]. In other words, classification derives a function or model that identifies the categorical class of an object based on its attributes [112]. In this study, a classifier is applied to find a "if-then rule" for making a decision about whether the posture is "Agile" or "Slouchy". The classifier is called as J48 in the software "Weka". Weka is a free software developed by Waikato University in the New Zealand. The purpose of the Weka project is declared in [30] that it aims to provide a comprehensive collection of machine learning algorithms and data preprocessing tools to researchers and practitioners alike. Weka has widespread acceptance in both academia and business [30]. C4.5 is a well-known decision tree algorithm developed by J. Ross Quinlan [30, 93]. C4.5 is named as J48 in Weka [117].

In [89], the developer of the C4.5 describes it as the collection of a set of programs. This set consists of four distinct programs, which are listed below:

1. the decision tree generator,
2. the production rule generator,
3. the decision tree interpreter, and
4. the production rule interpreter.

Open sources of C4.5 (unix-version) and j48 (java-version) can be found on the Internet: http://www2.cs.uregina.ca/ dbd/cs831/notes/ml/dtrees/c4.5/tutorial.html and http://weka.sourceforge.net/doc.dev/weka/classifiers/trees/J48.html. However, in this study, GUI version of Weka is used to run the J48 classifier. Additional information can be found at the following oficial web sites, http://www.cs.waikato.ac.nz/ml/weka/. Additionally, free educational material related to data mining with Weka can be found in the url:http://www.cs.waikato.ac.nz/ml/weka/mooc/dataminingwithweka/

Naturally, the main topic of this thesis is not data mining. Therefore, it is not preferred to give too much information about Weka and J48. However, above, it is just tried to show to be scientific and well-known method. (For more information, see all data mining textbooks, especially [117]).

In the next section, it will be discussed the way of extracting a rule from a decision tree. The mentioned software Weka and J48 classifier will be used for obtaining a decision tree and then extracting the corresponding "if-then rule".

8.2.3 Decision Three

The first step is to build a decision tree classifier from a set of training data. Therefore, chapter 2 in [89], which is referred to as "constructing decision trees", is summarized. The original example is replaced with the example, which contains initial posture configuration, final posture configuration, fatigue effect and decision about responses.

The method of constructing a decision tree from a set T of training cases is elegantly simple. Let the classes be denoted $\{C_1, C_2, \ldots, C_k\}$. There are three possibilities:

- T contains one or more cases, all belonging to a single class C_j: The decision tree for T is a leaf identifying class C_j.
- T contains no cases:
  The decision tree is again a leaf, but the class to be associated with the leaf must be determined from information other than T. For example, the leaf might be chosen in accordance with some background knowledge of the domain, such as the overall majority class. C4.5 uses the most frequent class at the parent of this node.
- T contains cases that belong to a mixture of classes:
  In this situation, the idea is to refine T into subsets of cases that are, or seem to be heading towards, single-class collections of cases. A $testT10$ is chosen, based on a single attribute; that has one or more mutually exclusive outcomes $\{O_1, O_2, \ldots, O_k\}$. T is partitioned into subsets $T_1, T_2, \ldots, T_k$ where T_i; contains all the cases in T that have outcome O_i of the chosen test. The decision tree for T consists of a decision node identifying the test, and one branch for each possible outcome. The same tree-building machinery is applied recursively to each subset of training cases, so that the i_{th} branch leads to the decision tree constructed from the subset T_i of training cases.

Example 8.2.1. *The successive division of the set of training cases proceeds until all the subsets consist of cases belonging to a single class. The illustration of the process involves the small training set of Table.8.2 in which there are seven attributes and two classes.*

Table 8.2: Training Set for Subject 2 Forward Trials

Initial Shank Angle	Initial Thigh Angle	Initial Trunk Angle	Final Shank Angle	Final Thigh Angle	Final Trunk Angle	Fatigue Effect	Decision
0.077835	-0.010344	-0.152514	0.109132	0.062044	-0.084534	First Ten	Agile
0.067942	-0.046347	-0.172938	0.092184	0.018609	-0.109702	First Ten	Agile
0.062542	-0.039526	-0.164461	0.110677	0.041225	-0.085236	First Ten	Agile
0.066812	-0.067289	-0.189021	0.11207	0.013843	-0.129525	First Ten	Agile
0.03464	-0.040155	-0.197792	0.10024	0.051389	-0.132434	First Ten	Slouchy
0.089481	-0.02287	-0.168175	0.085411	0.045801	-0.090692	First Ten	Slouchy
0.053907	-0.02054	-0.182708	0.10408	0.046624	-0.095737	First Ten	Agile
0.089915	-0.008524	-0.138105	0.095342	0.043112	-0.103919	First Ten	Agile
0.074438	-0.035566	-0.17756	0.099739	0.046988	-0.086583	First Ten	Agile
0.104557	-0.012136	-0.137971	0.105102	0.037842	-0.093385	Second Ten	Agile
0.109881	-0.010132	-0.142545	0.109207	0.018318	-0.123626	Second Ten	Agile
0.079042	-0.017367	-0.135704	0.103875	0.039772	-0.07451	Second Ten	Agile
0.054841	0.014915	-0.08282	0.11011	0.062495	-0.068041	Second Ten	Slouchy
0.069742	-0.005283	-0.122983	0.110056	0.082329	-0.047385	Second Ten	Agile
0.073456	-0.016553	-0.105995	0.081286	0.03687	-0.06353	Second Ten	Slouchy
0.034979	-0.049951	-0.130855	0.06226	0.044055	-0.029483	Second Ten	Slouchy
0.054471	-0.003314	-0.066479	0.097734	0.054737	-0.029913	Second Ten	Slouchy
0.091879	0.026783	-0.020819	0.091437	0.049356	-0.014245	Second Ten	Slouchy
0.068662	-0.01207	-0.06192	0.087851	0.041321	-0.020839	Second Ten	Slouchy

Evaluation of the given data set with visual inspection is very difficult, even with spread sheet software. Given data table is used as training set for drawing decision tree. There are 7 attributes and two classes. The attributes are the initial and final limb configurations [in rad.] and fatigue effect. The classes is "Agile" and "Slouchy" postures and responses.

The same data format are prepared for all subjects and for all directions. These datasets are evaluated with C.45 classifier (J48 in The Weka). The following figure Fig.8.6 shows the drawing decision tree for the given dataset by the Weka. The Weka's figure is drawn for more readability. Original visualized decision tree by the Weka can be seen in Appendix H. Additionally all outputs are given in Appendix H.

The following section is summarized from [31]. However, examples, figures, tables and some necessary explanation are added to strengthen the meaning.

Decision trees can become large and difficult to interpret. Therefore, it is applied to build a rule based classifier by extracting if-then rules from a decision tree. In comparison with a decision tree, the if-then rules may be easier for humans to understand, particularly if the decision tree is very large. To extract rules from a decision tree, one rule is created for each path from the root to a leaf node. An example decision tree can be seen in the Fig.8.6

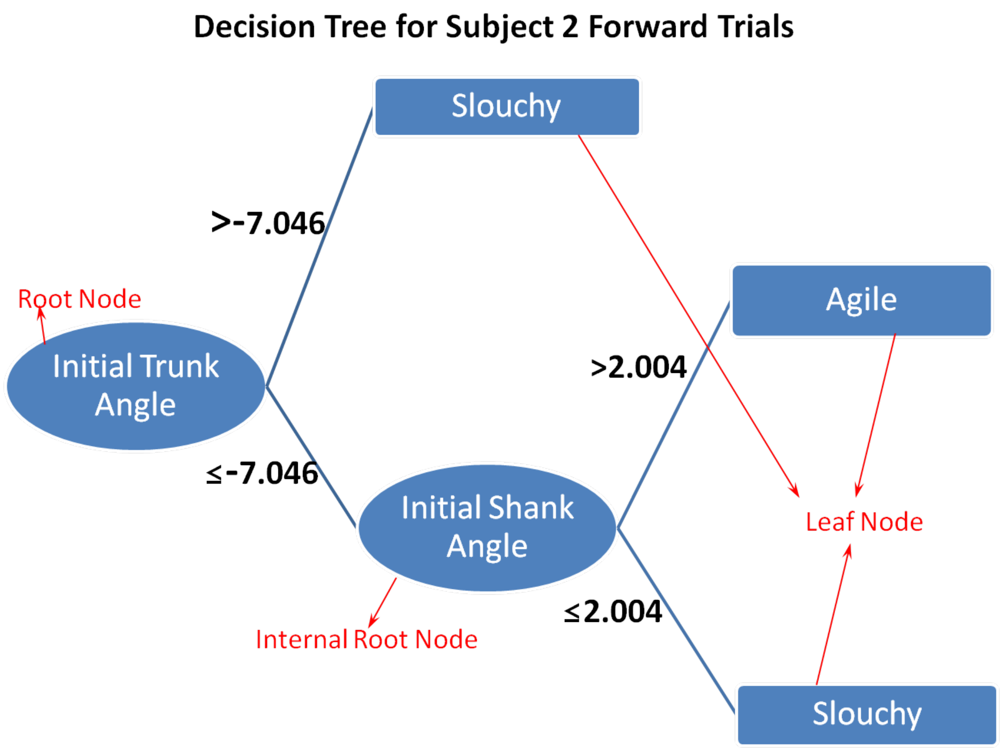

Figure 8.6: Decision Tree Showing "Agile" and "Slouchy" Postures together with the Related Terminology.

Each splitting criterion along a given path is finished with "logical AND" to form the rule antecedent ("IF" part). The leaf node holds the class prediction, forming the rule consequent ("THEN" part).

Example 8.2.2. *Extracting classification rules from a decision tree. The decision tree in Fig.8.6 can be converted to classification IF-THEN rules by tracing the path from the root node to each leaf node in the tree. The rules extracted from Fig.8.6 are*

R1: IF Initial Trunk Angle > -7.046 *THEN Postural Responses = Slouchy*

R2: IF Initial Trunk Angle ≤ -7.046 *AND Initial Shank Angle* ≤ 2.004 *THEN Postural Responses = Slouchy*

R3: IF Initial Trunk Angle ≤ -7.046 *AND Initial Shank Angle* > 2.004 *THEN Postural Responses = Agile*

A disjunction (logical OR) is implied between each of the extracted rules. Because the rules are extracted directly from the tree, they are mutually exclusive and exhaustive. By mutually exclusive, this means that it is impossible to appear a rule conflicts here because no two rules will be triggered for the same tuple. By exhaustive, there is one rule for each possible attribute-value combination, so that this set of rules does not require a default rule. Therefore, the order of the rules does not matter; they are unordered.

8.3 Statistical Evidence with Monte Carlo Simulations for Correlation between Initial Posture and Balance-Recovery Response

Four different rules are found for two subjects and two directions. These rules are tabulated below in Table.8.3. It is observed that trunk angle has a crucial role for keeping the posture.

Table 8.3: Extracted Rules

Subject 1

Forward	Backward

if $\theta_{tr-fin} \leq -0.1136$
    if $\theta_{sh-ini} \leq 0.1118$
        Response=Agile
    else
        Response=Slouchy
    end
else
        Response=Slouchy
end
	if $\theta_{th-fin} \leq -0.0062$
	        Response=Agile
	else
	    if $\theta_{sh-ini} \leq 0.072$
	        Response=Agile
	    else
	        Response=Slouchy
	    end
	end

Subject 2

Forward	Backward

if $\theta_{tr-ini} \leq -0.1230$
    if $\theta_{sh-ini} \leq 0.0350$
        Response=Slouchy
    else
        Response=Agile
    end
else
        Response=Slouchy
end
	if $\theta_{tr-ini} \leq -0.0466$
	        Response=Agile
	else
	        Response=Slouchy
	end

This result seems reasonable because trunk (trunk, arms and head) has a big portion of the body mass. Inevitably, balance-recovery responses will be more affected by the position of the relatively big mass. Appearance of the four distinct rules are expected result because of different behavioral patterns.

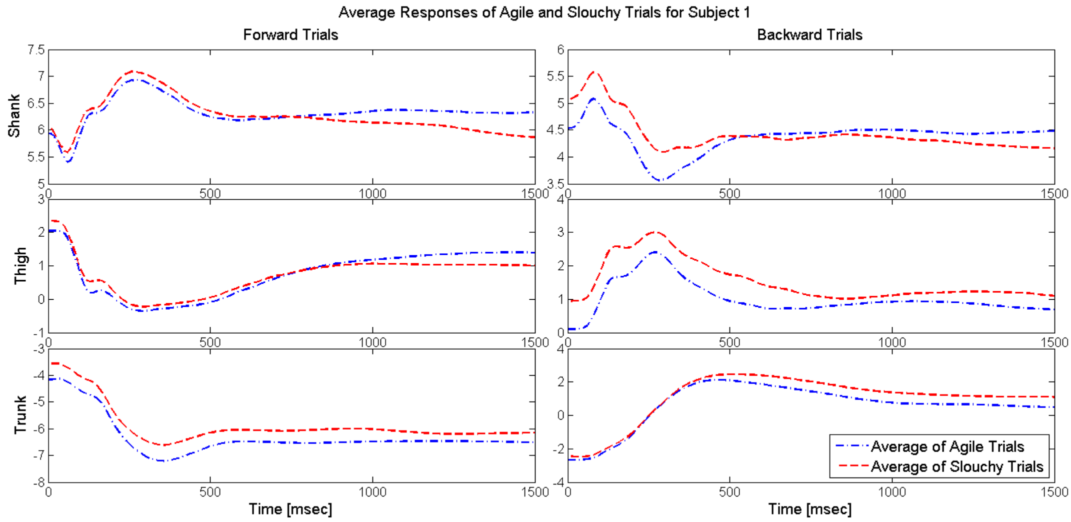

Figure 8.7: Averages of Agile and Slouchy Trials for Subject 1

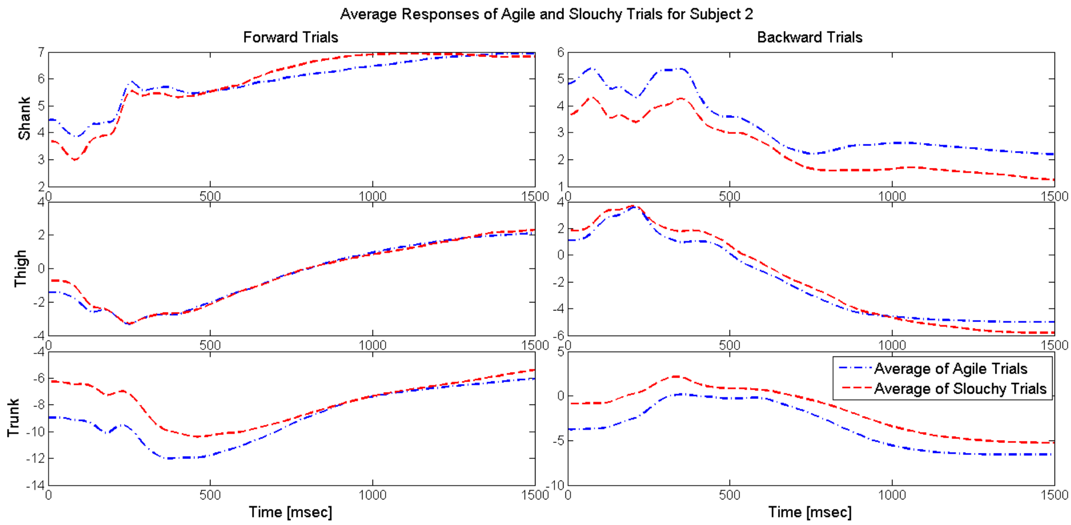

Figure 8.8: Averages of Agile and Slouchy Trials for Subject 2

Naturally, the extracted rules have to be checked whether or not the rules produce the expected responses. Therefore, it is applied to Monte Carlo Simulations for testing the rules, statistically. Before starting to run the simulations, first, the averages of agile and slouchy trials are found for four distinct cases. They can be seen in Fig.8.7

and Fig.8.8 As shown in the above figures, each average set can be thought as an independent trial. Then the control gains are estimated for these eight cases by using the LS method, which was explained in Chapter 6. As different from Chapter 6, they are saved for using at the next step to create new responses. At this point, it is needed to make a decision about randomly generated initial and final body configurations whether they are agile or slouchy by using extracted rules. For the simulations, this decision is important because it is needed a decision about which gain sets (agile or slouchy) have to be used. For sake of clarity, algorithm is tabulated as follows:

Table 8.4: Algorithm for Testing the Extracted Rules by Using MCS

Input Agile and Slouchy Trial Numbers.
Find Average Responses of Agile and Slouchy Trials.
Find Gain Set for Agile and Slouchy Responses.
Save these Sets differently such as Agile Gains and Slouchy Gains.
Find the max. and min limits for all the initial and final angles.
Randomly generate initial and final conditions within these limits.
Make a decision about randomly selected body configuration depending on extracted rules.
If it is Agile select Agile Gains else select Slouchy Gains.
Determine θ_{ref} depending on randomly generated initial and final conditions.
Start Simulation
Do it 20 times
Draw the results

By using algorithm above, the following initial posture and response relations are obtained. Fig.8.9 and Fig.8.10 belong to Subject 1. Similarly, random initial body configuration and balance recovery response relations for Subject 2 are given in Fig.8.11 and Fig.8.12. The first graphs represent forward trials, and the last graphs show backward trials for each graph pairs. The graphs are drawn on the experimental data to allow easier comparison. Blue thick and dash-dot lines represent randomly selected agile postures and corresponding responses. The same representation style with red color is used for slouchy postures and corresponding responses.

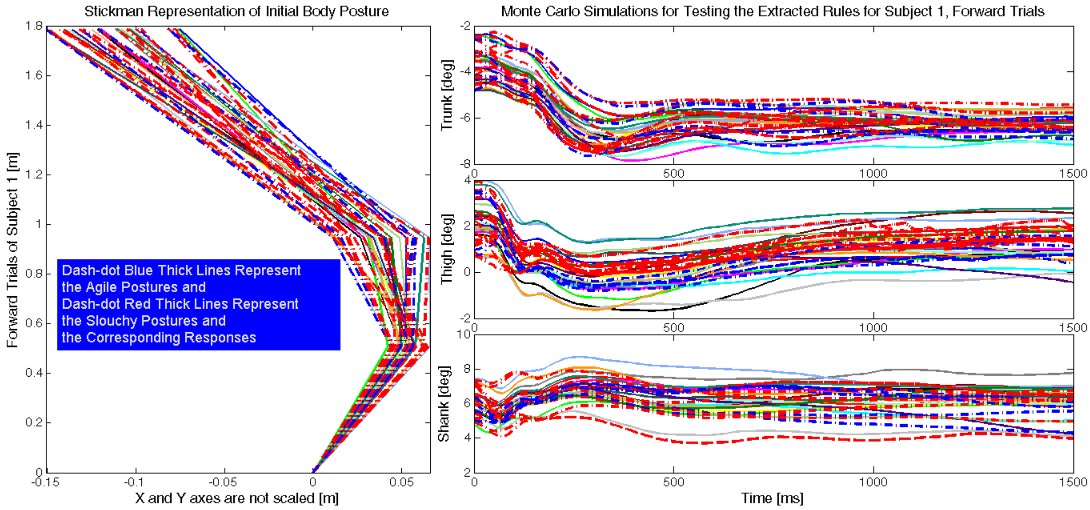

Figure 8.9: Monte Carlo Simulations for Testing the Extracted Rules for Subject 1, Forward Trials

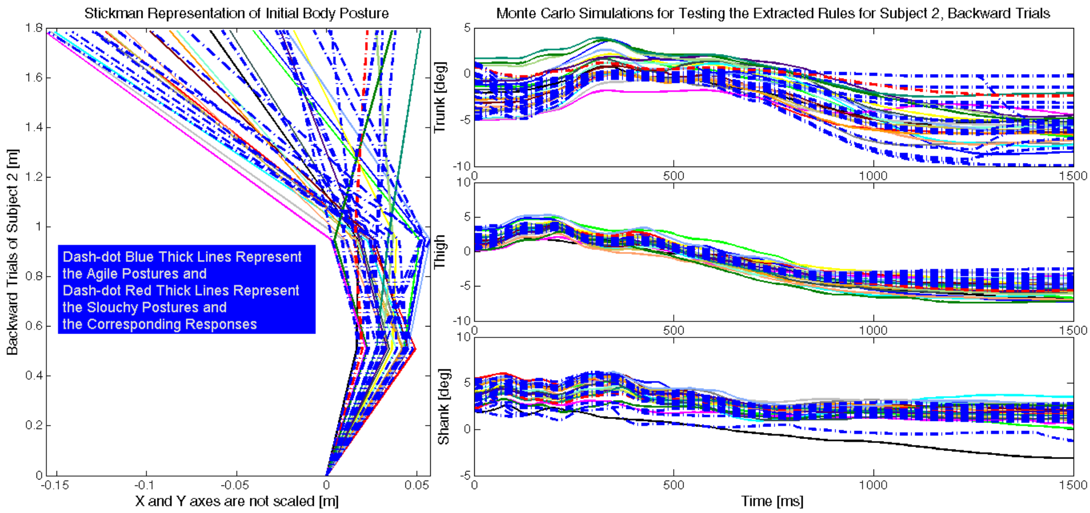

Figure 8.10: Monte Carlo Simulations for Testing the Extracted Rules for Subject 1, Backward Trials

In Fig.8.9 and Fig.8.10, as expected, both randomly generated body configuration, and corresponding responses are within the limits obtained by experimental data. However, Fig.8.10 shows that extracted rule for backward trials is not good enough. It can be seen in Table.8.3, this rule does not include trunk angle; it contains only final thigh angle and initial shank angle. Therefore, it is not sufficiently good at discriminating between agile and slouchy posture. It has to be accepted that the size of the used training set can be increased then the extracted rule will be changed. Therefore, the new rule may make more effective selections. With a more realistic view, final body configuration has not to be included the rule parameters. However, unfortunately, it is a necessity for modeling. This conflict can be noted for future works.

In the same way, Fig.8.11 and Fig.8.12 can be evaluated. It is surprisingly parallel to Subject 1, extracted rule for backward trials of Subject 2 is also does not work very well.

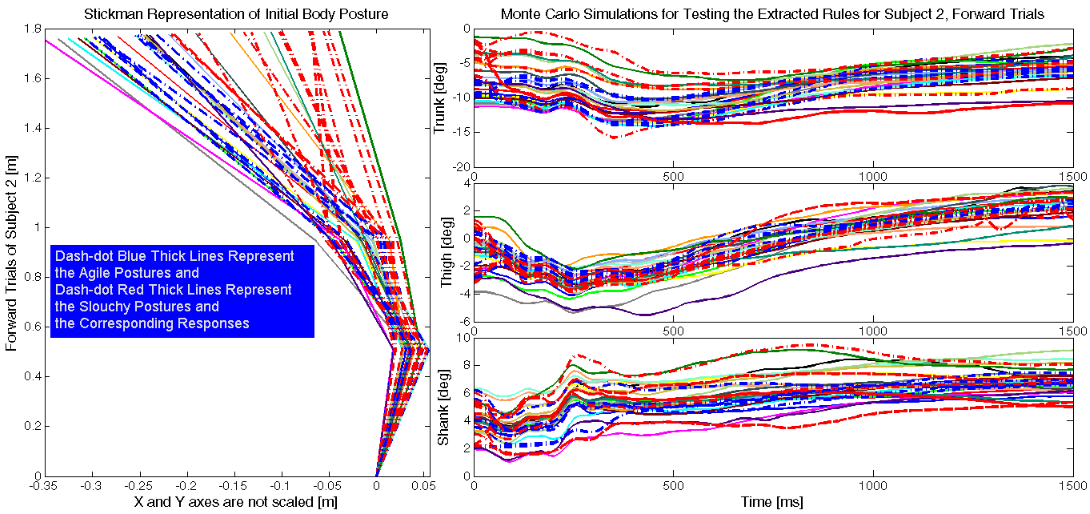

Figure 8.11: Monte Carlo Simulations for Testing the Extracted Rules for Subject 2, Forward Trials

Similarly, Fig.8.11 and Fig.8.12 are within the limits that are obtained from experimental data, but nevertheless the extracted rule for backward trials is not good enough as shown in Fig.8.12. This rule includes only initial trunk angle. It is said that trunk angle is a crucial role for the prediction of the responses depending on initial configuration. However, it is noticed that it is not enough alone.

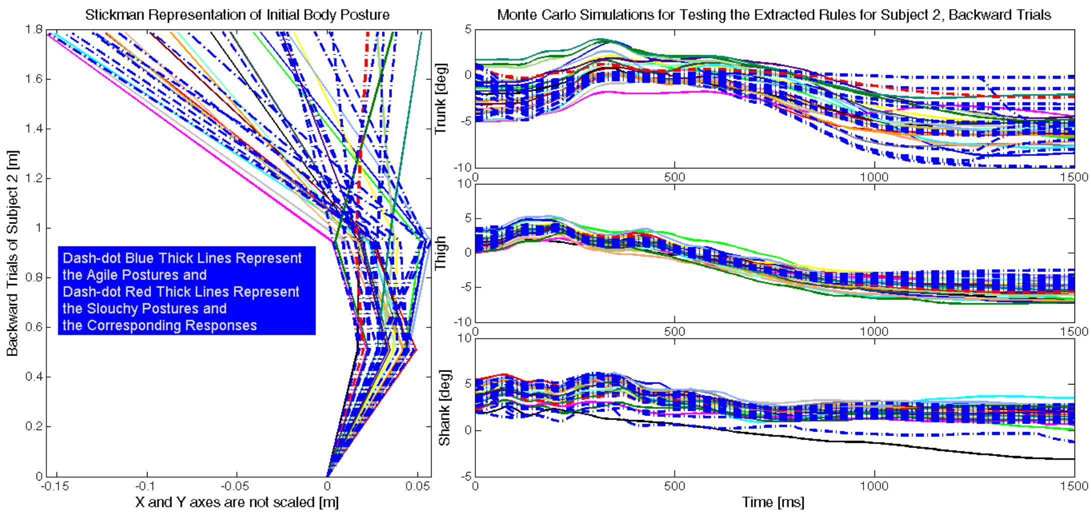

Figure 8.12: Monte Carlo Simulations for Testing the Extracted Rules for Subject 2, Backward Trials

As a summary of this chapter, the hypothesis, which claims that there is a correlation between the initial posture and the balance-recovery reactions against a sudden external disturbance, has kept validity. It has been demonstrated that an excessive initial backward or forward inclination of the trunk are the main causes of an ineffective balance recovery. However, it is not solely predictor for balance recovery. Shank angle is also an effective predictor.

The study in this chapter has supported the relation between the initial posture and the balance-recovery reactions. However, it has not clarified sufficient enough. The more studies are required on this topic for the disappearing of doubt and conflict. Moreover, there will be unknown effects on estimation of the balance-recovery reactions sourced from internal factors such as anxiety and fatigue. In this study, their effects have not been observed because of shortness of training set.

CHAPTER 9

SUMMARY AND CONCLUSIONS

This chapter consists of four sections as follows: summary of thesis, discussions, future prospects and conclusions. In the first section, it is given the summary of all the main points. In the discussion section, first of all, previously mentioned main points are interpreted in the context of literature. It is presented the principal findings, and it is commented their implications. Lastly, deficiencies and limitations of the study are discussed. In the third section, it is indicated to future prospects. In this section, it is tried to be drawn a directions for future research. This thesis has been finished with a conclusion section. Conclusion section includes evaluation of the thesis.

9.1 Summary of Thesis

The early and effective diagnosis of balance disorders and improvement of neuroprosthetics are directly related to the understanding of the balance-recovery reactions. However, the seemingly simple task of upright postural control is not well understood, yet.

This thesis is composed of nine chapters. The first four chapters are introductory chapters. The remaining four chapters (Chapter 5, 6, 7 and 8) include the basic and distinct aspects of this study.

In chapter 5, a control law to model automatic postural responses to sudden external disturbance has been conjectured. This conjecture is based on three main ideas and experimental observations. The first idea is that automatic postural responses depend on adjustable postural strategies and synergies, and this adjustment is realized by the central nervous system by evaluating the internal and external context. This phenomenon is observed as individual behavioral pattern resulting from balance-recovery response, experimentally. The second important basis of this conjecture is an observation that there is a diversity of the initial and final body configurations. Although it has not been found any correlation between the initial and final body configurations, there are powerful evidence about the relation between the initial body configuration and the corresponding postural response. However, the selection of the body configuration seems to be determined arbitrarily. The third idea is to use simplicity principle for explanation of the very complex system. In the lights of these ideas and observations, the control law has been suggested as simple as possible. Thus, PD control is proposed because of its compatibility of the physiological facts and its sufficiency for simulation of the behavior of the system. The feedback gains of this PD control are conjectured as time-varying. These gains are likely adjusted by CNS by using the bodily and environmentally acquired sensory information. According to the second observation, it has been proposed time-dependent upright reference angles (θ_{ref}). It has been claimed that the difference between the desired upright body segment position and sensed position is the main dynamics of producing the torque on muscles.

In Chapter 6, the conjectured control law has been tested and verified through detailed simulations on a 3 DoF biomechanical model. Firstly, the feedback gains have been identified by using LS (Least Square) algorithm and then, body reference angles have been determined. Lastly, the validation of the estimated time-varying feedback control gains and upright reference position (θ_{ref}) have been verified with the achievement of estimated parameters to fit the experimental data. Besides, simulations are repeated to test whether it is possible to obtain the individual behavioral pattern characteristic by using random initial body configuration.

Chapter 7 concentrates on revealing an adaptation law. Because, the central nervous system applies the conjectured PD control law by changing its gains according to a certain adaptation law. Adjustment of the gains is generally accepted theory that the CNS can modify the gain of even simple reflexes based on expectation, instruction and experience. In this chapter, an adaptation law has been proposed depending on bodily sensory information (measured position and velocity) and external disturbance (generated by support surface tilt platform). This adaptation law is identified by using CCA (Canonical Correlation Analysis). Then, it has been verified by using forward integration.

The penultimate chapter of this thesis examines the effect of initial body configuration on balance-recovery reactions. This chapter has arisen from examining the experimental results gathered from the repeated trials for different human subjects. With visual inspection and by using spread sheet software, it has been noticed a relation between initial body configuration and corresponding balance recovery responses. The result of this observation, initial body configurations are categorized into two fuzzy classes such as "Agile" and "Slouchy". The main aim of this chapter is to extract the rule, which can determine whether any random body configuration is "Agile" or "Slouchy". For verification of the extracted rules, they have been simulated by using two different gains set, which were found for averaged agile and averaged slouchy trials.

9.2 Discussion

In this section, as the same manner, the main four chapters are discussed separately. For all chapters, it is tried to explain principal implications including with comparison with the literature. Additionally, it is discussed and evaluated unexpected findings, conflicting results, limitations, and weaknesses, when necessary. Furthermore, the hypotheses tested in this thesis are stated why they are acceptable and how they are verified. These hypotheses also are examined depending on their consistency with previously published studies and experimental data.

Before starting to discuss each chapter of the main body of this thesis separately, it is needed to declare two important decision. These decisions are related to experimental setup and biomechanical model.

Experimental Setup

To understand the balance-recovery control against the sudden external disturbance is required to be evoked the body equilibrium and orientation by using any measurable disturbance source. In this study, the tilt of support surface has been selected as a disturbance generator. Because [21] has stated that tilt of support surface has a crucial role in understanding the basic mechanisms generating corrective postural reactions.

Biomechanical Model

The proposed model is confined to the sagittal plane with three degrees of freedom having the ankle, knee, and hip joints as the only actuated joints. This general assumption is a widely used approach in terms of simplification. In the sagittal plane, [7] has stated that the proposed model is valid for analysis of postural control mechanisms.

Discussion of Proposed Control Law (Ch. 5)

PD control strategy is widely used to model the human neural control. It is more convenient to simplification compared with optimal control strategies [49, 63]. The current study has contributed to "PD control strategy", which is to be used as physiological controller model with two main aspects. These contributions are "time-varying feedback gains" and "time-dependent upright reference angles" ideas. Time-varying feedback gains have been mentioned in several studies about adjustable strategies and synergies [38, 42, 84]. However, time-varying feedback gains are used in the model for the first time in this study. Moreover, in [84], upright reference angles are defined as constant, the second important contribution is related to the definition of the upright reference position. According to the evaluation of the experimental data, this study has proposed time-dependent upright reference angles. At this point, it has been hypothesized that upright reference body angles may also be modified by CNS. The positive effects of these two contributions have been seen in the simulations in terms of fitting the experimental data.

Furthermore, the conjectured control law is presented basis of the three main assumptions depending on simplicity principle. They can be listed as follows:

(i) Feedback gains are used in principle axis.

(ii) All sensors and actuators are assumed perfect.

(iii) Time delays are not included the model.

These simplifications do not have negative influences on the simulations.

Comparison of simulation results with experimental data (Ch. 6)

In this chapter, the experimentally observed motions of the human subjects have been simulated by using the 3 DoF-body model and the conjectured control law. Very satisfactory imitations are obtained by adjusting the control gains and the upright reference angles appropriately. No doubt, it is possible to obtain more similar results to the experimental data. For this purpose, the more convenient LS methods can be developed, or a different paradigm can be determined for upright reference angles.

Although it can be thought as future works, it is not fundamental issue for general purposes of this thesis.

In this chapter, preferred model-based approach is an advantage to describe phenomena, which are not fully understood. Nevertheless, there are more or less incompatibility between almost all obtained simulations and the experimental data. No doubt, it is possible to obtain more similar simulations to experimental data. However, it is an optimization problem. For more similar simulation results, it is needed to be spent more time for selection of methods, algorithms, and parameterization.

At this point, there are two solutions. First one is to abandon the running simulation automatically for all trials. It means that it must be done parameterization separately for all trials. For the second one, it is not to need to be given up automation. Instead, a correction method can be sought to obtain more successful simulations in terms of fitting experimental data. For instance, this correction method can be based on genetic algorithm. Additionally, new corrective terms can be added, which may represent the emotional factors such as anticipation, arousal, attention, expectations and prior experience. On the other hand, more powerful LS methods can be available in order to obtain more accurately estimate the control gains.

The Adaptation Law for Adaptive Modification of Automatic Postural Responses (Ch. 7)

It is widely accepted that automatic postural coordination has flexibility and adaptability to suit particular tasks and contexts based on the specific sensory information to each condition [36, 39, 40]. At this point, the most important contribution of this thesis is that a functional relationship about how time-varying gains are managed by CNS can be revealed. In addition to experimental studies, in fewer studies [110, 26], it has been attempted to identify the adaptation. A quantitative measure of adaptation can be used for the evaluation of balance disorders and diseases. In evaluating treatment efficacy, it can be an important tool in monitoring the progress of patients [26].

In this study, it has been found the functional relations, which can be expressed with the contributions of the variables involved in the adaptation process. For this purpose, the canonical correlation analysis method is selected. To verify the obtained results, the model is simulated by using these functions found by the canonical correlation analysis method.

According to obtained simulations, success expectation in the adaptation law has been realized. Adaptation law is formed by using bodily sensory information (measured position and velocity) and external disturbance (generated by support surface tilt platform). And it is estimated by using CCA. No doubt about that there is highly visible differences between experimental data and simulations. When necessary, it can be obtained more similar simulations to experimental data. It depends on selected estimation methods completely. It was discussed in the previous part. Additionally, it may be affected by added new sensory information or weighted sensory information, positively.

However, although there can be possible an improvement on simulations in terms of fitting to experimental data, it is not essential. At the beginning of this chapter, it was declared that estimation of the adaptation law was very difficult depending on many factors related to the past physiological and psychological experiences of the human beings. Nevertheless, it is achieved to estimate the functional relationships, which symbolize adjustment of sensory information and re-weighting by changing the environmental conditions. As a result, obtained simulations not only parallel to experimental data but also they support to the idea given in [36, 39]. This idea is that automatic postural coordination is flexible, and it can adapt to particular tasks and contexts based on the sensory information.

Correlation Between Initial Posture and Balance-Recovery Response (Ch. 8)

In this chapter, it has been examined whether the initial posture and the balance-recovery reactions against a sudden external disturbance are correlated. The experimental results of the subjects show that the initial posture of the subject happens to be different at each trial. It is also observed that the initial posture and the balance-recovery reaction patterns are noticeably correlated. In this respect, the initial postures are classified here into two fuzzy membership categories designated as "agile" and "slouchy" postures. To uncover of the evident correlation between the initial body configuration and the subsequent pattern of the balance-recovery reaction can be regarded as the second most important contribution of this thesis.

Although there are many studies about initial body configuration and its effects on balance-recovery reactions [64, 41, 39, 3, 10, 34, 16, 115, 78, 109], the controversy over the idea that postural responses are related with initial posture are continuing. At this point, the result of this study implies that initial posture and the response relations can be shown with extracted rules.

Naturally, the extracted rules have to be checked whether or not the rules produce the expected responses. Therefore, it is applied to Monte Carlo Simulations for the obtained rules testing as statistically. According to obtained results, the hypothesis, which claims that there is a correlation between the initial posture and the balance-recovery reactions against a sudden external disturbance, has kept validity. It has been demonstrated that an excessive initial backward or forward inclination of the trunk are the main causes of an ineffective balance recovery. However, it is not solely predictor for balance recovery. Shank angle is also an effective predictor.

The study in this chapter has supported the relation between the initial posture and the balance-recovery reactions. Moreover, there are unknown effects on estimation of the balance-recovery reactions sourced from internal factors such as anxiety and fatigue. In this study, their effects have not been observed because of shortness of training set.

9.3 Future Prospects

The future perspective of this study can be summarized into four main titles.

1. First of all, it has to be emphasized that the conditions of experimental studies differ from real experiences of humans. Therefore, future studies have to take advantage of wireless technologies to study postural behavior in "real-life" settings.

2. For more realistic experiments, experimental setup has to be improved to mimic the various real external disturbance.

3. Kinematic data is not solely sufficient for studies about automatic postural responses. Muscle activation patterns have to be taken into account for muscle activity during human balance-recovery reactions.

4. Formed general frame in this study has to be tested various questions and challenges. For this purpose, the model can be rebuilt gradually from simplicity to complexity adding some attributes. However, they should be tested each new adding attributes.

9.4 Conclusions

A significant contribution of this thesis is an adaptive PD control law conjectured to describe the automatic postural responses to sudden disturbances. It has been verified that this control law provides simulation results that fit quite well to the experimental results owing to its time-varying feedback gains and upright reference angles. As a consequent contribution, an adaptation rule is developed for the gains of the conjectured control law, which depends on the bodily sensory information and the size and speed of the external disturbance. In addition to these contributions, a rule is established to estimate the correlation between the initial body configuration and the corresponding balance recovery reaction. This rule is then verified to a reasonable extent by means of the Monte Carlo simulations.

REFERENCES

[1] Automatic postural response. In MarcD. Binder, Nobutaka Hirokawa, and Uwe Windhorst, editors, *Encyclopedia of Neuroscience*, pages 245–245. Springer Berlin Heidelberg, 2009.

[2] Stretch reflex. In MarcD. Binder, Nobutaka Hirokawa, and Uwe Windhorst, editors, *Encyclopedia of Neuroscience*, pages 3865–3865. Springer Berlin Heidelberg, 2009.

[3] J.H.J. Allum, B.R. Bloem, M.G. Carpenter, M. Hulliger, and M. Hadders-Algra. Proprioceptive control of posture: A review of new concepts. *Gait and Posture*, 8(3):214–242, 1998. cited By 110.

[4] J.H.J. Allum, M.G. Carpenter, and F. Honegger. Directional aspects of balance corrections in man. *Engineering in Medicine and Biology Magazine, IEEE*, 22(2):37–47, March 2003.

[5] J.H.J. Allum and F. Honegger. Chapter 30 synergies and strategies underlying normal and vestibulary deficient control of balance: implication for neuroprosthetic control. In F.P. Harris J.H.J. Allum, D.J. Allum-Mecklenburg and R. Probst, editors, *Natural and Artificial Control of Hearing and Balance*, volume 97 of *Progress in Brain Research*, pages 331 – 348. Elsevier, 1993.

[6] Lockhart D. B. Prediction of muscle activation patterns during postural perturbations using a feedback control model. Master's thesis, Woodruff School of Mechanical Engineering, Georgia Institute of Technology, 2005.

[7] K. Barin. Evaluation of a generalized model of human postural dynamics and control in the sagittal plane. *Biological Cybernetics*, 61(1):37–50, 1989.

[8] M. Basseville and I. V. Nikiforov. *Detection of Abrupt Changes: Theory and Application*. Prentice-Hall, Inc., Upper Saddle River, NJ, USA, 1993.

[9] Bastiaan R Bloem, Vibeke V Valkenburg, Mathilde Slabbekoorn, and Mirjam D Willemsen. The multiple tasks test: Development and normal strategies. *Gait and Posture*, 14(3):191 – 202, 2001.

[10] B.R. Bloem, D.J. Beckley, and J.G. Van Dijk. Are automatic postural responses in patients with parkinson's disease abnormal due to their stooped posture? *Experimental Brain Research*, 124(4):481–488, 1999.

[11] S. J. Bonasera and T. R. Nichols. Mechanical actions of heterogenic reflexes linking long toe flexors with ankle and knee extensors of the cat hindlimb. *Journal of Neurophysiology*, 71(3):1096–1110, 1994.

[12] Kenan Bozkaya and Metin Akkök. *A study on the reliability analysis during preliminary design : a rocket motor example. [Electronic resource].* Ankara : METU ; 2006., n.d.

[13] James R Carey, Robert Patterson, and Paula J Hollenstein. Sensitivity and reliability of force tracking and joint-movement tracking scores in healthy subjects. *Physical Therapy*, 68(7):1087–1091, 1988.

[14] M. G. Carpenter, J. S. Frank, A. L. Adkin, A. Paton, and J.H.J. Allum. Influence of postural anxiety on postural reactions to multi-directional surface rotations. *Journal of Neurophysiology*, 92(6):3255–3265, 2004.

[15] Mark G. Carpenter, Allan L. Adkin, Lawrence R. Brawley, and James S. Frank. Postural, physiological and psychological reactions to challenging balance: does age make a difference? *Age and Ageing*, 35(3):298–303, 2006.

[16] M.G. Carpenter, J.S. Frank, A.L. Adkin, A. Paton, and J.H.J. Allum. Influence of postural anxiety on postural reactions to multi-directional surface rotations. *Journal of Neurophysiology*, 92(6):3255–3265, 2004. cited By 65.

[17] SH Collins and A Ruina. A bipedal walking robot with efficient and human-like gait. In *2005 IEEE International Conference on Robotics and Automation (ICRA), Vols 1-4*, IEEE International Conference on Robotics and Automation, pages 1983–1988. IEEE, 2005. IEEE International Conference on Robotics and Automation (ICRA), Barcelona, SPAIN, APR 18-22, 2005.

[18] Collins English Dictionary – Complete and Unabridged. afferent. Aug 2015.

[19] P. J. Cordo and L. M. Nashner. Properties of postural adjustments associated with rapid arm movements. *Journal of Neurophysiology*, 47(2):287–302, 1982.

[20] Nicolle M. Correa, Tom Eichele, Tülay Adalı, Yi-Ou Li, and Vince D. Calhoun. Multi-set canonical correlation analysis for the fusion of concurrent single trial {ERP} and functional {MRI}. *NeuroImage*, 50(4):1438 – 1445, 2010.

[21] Tatiana G. Deliagina, Pavel V. Zelenin, and Grigori N. Orlovsky. Physiological and circuit mechanisms of postural control. *Current Opinion in Neurobiology*, 22(4):646–652, AUG 2012.

[22] Mosby's Medical Dictionary. limit of stability, 2015. [Online; accessed 1-August-2015].

[23] Benoni B. Edin. Cutaneous afferents provide information about knee joint movements in humans. *The Journal of Physiology*, 531(1):289–297, 2001.

[24] A. Aldo Faisal, Luc P. J. Selen, and Daniel M. Wolpert. Noise in the nervous system. *Nat Rev Neurosci*, 9(4):292–303, 2008.

[25] AnatolG. Feldman, Tal Krasovsky, MelanieC. Baniña, Anouk Lamontagne, and MindyF. Levin. Changes in the referent body location and configuration may underlie human gait, as confirmed by findings of multi-muscle activity minimizations and phase resetting. *Experimental Brain Research*, 210(1):91–115, 2011.

[26] P.-A Fransson, R Johansson, A Hafström, and M Magnusson. Methods for evaluation of postural control adaptation. *Gait and Posture*, 12(1):14 – 24, 2000.

[27] Carolyn L. M. Geh, Mark R. Beauchamp, Peter. R. E. Crocker, and Mark G. Carpenter. Assessed and distressed: White-coat effects on clinical balance performance. *Journal of Psychosomatic Research*, 70(1):45–51, JAN 2011.

[28] H Gomi and M Kawato. Equilibrium-point control hypothesis examined by measured arm stiffness during multijoint movement. *Science*, 272(5258):117–120, APR 5 1996.

[29] Joseph F. Hair, Ronald L. Tatham, Rolph E. Anderson, and William Black. *Multivariate Data Analysis (5th Edition)*. Prentice Hall, 5th edition, March 1998.

[30] Mark Hall, Eibe Frank, Geoffrey Holmes, Bernhard Pfahringer, Peter Reutemann, and Ian H. Witten. The weka data mining software: an update. *SIGKDD Explor. Newsl.*, 11(1):10–18, 2009.

[31] Jiawei Han, Micheline Kamber, and Jian Pei. *Data Mining: Concepts and Techniques*. Morgan Kaufmann Publishers Inc., San Francisco, CA, USA, 3rd edition, 2011.

[32] W.K. Härdle and L. Simar. *Applied Multivariate Statistical Analysis*. Springer Berlin Heidelberg, 2007.

[33] Sharon M. Henry, Joyce Fung, and Fay B. Horak. Emg responses to maintain stance during multidirectional surface translations. *Journal of Neurophysiology*, 80(4):1939–1950, 1998.

[34] Sharon M. Henry, Joyce Fung, and Fay B. Horak. Effect of stance width on multidirectional postural responses. *Journal of Neurophysiology*, 85(2):559–570, 2001.

[35] F. B. Horak and H. C. Diener. Cerebellar control of postural scaling and central set in stance. *Journal of Neurophysiology*, 72(2):479–493, 1994.

[36] Fay Horak and Art Kuo. Postural adaptation for altered environments, tasks, and intentions. In JackM. Winters and PatrickE. Crago, editors, *Biomechanics and Neural Control of Posture and Movement*, pages 267–281. Springer New York, 2000.

[37] Fay B. Horak. Postural orientation and equilibrium: what do we need to know about neural control of balance to prevent falls? *Age and Ageing*, 35(2):7–11, Sep 2006.

[38] Fay B. Horak. Postural control. In MarcD. Binder, Nobutaka Hirokawa, and Uwe Windhorst, editors, *Encyclopedia of Neuroscience*, pages 3212–3219. Springer Berlin Heidelberg, 2009.

[39] Fay B Horak, Sharon M Henry, and Anne Shumway-Cook. Postural perturbations: New insights for treatment of balance disorders. *Physical Therapy*, 77(5):517–533, 1997.

[40] FB Horak. Adaptation of automatic postural responses. In Bloedel, JR and Ebner, TJ and Wise, SP, editor, *Acquisition of Motor Behavior in Vertebrates*, pages 57–85, 1996. Satellite Seminar on the Acquisition of Motor Behavior in Vertebrates, at the 5th Annual Neural Control of Movement Meeting, KEY WEST, FL, APR 23-25, 1995.

[41] FB Horak and SP Moore. The effect of prior leaning on human postural responses. *Gait and Posture*, 1(4):203 – 210, 1993.

[42] FB Horak and LM Nashner. Central programming of postural movements - adaptation to altered support-surface configurations. *Journal of Neurophysiology*, 55(6):1369–1381, JUN 1986.

[43] Harold Hotelling. Relations between two sets of variates. *Biometrika*, 28:321–377, 1936.

[44] http://home.hit.no. Estimation of model parameters, 2015. [Online; accessed 2-March-2015].

[45] Hua Huang, Huiting He, Xin Fan, and Junping Zhang. Super-resolution of human face image using canonical correlation analysis. *Pattern Recognition*, 43(7):2532 – 2543, 2010.

[46] M.E. Ioffe. Cerebellar control of posture. In Mario Manto, JeremyD. Schmahmann, Ferdinando Rossi, DonnaL. Gruol, and Noriyuki Koibuchi, editors, *Handbook of the Cerebellum and Cerebellar Disorders*, pages 1221–1240. Springer Netherlands, 2013.

[47] J. V. Jacobs and F. B. Horak. Cortical control of postural responses. *Journal of Neural Transmission*, 114(10):1339–1348, OCT 2007.

[48] Jesse V. Jacobs, Katsuo Fujiwara, Hidehito Tomita, Naoe Furune, Kenji Kunita, and Fay B. Horak. Changes in the activity of the cerebral cortex relate to postural response modification when warned of a perturbation. *Clinical Neurophysiology*, 119(6):1431 – 1442, 2008.

[49] John Jeka and Tim Kiemel. Modeling of human postural control. In MarcD. Binder, Nobutaka Hirokawa, and Uwe Windhorst, editors, *Encyclopedia of Neuroscience*, pages 2381–2384. Springer Berlin Heidelberg, 2009.

[50] Jin Jiang and Youmin Zhang. A revisit to block and recursive least squares for parameter estimation. *Computers and Electrical Engineering*, 30(5):403 – 416, 2004.

[51] Sungho Jo. *Hierarchical neural control of human postural balance and bipedal walking in sagittal plane*. PhD thesis, MIT, 2006.

[52] Eric R. Kandel, J. H. Schwartz, and Thomas M. Jessell. *Principles of Neural Science*. McGraw-Hill Medical, 4th edition, July 2000.

[53] Mitsuo Kawato. Internal models for motor control and trajectory planning. *Current Opinion in Neurobiology*, 9(6):718 – 727, 1999.

[54] Seyoung Kim, Christopher G. Atkeson, and Sukyung Park. Perturbation-dependent selection of postural feedback gain and its scaling. *Journal of Biomechanics*, 45(8):1379 – 1386, 2012.

[55] UrsulaMargareta Küng, C.G.C. Horlings, F. Honegger, J.E.J. Duysens, and J.H.J. Allum. Control of roll and pitch motion during multi-directional balance perturbations. *Experimental Brain Research*, 194(4):631–645, 2009.

[56] M Koroglu. Analysis and Model Identification of Ionosphere Dynamics. Master's thesis, Hacettepe University, Turkey, 2012.

[57] Arthur D. Kuo. An optimal state estimation model of sensory integration in human postural balance. *Journal of Neural Engineering*, 2(3, SI), Sep 2005.

[58] Arthur D. Kuo and Felix E. Zajac. Chapter 31 human standing posture: multi-joint movement strategies based on biomechanical constraints. In F.P. Harris J.H.J. Allum, D.J. Allum-Mecklenburg and R. Probst, editors, *Natural and Artificial Control of Hearing and Balance*, volume 97 of *Progress in Brain Research*, pages 349 – 358. Elsevier, 1993.

[59] Mark L. Latash, Mindy F. Levin, John P. Scholz, and Gregor Schoener. Motor control theories and their applications. *Medicine-Lithuania*, 46(6):382–392, 2010.

[60] Yao Li. *An Optimal Control Model For Human Postural Regulation*. PhD thesis, University of Maryland, 2010.

[61] Yao Li, W.S. Levine, and G.E. Loeb. A two-joint human posture control model with realistic neural delays. *Neural Systems and Rehabilitation Engineering, IEEE Transactions on*, 20(5):738–748, Sept 2012.

[62] G. E. Loeb, I. E. Brown, and E. J. Cheng. A hierarchical foundation for models of sensorimotor control. *Experimental Brain Research*, 126(1):1–18, 1999.

[63] GeraldE. Loeb. Optimal isn't good enough. *Biological Cybernetics*, 106(11-12):757–765, 2012.

[64] J.M. Macpherson, F.B. Horak, D.C. Dunbar, and R.S. Dow. Stance dependence of automatic postural adjustments in humans. *Experimental Brain Research*, 78(3):557–566, 1989.

[65] B. E. Maki and W. E. McIlroy. Cognitive demands and cortical control of human balance-recovery reactions. *Journal of Neural Transmission*, 114(10):1279–1296, 2007.

[66] Brian E Maki B. E. and William E McIlroy. The role of limb movements in maintaining upright stance: The "change-in-support" strategy. *Physical Therapy*, 77(5):488–507, 1997.

[67] BrianE. Maki B. E. Postural strategies. In MarcD. Binder, Nobutaka Hirokawa, and Uwe Windhorst, editors, *Encyclopedia of Neuroscience*, pages 3222–3227. Springer Berlin Heidelberg, 2009.

[68] Bryan F.J. Manly. *Multivariate Statistical Methods: A Primer, Second Edition*. Chapman and Hall, 2 edition, July 1994.

[69] Mario Manto, JamesM. Bower, AdrianaBastos Conforto, JoséM. Delgado-García, SuzeteNascimentoFarias da Guarda, Marcus Gerwig, Christophe Habas, Nobuhiro Hagura, RichardB. Ivry, Peter Mariën, Marco Molinari, Eiichi Naito, DennisA. Nowak, Nordeyn Oulad Ben Taib, Denis Pelisson, ClaudiaD. Tesche, Caroline Tilikete, and Dagmar Timmann. Consensus paper: Roles of the cerebellum in motor control—the diversity of ideas on cerebellar involvement in movement. *The Cerebellum*, 11(2):457–487, 2012.

[70] Kei Masani, Milos R. Popovic, Kimitaka Nakazawa, Motoki Kouzaki, and Daichi Nozaki. Importance of body sway velocity information in controlling ankle extensor activities during quiet stance. *Journal of Neurophysiology*, 90(6):3774–3782, 2003.

[71] Kei Masani, Albert H. Vette, and Milos R. Popovic. Controlling balance during quiet standing: Proportional and derivative controller generates preceding motor command to body sway position observed in experiments. *Gait and Posture*, 23(2):164 – 172, 2006.

[72] William Evans McIlroy, Darcy Claire Bishop, William Richard Staines, Aimee Jennifer Nelson, Brian Edward Maki, and John Dennis Brooke. Modulation of afferent inflow during the control of balancing tasks using the lower limbs. *Brain Research*, 961(1):73 – 80, 2003.

[73] J Mcintyre and E Bizzi. Servo hypotheses for the biological-control of movement. *Journal of Motor Behavior*, 25(3):193–202, SEP 1993.

[74] Mark M. Meerschaert. Chapter 9 - simulation of probability models. In Mark M. Meerschaert, editor, *Mathematical Modeling (Fourth Edition)*, pages 301 – 358. Academic Press, Boston, fourth edition edition, 2013.

[75] METU-Modsim. Posture laboratory — modeling and simulation research and development center, 2015. [Online; accessed 12-July-2015].

[76] Theodore E. Milner and Mitsuo Kawato. The central nervous system stabilizes unstable dynamics by learning optimal impedance. *Nature*, 9(414):446 – 449, 2001.

[77] Djordje Mitrovic, Stefan Klanke, Rieko Osu, Mitsuo Kawato, and Sethu Vijayakumar. A computational model of limb impedance control based on principles of internal model uncertainty. *PLoS ONE*, 5(10):e13601, 10 2010.

[78] Gabriel Bueno Lahoz Moya, Cassio Marinho Siqueira, Rene Rogieri Caffaro, Carolina Fu, and Clarice Tanaka. Can quiet standing posture predict compensatory postural adjustment? *Clinics*, 64:791 – 796, 00 2009.

[79] Ferdinando A. Mussa-Ivaldi and Sara A. Solla. Models of motor control. In *The Cambridge Handbook of Computational Psychology*, pages 635–664. Cambridge University Press, 2008. Cambridge Books Online.

[80] L.M. Nashner. Balance and posture control. In Larry R. Squire, editor, *Encyclopedia of Neuroscience*, pages 21 – 29. Academic Press, Oxford, 2009.

[81] T. Richard Nichols and James C. Houk. Reflex compensation for variations in the mechanical properties of a muscle. *Science*, (4095):182, 1973.

[82] Gergo Orban and Daniel M Wolpert. Representations of uncertainty in sensorimotor control. *Current Opinion in Neurobiology*, 21(4):629 – 635, 2011. Sensory and motor systems.

[83] Yi-Chung Pai and James Patton. Center of mass velocity-position predictions for balance control. *Journal of Biomechanics*, 30(4):347 – 354, 1997.

[84] Sukyung Park, FayB. Horak, and ArthurD. Kuo. Postural feedback responses scale with biomechanical constraints in human standing. *Experimental Brain Research*, 154(4):417–427, 2004.

[85] Stephen Douglas Peny. *The Role Of Plantar Cutaneous Mechanoreceptors In The Control Of Compensatory Stepping In The Young And Older Adult.* PhD thesis, University of Toronto, 2000.

[86] R.J. Peterka. Simplifying the complexities of maintaining balance. *Engineering in Medicine and Biology Magazine, IEEE*, 22(2):63–68, March 2003.

[87] RobertJ. Peterka. Posture – sensory integration. In MarcD. Binder, Nobutaka Hirokawa, and Uwe Windhorst, editors, *Encyclopedia of Neuroscience*, pages 3234–3239. Springer Berlin Heidelberg, 2009.

[88] Arthur Prochazka. Feedback control of movement. In MarcD. Binder, Nobutaka Hirokawa, and Uwe Windhorst, editors, *Encyclopedia of Neuroscience*, pages 1560–1564. Springer Berlin Heidelberg, 2009.

[89] J. Ross Quinlan. *C4.5: Programs for Machine Learning*. Morgan Kaufmann Publishers Inc., San Francisco, CA, USA, 1993.

[90] S. Ratick and G. Schwarz. Monte carlo simulation. In Rob KitchinNigel Thrift, editor, *International Encyclopedia of Human Geography*, pages 175 – 184. Elsevier, Oxford, 2009.

[91] CF Runge, CL Shupert, FB Horak, and FE Zajac. Role of vestibular information in initiation of rapid postural responses. *Experimental Brain Research*, 122(4):403–412, OCT 1998.

[92] C.F Runge, C.L Shupert, F.B Horak, and F.E Zajac. Ankle and hip postural strategies defined by joint torques. *Gait and Posture*, 10(2):161 – 170, 1999.

[93] StevenL. Salzberg. C4.5: Programs for machine learning by j. ross quinlan. morgan kaufmann publishers, inc., 1993. *Machine Learning*, 16(3):235–240, 1994.

[94] Gregor Schöner. Dynamical systems approaches to cognition. In *The Cambridge Handbook of Computational Psychology*, pages 101–126. Cambridge University Press, 2008. Cambridge Books Online.

[95] Luc P. J. Selen, David W. Franklin, and Daniel M. Wolpert. Impedance control reduces instability that arises from motor noise. *The Journal of Neuroscience*, 29(40):12606–12616, 2009.

[96] Hyejin Shin and Seokho Lee. Canonical correlation analysis for irregularly and sparsely observed functional data. *Journal of Multivariate Analysis*, 134:1 – 18, 2015.

[97] K.-S. Tang, F. Honegger, and J.H.J. Allum. Movement patterns underlying first trial responses in human balance corrections. *Neuroscience*, 225(0):140 – 151, 2012.

[98] W. Taube, M. Gruber, and A. Gollhofer. Spinal and supraspinal adaptations associated with balance training and their functional relevance. *Acta Physiologica*, 193(2):101–116, 2008.

[99] Lena H. Ting, Stacie A. Chvatal, Seyed A. Safavynia, and J. Lucas McKay. Review and perspective: neuromechanical considerations for predicting muscle activation patterns for movement. *International Journal for Numerical Methods in Biomedical Engineering*, 28(10):1003–1014, 2012.

[100] Lena H. Ting and Jane M. Macpherson. A limited set of muscle synergies for force control during a postural task. *Journal of Neurophysiology*, 93(1):609–613, 2004.

[101] LenaH. Ting. Postural synergies. In MarcD. Binder, Nobutaka Hirokawa, and Uwe Windhorst, editors, *Encyclopedia of Neuroscience*, pages 3228–3233. Springer Berlin Heidelberg, 2009.

[102] K. G. Toker. System Identification via Canonical Correlation Analysis. Master's thesis, Hacettepe University, Turkey, 2013.

[103] Gelsy Torres-Oviedo and Lena H. Ting. Muscle synergies characterizing human postural responses. *Journal of Neurophysiology*, 98(4):2144–2156, 2007.

[104] Matthew Tresch and DevinL. Jindrich. Spinal and neuromechanical integration: Overview. In Dieter Jaeger and Ranu Jung, editors, *Encyclopedia of Computational Neuroscience*, pages 1–2. Springer New York, 2014.

[105] Matthew C Tresch and Anthony Jarc. The case for and against muscle synergies. *Current Opinion in Neurobiology*, 19(6):601 – 607, 2009.

[106] H van der Kooij, R Jacobs, B Koopman, and H Grootenboer. A multisensory integration model of human stance control. *Biological Cybernetics*, 80(5):299–308, MAY 1999.

[107] H Van der Kooij, R Jacobs, B Koopman, and F Van der Helm. An adaptive model of sensory integration in a dynamic environment applied to human stance control. *Biological Cybernetics*, 84(2):103–115, FEB 2001.

[108] Jasper E. Visser, Mark G. Carpenter, Herman van der Kooij, and Bastiaan R. Bloem. The clinical utility of posturography. *Clinical Neurophysiology*, 119(11):2424 – 2436, 2008.

[109] Vivian Weerdesteyn, Andrew C. Laing, and Stephen N. Robinovitch. The body configuration at step contact critically determines the successfulness of balance recovery in response to large backward perturbations. *Gait & Posture*, 35(3):462–466, MAR 2012.

[110] Torrence D. J. Welch and Lena H. Ting. Mechanisms of motor adaptation in reactive balance control. *PLoS ONE*, 9(5):e96440, 05 2014.

[111] Wikipedia. Canonical correlation — wikipedia, the free encyclopedia, 2015. [Online; accessed 7-August-2015].

[112] Wikipedia. Data mining — wikipedia, the free encyclopedia, 2015. [Online; accessed 14-August-2015].

[113] Wikipedia. Muscle spindle — wikipedia, the free encyclopedia, 2015. [Online; accessed 8-July-2015].

[114] Wikipedia. Sensory-motor coupling — wikipedia, the free encyclopedia, 2015. [Online; accessed 4-August-2015].

[115] E.L. Wilson, M.L. Madigan, B.S. Davidson, and M.A. Nussbaum. Postural strategy changes with fatigue of the lumbar extensor muscles. *Gait and Posture*, 23(3):348–354, 2006. cited By 28.

[116] David A. Winter. *Anthropometry*, pages 82–106. John Wiley and Sons, Inc., 2009.

[117] I.H. Witten, E. Frank, and M.A. Hall. *Data Mining: Practical Machine Learning Tools and Techniques: Practical Machine Learning Tools and Techniques*. The Morgan Kaufmann Series in Data Management Systems. Elsevier Science, 2011.

[118] Daniel M. Wolpert, Zoubin Ghahramani, and Michael I. Jordan. An internal model for sensorimotor integration. *Science*, (5232):1880, 1995.

[119] M Woollacott and A Shumway-Cook. Attention and the control of posture and gait: a review of an emerging area of research. *Gait & Posture*, 16(1):1–14, AUG 2002.

[120] "Xsens Technologies ", "www.xsens.com". *"MVN user Manual"*, "2012".

[121] V. Zatsiorsky and V. Seluyanov. The mass and inertia characteristics of the main segments of the human body. In *Biomechanics VIII: proceedings of the Eighth International Congress of Biomechanics*, pages 1152–1159. Human Kinetics Publishers, 1983.

APPENDIX A

DERIVATION OF EQUATIONS FOR MUSCULOSKELETAL STRUCTURE

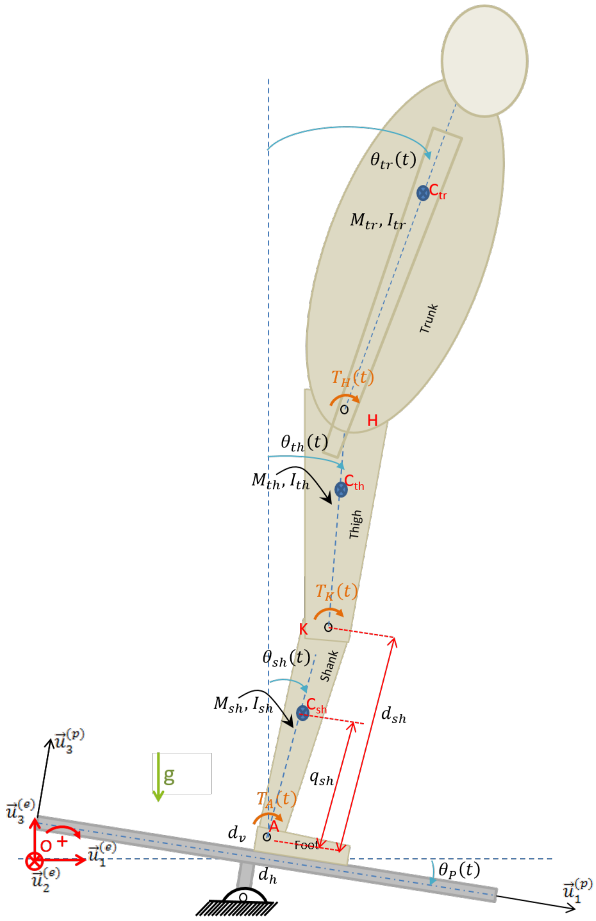

Figure A.1: Proposed model for a subject standing on a tilt platform.

In this model, the masses and inertias of the body members are represented by the symbols $M_{sh}, I_{sh}, M_{th}, I_{th}$, M_{tr}, and I_{tr} where "*sh*", "*th*" and "*tr*" represent the shank, the thigh and the trunk, respectively. Similarly, d_{sh}, d_{th} and d_{tr} show the lengths of the limbs, while q_{sh}, q_{th} and q_{tr} show the distances of the mass centers (C_{sh}, C_{th} and C_{tr}) from the joint centers. The subjects use the torques $(T_A(t), T_K(t)$ and $T_H(t))$ to maintain their balance. The motions of the body members (shank, thigh, and trunk) are described by the angles $\theta_{sh}(t), \theta_{th}(t)$ and $\theta_{tr}(t)$ which denote the deviations from the vertical axis represented by $\vec{u}_3^{(e)}$. Therefore, the differential equations of motion have been derived for these angles. The angle $\theta_p(t)$ represents the specified disturbance. The distances d_h and d_v are constant parameters that describe the geometric features of the tilt platform (See Fig.A.2). The inertial parameters for the model have been obtained by using the proposed method in [2] (see Appendix B for the details).

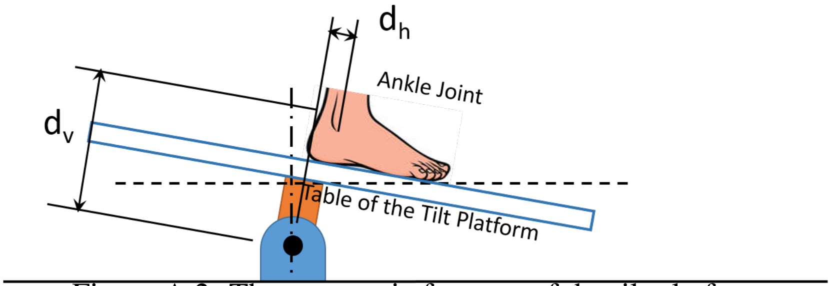

Figure A.2: The geometric features of the tilt platform.

SOLUTION

First Step: express all the relevant angular and linear positions in terms of the variables $\theta_{sh}(t), \theta_{th}(t)$ and $\theta_{tr}(t)$, and their first and second derivatives.

Positions;

$$\begin{aligned}
\vec{r}_{A/O} &= (d_h \cos\theta_p + d_v \sin\theta_p)\vec{u}_1^{(e)} - (d_h \sin\theta_p - d_v \cos\theta_p)\vec{u}_2^{(e)} \\
\vec{r}_{C_{sh}/O} &= (q_{sh}\sin\theta_{sh} + d_h\cos\theta_p + d_v\sin\theta_p)\vec{u}_1^{(e)} + (q_{sh}\cos\theta_{sh} - d_h\sin\theta_p + d_v\cos\theta_p)\vec{u}_2^{(e)} \\
\vec{r}_{C_{th}/O} &= (q_{th}\sin\theta_{th} + d_{sh}\sin\theta_{sh} + d_h\cos\theta_p + d_v\sin\theta_p)\vec{u}_1^{(e)} \\
&\quad + (q_{th}\cos\theta_{th} + d_{sh}\cos\theta_{sh} - d_h\sin\theta_p + d_v\cos\theta_p)\vec{u}_2^{(e)} \\
\vec{r}_{C_{tr}/O} &= (q_{tr}\sin\theta_{tr} + d_{th}\sin\theta_{th} + d_{sh}\sin\theta_{sh} + d_h\cos\theta_p + d_v\sin\theta_p)\vec{u}_1^{(e)} \\
&\quad + (q_{tr}\cos\theta_{tr} + d_{th}\cos\theta_{th} + d_{sh}\cos\theta_{sh} - d_h\sin\theta_p + d_v\cos\theta_p)\vec{u}_2^{(e)}
\end{aligned}$$

Linear Velocities;

$$\begin{aligned}
\vec{\nu}_{C_{sh}/O} &= (\dot{\theta}_{sh} q_{sh}\cos\theta_{sh} + \dot{\theta}_p(-d_h\sin\theta_p + d_v\cos\theta_p))\vec{u}_1^{(e)} \\
&\quad - (\dot{\theta}_{sh} q_{sh}\sin\theta_{sh} + \dot{\theta}_p(d_h\cos\theta_p + d_v\sin\theta_p))\vec{u}_2^{(e)} \\
\vec{\nu}_{C_{th}/O} &= (\dot{\theta}_{th} q_{th}\cos\theta_{th} + \dot{\theta}_{sh} d_{sh}\cos\theta_{sh} + \dot{\theta}_p(-d_h\sin\theta_p + d_v\cos\theta_p))\vec{u}_1^{(e)} \\
&\quad - (\dot{\theta}_{th} q_{th}\sin\theta_{th} + \dot{\theta}_{sh} d_{sh}\sin\theta_{sh} + \dot{\theta}_p(d_h\cos\theta_p + d_v\sin\theta_p))\vec{u}_2^{(e)} \\
\vec{\nu}_{C_{tr}/O} &= (\dot{\theta}_{tr} q_{tr}\cos\theta_{tr} + \dot{\theta}_{th} d_{th}\cos\theta_{th} + \dot{\theta}_{sh} d_{sh}\cos\theta_{sh} \\
&\quad + \dot{\theta}_p(-d_h\sin\theta_p + d_v\cos\theta_p))\vec{u}_1^{(e)} \\
&\quad - (\dot{\theta}_{tr} q_{tr}\sin\theta_{tr} + \dot{\theta}_{th} d_{th}\sin\theta_{th} \\
&\quad + \dot{\theta}_{sh} d_{sh}\sin\theta_{sh} + \dot{\theta}_p(d_h\cos\theta_p + d_v\sin\theta_p))\vec{u}_2^{(e)}
\end{aligned}$$

The equation of motion is derived by using Lagrange's equations as follows

Remember the Lagrange's equations:

$$\dot{P}_k - \frac{\partial K}{\partial q_k} + \frac{\partial D}{\partial \dot{q}_k} + \frac{\partial U}{\partial q_k} = Q_k \qquad k = 1, 2, 3, \ldots, n$$

$$P_k = \frac{\partial K}{\partial \dot{q}_k}$$

Second step: write the kinetic and potential energy equations; differentiate them due to given rule and obtain the equation of the motion.

Kinetic Energy

$$K = \frac{1}{2}\sum_{i=1}^{3} m_i \nu_i^2 + \frac{1}{2}\sum_{i=1}^{3} J_i \omega_i^2$$

Potential Energy

$$U = m_i g r_i^y$$

The generalized forces Q_k where k=1,2,3,...,n

$Q_1 = T_A - T_K$
$Q_2 = T_K - T_H$
$Q_3 = T_H$

Three equations are obtained as follow.

First equation is

$$\begin{aligned}
&\left[I_{sh} + m_{sh}{q_{sh}}^2 + (m_{th} + m_{tr})\,{d_{sh}}^2\right]\ddot{\theta}_{sh} \\
&\quad + [d_{sh}q_{th}m_{th} + d_{sh}d_{th}m_{tr}]\cos(\theta_{sh} - \theta_{th})\ddot{\theta}_{th} \\
&\quad + d_{sh}q_{tr}m_{tr}\cos(\theta_{sh} - \theta_{tr})\ddot{\theta}_{tr} \\
&\quad + [(q_{sh}d_v m_{sh} + d_{sh}d_v(m_{th} + m_{tr}))\cos(\theta_{sh} - \theta_p) \\
&\qquad\qquad + (q_{sh}d_h m_{sh} + d_{sh}d_h(m_{th} + m_{tr}))\sin(\theta_{sh} - \theta_p)]\ddot{\theta}_p \\
&\quad + [(q_{sh}d_v m_{sh} + d_{sh}d_v(m_{th} + m_{tr}))\sin(\theta_{sh} - \theta_p) \\
&\qquad\qquad - (q_{sh}d_h m_{sh} + d_{sh}d_h(m_{th} + m_{tr}))\cos(\theta_{sh} - \theta_p)]\dot{\theta}_p^2 \\
&\quad + d_{sh}\,(m_{th}q_{th} + m_{tr}d_{th})\sin(\theta_{sh} - \theta_{th})\dot{\theta}_{th}^2 \\
&\quad + (d_{sh}q_{tr}m_{tr})\sin(\theta_{sh} - \theta_{tr})\dot{\theta}_{tr}^2 \\
&\quad - (m_{th} + m_{tr})\,d_{sh}g\sin(\theta_{sh}) - m_{sh}q_{sh}g\sin(\theta_{sh}) = T_A - T_K
\end{aligned}$$

Second equation is

$$
\begin{aligned}
&(d_{sh}q_{sh}m_{th} + d_{sh}d_{th}m_{tr})\cos(\theta_{sh}-\theta_{th})\ddot{\theta}_{sh} + \left(I_{th} + q_{th}^2 m_{th} + d_{th}^2 m_{tr}\right)\ddot{\theta}_{th}\\
&\quad + d_{th}q_{tr}m_{tr}\cos(\theta_{th}-\theta_{tr})\ddot{\theta}_{tr}\\
&\quad - (d_{sh}q_{th}m_{th} + d_{sh}d_{th}m_{tr})\sin(\theta_{sh}-\theta_{th})\dot{\theta}_{sh}^2\\
&\quad + d_{th}q_{tr}m_{tr}\sin(\theta_{th}-\theta_{tr})\dot{\theta}_{tr}^2\\
&\quad + \left[(d_v q_{th}m_{th} + d_v d_{th}m_{tr})\cos(\theta_p-\theta_{th}) - (d_h q_{th}m_{th} + d_h d_{th}m_{tr})\sin(\theta_p-\theta_{th})\right]\ddot{\theta}_p\\
&\quad - \left[(d_v q_{th}m_{th} + d_v d_{th}m_{tr})\sin(\theta_p-\theta_{th}) - (d_h q_{th}m_{th} + d_h d_{th}m_{tr})\cos(\theta_p-\theta_{th})\right]\dot{\theta}_p^2\\
&\quad - (q_{th}m_{th} + d_{th}m_{tr})\, g\sin(\theta_{th}) = T_K - T_H
\end{aligned}
$$

Third equation is

$$
\begin{aligned}
&d_{sh}q_{tr}m_{tr}\cos(\theta_{sh}-\theta_{tr})\ddot{\theta}_{sh} + d_{th}q_{tr}m_{tr}\cos(\theta_{th}-\theta_{tr})\ddot{\theta}_{th} + \left(I_{tr} + q_{tr}^2 m_{tr}\right)\ddot{\theta}_{tr}\\
&\quad - d_{sh}q_{tr}m_{tr}\sin(\theta_{sh}-\theta_{tr})\dot{\theta}_{sh}^2 - d_{th}q_{tr}m_{tr}\sin(\theta_{th}-\theta_{tr})\dot{\theta}_{th}^2\\
&\quad + \left[d_v q_{tr}m_{tr}\cos(\theta_p-\theta_{tr}) - d_h q_{tr}m_{tr}\sin(\theta_p-\theta_{tr})\right]\ddot{\theta}_p\\
&\quad - \left[d_v q_{tr}m_{tr}\sin(\theta_p-\theta_{tr}) + d_h q_{tr}m_{tr}\cos(\theta_p-\theta_{tr})\right]\dot{\theta}_p^2\\
&\quad - q_{tr}m_{tr}g\sin(\theta_{tr}) = T_H
\end{aligned}
$$

These three equations can be written in a more compact form as follows

$$M(\theta)\ddot{\theta} + V(\theta,\dot{\theta})\dot{\theta} + D + G = Q$$

Where $\theta = [\theta_{sh} \quad \theta_{th} \quad \theta_{tr}]^T$ and the components of the mass matrix are

$$
\begin{aligned}
&M_{11} = \left[I_{sh} + m_{sh}{q_{sh}}^2 + (m_{th} + m_{tr})\,{d_{sh}}^2\right]\\
&M_{22} = (I_{th} + q_{th}^2 m_{th} + d_{th}^2 m_{tr})\\
&M_{33} = (I_{tr} + q_{tr}^2 m_{tr})\\
&M_{12} = M_{21} = (d_{sh}q_{sh}m_{th} + d_{sh}d_{th}m_{tr})\cos(\theta_{sh}-\theta_{th})\\
&M_{13} = M_{31} = d_{sh}q_{tr}m_{tr}\cos(\theta_{sh}-\theta_{tr})\\
&M_{23} = M_{32} = d_{th}q_{tr}m_{tr}\cos(\theta_{th}-\theta_{tr})
\end{aligned}
$$

Components of the centrifugal and Coriolis forces matrix are

$$
\begin{aligned}
&V_{11} = V_{22} = V_{33} = 0\\
&V_{12} = -V_{21} = d_{sh}\,(m_{th}q_{th} + m_{tr}d_{th})\sin(\theta_{sh}-\theta_{th})\dot{\theta}_{th}\\
&V_{13} = -V_{31} = (d_{sh}q_{tr}m_{tr})\sin(\theta_{sh}-\theta_{tr})\dot{\theta}_{tr}\\
&V_{23} = -V_{32} = d_{th}q_{tr}m_{tr}\sin(\theta_{th}-\theta_{tr})\dot{\theta}_{tr}
\end{aligned}
$$

Components of the vector dependent on external perturbation are

$$
\begin{aligned}
D_1 = &\left[(q_{sh} d_v m_{sh} + d_{sh} d_v (m_{th} + m_{tr})) \cos(\theta_{sh} - \theta_p) \right. \\
&\qquad \left. + (q_{sh} d_h m_{sh} + d_{sh} d_h (m_{th} + m_{tr})) \sin(\theta_{sh} - \theta_p)\right] \ddot{\theta}_p \\
&+ \left[(q_{sh} d_v m_{sh} + d_{sh} d_v (m_{th} + m_{tr})) \sin(\theta_{sh} - \theta_p) \right. \\
&\qquad \left. - (q_{sh} d_h m_{sh} + d_{sh} d_h (m_{th} + m_{tr})) \cos(\theta_{sh} - \theta_p)\right] \dot{\theta}_p^2 \\
D_2 = &\, (d_v q_{th} m_{th} + d_v d_{th} m_{tr}) \cos(\theta_p - \theta_{th}) \ddot{\theta}_p \\
&\qquad\qquad - (d_h q_{th} m_{th} + d_h d_{th} m_{tr}) \sin(\theta_p - \theta_{th}) \ddot{\theta}_p \\
&- (d_v q_{th} m_{th} + d_v d_{th} m_{tr}) \sin(\theta_p - \theta_{th}) \dot{\theta}_p^2 \\
&\qquad\qquad - (d_h q_{th} m_{th} + d_h d_{th} m_{tr}) \cos(\theta_p - \theta_{th}) \dot{\theta}_p^2 \\
D_3 = &\left[d_v q_{tr} m_{tr} \cos(\theta_p - \theta_{tr}) - d_h q_{tr} m_{tr} \sin(\theta_p - \theta_{tr})\right] \ddot{\theta}_p \\
&- \left[d_v q_{tr} m_{tr} \sin(\theta_p - \theta_{tr}) + d_h q_{tr} m_{tr} \cos(\theta_p - \theta_{tr})\right] \dot{\theta}_p^2
\end{aligned}
$$

Components of the vector of gravity dependent terms are

$$
\begin{aligned}
G_1 &= -(m_{th} + m_{tr}) d_{sh} g \sin(\theta_{sh}) - m_{sh} q_{sh} g \sin(\theta_{sh}) \\
G_2 &= -(q_{th} m_{th} + d_{th} m_{tr}) g \sin(\theta_{th}) \\
G_3 &= -q_{tr} m_{tr} g \sin(\theta_{tr})
\end{aligned}
$$

APPENDIX B

THE METHOD FOR ESTIMATION OF THE MODEL INERTIAL PARAMETERS

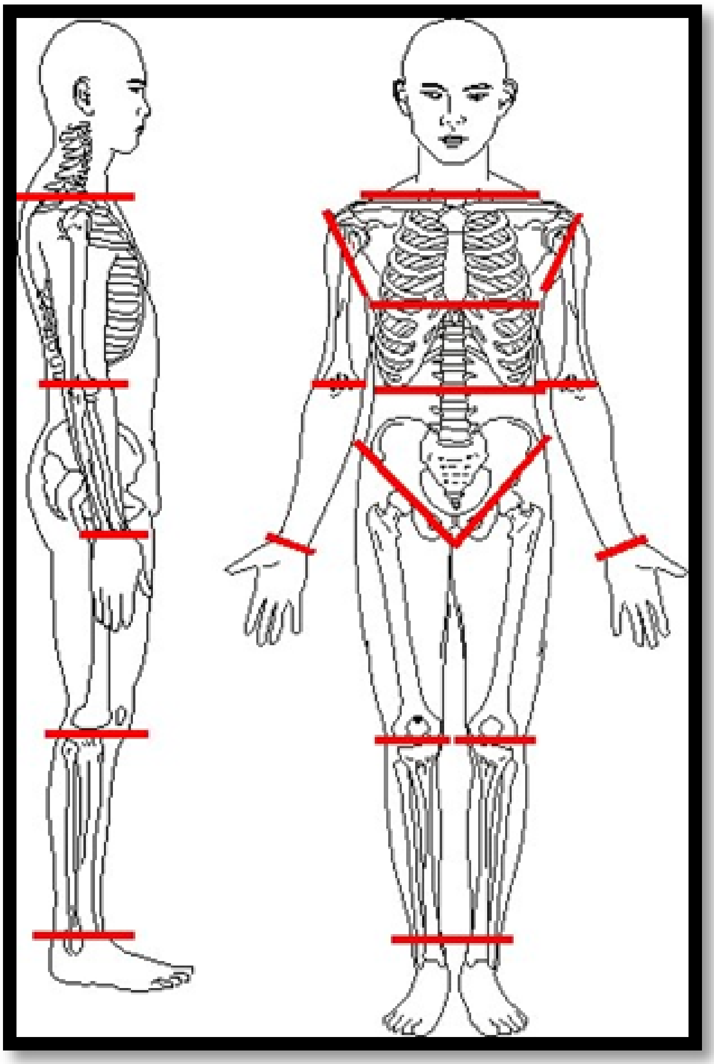

Figure B.1: Body Segment Parameters (Adapted from [121])

Definition of Body Segmentation ([116, 121])

16segments:

Head

Upper part of torso

Middle part of torso

Lower part of torso

Right Thigh

Right Foot

Right Calf

Right Upper arm

Right Forearm

Right Hand

Left Limbs are symmetric;

Note: the origin of the coordinate system for each segment is the center of gravity of that segment. The x-axis is defined origin towards the front of the body. The y-axis is defined as the saggital axis and +y is the direction as the frontal axis and +x is the direction from the origin towards the left of the body. The z-axis is defined as the horizontal-axis and +z is direction from the origin towards the head.

Masses of Segments : the following table shows regression coefficients.

Ex.) Head mass(kg)=1.29600 + 0.01710 $\times$ body weight (kg) + 0.01430 $\times$ stature (cm)

Body Part	Constant	Body Weight	Sature
Head	1.29	0.0171	0.0143
Upper Part of Torso	8.2144	0.1862	-0.0584
Middle Part of Torso	7.181	0.2234	-0.06663
Lower Part of Torso	-7.498	0.0976	0.04896
Upper Arm	0.25	0.03012	-0.0027
Forearm	0.3185	0.01445	-0.00114
Hand	-0.1165	0.0036	0.00175
Thight	-2.649	0.1463	0.0137
Calf	-1.592	0.036	0.0121
Foot	-0.829	0.0077	0.0073

Figure B.2: Regression Coefficients (Adapted from [121])

Moment of Inertia: the following table shows regression coefficients.

Where mass in kg, moment of inertia in kg/cm^2, stature in cm.

Ex.) Moment of inertia of the head around x-axis (kg/cm^2)

I_{xx}=-78 + 1.171 $\times$ body weight (kg) + 1.519 $\times$ stature (cm)

Moment of Inertia around x-axis	Constant	Body Weight	Length
Head	-78	1.171	1.519
Upper Part of Torso	81.2	36.73	-5.97
Middle Part of Torso	618.5	39.8	-12.87
Lower Part of Torso	-1568	12	7.741
Upper Arm	-250.7	1.56	1.512
Forearm	-64	0.95	0.34
Hand	-19.5	0.17	0.116
Thight	-3557	31.7	18.61
Calf	-1105	4.59	6.63
Foot	-100	0.48	0.626
Moment of Inertia around y-axis	**Constant**	**Body Weight**	**Length**
Head	-112	1.43	1.73
Upper Part of Torso	367	18.3	-5.73
Middle Part of Torso	263	26.7	-8
Lower Part of Torso	-934	11.8	3.44
Upper Arm	-232	1.525	1.343
Forearm	-67.9	0.855	0.376
Hand	-13.68	0.088	0.092
Thight	-3690	32.02	19.24
Calf	-1152	4.594	6.815
Foot	-97.09	0.414	0.614
Moment of Inertia around z-axis	**Constant**	**Body Weight**	**Length**
Head	61.6	1.72	0.0814
Upper Part of Torso	561	36.03	-9.98
Middle Part of Torso	5615.1	43.14	-19.8
Lower Part of Torso	-775	14.7	1.685
Upper Arm	-16.9	0.662	0.0435
Forearm	5.66	0.306	-0.088
Hand	-6.26	0.0762	0.0347
Thight	-13.5	11.3	-2.28
Calf	-70.5	1.134	0.3
Foot	-15.48	0.144	0.088

Figure B.3: Regression Coefficients (Adapted from [121])

APPENDIX C

ANTHROPOMETRIC MEASURES

C.1 Segment Dimensions

Human movement analysis requires kinetic measures such as masses, moments of inertias, and their locations. An average set of segment lengths expressed as a percentage of body height is shown in Fig.C.1

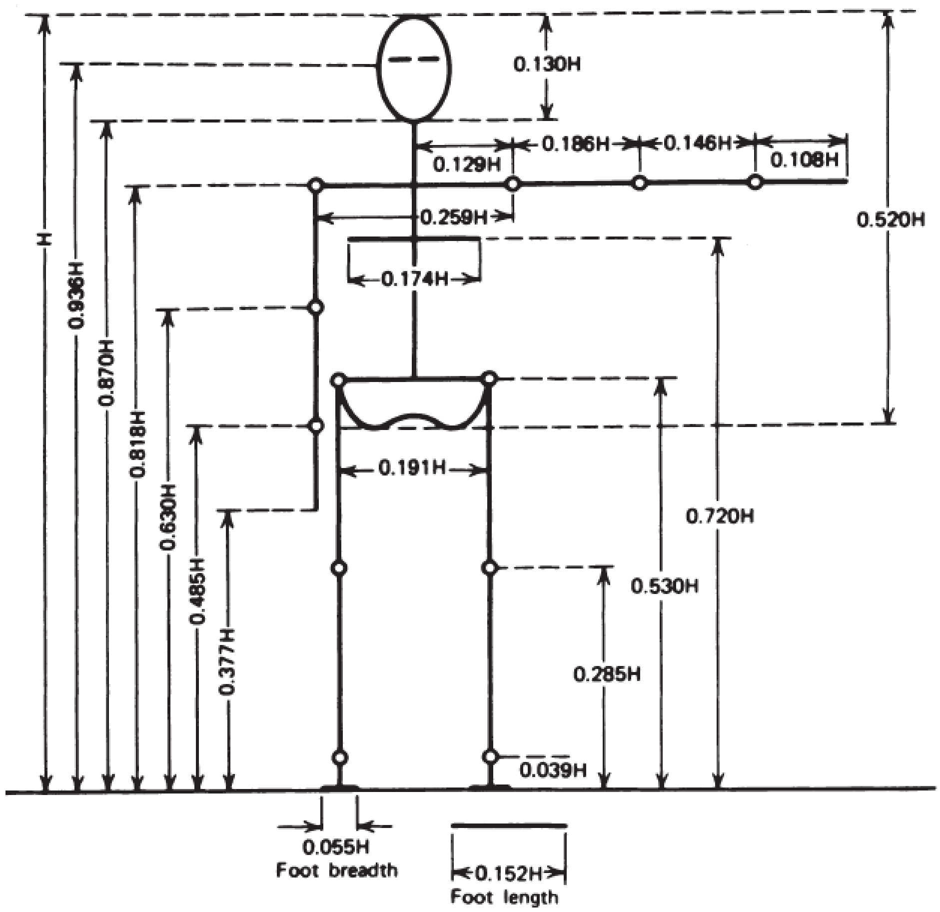

Figure C.1: Body segment lengths expressed as a fraction of body height H (Adapted from [116])

C.2 Center of Masses of the Segments

TABLE 4.1 Anthropometric Data

Segment	Definition	Segment Weight/Total Body Weight	Center of Mass/Segment Length		Radius of Gyration/Segment Length			Density
			Proximal	Distal	C of G	Proximal	Distal	
Hand	Wrist axis/knuckle II middle finger	0.006 M	0.506	0.494 P	0.297	0.587	0.577 M	1.16
Forearm	Elbow axis/ulnar styloid	0.016 M	0.430	0.570 P	0.303	0.526	0.647 M	1.13
Upper arm	Glenohumeral axis/elbow axis	0.028 M	0.436	0.564 P	0.322	0.542	0.645 M	1.07
Forearm and hand	Elbow axis/ulnar styloid	0.022 M	0.682	0.318 P	0.468	0.827	0.565 P	1.14
Total arm	Glenohumeral joint/ulnar styloid	0.050 M	0.530	0.470 P	0.368	0.645	0.596 P	1.11
Foot	Lateral malleolus/head metatarsal II	0.0145 M	0.50	0.50 P	0.475	0.690	0.690 P	1.10
Leg	Femoral condyles/medial malleolus	0.0465 M	0.433	0.567 P	0.302	0.528	0.643 M	1.09
Thigh	Greater trochanter/femoral condyles	0.100 M	0.433	0.567 P	0.323	0.540	0.653 M	1.05
Foot and leg	Femoral condyles/medial malleolus	0.061 M	0.606	0.394 P	0.416	0.735	0.572 P	1.09
Total leg	Greater trochanter/medial malleolus	0.161 M	0.447	0.553 P	0.326	0.560	0.650 P	1.06
Head and neck	C7–T1 and 1st rib/ear canal	0.081 M	1.000	— PC	0.495	0.116	— PC	1.11
Shoulder mass	Sternoclavicular joint/glenohumeral axis	—	0.712	0.288	—	—	—	1.04
Thorax	C7–T1/T12–L1 and diaphragm*	0.216 PC	0.82	0.18	—	—	—	0.92
Abdomen	T12–L1/L4–L5*	0.139 LC	0.44	0.56	—	—	—	—
Pelvis	L4–L5/greater trochanter*	0.142 LC	0.105	0.895	—	—	—	—
Thorax and abdomen	C7–T1/L4–L5*	0.355 LC	0.63	0.37	—	—	—	—
Abdomen and pelvis	T12–L1/greater trochanter*	0.281 PC	0.27	0.73	—	—	—	1.01
Trunk	Greater trochanter/glenohumeral joint*	0.497 M	0.50	0.50	—	—	—	1.03
Trunk head neck	Greater trochanter/glenohumeral joint*	0.578 MC	0.66	0.34 P	0.503	0.830	0.607 M	—
Head, arms, and trunk (HAT)	Greater trochanter/glenohumeral joint*	0.678 MC	0.626	0.374 PC	0.496	0.798	0.621 PC	—
HAT	Greater trochanter/mid rib	0.678	1.142	—	0.903	1.456	—	—

*NOTE: These segments are presented relative to the length between the greater trochanter and the glenohumeral joint.

Source Codes: M, Dempster via Miller and Nelson; *Biomechanics of Sport*, Lea and Febiger, Philadelphia, 1973. P, Dempster via Plagenhoef; *Patterns of Human Motion*, Prentice-Hall, Inc. Englewood Cliffs, NJ, 1971. L, Dempster via Plagenhoef from living subjects; *Patterns of Human Motion*, Prentice-Hall, Inc., Englewood Cliffs, NJ, 1971. C, Calculated.

Figure C.2: Body segment lengths expressed as a fraction of body height H (Adapted from [116])

APPENDIX D

INITIAL AND FINAL LIMB ANGLES

In this appendix, it is given the initial and final limb angles, which base on the calculation of correlation between them.

Table D.1: Initial and final limb angles for forward trials of subject 1

	Shank		Thigh		Trunk	
Trials	Initial	Final	Initial	Final	Initial	Final
1	5.5295	6.4388	1.6243	0.9693	-3.8881	-6.4568
2	6.2101	5.8467	2.3778	0.727	-3.343	-5.5655
3	4.8671	5.98	1.896	0.7537	-2.4646	-6.1625
4	5.9168	6.1159	3.1721	0.9781	-2.4069	-5.942
5	6.5776	7.7504	1.8939	1.463	-3.5729	-6.6194
6	6.0661	6.1934	1.7566	0.9711	-3.8238	-6.6165
7	6.0364	6.0864	1.935	1.4246	-4.479	-6.5685
8	5.5199	5.0298	1.9275	0.0409	-4.345	-7.1777
9	5.1324	4.1296	0.6613	-0.0894	-4.464	-5.7897
10	5.8649	6.856	2.4323	2.5554	-4.491	-6.4057
11	5.4572	6.1068	1.9805	1.3748	-3.99	-6.3866
12	5.8556	5.9338	2.1209	0.8443	-4.4164	-6.956
13	5.6033	6.621	1.9126	1.8822	-3.4565	-5.6214
14	7.0912	6.1726	0.7619	0.5221	-4.748	-6.5894
15	7.3944	7.0206	3.9693	2.3583	-3.2928	-6.2121
16	6.3676	6.3823	2.4806	1.9781	-4.814	-6.1891
17	6.3613	4.1938	2.0311	-0.4966	-4.3349	-6.1361
18	6.0459	4.9071	2.9302	0.7565	-3.511	-5.9046
19	5.5581	6.8407	2.6473	1.7686	-3.3117	-6.7725
20	6.3539	6.8511	3.781	2.7939	-3.5143	-6.2638

Table D.2: Initial and final limb angles for backward trials of subject 1

	Shank		Thigh		Trunk	
Trials	Initial	Final	Initial	Final	Initial	Final
1	3.866	3.308	1.059	1.34	-2.474	1.555
2	4.008	3.911	-0.1439	0.4835	-1.967	1.399
3	5.139	4.841	0.7517	2.071	-2.643	1.434
4	4.055	2.278	1.002	-1.448	-0.8471	2.021
5	4.068	4.13	0.3871	1.083	-1.882	1.06
6	4.144	3.002	0.5075	0.364	-1.716	2.503
7	3.262	3.791	-0.1993	0.4881	-1.79	0.9414
8	4.811	4.521	1.453	2.479	-2.555	1.576
9	5.012	3.25	1.247	-0.002287	-2.158	1.319
10	5.196	4.308	1.376	1.852	-1.711	1.586
11	5.441	4.538	0.7146	1.815	-2.346	1.653
12	4.657	5.383	-0.4493	1.728	-2.942	-0.702
13	5.895	5.131	1.012	2.332	-2.992	0.6629
14	5.235	4.382	0.4309	0.582	-3.83	-0.3535
15	4.378	4.221	-0.5311	-0.1386	-3.319	-0.3475
16	4.998	5.525	-0.378	0.5326	-3.272	-0.1151
17	5.477	3.735	0.1062	-1.22	-3.262	0.3008
18	5.054	4.748	-0.09306	-0.08688	-2.192	0.2691
19	6.915	6.001	3.078	2.982	-4.02	-0.2775
20	5.032	5.156	-0.00889	0.7621	-3.123	-0.224

Table D.3: Initial and final limb angles for forward trials of subject 2

	Shank		Thigh		Trunk	
Trials	Initial	Final	Initial	Final	Initial	Final
1	4.16	6.798	-0.751	3.444	-7.793	-4.246
2	4.456	6.324	-0.6152	2.609	-8.773	-5.471
3	3.896	6.506	-2.67	2.079	-9.921	-5.123
4	3.579	5.765	-2.293	1.606	-9.42	-5.133
5	3.837	7.303	-3.848	2.315	-10.82	-5.802
6	1.951	6.072	-2.223	3.301	-11.3	-6.784
7	5.12	7.163	-1.332	-0.1513	-9.659	-8.772
8	3.108	6.88	-1.219	2.573	-10.48	-6.895
9	5.168	6.576	-0.4731	2.111	-7.899	-5.977
10	4.256	7.238	-1.986	1.866	-10.13	-7.123
11	5.998	6.218	-0.6894	0.816	-7.898	-6.707
12	6.313	8.455	-0.578	2.195	-8.165	-6.229
13	4.541	8.176	-1.037	2.099	-7.858	-6.281
14	3.224	6.833	0.8404	3.247	-4.957	-5.126
15	4.002	6.999	-0.3065	2.927	-7.051	-5.785
16	4.232	6.371	-0.9707	3.768	-6.116	-3.862
17	2.04	6.165	-2.886	-0.3593	-7.685	-10.49
18	3.135	9.076	-0.191	3.615	-3.816	-2.224
19	5.263	7.713	1.542	2.944	-1.245	-2.935
20	3.942	5.302	-0.7056	0.9348	-3.558	-4.181

Table D.4: Initial and final limb angles for backward trials of subject 2

	Shank		Thigh		Trunk	
Trials	Initial	Final	Initial	Final	Initial	Final
1	1.903	-3.134	1.065	-6.86	-2.065	-5.277
2	5.55	1.696	1.462	-3.795	-3.925	-6.472
3	4.856	0.0926	3.136	-6.678	-1.307	-6.816
4	4.919	1.862	3.309	-7.218	-1.188	-8.425
5	4.743	2.439	1.445	-4.708	-4.093	-7.612
6	2.496	0.583	0.1581	-3.302	-5	-4.429
7	4.106	1.569	2.355	-4.948	-0.5862	-5.566
8	5.129	3.511	1.347	-5.986	-4.843	-7.623
9	4.906	2.613	0.5656	-3.349	-4.901	-5.566
10	5.116	2.088	1.593	-4.876	-3.144	-6.351
11	3.917	1.867	0.6474	-6.889	-3.577	-7.166
12	4.378	2.619	1.011	-3.858	-2.653	-5.629
13	4.834	0.9955	1.025	-5.783	-3.899	-6.072
14	4.761	1.959	0.9077	-5.623	-2.781	-6.576
15	5.067	2.706	3.474	-4.857	-0.7118	-5.382
16	3.924	1.257	1.193	-6.013	-1.715	-5.184
17	3.764	2.03	1.12	-5.465	-0.8206	-4.486
18	3.465	2.637	2.228	-6.056	0.8836	-5.392
19	2.574	2.582	0.2744	-7.131	1.168	-4.768
20	3.121	1.475	2.074	-5.391	1.672	-2.084

APPENDIX E

DETAILED ANALYSIS: COMPARISON OF SIMULATIONS AND EXPERIMENTAL DATA

In this appendix, the analysis results of simulations are given in terms of the fitting to experimental data. Each table includes two-type analysis. These analyses are the final value differences and root mean square deviation which measures the deviation between the simulated and experimental data. In tables, upper header shows direction, middle header involves type of analysis and each lower headers describes related angles.

Table E.1: The analysis results of simulations of subject 1

	Forward Trials						Backward Trials					
	Final Value			RMS			Final Value			RMS		
Trials	Shank	Thigh	Trunk	Shank	Thigh	Trunk	Shank	Thigh	Trunk	Shank	Thigh	Trunk
1	-0.345	0.366	-0.1136	0.0138	0.0153	0.0054	-0.224	0.2898	-0.1541	0.0076	0.0095	0.0048
2	-0.3034	0.3121	-0.0864	0.0124	0.0133	0.0043	-0.3125	0.4174	-0.2305	0.0106	0.0141	0.0078
3	-0.2912	0.2987	-0.0803	0.0115	0.0123	0.0039	-0.2832	0.3592	-0.1852	0.0098	0.0125	0.0065
4	-0.2871	0.2774	-0.0585	0.0109	0.0108	0.0026	-0.3165	0.4403	-0.2563	0.0097	0.0132	0.0076
5	-0.3521	0.3638	-0.1048	0.0137	0.0146	0.0047	-0.2781	0.3605	-0.191	0.0092	0.0119	0.0063
6	-0.298	0.2913	-0.0622	0.0119	0.0121	0.0032	-0.2647	0.3578	-0.2031	0.0088	0.0117	0.0065
7	-0.2054	0.1633	0.0103	0.009	0.008	0.0008	-0.2799	0.37	-0.2009	0.0091	0.0121	0.0066
8	-0.2667	0.2527	-0.0417	0.0108	0.0107	0.0024	-0.2286	0.2872	-0.1476	0.008	0.01	0.0051
9	-0.2801	0.2925	-0.0812	0.0113	0.0122	0.0037	-0.2494	0.3306	-0.1828	0.0074	0.0097	0.0054
10	-0.1917	0.1389	0.0268	0.0086	0.0074	0.0005	-0.2474	0.3161	-0.1667	0.0082	0.0103	0.0055
11	-0.2173	0.1811	-0.0014	0.0092	0.0084	0.0012	-0.2704	0.3385	-0.1712	0.0097	0.0121	0.0061
12	-0.2538	0.2282	-0.024	0.0105	0.0101	0.002	-0.2675	0.3097	-0.1307	0.0096	0.0111	0.0047
13	-0.2455	0.2237	-0.0293	0.0103	0.0101	0.0023	-0.2302	0.2795	-0.1352	0.0076	0.0093	0.0046
14	-0.3443	0.3609	-0.1079	0.0142	0.0154	0.0053	-0.2676	0.3258	-0.1529	0.0087	0.0104	0.0047
15	-0.2272	0.1781	0.0098	0.0099	0.0086	0.0009	-0.331	0.4213	-0.2115	0.0112	0.0141	0.007
16	-0.1812	0.1195	0.0427	0.0077	0.0058	0.0008	-0.3596	0.4538	-0.2263	0.0122	0.0154	0.0076
17	-0.268	0.2539	-0.0438	0.011	0.0107	0.0022	-0.366	0.4695	-0.2389	0.0124	0.0154	0.0074
18	-0.1573	0.1009	0.041	0.0071	0.0054	0.0006	-0.3452	0.4428	-0.2278	0.0115	0.0147	0.0075
19	-0.2138	0.1719	0.0069	0.0089	0.0079	0.0008	-0.1557	0.1364	-0.0213	0.0046	0.0033	0.0003
20	-0.1506	0.0742	0.0681	0.0069	0.0046	0.0014	-0.3143	0.3898	-0.189	0.0105	0.0129	0.0061
Averages Absolute	0.254	0.2325	0.052	0.0105	0.0102	0.0025	0.2796	0.3548	0.1812	0.0093	0.0117	0.0059

Table E.2: The analysis results of simulations of subject 2

	Forward Trials						Backward Trials					
	Final Value			RMS			Final Value			RMS		
Trials	Shank	Thigh	Trunk	Shank	Thigh	Trunk	Shank	Thigh	Trunk	Shank	Thigh	Trunk
1	-0.216	0.1986	-0.0273	0.0076	0.0072	0.0012	-0.2547	0.4492	-0.3339	0.0117	0.0218	0.0174
2	-0.1205	0.0562	0.0685	0.0057	0.0039	0.0016	-0.2222	0.2653	-0.1107	0.0064	0.0073	0.0028
3	-0.2504	0.2512	-0.053	0.0105	0.0111	0.0029	-0.1814	0.224	-0.1018	0.0036	0.0036	0.0011
4	-0.2351	0.2223	-0.0314	0.0097	0.0097	0.0019	-0.1601	0.1938	-0.0817	0.0027	0.0026	0.0006
5	-0.309	0.3139	-0.0758	0.0125	0.0133	0.0038	-0.2243	0.2698	-0.1137	0.0057	0.0066	0.0026
6	-0.1516	0.0818	0.0712	0.008	0.0063	0.001	-0.2128	0.268	-0.1228	0.0051	0.0057	0.0019
7	-0.2953	0.2875	-0.0519	0.0105	0.0103	0.0018	-0.2372	0.3032	-0.1494	0.0062	0.0075	0.0035
8	-0.2124	0.1739	0.0118	0.009	0.0083	0.0007	-0.2347	0.3054	-0.1517	0.006	0.0076	0.0037
9	-0.1761	0.1288	0.0289	0.007	0.0057	0.0003	-0.258	0.3175	-0.1433	0.0076	0.0091	0.0039
10	-0.3217	0.3118	-0.0582	0.0138	0.0143	0.0036	-0.2612	0.3342	-0.1633	0.0074	0.0093	0.0044
11	-0.2264	0.1997	-0.0115	0.0087	0.0081	0.001	-0.2976	0.3892	-0.1936	0.0088	0.0112	0.0054
12	-0.3325	0.3246	-0.068	0.0133	0.0135	0.0033	-0.246	0.3141	-0.1529	0.0066	0.0082	0.0039
13	-0.3247	0.3288	-0.0824	0.0125	0.0132	0.0038	-0.2873	0.3766	-0.1901	0.0083	0.0107	0.0053
14	-0.1818	0.1413	0.0139	0.0081	0.0076	0.0012	-0.2684	0.3434	-0.1663	0.0075	0.0093	0.0043
15	-0.2119	0.1729	0.0069	0.0092	0.0085	0.0011	-0.2243	0.2804	-0.1336	0.0051	0.0058	0.0025
16	-0.1697	0.1321	0.0158	0.0078	0.0074	0.001	-0.239	0.3192	-0.1665	0.0059	0.0077	0.0039
17	-0.3164	0.3288	-0.0828	0.0124	0.0137	0.0044	-0.2863	0.3823	-0.2027	0.0081	0.0105	0.0054
18	-0.328	0.3543	-0.1206	0.0116	0.0129	0.0047	-0.2712	0.3601	-0.1895	0.0071	0.009	0.0047
19	-0.2127	0.1982	-0.035	0.0065	0.006	0.0009	-0.2797	0.3842	-0.2101	0.0078	0.0106	0.0059
20	-0.259	0.2747	-0.0805	0.0093	0.0103	0.0034	-0.26	0.354	-0.1945	0.0061	0.0081	0.0044
Averages Absolute	0.2426	0.2241	0.0498	0.0097	0.0096	0.0022	0.2453	0.3217	0.1636	0.0067	0.0086	0.0044

APPENDIX F

CANONICAL CORRELATION ANALYSIS METHOD

For sake of integrity of the thesis, theoretical background and mathematical description of the canonical correlation analysis method are presented in here on the basis of [32], directly.

Suppose we are given two random variables $X \in R^q$ and $Y \in R^p$. The idea is to find an index describing a (possible) link between X and Y . The canonical correlation analysis (CCA) is based on linear indices, i.e., linear combinations

$$a^T X \text{ and } b^T Y$$

of the random variables. The canonical correlation analysis searches for vectors a and b such that the relation of the two indices $a^T X$ and $b^T Y$ is quantified in some interpretable way. More precisely, one is looking for the "*most interesting*" projections a and b in the sense that they maximize the correlation

$$\rho(a, b) = \rho a^T X b^T Y \tag{F.1}$$

between the two indices.

Let us consider the correlation $\rho(a, b)$ between the two projections in more detail. Suppose that

$$\begin{pmatrix} X \\ Y \end{pmatrix} \sim \left(\begin{pmatrix} \mu \\ \nu \end{pmatrix}, \begin{pmatrix} \Sigma_{XX} & \Sigma_{XY} \\ \Sigma_{YX} & \Sigma_{YY} \end{pmatrix} \right)$$

where the sub-matrices of this covariance structure are given by

$$\mathrm{Var}(X) = \Sigma_{XX}(q \times q)$$

$$\mathrm{Var}(Y) = \Sigma_{YY}(p \times p)$$

$$\mathrm{Cov}(X, Y) = E(X - \mu)(Y - \nu)^T = \Sigma_{XY} = \Sigma_{YX}^T(q \times p)$$

$$\rho(X, Y) = \frac{\mathrm{Cov}(X, Y)}{\sqrt{\mathrm{Var}(X)\,\mathrm{Var}(Y)}} \tag{3.7}$$

$$\mathrm{Cov}(AX, BY) = A\,\mathrm{Cov}(X, Y)B^T \tag{4.26}$$

Using Eq.3.7 and Eq.4.26

$$\rho(a, b) = \frac{a^T \Sigma_{XY} b}{(a^T \Sigma_{XX} a)^{1/2}\,(b^T \Sigma_{YY} b)^{1/2}} \tag{F.2}$$

Therefore, $\rho(ca, b) = \rho(a, b)$ for any $c \in R^+$. Given the invariance of scale we may rescale projections a and b and thus we can equally solve

$$\max_{a,b} = a^T \Sigma_{XY} b$$

under the constraints

$$a^T \Sigma_{XX} a = 1$$
$$b^T \Sigma_{YY} b = 1$$

For this problem, define

$$\kappa = \Sigma_{XX}^{-1/2} \Sigma_{XY} \Sigma_{YY}^{-1/2} \tag{F.3}$$

THEOREM 2. 1. *(Jordan Decomposition) Each symmetric matrix $A(n \times p)$ can be written as*

$$A = \Gamma \Lambda \Gamma^T = \sum_j = 1^p \lambda_j \gamma_j \gamma_j^T$$

where

$$\Lambda = \mathrm{diag}(\lambda_1, \ldots, \lambda_p)$$

and where

$$\Gamma = diag(\gamma_1, \ldots, \gamma_p)$$

is an orthogonal matrix consisting of the eigenvectors γ_j of A.

THEOREM 2. 2. *(Singular Value Decomposition) Each matrix $A(n \times p)$ with rank r can be decomposed as*

$$A = \mathit{\Gamma} \mathit{\Lambda} \Delta^T,$$

where $\mathit{\Gamma}(n \times r)$ and $\Delta(p \times r)$. Both $\mathit{\Gamma}$ and Δ are column orthonormal, i.e., $\mathit{\Gamma}^T \mathit{\Gamma} = \Delta^T \Delta = I_r$ and $\mathit{\Lambda} = \operatorname{diag}\left(\lambda_1^{1/2}, \ldots, \lambda_r^{1/2}\right), \lambda_j > 0$. The values $\lambda_1, \ldots, \lambda_r$ are the non-zero eigenvalues of the matrices AA^T and $A^T A$. $\mathit{\Gamma}$ and Δ consist of the corresponding r eigenvectors of these matrices.

This is obviously a generalization of Theorem 2.1 (Jordan decomposition). With Theorem 2.2, we can find a G-inverse A^- of A. Indeed, define $A^- = \Delta \mathit{\Lambda}^{-1} \mathit{\Gamma}^T$. Then $AA^-A = \mathit{\Gamma} \mathit{\Lambda} \Delta^T = A$. Note that the G-inverse is not unique.

THEOREM 2. 5. *If A and B are symmetric and $B > 0$, then the maximum of $\frac{x^T Ax}{x^T Bx}$ is given by the largest eigenvalue of $B^{-1}A$. More generally,*

$$\max_a \frac{x^T Ax}{x^T Bx} = \lambda_1 \geq \lambda_2 \geq \cdots \geq \lambda_p = \min_a \frac{x^T Ax}{x^T Bx}$$

where $\lambda_1, \ldots, \lambda_p$ denote the eigenvalues of $B^{-1}A$. The vector which maximizes (minimizes) $\frac{x^T Ax}{x^T Bx}$ is the eigenvector of $B^{-1}A$ which corresponds to the largest (smallest) eigenvalue of $B^{-1}A$. If $x^T Bx = 1$, we get

$$\max_a x^T Ax = \lambda_1 \geq \lambda_2 \geq \cdots \geq \lambda_p = \min_a x^T Ax$$

Proof. See [32] for proof. □

Recall the singular value decomposition of $\kappa(q \times p)$ from Theorem 2.2. The matrix κ may be decomposed as

$$\kappa = \mathit{\Gamma} \mathit{\Lambda} \Delta^T$$

with

$$\begin{aligned} \mathit{\Gamma} &= (\gamma_1, \ldots, \gamma_k) \\ \Delta &= (\delta_1, \ldots, \delta_k) \\ \mathit{\Lambda} &= \operatorname{diag}\left(\lambda_1^{1/2}, \ldots, \lambda_r^{1/2}\right) \end{aligned} \tag{F.4}$$

$$\operatorname{rank}(ABC) = \operatorname{rank}(B) \text{ for nonsingular A,C} \tag{2.15}$$

where by (F.3) and (2.15),

$$k = \text{rank}(\kappa) = \text{rank}(\Sigma_{XY}) = \text{rank}(\Sigma_{YX}),$$

and $\lambda_1 \geq \lambda_2 \geq \ldots \lambda_k$ are the nonzero eigenvalues of $N_1 = KK^T$ and $N_2 = K^T K$ and γ_i and δ_j are the standardized eigenvectors of N_1 and N_2 respectively. Define now for $i = 1, \cdots, k$ the vectors

$$a_i = \Sigma_{XX}^{-1/2} \gamma_i, \tag{F.5}$$

$$b_i = \Sigma_{YY}^{-1/2} \delta_i, \tag{F.6}$$

which are called the canonical correlation vectors. Using these canonical correlation vectors we define the canonical correlation variables

$$\eta_i = a_i^T X, \tag{F.7}$$

$$\varphi_i = b_i^T Y, \tag{F.8}$$

The quantities $\rho_i = \lambda_i^{1/2}$ for $i = 1, \cdots, k$ are called the canonical correlation coefficients. From the properties of the singular value decomposition given in (**??**) we have

$$\text{Cov}(\eta_i, \eta_j) = a_i^T \Sigma_{XX} a_j = \gamma_i^T \gamma_j = \begin{cases} 1 & i = j \\ 0 & i \neq j \end{cases} \tag{F.9}$$

The same is true for $\text{Cov}(\varphi_i, \varphi_j)$. The following theorem tells us that the canonical vectors are the solution to the maximization problem of (F.1).

THEOREM F.0.1. *For any given r, $1 \leq r \leq k$, the maximum*

$$C(r) = \max_{a,b} = a^T \Sigma_{XY} b \tag{F.10}$$

subject to

$$a^T \Sigma_{XX} a = 1, \; b^T \Sigma_{YY} b = 1$$

and

$$a_i^T \Sigma_{XX} a = 0, \textit{ for } i = 1, \ldots, r-1$$

is given by

$$C(r) = \rho r = \lambda_r^{1/2}$$

and is attained when $a = a_r$ and $b = b_r$.

Proof. The proof is given in three steps.

i Fix a and maximize over b, i.e., solve:

$$\max_b \left(a^T \Sigma_{XY} b\right)^2 = \max_b \left(b^T \Sigma_{YX} a\right)\left(a^T \Sigma_{XY} b\right)$$

subject to $b^T \Sigma_{YY} b = 1$ By Theorem 2.5 the maximum is given by the largest eigenvalue of the matrix

$$\Sigma_{YY}^{-1} \Sigma_{YX} a a^T \Sigma_{XY}$$

By Corollary 2.2, the only nonzero eigenvalue equals

Note: Corallary 2.2 is $\mathrm{rank}(Aab^T B) \leq 1$. The non-zero eigenvalue, if it exists, equals $b^T BAa$ (with eigenvector Aa).

$$a^T \Sigma_{XY} \Sigma_{YY}^{-1} \Sigma_{YX} a \tag{F.11}$$

ii Maximize (F.11) over a subject to the constraints of the Theorem. Put $\gamma = \Sigma_{XX}^{1/2} a$ and observe that (F.11) equals

$$\gamma^T \Sigma_{XX}^{-1/2} \Sigma_{XY} \Sigma_{YY}^{-1} \Sigma_{YX} \Sigma_{XX}^{-1/2} \gamma = \gamma^T \kappa^T \kappa \gamma.$$

Thus, solve the equivalent problem

$$max_a \gamma^T N_1 \gamma \tag{F.12}$$

subject to $\gamma^T \gamma = 1$ for $i = 1, \ldots, r-1$. Note that the γ_is are the eigenvectors of N_1 corresponding to its first $r-1$ largest eigenvalues.Thus, as in Theorem 9.3 (see below), the maximum in (F.12) is obtained by setting γ equal to the eigenvector corresponding to the r-th largest eigenvalue, i.e., $\gamma = \gamma_r$ or equivalently $a = a_r$. This yields

$$C^2(r) = \gamma_r^T N_1 \gamma_r = \lambda_r \gamma_r^T \gamma = \lambda_r.$$

THEOREM 9. 3. *If $Y = a^T X$ is a standardized linear combination that is not correlated with the first k principal components of X, then the variance of Y is maximized by choosing it to be the $(k+1)$-st principal component.*

iii Show that the maximum is attained for $a = a_r$ and $b = b_r$. From the singular value decomposition of κ we conclude that $\kappa \delta_r = \rho_r \gamma_r$ and hence

$$a_r^T \Sigma_{XY} b_r = \gamma_r^T \kappa \delta_r = \rho_r \gamma_r^T \gamma_r = \rho_r.$$

$\square$

Let

$$\begin{pmatrix} X \\ Y \end{pmatrix} \sim \left(\begin{pmatrix} \mu \\ \nu \end{pmatrix}, \begin{pmatrix} \Sigma_{XX} & \Sigma_{XY} \\ \Sigma_{YX} & \Sigma_{YY} \end{pmatrix} \right)$$

$$a_1 = \Sigma_{XX}^{-1/2} \gamma_1,$$

$$b_1 = \Sigma_{YY}^{-1/2} \delta_1,$$

maximize the correlation between the canonical variables

$$\eta_1 = a_1^T X,$$

$$\varphi_1 = b_1^T Y.$$

The covariance of the canonical variables η and φ is given in the next theorem.

THEOREM F.0.2. *Let η_i and φ_i be the i-th canonical correlation variables ($i = 1, \ldots, k$). Define $\eta = (\eta_1, \ldots, \eta_k)$ and $\varphi = (\varphi_1, \ldots, \varphi_k)$. Then*

$$Var \begin{pmatrix} \eta \\ \varphi \end{pmatrix} = \begin{pmatrix} I_k & \Lambda \\ \Lambda & I_k \end{pmatrix}$$

with Λ given in (F.4).

This theorem shows that the canonical correlation coefficients, $\rho_i = \lambda_i^{1/2}$, are the covariances between the canonical variables η_i and φ_i and that the indices $\eta_i = a_1^T X$ and $\varphi_i = b_1^T Y$ have the maximum covariance $\sqrt{\lambda_1} = \rho_1$.

The following theorem shows that canonical correlations are invariant w.r.t. linear transformations of the original variables.

THEOREM F.0.3. *Let $X^* = U^T X + u$ and $Y^* = V^T Y + v$ where U and V are nonsingular matrices. Then the canonical correlations between X^* and Y^* are the same as those between X and Y . The canonical correlation vectors of X^* and Y^* are given by*

$$\begin{aligned} a_i^* &= U^{-1} a_i, \\ b_i^* &= V^{-1} b_i. \end{aligned} \tag{F.13}$$

APPENDIX G

TABULATED RESULTS OF STATISTICAL ANALYSIS FOR CCA

In this appendix, tabulated results of statistical analysis are given. These results are obtained by comparing to simulations with the experimental data. Adaptation law, which are found by using CCA, are simulated for all subjects and all trials, then obtained results are evaluated by using two type simple statistical analysis methods. They are the final value differences and root mean square deviation which measures the deviation between the simulated and the experimental data.

Table G.1: Tabulated results of statistical analysis for subject 1

	Forward Trials						Backward Trials					
	Final Value			RMS			Final Value			RMS		
Trials	Shank	Thigh	Trunk	Shank	Thigh	Trunk	Shank	Thigh	Trunk	Shank	Thigh	Trunk
1	0.1159	-0.4957	-1.336	0.0197	0.0426	0.018	1.7474	-2.926	4.0688	0.0497	0.0842	0.3127
2	-0.1027	-0.1085	-0.273	0.0036	0.0163	0.0158	0.2665	-0.5607	2.9127	0.003	0.01	0.2395
3	-0.7765	0.8452	-2.8737	0.0394	0.0476	0.1307	0.2438	-0.5754	2.9706	0.006	0.0009	0.2502
4	-0.68	0.7064	-1.5587	0.0159	0.0109	0.0686	1.664	-2.8588	5.6829	0.0342	0.0606	0.3537
5	-1.6066	2.4395	-4.268	0.0319	0.0395	0.1232	0.2159	-0.5377	2.3621	0.0016	0.0044	0.1956
6	-1.039	1.305	-2.6538	0.0425	0.056	0.1382	-1.034	1.2977	-0.576	0.0187	0.0317	0.0269
7	-1.0252	1.2097	-2.0828	0.0331	0.0402	0.0709	0.2322	-0.4951	2.0558	0.0024	0.0082	0.1801
8	-1.2893	1.5959	-1.6997	0.0366	0.0438	0.0673	0.6662	-1.4012	3.3188	0.01	0.0279	0.2807
9	-1.3473	1.766	-1.4965	0.047	0.0636	0.0378	0.187	-0.4893	4.9428	0.0155	0.0161	0.3242
10	-0.0424	-0.2064	-1.7033	0.0018	0.0067	0.0467	0.4236	-0.8505	2.9668	0.0047	0.0142	0.2532
11	-1.8674	2.5569	-3.2348	0.0689	0.0931	0.1314	0.2928	-0.6517	3.0593	0.0038	0.0017	0.2033
12	-0.7292	0.8008	-1.5503	0.0266	0.0277	0.0687	-0.3068	0.3939	0.0163	0.0234	0.0315	0.0241
13	-0.4229	0.4179	-2.2307	0.0142	0.0125	0.0896	-0.1568	0.0724	2.9441	0.0226	0.0254	0.2812
14	-1.087	1.2804	-2.1668	0.0461	0.0544	0.0903	-0.0916	0.0175	3.3963	0.0083	0.0075	0.2317
15	-1.4303	1.6963	-2.0326	0.0769	0.0988	0.1025	-0.2192	0.2392	2.5535	0.0178	0.023	0.1735
16	-1.1466	1.5591	-1.7204	0.0542	0.071	0.0726	-0.6156	0.8849	2.1337	0.0286	0.0399	0.1669
17	0.0363	-0.2207	0.9719	0.0034	0.0102	0.0096	1.7669	-3.0638	5.263	0.0271	0.0508	0.2653
18	-0.1629	0.0211	-0.003	0.0019	0.0126	0.0122	0.1264	-0.2585	2.5203	0.0047	0.0093	0.1532
19	-0.4711	0.4119	-2.6054	0.0196	0.0168	0.0958	0.1206	-0.3353	3.9025	0.0021	0.0028	0.257
20	-0.2188	0.045	-1.5263	0.0017	0.0143	0.0474	0.0884	-0.3078	2.1885	0.0004	0.0064	0.1731
Averages Absolute	0.7799	0.9844	1.8994	0.0293	0.0389	0.0719	0.5233	0.9109	2.9917	0.0142	0.0228	0.2173

In these tables, the analysis results of simulations are given in terms of fitting to experimental data. Each table includes "upper headers shown direction", "middle headers involved type of analysis" and "lower headers described related angles".

Table G.2: Tabulated results of statistical analysis for subject 2

	Forward Trials						Backward Trials					
	Final Value			RMS			Final Value			RMS		
Trials	Shank	Thigh	Trunk	Shank	Thigh	Trunk	Shank	Thigh	Trunk	Shank	Thigh	Trunk
1	-0.3759	0.3298	-0.6649	0.0122	0.0109	0.0713	-1.4879	1.9438	3.7411	0.0523	0.0716	0.2022
2	-1.1152	1.4599	-0.7222	0.0435	0.0564	0.0809	-1.3352	1.6578	2.0682	0.0677	0.0866	0.1606
3	-0.8167	0.9837	-0.3369	0.026	0.0283	0.0507	-0.286	0.2159	4.3146	0.0013	0.0067	0.2427
4	0.789	-1.1997	1.2637	0.0377	0.057	0.006	-1.2419	1.5617	2.4927	0.0272	0.025	0.3062
5	0.7691	-1.2405	-0.3236	0.0443	0.0678	0.0512	-1.8628	2.6051	1.117	0.0805	0.1125	0.1595
6	-0.7214	0.8438	-1.3917	0.031	0.0359	0.1147	-0.5	0.4933	4.104	0.0436	0.0574	0.2599
7	-0.9566	1.2366	-0.9778	0.0505	0.0669	0.0995	-1.1871	1.6034	1.5698	0.03	0.033	0.1703
8	-0.7924	0.9845	-0.6238	0.0394	0.0504	0.075	1.1244	-2.117	6.2735	0.0229	0.0517	0.4946
9	0.2821	-0.5701	-0.2472	0.0147	0.0269	0.0545	-1.05	1.3027	2.5444	0.0583	0.0784	0.2018
10	0.5691	-0.9484	-0.2036	0.0347	0.0551	0.0395	-0.6488	0.7333	3.0645	0.0347	0.0415	0.25
11	-0.89	1.0895	-0.8097	0.0311	0.0363	0.077	-1.6153	2.089	2.839	0.08	0.1064	0.2277
12	-1.6493	2.3871	-2.3413	0.0686	0.097	0.1587	-0.7932	0.9985	1.3932	0.06	0.0801	0.1972
13	-0.6091	0.7031	-1.8952	0.0253	0.0279	0.1348	-1.5332	1.9852	3.6541	0.0834	0.1103	0.2491
14	-0.3601	0.3878	-2.941	0.0097	0.0203	0.1433	-0.4958	0.5739	2.6507	0.028	0.0352	0.1697
15	0.9777	-1.5064	-1.0463	0.0396	0.0633	0.0777	-1.1575	1.3743	2.9302	0.0486	0.0568	0.2141
16	-0.7787	1.0974	-3.4928	0.0395	0.0561	0.2184	-1.6697	2.1343	2.7331	0.0663	0.0831	0.2367
17	-0.9777	1.4818	-6.4055	0.0318	0.0437	0.2993	-1.2789	1.7271	2.0126	0.0655	0.0893	0.2013
18	1.2468	-1.6331	-1.4103	0.0425	0.0569	0.1444	-0.705	0.7248	1.876	0.0311	0.0326	0.1838
19	-0.2191	0.1865	-3.5456	0.0006	0.004	0.207	-2.0731	2.7018	0.0791	0.1022	0.1364	0.0849
20	-0.0273	-0.0948	-2.26	0.0178	0.019	0.1927	-2.3179	2.8969	2.2793	0.1083	0.1381	0.1217
Averages Absolute	0.7462	1.0182	1.6452	0.032	0.044	0.1148	1.2182	1.572	2.6869	0.0546	0.0716	0.2167

APPENDIX H

IDENTIFICATION OF THE "AGILE" AND "SLOUCHY" INITIAL STANCE

In this appendix, it is given the initial limb angles, root mean square deviation which measures the deviation between the response data obtained each trial and average of all 20 trials responses. (Note that: there are 40 trials for each subject, the direction of half is forward and the other is backward). Obtained average standard deviation for each limb is also given. At the last two column are "Knee angle" and "Hip angle". Four different table include the data of two different subjects for two different directions.

Additionally, in this appendix, outputs of the using classification algorithm are presented as Fig.H.1, Fig.H.2, Fig.H.3 and Fig.H.4.

Table H.1: Subject#1, Statistics for Forward Trials

	Initial Conditions			Standard Deviations			Extra Measures		
No	Sh. Ang.	Th. Ang.	Tr. Ang.	SD_Sh.	SD_Th.	SD_Tr.	Ave. SD	Knee Ang.	Hip Ang.
1	5.5295	1.6243	-3.8881	0.3839	0.9734	0.2653	0.6786	3.9052	5.5124
2	6.2101	2.3778	-3.343	0.366	0.4604	0.7664	0.4132	3.8323	5.7207
3	4.8671	1.896	-2.4646	0.6632	0.5671	0.5754	0.6151	2.9711	4.3606
4	5.9168	3.1721	-2.4069	0.3054	0.3566	0.5885	0.331	2.7448	5.5789
5	6.5776	1.8939	-3.5729	1.8944	0.6095	0.2404	1.2519	4.6836	5.4668
6	6.0661	1.7566	-3.8238	0.3021	0.6089	0.5377	0.4555	4.3095	5.5804
7	6.0364	1.935	-4.479	0.3037	0.3021	0.2721	0.3029	4.1014	6.4141
8	5.5199	1.9275	-4.345	1.052	1.3662	0.9378	1.2091	3.5924	6.2726
9	5.1324	0.6613	-4.464	1.3858	1.1084	0.3406	1.2471	4.4711	5.1252
10	5.8649	2.4323	-4.491	0.4824	0.836	0.2376	0.6592	3.4326	6.9233
11	5.4572	1.9805	-3.99	0.2632	0.2847	0.0789	0.2739	3.4767	5.9705
12	5.8556	2.1209	-4.4164	0.1744	0.2386	0.6035	0.2065	3.7347	6.5373
13	5.6033	1.9126	-3.4565	0.4471	0.6772	0.7716	0.5621	3.6907	5.3691
14	7.0912	0.7619	-4.748	0.4119	0.76	0.3206	0.586	6.3292	5.5099
15	7.3944	3.9693	-3.2928	1.0953	1.29	0.2968	1.1926	3.4251	7.2621
16	6.3676	2.4806	-4.814	0.7449	1.0336	0.5788	0.8892	3.8869	7.2947
17	6.3613	2.0311	-4.3349	1.7466	2.0032	0.4769	1.8749	4.3302	6.366
18	6.0459	2.9302	-3.511	0.7623	0.6723	0.5255	0.7173	3.1157	6.4411
19	5.5581	2.6473	-3.3117	0.5026	0.7376	0.403	0.6201	2.9108	5.9591
20	6.3539	3.781	-3.5143	0.752	1.6193	0.2726	1.1857	2.5728	7.2953

Table H.2: Subject#1, Statistics for Backward Trials

	Initial Conditions			Standard Deviations			Extra Measures		
No	Sh. Ang.	Th. Ang.	Tr. Ang.	SD_Sh.	SD_Th.	SD_Tr.	Ave. SD	Knee Ang.	Hip Ang.
1	3.8664	1.0587	-2.4742	0.9633	0.4473	0.6267	0.6791	2.8077	3.5328
2	4.008	-0.1439	-1.9668	0.4329	0.5344	0.8901	0.6191	4.1519	1.823
3	5.1395	0.7517	-2.6432	0.3728	1.048	0.8293	0.75	4.3878	3.3949
4	4.0547	1.0015	-0.8471	1.3875	1.4435	1.2745	1.3685	3.0532	1.8486
5	4.0683	0.3871	-1.8821	0.3147	0.2809	0.3255	0.307	3.6812	2.2692
6	4.1437	0.5075	-1.7162	1.2279	0.4708	1.3604	1.0197	3.6362	2.2237
7	3.2616	-0.1993	-1.7903	0.7589	0.5079	0.3143	0.527	3.4609	1.5911
8	4.8108	1.4533	-2.5551	0.2209	1.2878	0.552	0.6869	3.3574	4.0084
9	5.0118	1.247	-2.1577	0.8123	0.6278	0.8809	0.7737	3.7648	3.4047
10	5.1957	1.3759	-1.7112	0.2093	0.7641	0.8121	0.5951	3.8198	3.0871
11	5.4414	0.7146	-2.3465	0.3781	0.6516	0.6769	0.5689	4.7269	3.0611
12	4.6574	-0.4493	-2.942	0.8351	0.7319	1.5584	1.0418	5.1068	2.4927
13	5.8953	1.0118	-2.9921	0.4868	0.9584	0.3306	0.5919	4.8834	4.0039
14	5.235	0.4309	-3.8299	0.3142	0.1968	1.1418	0.5509	4.8041	4.2607
15	4.3781	-0.5311	-3.3188	0.3094	0.8844	1.1671	0.787	4.9092	2.7877
16	4.9975	-0.378	-3.2717	0.8669	0.5706	0.8768	0.7714	5.3755	2.8936
17	5.4765	0.1062	-3.2616	0.7312	1.3205	0.6926	0.9148	5.3703	3.3679
18	5.0537	-0.0931	-2.1917	0.4307	0.7249	0.4423	0.5327	5.1468	2.0986
19	6.915	3.0781	-4.0203	1.807	1.5814	1.4278	1.6054	3.837	7.0984
20	5.0319	-0.0089	-3.1226	0.4764	0.5121	1.0828	0.6904	5.0408	3.1137

Table H.3: Subject#2, Statistics for Forward Trials

	Initial Conditions			Standard Deviations			Extra Measures		
No	Sh. Ang.	Th. Ang.	Tr. Ang.	SD_Sh.	SD_Th.	SD_Tr.	Ave. SD	Knee Ang.	Hip Ang.
1	4.1598	-0.751	-7.7928	0.808	1.589	0.9737	1.1236	4.9108	7.0418
2	4.4557	-0.6152	-8.7726	0.5858	0.6849	0.598	0.6229	5.0709	8.1574
3	3.8961	-2.6702	-9.9208	0.5708	1.1542	1.5798	1.1016	6.5662	7.2506
4	3.5787	-2.2926	-9.4203	0.8588	0.443	0.7636	0.6885	5.8713	7.1277
5	3.837	-3.848	-10.8212	0.8321	1.1474	1.7168	1.2321	7.685	6.9732
6	1.9511	-2.2231	-11.3	1.2114	0.8224	2.1382	1.3907	4.1742	9.0769
7	5.1205	-1.3319	-9.6589	0.7437	1.212	2.0445	1.3334	6.4524	8.327
8	3.1084	-1.2194	-10.4787	0.5259	0.3326	1.4571	0.7718	4.3278	9.2593
9	5.1684	-0.4731	-7.8987	0.6265	0.4018	1.1347	0.721	5.6415	7.4256
10	4.256	-1.9863	-10.1292	0.4312	0.6838	1.0416	0.7189	6.2423	8.1428
11	5.9985	-0.6894	-7.8983	0.7785	0.9491	0.8389	0.8555	6.6879	7.2089
12	6.3133	-0.578	-8.1653	1.2255	0.8778	1.5224	1.2086	6.8913	7.5872
13	4.5411	-1.0371	-7.8577	1.3782	0.6844	1.0905	1.051	5.5783	6.8206
14	3.2236	0.8404	-4.9566	0.4944	1.0748	1.22	0.9297	2.3832	5.797
15	4.0017	-0.3065	-7.0513	0.4109	1.3162	0.942	0.8897	4.3082	6.7447
16	4.2319	-0.9707	-6.1159	0.8539	0.7057	1.5127	1.0241	5.2026	5.1452
17	2.0401	-2.8857	-7.6846	1.2881	1.7254	2.7577	1.9237	4.9258	4.7989
18	3.1347	-0.191	-3.8155	1.3884	0.9465	3.0937	1.8095	3.3257	3.6245
19	5.2627	1.5416	-1.2451	1.3222	0.8878	3.9903	2.0668	3.7211	2.7867
20	3.9423	-0.7056	-3.5576	1.5035	0.8095	2.8682	1.7271	4.6479	2.8519

Table H.4: Subject#2, Statistics for Backward Trials

	Initial Conditions			Standard Deviations			Extra Measures		
No	Sh. Ang.	Th. Ang.	Tr. Ang.	SD_Sh.	SD_Th.	SD_Tr.	Ave. SD	Knee Ang.	Hip Ang.
1	1.9034	1.0655	-2.0645	3.6466	1.431	0.8292	1.969	0.8379	3.13
2	5.5497	1.4615	-3.9255	0.7095	1.1272	1.4238	1.0868	4.0882	5.387
3	4.8555	3.1364	-1.3073	1.0617	2.0022	2.2142	1.7594	1.7191	4.4437
4	4.9193	3.3089	-1.1879	0.5671	2.2573	2.7011	1.8418	1.6105	4.4968
5	4.743	1.4449	-4.093	0.8043	0.4253	2.3142	1.1812	3.2982	5.5379
6	2.496	0.1581	-4.9998	1.8474	0.9948	1.5502	1.4642	2.3379	5.1579
7	4.1056	2.3553	-0.5862	0.7354	0.7895	1.2713	0.9321	1.7502	2.9416
8	5.1294	1.347	-4.8425	0.8967	0.8866	1.115	0.9661	3.7824	6.1895
9	4.9057	0.5656	-4.9007	0.6922	1.2217	1.0813	0.9984	4.3401	5.4663
10	5.1163	1.5929	-3.1439	0.4538	0.4697	0.6989	0.5408	3.5234	4.7368
11	3.917	0.6474	-3.5773	0.6185	1.0855	1.3378	1.0139	3.2696	4.2247
12	4.3781	1.0107	-2.6531	0.9673	1.3432	0.4884	0.933	3.3674	3.6638
13	4.8336	1.0253	-3.8985	0.5847	0.4868	0.97	0.6805	3.8083	4.9239
14	4.7608	0.9077	-2.781	0.6874	0.3707	1.3584	0.8055	3.8531	3.6887
15	5.0672	3.4744	-0.7118	1.0476	1.061	0.6126	0.9071	1.5928	4.1862
16	3.9239	1.1926	-1.715	0.4701	0.5629	1.5315	0.8548	2.7313	2.9076
17	3.7638	1.1201	-0.8206	1.2964	1.3087	1.9207	1.5086	2.6437	1.9407
18	3.4654	2.2282	0.8836	1.0227	1.3564	2.8934	1.7575	1.2372	1.3446
19	2.5741	0.2744	1.1678	1.5476	1.1486	3.4731	2.0565	2.2996	-0.8934
20	3.1206	2.0737	1.6715	0.3633	0.4463	3.2347	1.3481	1.0469	0.4022

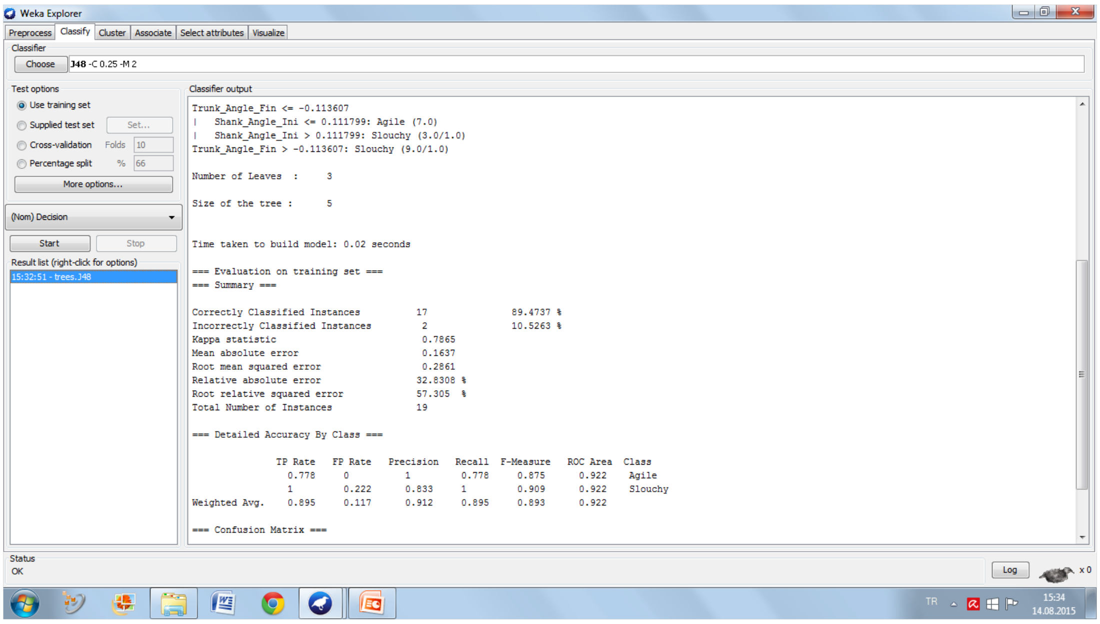

Figure H.1: Weka Output for decision three, Forward Trials of Subject 1

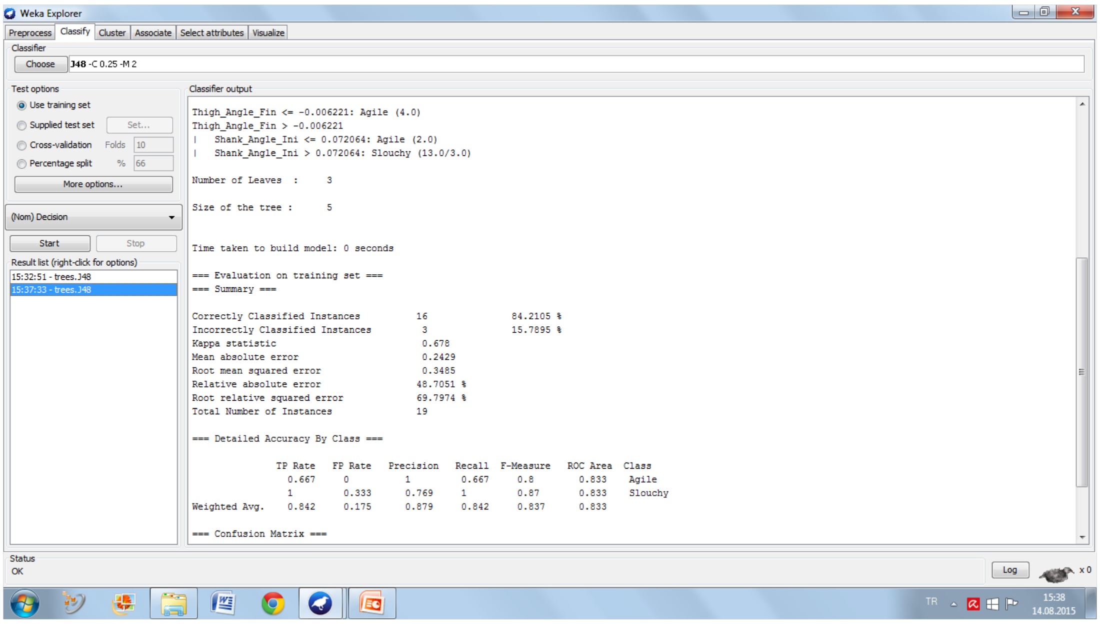

Figure H.2: Weka Output for decision three, Backward Trials of Subject 1

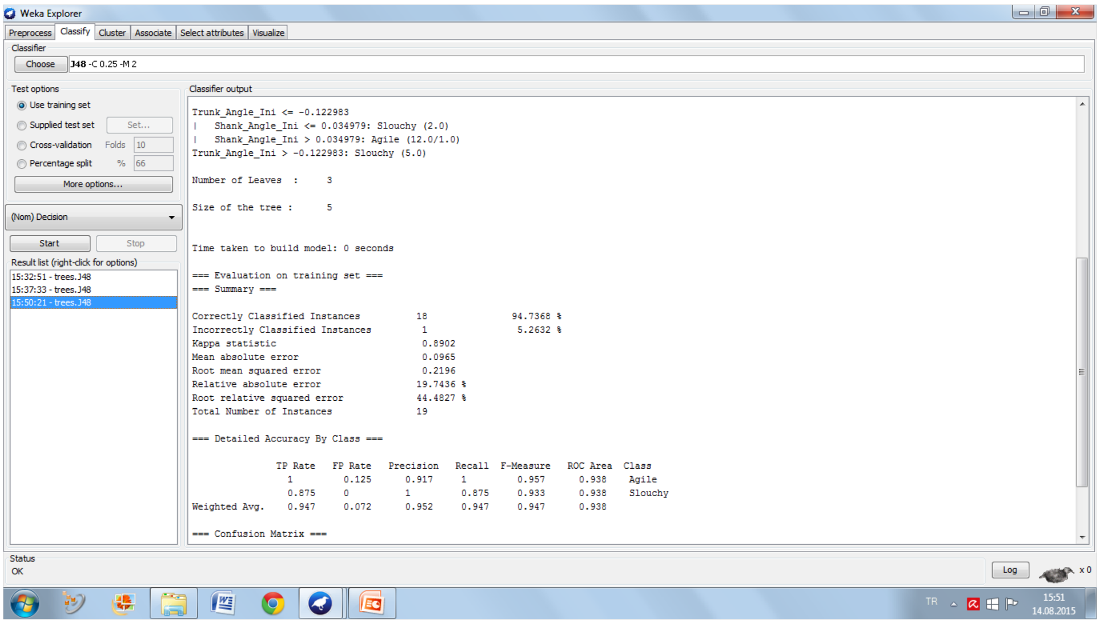

Figure H.3: Weka Output for decision three, Forward Trials of Subject 2

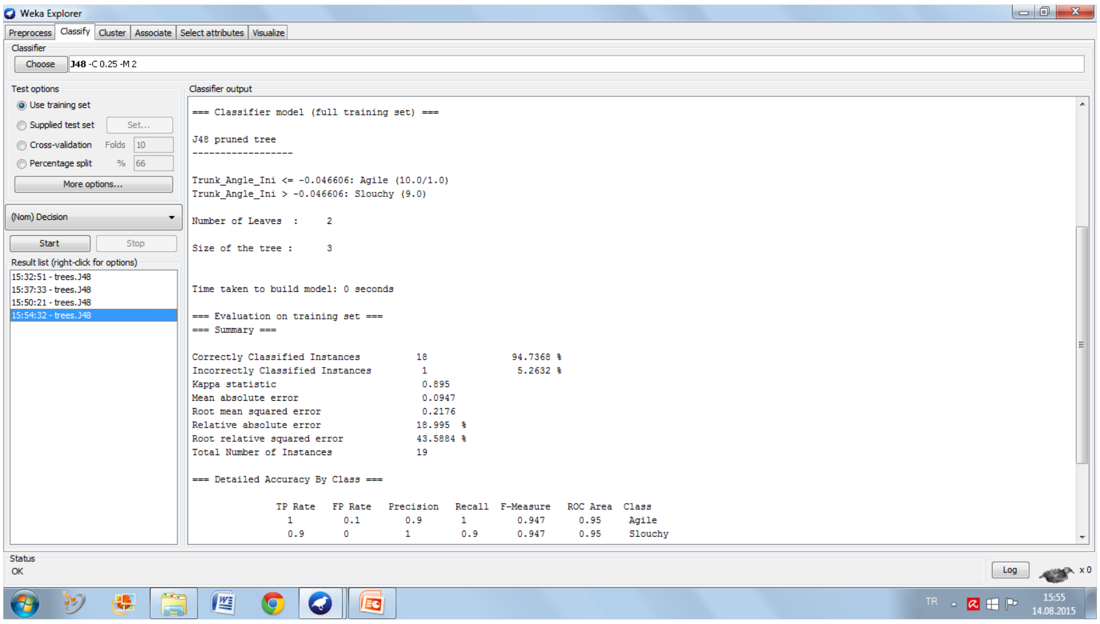

Figure H.4: Weka Output for decision three, Backward Trials of Subject 2

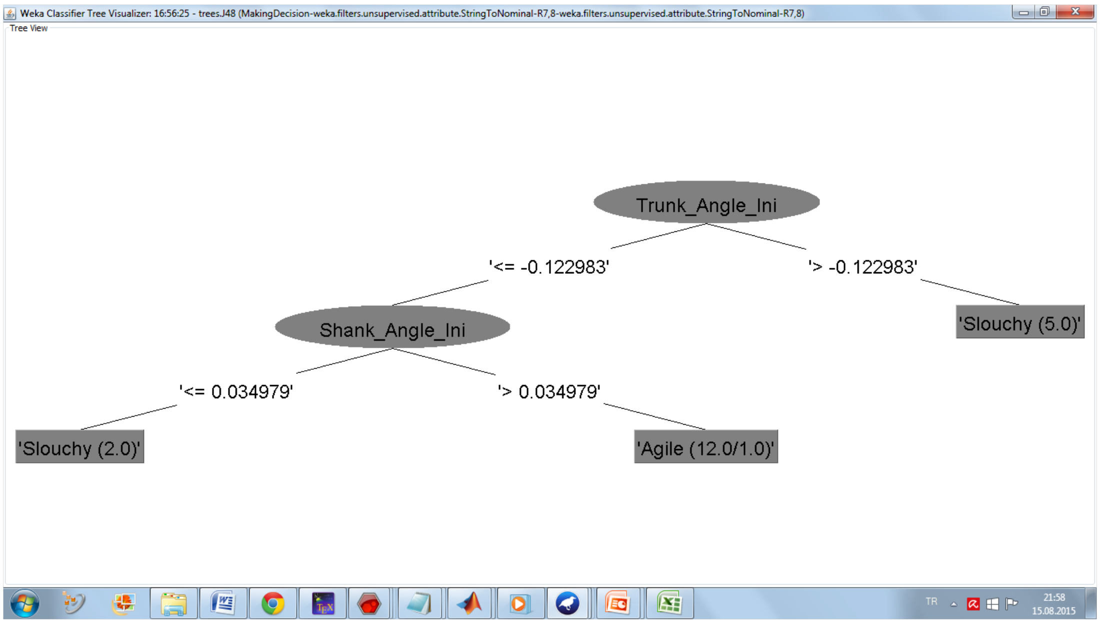

Figure H.5: Visualized Decision Tree by Weka, Forward Trials of Subject 2

CURRICULUM VITAE

PERSONAL INFORMATION

Surname, Name: Bilgin, Nurdan
Nationality: Turkish (TC)
Date and Place of Birth: 31.07.1971, Samsun
Marital Status: Single
Phone: 0 542 2927616
Fax: 0 312 2308434

EDUCATION

Degree	Institution	Year of Graduation
M.S.	Gazi University/Mechanical Engineering Dep.	2007
B.S.	Gazi University/Mechanical Engineering Dep.	2003
A.S.	METU/Technical Vocational School/Automation	1995
B.S.	METU/Department of Physics Education	1993-uncompleted
High School	Ladik Lycee	1988

PROFESSIONAL EXPERIENCE

Year	Place	Enrollment
2011-	Gazi University/Mechanical Engineering Department	Engineer
2001-2011	Gazi University/Gazi Hospital/IT Department	Engineer
1998-2001	Ondokuz Mayıs University/IT Department	Technician
1996-1998	Işık A.Ş./IT and Design Departments	Technician
1995-1996	Orkimsen A.Ş./Design Departments	Technician

PUBLICATIONS

International Conference Publications

1. Nurdan Bilgin, Metin U. Salamci, 2014. Determination of Optimal Feedback Gain Matrix for a Class of Nonlinear Systems , 2014 15th International Carpathian Control Conference (ICCC) Velke Karlovice, Czech Republic
2. Nurdan Bilgin, Metin U. Salamci, 2014. Sliding Mode Control Design for Nonlinear Systems without Reaching Pase and its Applications to a Flexible Spacecraft , Proceedings of the ASME 2014 12th Biennial Conference on Engineering Systems Design and Analysis ESDA2014 Copenhagen, Denmark
3. Metin U. Salamci, Nurdan Bilgin, Sinan Özcan and Emin Yusuf Avan, 2011. Sliding Mode Control Design for Nonlinear Systems without Reaching Phase , ACD 2011 : 9th European Workshop on Advanced Control and Diagnosis Budapest/Hungary

National Conference Publications

1. Nurdan Bilgin, M. Kemal Özgören, 2015. İnsanların denge-kurtarma kontrolüne ait uyarlama kuralının kanonik korelasyon analizi ile tanılanması, TOK 2015, Denizli.
2. Nurdan Bilgin, M. Kemal Özgören, 2015. İnsanlarda denge kurtarma kontrolcusunun zamanla değişen parametrelerinin kestirimi için kullanılan yöntemlerin karşılaştırılması, TOK 2015, Denizli.
3. Nurdan Bilgin, M. Kemal Özgören, 2015. Dik Duruş Sırasında İnsanın Ani Bir Dış Etki Karşısında Denge Korumak İçin Kullanmış Olabileceği Kontrol Kuralı Önerisi ve Deneysel Doğrulanması, 17. Ulusal Makine Teorisi Sempozyumu, İzmir
4. Nurdan Bilgin, M. Kemal Özgören, 2015. Ani Bir Dış Etki Karşısında Dik Duruş Dengesini Sağlayan Kontrol Parametreleri için Merkezi Sinir Sistemi Tarafından Kullanılan Olası Uyarlama Kuralı Hakkında Bir Çalışma, 17. Ulusal Makine Teorisi Sempozyumu, İzmir

5. Nurdan Bilgin, Senih Gürses, 2013. Kişisel Alan İhlalinin İnsanın Dik Duruş Cevabına Etkisinin İncelenmesi, Ulusal Makine Teorisi Sempozyumu, Erzurum

6. Nurdan Bilgin, Metin Uymaz Salamcı, 2013. Rijit Bir Uydu İçin Durum Geri Besleme Denetim Algoritması Tasarımı, Ulusal Makine Teorisi Sempozyumu, Erzurum

7. Nurdan Bilgin, Metin Uymaz Salamcı, 2013. Doğrusal Olmayan Sistemlerin Optimal Denetimi için Yakınsama Yaklaşımı ve Uygulaması , TOK2013 Malatya

8. Nurdan Bilgin, Metin U. Salamcı, 2011. Bir Uydu Modelinin Kayan Kipli Denetçi ile Konum ve Titreşim Kontrolü için iki Farklı Denetim Yöntem, TOK 2011 İzmir

9. Nurdan Bilgin, Metin U. Salamcı, 2007. Esnek Kanada Sahip Bir Uydu Modeli İçin Kayan Kipli Denetci Tasarımı , 13. Ulusal Makine Teorisi Sempozyumu Sivas